NASA Technical Memorandum 103934

Dynamic Response of Induced Pressures, Suckdown, and Temperatures for Two Tandem Jet STOVL Configurations

Douglas A. Wardwell, Victor R. Corsiglia, and Richard E. Kuhn
Ames Research Center, Moffett Field, California

July 1992

National Aeronautics and
Space Administration

Ames Research Center
Moffett Field, California 94035-1000

Dynamic Response of Induced Pressures, Suckdown, and Temperatures for Two Tandem Jet STOVL Configurations

DOUGLAS A. WARDWELL, VICTOR R. CORSIGLIA, AND RICHARD E. KUHN*

Ames Research Center

Summary

NASA Ames Research Center has been conducting a program to improve the methods for predicting the jet-induced lift loss (suckdown) and hot gas ingestion on jet Short Takeoff and Vertical Landing (STOVL) aircraft during hover near the ground. As part of that program, small-scale hover tests were conducted to expand the current data base and to improve upon the current empirical methods for predicting jet-induced lift loss and hot gas ingestion (HGI) effects.

This report is one of three data reports covering data obtained from hover tests conducted at Lockheed Aeronautical Systems, Rye Canyon Facility. It will include dynamic (time dependent) test data for both lift loss and HGI parameters (height, nozzle temperature, nozzle pressure ratio, and inlet location). The flat plate models tested were tandem jet configurations with three planform variations and variable position side-by-side sucking inlets mounted above the planform.

Temperature time lags from 8–15 seconds were observed before the model temperatures stabilized. This was larger than the expected 1.5-second lag calculated from literature. Several possible explanations for the flow temperatures to stabilize may include some, or all, of the following: thermocouple lag, radiation to the model surface, and heat loss to the ground board. Further investigations will be required to understand the reasons for this temperature lag.

Nomenclature

c_p	pressure coefficient, $\frac{\Delta P \times 2 \times A_{jet}}{Thrust}$
$\overline{D}$	equivalent model diameter, ft, $\frac{1}{\pi}\int_0^{2\pi} r d\Theta$
HGI	hot gas ingestion
LID	lift improvement device
NPR	nozzle pressure ratio; nozzle total pressure divided by ambient pressure
S_{plan}	total planform area, ft^2
S_{jet}	total jet exit area, ft^2
Thrust	total jet thrust, lb
T_{amb}	ambient room temperature, °F
T_{jet}	jet total temperature, °F
T_x	temperature at measured location, °F
ΔL	jet-induced lift, lb
$\frac{\Delta L}{T}$	jet-induced lift divided by total jet thrust
θ	temperature ratio, $\frac{T_x - T_{amb}}{T_{jet} - T_{amb}}$

Introduction

Throughout the 1950's and 1960's there were efforts to evaluate the effects of propulsion induced aerodynamics on a diverse set of Short Takeoff Vertical Landing (STOVL) designs. Reference 1 (Wyatt) was the first of these efforts to predict the suckdown. There was no pressure distribution data within that study and very little in subsequent studies. Additionally, most of the studies in the literature included only force and moment data on complete STOVL configurations with little or no documentation on the models, nozzles, room size, etc.

What has been needed is a systematic variation of parameters to create a large database for predicting the suckdown and hot gas ingestion (HGI) on potential STOVL designs. The propulsion induced aerodynamics experienced by jet STOVL aircraft hovering near the ground is the subject of investigation at NASA Ames Research Center. Part of this program, partially reported here, was to conduct small-scale hover tests to expand the current data base and then to try to improve the current methods for empirically predicting jet-induced lift loss and HGI effects.

*STO-VL Technology, San Diego, CA.

To implement this task, a hover test rig was built to test small-scale planforms in and out of ground effect during hover. To obtain HGI data on these models, it was necessary to use Lockheed Aeronautical Systems, Rye Canyon facility because they had a source of 800°F air, which at the time was unavailable at NASA Ames. All planforms tested were flat plate models.

Reference 2 presents the single-jet data obtained in evaluating the adequacy of the facility used for the tests at Ames and Rye Canyon. Reference 3 presents static data taken during the test at Rye Canyon. This report will present dynamic (time dependent) test data for both lift loss and HGI parameters (height, nozzle temperature, nozzle pressure ratio, and inlet location). The models tested were tandem jet configurations with three planform variations and variable position side-by-side sucking inlets mounted above the planform.

Figure 1 shows a side view of the flow field generated by a multiple jet configuration in ground effect. The jet flow impinges on the ground and forms a wall jet that entrains surrounding air. This entrainment induces a low-pressure area on the lower surface of the aircraft called suckdown. Meanwhile, a fountain upwash is generated in the area between the jets, inducing a high-pressure area called fountain lift. The resultant of these two forces (suckdown and fountain lift) is the jet-induced lift or ΔL. Hot gas ingestion is caused by the hot wall jet (far field) and/or fountain flow (near field) being drawn into the engine inlet.

Description of Rye Canyon Test Setup

The test setup at the Lockheed, Rye Canyon facility and most hardware is fully described in reference 2. Only a general description of those test items used in reference 2 will be repeated below. Hardware unique to the HGI portion of the tests will be described in detail.

Models

Three flat plate configurations were tested: the body alone (fig. 2); the wing/body (fig. 3); and the delta wing (fig. 4).

The models were constructed of 1/4 in. thick aluminum. Each model was 34 in. long and both the wing/body and delta planforms had a wing span of 20 in. The body was 4 in. wide. The jet spacing for all three configurations was constant at 14.7 in. The top edges were chamfered as shown in figures 2-4. The moment reference point is constant at 17.0 in. aft of the model nose of each configuration.

The body only model (fig. 2) had a planform area to jet area ratio (S_{plan}/S_{jet}) of 50.2 and an equivalent model diameter ($\overline{D}$) of 9.95 in. (calculated from the moment reference point). The equivalent model diameter ($\overline{D}$) is defined by Wyatt (ref. 1) and is used for suckdown prediction techniques. The balance attachment point was at a model station of 18 in. from the nose (1 in. aft of the moment reference point).

The wing/body model (fig. 3) had a leading edge sweep of 49° and a trailing edge sweep of –8°. It had an aspect ratio of 2.28, a planform area to jet area ratio of 105, and an equivalent model diameter ($\overline{D}$) of 16.9 in. (calculated from the moment reference point). The balance attachment point was also at a model station of 18 in. from the nose.

The delta wing model (fig. 4) had a leading edge sweep of 71° and a trailing edge sweep of –8°. It had an aspect ratio of 1.08, a planform area to jet area ratio of 156, and an equivalent model diameter ($\overline{D}$) of 20.1 in. (calculated from the moment reference point). The task balance attachment point was the same as for the wing/body model at a model station of 18 in. from the nose.

The bottom pressure taps for the body only, wing/body, and the delta wing are shown in figures 5 and 6. The first longitudinal row of pressure taps is offset from the center by 0.25 in. Although the wing/body had 67 pressure taps and the delta wing had 78 for static testing, only three per model were used during the dynamic tests. These three taps were located at 13, 17, and 21 in. aft of the nose and along the centerline (0.25 in. offset) of the model. These were used to measure the fountain center pressure and the pressures associated with the lift improvement devices. The wing/body and the delta wing are shown installed at the Rye Canyon test cell in figures 7 and 8, respectively.

For some tests lift improvement devices (LIDs) were installed on the body only and wing/body configurations (figs. 9 and 10) to evaluate their influence on lift loss and HGI. The LIDs were made of 1/16 in. thick steel that was 1-1/2 in. wide, bent at a 90° angle, and attached to the bottom of the model so that they were protruded down 3/4 in.

Balance

A six component TASK 1.5 MK IIC strain gage balance was used to measure the jet-induced forces on the models. The axial force component (100 lb max) was used to measure the jet-induced lift. The side force components (500 lb max) were used to determine the pitching moment. No interactions between the balance gages were used in calculating the balance forces.

Hover Test Rig

The hover test rig is shown in figures 11, 12, and 13. The rig has an 8 ft × 8 ft movable ground plane with a manually operated pneumatic trap door. The trap door sits under the jets, and while open, allows the hot jet air to be exhausted from the room through the ducting attached to the underside of the ground plane. The trap door is in the open position while the run parameters (i.e. ground height, nozzle pressure ratio (NPR), and nozzle temperature) are set so that the model, ground plane, and room do not get overheated. Once the parameters are set, the trap doors are closed, data is taken, and the trap doors reopened.

Figure 13 shows the room size and rig position at the Rye Canyon facility. Reference 2 presents data on room size variations and shows that the room size does slightly affect the out-of-ground effect suckdown.

The models were mounted to the balance while the nozzles and plenums were mounted directly to the hover test rig. A 0.05 in. gap was maintained between the nozzle exit and the model making the model non-metric because the nozzles did not touch the model. An electrical fouling circuit was used to insure that the metric break was maintained. Therefore the task balance only measured jet-induced aerodynamic loads on the models. The balance, nozzles, plenums, and high-pressure lines bringing air to the plenums were wrapped with insulation material to reduce the warm-up time and to isolate the balance from the hot environment.

Nozzle and Plenum

The two circular nozzles were made of 321 stainless steel and were bolted to rectangular plenums made of 304 stainless steel (fig. 14). The nozzles had three porous plates to improve flow quality and an ASME long-radius nozzle exit design (fig. 15) to simplify the thrust calculations. Each nozzle had an exit diameter of 1.23 in.

The rectangular plenums had 3/8 in. diameter steel rods welded in place to increase the plenum wall stiffness (fig. 14). Each plenum pressure was controlled separately but maintained at the same pressure. The maximum flow throughout each plenum was 2.5 lb/sec at an NPR of 6; most data was taken at an NPR of 2, and a total mass flow of approximately 1.44 lb/sec (59 °F), depending upon temperature.

Kiel Probe

A Kiel probe assembly was used to measure the total pressure and total temperature of each ASME nozzle that was used to calculate nozzle thrust. The probes were located 3.5 in. upstream of the nozzle exit and 2 in. (26 hole diameters) downstream of the last porous plate (fig. 15). The Kiel probe had a shield diameter of 0.095 in. At the location of the Kiel probe, the inner diameter of the duct leading to the nozzle was 1.935 in. A gap of 0.050 in. was maintained between the model and the nozzle at the exit plane (fig. 15).

Inlet

The inlet layout (with respect to the model) is shown in figures 16 and 17. The left and right inlet temperature probes were vertically stacked at the entrance of each inlet; the middle temperature probe (T22 in fig. 18) of the left inlet malfunctioned at the start and was never used.

A vacuum system at the Rye Canyon test facility was used to generate inlet flow. To measure the mass flow of the inlet, a venturi was located downstream of the inlet. The venturi contained two pressure transducers to measure total and static pressure, plus a thermocouple to measure total temperature. The suction system venturi became choked at a mass flow of 0.53 to 0.55 lb/sec. A valve downstream of the venturi was used to vary the mass flow for some runs; however, most runs were done with the valve fully open.

Thermocouples

Thirteen thermocouples were used for each model: one monitored the ambient temperature (Copper-Constantan), type-T; two others monitored the total nozzle air temperature (Chromel-Alumel), type-K; five monitored the inlet temperatures (type-T); two monitored the edge and belly temperatures (type-T); two field thermocouples monitored the external flow field temperatures (type-T); and the final one measured the total temperature of the venturi (type-K) used in the inlet suction system. Figures 17 and 18 show the inlet thermocouple locations. The belly thermocouple was located in the model along the longitudinal axis in the center of the fountain region (17 in. from the nose). The model edge thermocouple moved with the inlet longitudinal X-position with its lateral Y-location following the edge of the planform (see fig. 16). All thermocouples were wired to a 150 °F hot box reference junction. The field thermocouples were placed at various locations around the model, but always at axial distance of 15.5 in. and 21.0 in. away from the front nozzle. Figures preceding each data set will show the locations of the inlets, field thermocouples, and belly and edge thermocouples.

Instrumentation and Data Acquisition System

The model and hover test rig instrumentation consisted of the following:

- two nozzle pressure transducers (100 psig; used to determine NPR);
- three scanivalve pressure transducers (1 psig) that were used on three 48-port scanivalve modules—only one port per transducer was used during the dynamic tests;
- an ambient pressure transducer (25 psia);
- thirteen (K & T type) thermocouples, including ambient temperature;
- two pressure transducers for the inlet suction venturi;
- two trap door position switches;
- a six-component strain gage balance; and
- a string-potentiometer to measure ground height.

Figure 19 shows a schematic of the data system.

The task balance, pressure transducers, and ground height potentiometer were supplied an excitation voltage by a group of signal conditioners; one conditioner per instrument. All instrumentation was fed into a set of amplifiers and digitized.

During the data acquisition sequence data taking was started, the trap doors were manually closed after approximately two seconds, data taking progressed, the trap doors were manually opened approximately two seconds before the predetermined time limit, and data taking was stopped. The data was then stored on a hard disk, converted to engineering units, and summarized on an output to a printer.

Computer memory limited on-line data storage to 280 points/channel (40 channels max in the system). To accommodate this, five samples from the multiprogrammer were averaged into one data point on the computer. Due to memory limits, the time duration for each run was limited to 30 seconds. This meant that with 40 channels, the sampling rate limit was 45 samples per second; which equates to 9 (45 samples/(5 samples/data point)) data points per second per channel for each run.

Data Sets

The test conditions for the 13 data sets obtained are listed in Table 1. The time history data obtained from the tests are shown for each run point in each data set (figs. 20-56). Proceeding each data set is a figure that shows the model planform used, inlet location, and thermocouple locations. There are six plots per run point: (1) upper left-hand corner shows pressure coefficients, C_p, at three model locations of 13, 17, and 21 in. from the nose of the model (see fig. 6); (2) middle upper row shows room and, if applicable, field temperatures; (3) upper right-hand corner shows the air temperature ratios for the model belly and edge; (4) lower left-hand corner shows the jet-induced lift increment as measured by the balance; (5) middle lower row shows the air temperature ratios for the left inlet; and (6) lower right-hand corner shows the air temperature ratios for the right inlet. For runs 66 through 68 (figs. 21, 23, and 25), no field temperatures were taken.

The room temperature was measured at the top of the hover test rig. The field temperatures were measured at various places around the model as shown in the figure proceeding each data set. The belly temperature was measured by a thermocouple protruding from the underside of the model, located at the centerline station 17 in. from the model nose. The edge temperature was placed along the edge of the planform at the same longitudinal X-station location as the mouth of the inlet. The inlet was nominally at maximum suction capacity (0.53 to 0.55 lb/sec) for all runs; exceptions will be noted.

The trap door position was measured by two limit switches that indicated when the doors were in the full-open or full-closed positions. The trap door position is plotted on all graphs. Zero time is when the trap door was fully closed.

Discussion of Results

General

As expected, the pressure and lift response were almost instantaneous with the closing of the trap doors. Although no attempt was made to establish the time history of the development of the flow field, the pressure and lift increment data suggest that the time to establish the flow field was less than 0.1 seconds.

The sensitivity of inlet mass flow to the inlet temperatures was briefly explored. Runs 71P1 to 71P5 (figs. 29(a)-29(e)) attempted to vary only the inlet mass flow; however, the jet temperatures increased around 4% (from 480 °F to 497 °F) as the mass flow was incrementally decreased. The inlet was 17 in. from the model nose, the model height was 4 in. from the ground, the model was the body alone, and the jets were at an NPR of 2.0. The inlet temperature rise was constant for air flows from 0.532 to 0.245 lb/sec. The runs with inlet flow variations took from 8–10 sec for the temperatures to stabilize, while the temperature for the zero-mass-flow run never did

stabilize in the 30 sec data interval. The zero-mass-flow run did, however, reach approximately the same ending temperature as those with inlet flow. This suggests that the fountain flow was the major driver in establishing the inlet temperatures for this configuration.

All the temperature time histories taken during these tests showed a time lag of 8–15 sec before the temperature stabilized; this was not expected, especially for the belly and edge temperatures. The lag of the inlet temperatures could be due to the time required for the hot jet flow to mix with the entrained flow. However, the temperature of the air measured on the belly (in the fountain impingement region) was expected to respond as quickly as the flow field pressures. Several possible explanations for the observed lag in stabilizing the temperature are suggested: (1) thermocouple lag; (2) radiation to the nearby cooler model surfaces; and (3) heat loss to the ground board in the impingement region. The possible effect of each of these factors on the observed thermocouple time histories are briefly discussed below.

Thermocouple Lag

The thermocouples used in the present investigation were made from Copper-Constantan 28 gage (app. 0.013 in. diameter) wire with a bulb size of 0.010 in. Reference 4 presents the thermocouple time constants (the time required for the indicated temperature to rise to 63% of the temperature of the air it is measuring) for a range of wire sizes and air velocities. For the inlet velocities involved in this study, reference 4 indicates that the time constant should be about 0.9 sec.

For the thermocouples on the lower surface of the models, the effective velocity of the air is unknown. Reference 4 indicates that for the size of wire used, the time constant should be between 0.3 and 1.3 sec depending upon the magnitude of the effective velocity at the thermocouple. If these time constants are correct, something else must be causing the lag in the thermocouple temperature measurements. More experimentation needs to be done to determine the true time constant for the conditions encountered in this test.

Radiation to Model Surface

At the beginning of a run, the model surface is at a lower temperature than the air impinging on the model or entering the inlet. If the thermocouple junction is hotter than the model surface, it will lose heat to the cooler model. However, at the beginning of a run (immediately after the ground board trap doors close), the junction is cool and both it and the model should warm up together. It is not clear if radiation to the model can have a significant effect on the temperature time history.

Loss of Heat to the Ground Board

At the beginning of a run, the trap doors in the ground board (on which the jets impinge) are cooler than the air that impinges on it; but they heat up rapidly. At the end of a typical 30 sec run the ground board trap doors were too hot to touch. At the beginning of the run, more heat was lost to the doors than later in the run. Therefore, the air that reached the model was cooler at the beginning than at the end of the run. Again, it is not clear if heat loss to the ground board had a significant effect.

Concluding Remarks

As expected, the pressure and lift response were almost instantaneous with the closing of the trap doors. However, an unexpected time lag in the stabilization of the temperature was encountered in the temperature measurements. Additional testing and data analysis will be required to fully understand the reasons for this temperature lag. Further investigations should be undertaken to evaluate the response time of thermocouples used, the effects of radiation to the cooler model surfaces, and the effects of heat loss into the ground board.

References

1. Wyatt, L. A.: Static Test of Ground Effect on Planforms Fitted With a Centrally-Located Round Lifting Jet. Ministry of Aviation. London, England. CP 749, June 1962.

2. Bellavia, D. C.; Wardwell, D. A.; Corsiglia, V. R.; and Kuhn, R. E.: Forces and Pressures Induced on Circular Plates by a Single Lifting Jet in Ground Effect. NASA TM-102816, April 1991.

3. Bellavia, D. C.; Wardwell, D. A.; Corsiglia, V. R.; and Kuhn, R. E.: Suckdown, Fountain Lift, and Pressures Induced on Several Tandem Jet V/STOL Configurations. NASA TM-102817, April 1991.

4. Moffat, R. J.: Design of Thermocouples for Response Rate. ASME Transactions, Feb. 1958, pp. 257–262.

Table 1. Summary of model configurations tested.

Data Set	Config	Height	LID	Inlet		Jets			Field probes	Run/ Point	Figure
				position	suction	NPR	thrust	Tjet			
1	Body alone	4	None	13	0.551	2	50	470	None	66/1	21a
1	Body alone	6	None	13	0.551	2	50	475	None	66/2	21b
1	Body alone	8	None	13	0.551	2	50	480	None	66/3	21c
1	Body alone	10	None	13	0.551	2	50	490	None	66/4	21d
1	Body alone	20	None	13	0.551	2	50	500	None	66/6	21e
1	Body alone	30	None	13	0.551	2	50	500	None	66/7	21f
1	Body alone	40	None	13	0.551	2	50	505	None	66/8	21g
2	Body alone	4	None	9.66	0.551	2	50	485	None	67/1	21a
2	Body alone	6	None	9.66	0.551	2	50	500	None	67/2	23b
2	Body alone	8	None	9.66	0.551	2	50	505	None	67/3	23c
3	Delta wing	4	None	9.66	0.551	2	50	400	None	68/1	25a
3	Delta wing	6	None	9.66	0.551	2	50	419	None	68/2	25b
3	Delta wing	8	None	9.66	0.551	2	50	433	None	68/3	25c
3	Delta wing	10	None	9.66	0.551	2	50	445	None	68/4	25d
4	Delta wing	4	None	9.66	0.551	2	50	415	top/side	70/1	27a
4	Delta wing	4	None	9.66	0.437	2	50	440	top/side	70/2	27b
4	Delta wing	4	None	9.66	0.347	2	50	453	top/side	70/3	27c
4	Delta wing	4	None	9.66	0.551	2	50	499	top/side	70/4	27d
4	Delta wing	6	None	9.66	0.551	2	50	503	top/side	70/5	27e
4	Delta wing	8	None	9.66	0.551	2	50	506	top/side	70/6	27f
4	Delta wing	10	None	9.66	0.551	2	50	508	top/side	70/7	27g
4	Delta wing	15	None	9.66	0.551	2	50	510	top/side	70/8	27h
4	Delta wing	20	None	9.66	0.551	2	50	511	top/side	70/9	27i
4	Delta wing	30	None	9.66	0.551	2	50	512	top/side	70/10	27j
4	Delta wing	40	None	9.66	0.551	2	50	514	top/side	70/11	27k

Table 1. (Continued.)

Data Set	Config	Height	LID	Inlet		Jets			Field probes	Run/ Point	Figure
				position	suction	NPR	thrust	Tjet			
5	Body alone	4	None	17	0.532	2	50	469	top/side	71/1	29a
5	Body alone	4	None	17	0.425	2	50	480	top/side	71/2	29b
5	Body alone	4	None	17	0.346	2	50	486	top/side	71/3	29c
5	Body alone	4	None	17	0.245	2	50	492	top/side	71/4	29d
5	Body alone	4	None	17	0	2	50	497	top/side	71/5	29e
5	Body alone	6	None	17	0.551	2	50	502	top/side	71/6	29f
5	Body alone	8	None	17	0.551	2	50	505	top/side	71/7	29g
5	Body alone	10	None	17	0.551	2	50	507	top/side	71/8	29h
5	Body alone	15	None	17	0.551	2	50	510	top/side	71/9	29i
5	Body alone	4	None	17	0.551	2	50	671	top/side	72/1	30a
5	Body alone	6	None	17	0.551	2	50	696	top/side	72/2	30b
5	Body alone	8	None	17	0.551	2	50	698	top/side	72/3	30c
5	Body alone	10	None	17	0.551	2	50	699	top/side	72/4	30d
5	Body alone	15	None	17	0.551	2	50	699	top/side	72/5	30e
5	Body alone	20	None	17	0.551	2	50	701	top/side	72/6	30f
5	Body alone	30	None	17	0.551	2	50	702	top/side	72/7	30g
5	Body alone	40	None	17	0.551	2	50	703	top/side	72/8	30h
5	Body alone	4	None	17	0.551	2	50	174	top/side	73/1	31a
5	Body alone	6	None	17	0.551	2	50	188	top/side	73/2	31b
5	Body alone	8	None	17	0.551	2	50	192	top/side	73/3	31c
5	Body alone	10	None	17	0.551	2	50	201	top/side	73/4	31d
5	Body alone	15	None	17	0.551	2	50	204	top/side	73/5	31e
5	Body alone	20	None	17	0.551	2	50	208	top/side	73/6	31f
5	Body alone	30	None	17	0.551	2	50	210	top/side	73/7	31g

Table 1. (Continued.)

Data Set	Config	Height	LID	Inlet		Jets			Field probes	Run/ Point	Figure
				position	suction	NPR	thrust	Tjet			
6	Body alone	4	None	17	0.551	2	50	480	inlet/side	74/1	33a
6	Body alone	8	None	17	0.551	2	50	485	inlet/side	74/2	33b
6	Body alone	4	None	17	0.551	3	92	500	inlet/side	74/3	33c
6	Body alone	8	None	17	0.551	3	92	509	inlet/side	74/4	33d
6	Body alone	4	None	17	0.551	4	133	525	inlet/side	75/1	34a
6	Body alone	8	None	17	0.551	4	133	533	inlet/side	75/2	34b
6	Body alone	4	None	17	0.551	5	176	545	inlet/side	76/1	35a
6	Body alone	8	None	17	0.551	5	176	550	inlet/side	76/2	35b
6	Body alone	4	None	17	0.551	6	219	560	inlet/side	77/1	36a
6	Body alone	8	None	17	0.551	6	219	562	inlet/side	77/2	36b
6	Body alone	4	Box 13/21	17	0.551	2	50	482	inlet/side	78/1	37a
6	Body alone	6	Box 13/21	17	0.551	2	50	488	inlet/side	78/2	37b
6	Body alone	8	Box 13/21	17	0.551	2	50	493	inlet/side	78/3	37c
6	Body alone	10	Box 13/21	17	0.551	2	50	498	inlet/side	78/4	37d
6	Body alone	15	Box 13/21	17	0.551	2	50	502	inlet/side	78/5	37e
6	Body alone	17	Box 13/21	17	0.551	2	50	505	inlet/side	78/6	37f
6	Body alone	20	Box 13/21	17	0.551	2	50	508	inlet/side	78/7	37g
6	Body alone	40	Box 13/21	17	0.551	2	50	511	inlet/side	78/8	37h
7	Body alone	4	Box 13/21	13	0.551	2	50	497	inlet/side	79/1	39a
7	Body alone	6	Box 13/21	13	0.551	2	50	501	inlet/side	79/2	39b
7	Body alone	8	Box 13/21	13	0.551	2	50	505	inlet/side	79/3	39c
7	Body alone	10	Box 13/21	13	0.551	2	50	508	inlet/side	79/4	39d
7	Body alone	15	Box 13/21	13	0.551	2	50	511	inlet/side	79/5	39e
7	Body alone	20	Box 13/21	13	0.551	2	50	514	inlet/side	79/6	39f
7	Body alone	30	Box 13/21	13	0.551	2	50	515	inlet/side	79/7	39g
7	Body alone	40	Box 13/21	13	0.551	2	50	517	inlet/side	79/8	39h
8	Body alone	4	Box 13/21	9.66	0.551	2	50	500	inlet/side	80/1	41a
8	Body alone	6	Box 13/21	9.66	0.551	2	50	506	inlet/side	80/2	41b
8	Body alone	8	Box 13/21	9.66	0.551	2	50	508	inlet/side	80/3	41c
8	Body alone	10	Box 13/21	9.66	0.551	2	50	510	inlet/side	80/4	41d
8	Body alone	15	Box 13/21	9.66	0.551	2	50	512	inlet/side	80/5	41e
8	Body alone	20	Box 13/21	9.66	0.551	2	50	514	inlet/side	80/6	41f

Table 1. (Continued.)

Data Set	Config	Height	LID	Inlet		Jets			Field probes	Run/ Point	Figure
				position	suction	NPR	thrust	Tjet			
8	Body alone	30	Box 13/21	9.66	0.551	2	50	516	inlet/side	80/7	41g
8	Body alone	40	Box 13/21	9.66	0.551	2	50	517	inlet/side	80/8	41h
8	Body alone	4	Box 13/21	9.66	0.551	2	50	510	inlet/side	81/1	42a
8	Body alone	6	Box 13/21	9.66	0.551	2	50	511	inlet/side	81/2	42b
8	Body alone	8	Box 13/21	9.66	0.551	2	50	513	inlet/side	81/3	42c
8	Body alone	10	Box 13/21	9.66	0.551	2	50	515	inlet/side	81/4	42d
8	Body alone	15	Box 13/21	9.66	0.551	2	50	517	inlet/side	81/5	42e
8	Body alone	20	Box 13/21	9.66	0.551	2	50	518	inlet/side	81/6	42f
8	Body alone	30	Box 13/21	9.66	0.551	2	50	518	inlet/side	81/7	42g
8	Body alone	40	Box 13/21	9.66	0.551	2	50	520	inlet/side	81/8	42h
9	Body alone	4	None	13	0.551	2	50	495	nlet/fron	82/1	44a
9	Body alone	6	None	13	0.551	2	50	500	nlet/fron	82/2	44b
9	Body alone	8	None	13	0.551	2	50	503	nlet/fron	82/3	44c
9	Body alone	10	None	13	0.551	2	50	506	nlet/fron	82/4	44d
9	Body alone	20	None	13	0.551	2	50	511	nlet/fron	82/6	44e
9	Body alone	30	None	13	0.551	2	50	514	nlet/fron	82/7	44f
9	Body alone	40	None	13	0.551	2	50	515	nlet/fron	82/8	44g
10	Body alone	4	None	17	0.551	2	50	506	nlet/fron	83/1	46a
10	Body alone	6	None	17	0.551	2	50	508	nlet/fron	83/2	46b
10	Body alone	8	None	17	0.551	2	50	511	nlet/fron	83/3	46c
10	Body alone	10	None	17	0.551	2	50	513	nlet/fron	83/4	46d
10	Body alone	15	None	17	0.551	2	50	514	nlet/fron	83/5	46e
10	Body alone	20	None	17	0.551	2	50	516	nlet/fron	83/6	46f
10	Body alone	40	None	17	0.551	2	50	518	nlet/fron	83/8	46g
11	Wing/body	4	None	9.66	0.551	2	50	488	top/front	84/1	48a
11	Wing/body	6	None	9.66	0.551	2	50	495	top/front	84/2	48b
11	Wing/body	8	None	9.66	0.551	2	50	498	top/front	84/3	48c
11	Wing/body	10	None	9.66	0.551	2	50	502	top/front	84/4	48d
11	Wing/body	15	None	9.66	0.551	2	50	506	top/front	84/5	48e
11	Wing/body	20	None	9.66	0.551	2	50	509	top/front	84/6	48f
11	Wing/body	30	None	9.66	0.551	2	50	511	top/front	84/7	48g
11	Wing/body	40	None	9.66	0.551	2	50	514	top/front	84/8	48h

Table 1. (Continued.)

Data Set	Config	Height	LID	Inlet		Jets			Field probes	Run/ Point	Figure
				position	suction	NPR	thrust	Tjet			
11	Wing/body	6	Box 12/21	9.66	0.551	2	50	512	top/front	89/2	49a
11	Wing/body	8	Box 12/21	9.66	0.551	2	50	514	top/front	89/3	49b
11	Wing/body	10	Box 12/21	9.66	0.551	2	50	514	top/front	89/4	49c
11	Wing/body	15	Box 12/21	9.66	0.551	2	50	515	top/front	89/5	49d
11	Wing/body	20	Box 12/21	9.66	0.551	2	50	515	top/front	89/6	49e
11	Wing/body	30	Box 12/21	9.66	0.551	2	50	517	top/front	89/7	49f
11	Wing/body	40	Box 12/21	9.66	0.551	2	50	517	top/front	89/8	49g
11	Wing/body	4	Box 12/no rear	9.66	0.551	2	50	507	top/front	90/1	50a
11	Wing/body	6	Box 12/no rear	9.66	0.551	2	50	509	top/front	90/2	50b
11	Wing/body	8	Box 12/no rear	9.66	0.551	2	50	510	top/front	90/3	50c
11	Wing/body	10	Box 12/no rear	9.66	0.551	2	50	510	top/front	90/4	50d
11	Wing/body	15	Box 12/no rear	9.66	0.551	2	50	512	top/front	90/5	50e
11	Wing/body	20	Box 12/no rear	9.66	0.551	2	50	514	top/front	90/6	50f
11	Wing/body	30	Box 12/no rear	9.66	0.551	2	50	515	top/front	90/7	50g
12	Wing/body	4	None	13	0.551	2	50	493	top/front	85/1	52a
12	Wing/body	6	None	13	0.551	2	50	498	top/front	85/2	52b
12	Wing/body	8	None	13	0.551	2	50	503	top/front	85/3	52c
12	Wing/body	10	None	13	0.551	2	50	506	top/front	85/4	52d
12	Wing/body	15	None	13	0.551	2	50	510	top/front	85/5	52e
12	Wing/body	20	None	13	0.551	2	50	513	top/front	85/6	52f
12	Wing/body	30	None	13	0.551	2	50	515	top/front	85/7	52g
12	Wing/body	40	None	13	0.551	2	50	517	top/front	85/8	52h
12	Wing/body	4	Box 12/21	13	0.551	2	50	495	top/front	88/1	53a
12	Wing/body	6	Box 12/21	13	0.551	2	50	499	top/front	88/2	53b
12	Wing/body	8	Box 12/21	13	0.551	2	50	502	top/front	88/3	53c
12	Wing/body	10	Box 12/21	13	0.551	2	50	504	top/front	88/4	53d
12	Wing/body	15	Box 12/21	13	0.551	2	50	507	top/front	88/5	53e
12	Wing/body	20	Box 12/21	13	0.551	2	50	508	top/front	88/6	53f
12	Wing/body	30	Box 12/21	13	0.551	2	50	511	top/front	88/7	53g
12	Wing/body	40	Box 12/21	13	0.551	2	50	512	top/front	88/8	53h
13	Wing/body	4	None	17	0.551	2	50	476	top/front	86/1	55a
13	Wing/body	6	None	17	0.551	2	50	478	top/front	86/2	55b

Table 1. (Concluded.)

Data Set	Config	Height	LID	Inlet		Jets			Field probes	Run/ Point	Figure
				position	suction	NPR	thrust	Tjet			
13	Wing/body	8	None	17	0.551	2	50	479	top/front	86/3	55c
13	Wing/body	10	None	17	0.551	2	50	481	top/front	86/4	55d
13	Wing/body	15	None	17	0.551	2	50	483	top/front	86/5	55e
13	Wing/body	20	None	17	0.551	2	50	485	top/front	86/6	55f
13	Wing/body	30	None	17	0.551	2	50	487	top/front	86/7	55g
13	Wing/body	40	None	17	0.551	2	50	489	top/front	86/8	55h
13	Wing/body	4	Box 12/21	17	0.551	2	50	509	top/front	87/1	56a
13	Wing/body	6	Box 12/21	17	0.551	2	50	510	top/front	87/2	56b
13	Wing/body	8	Box 12/21	17	0.551	2	50	510	top/front	87/3	56c
13	Wing/body	10	Box 12/21	17	0.551	2	50	511	top/front	87/4	56d
13	Wing/body	15	Box 12/21	17	0.551	2	50	511	top/front	87/5	56e
13	Wing/body	30	Box 12/21	17	0.551	2	50	511	top/front	87/7	56f
13	Wing/body	40	Box 12/21	17	0.551	2	50	511	top/front	87/8	56g

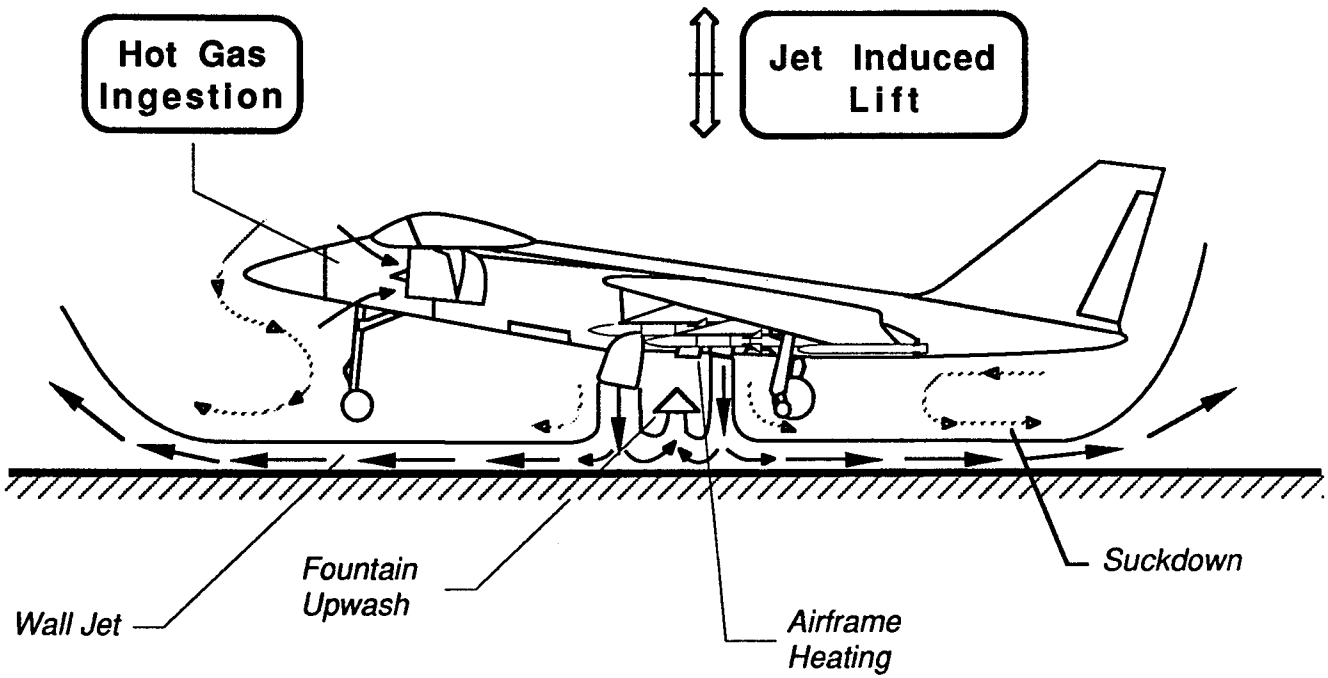

Figure 1. General STOVL aircraft in ground effect.

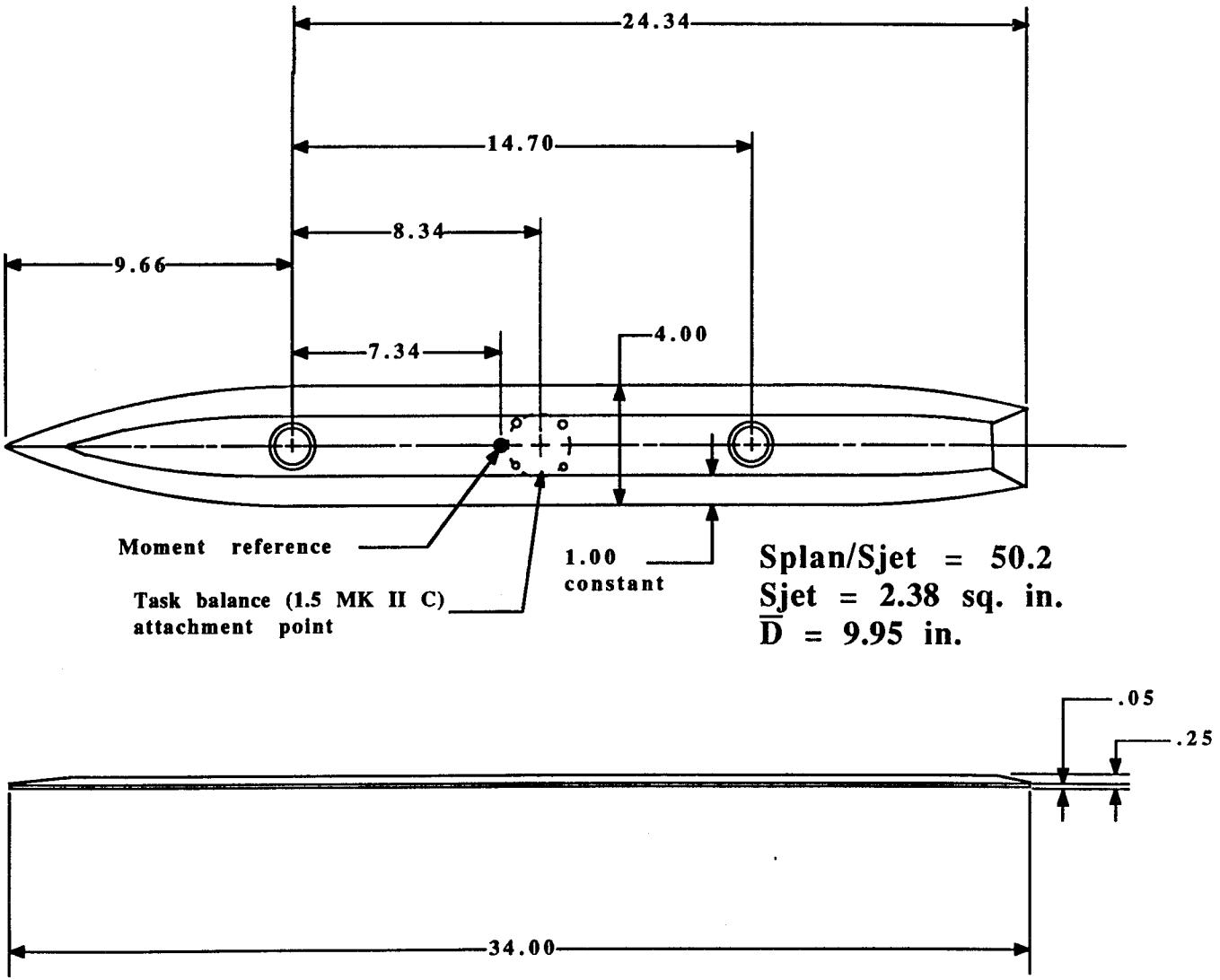

Figure 2. Flat plate body model. Dimensions in inches.

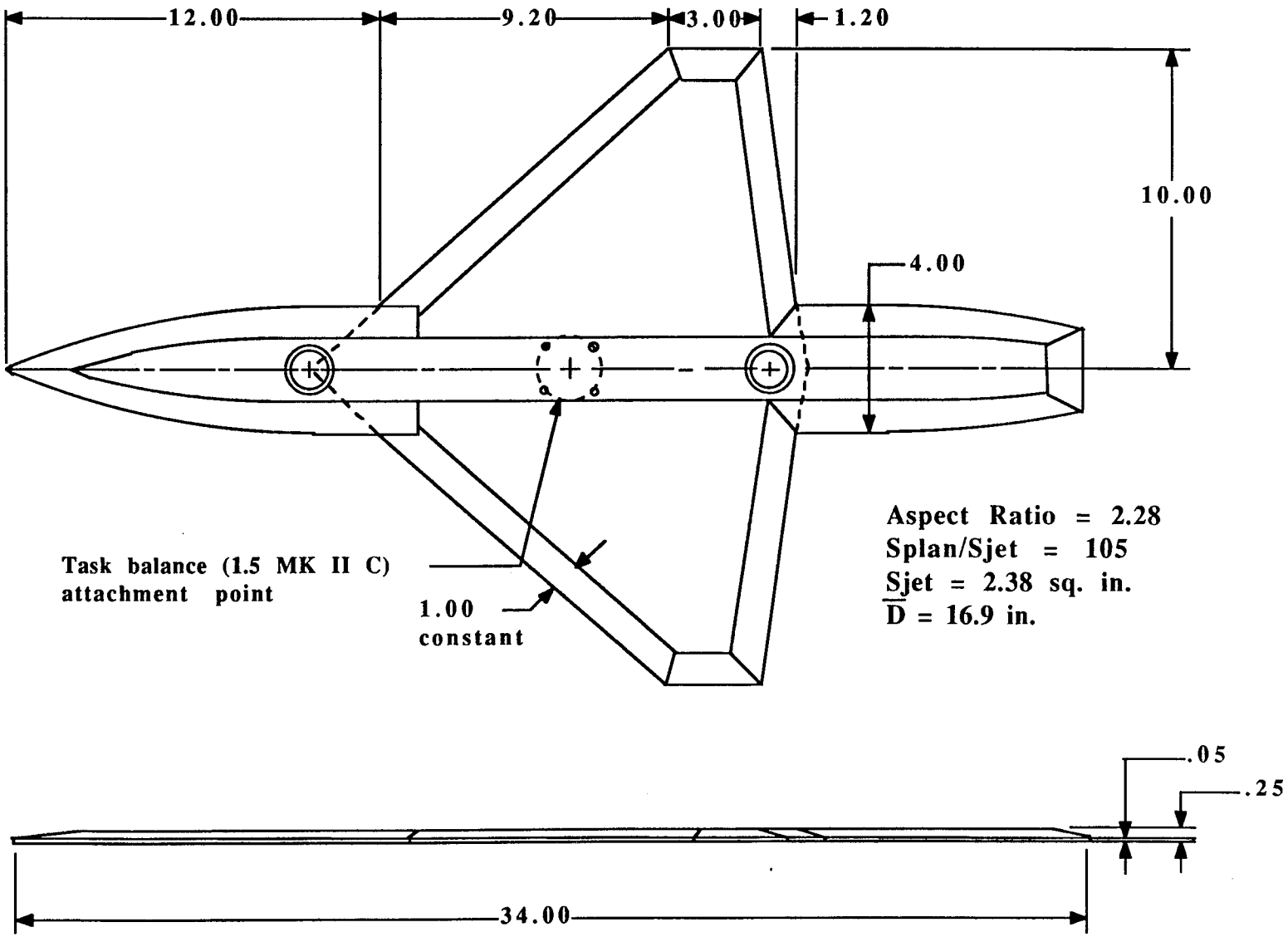

Figure 3. Flat plate wing/body model. Dimensions in inches.

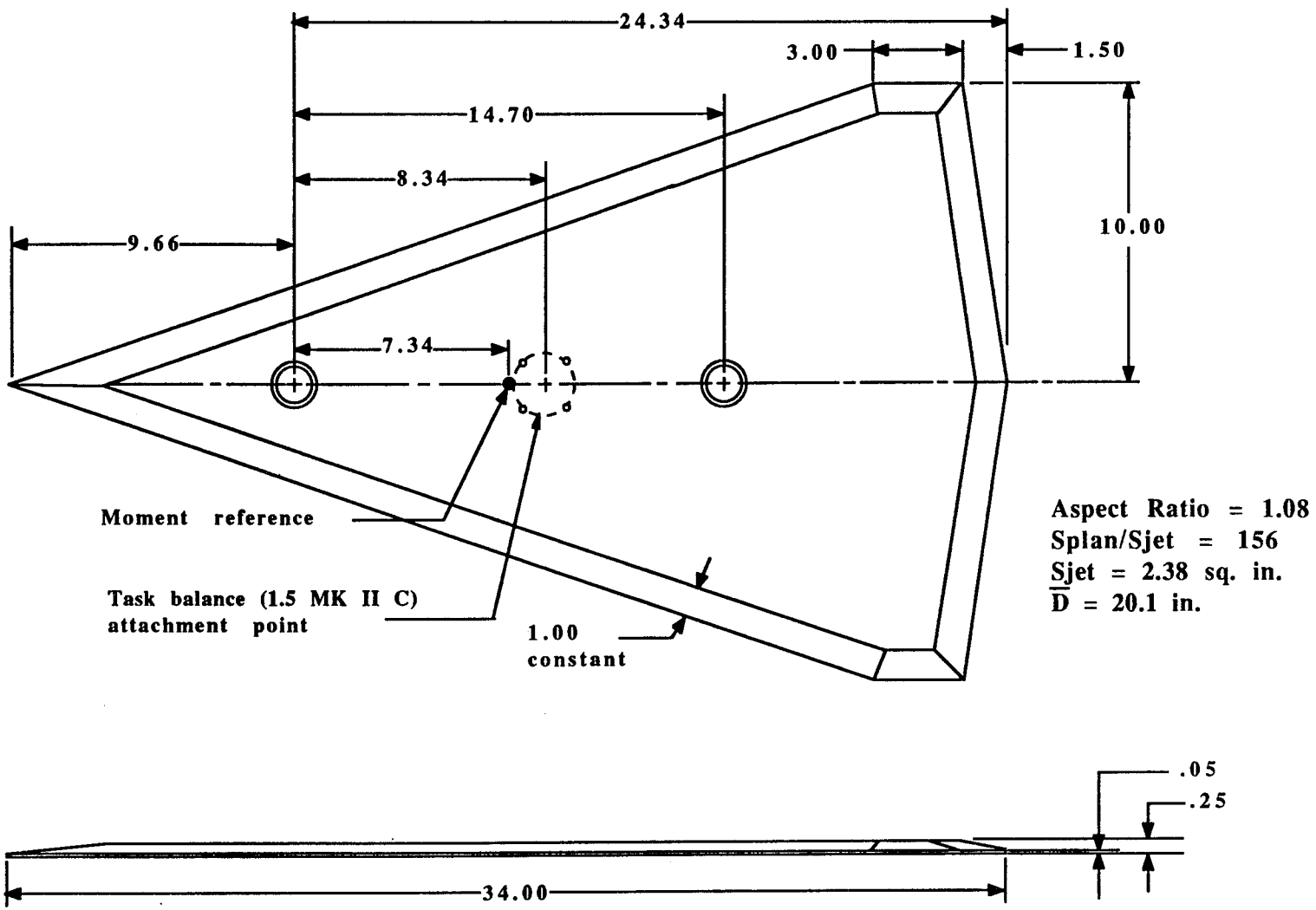

Figure 4. Flat plate delta wing model. Dimensions in inches.

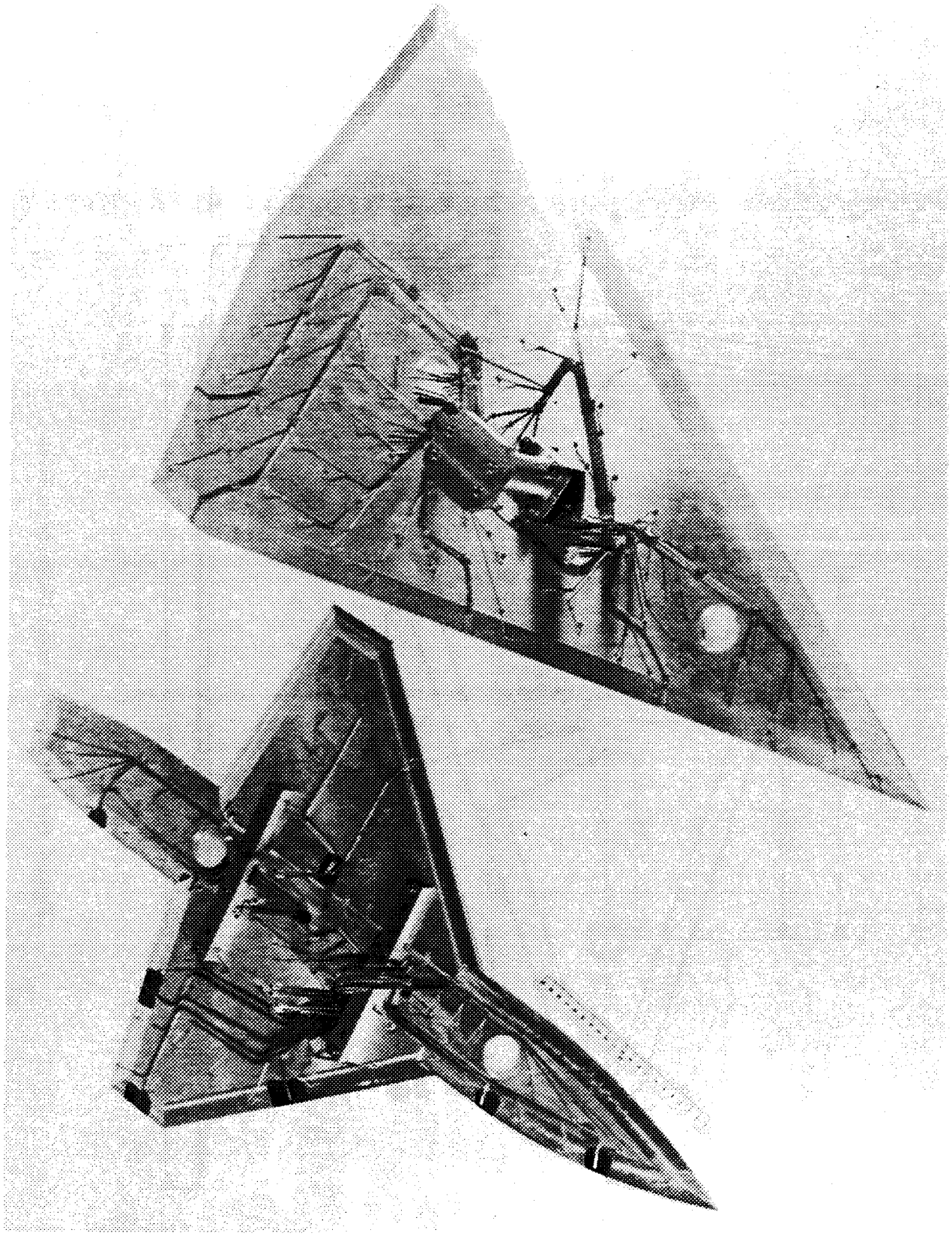

Figure 5. Photograph of the wing/body and delta wing models.

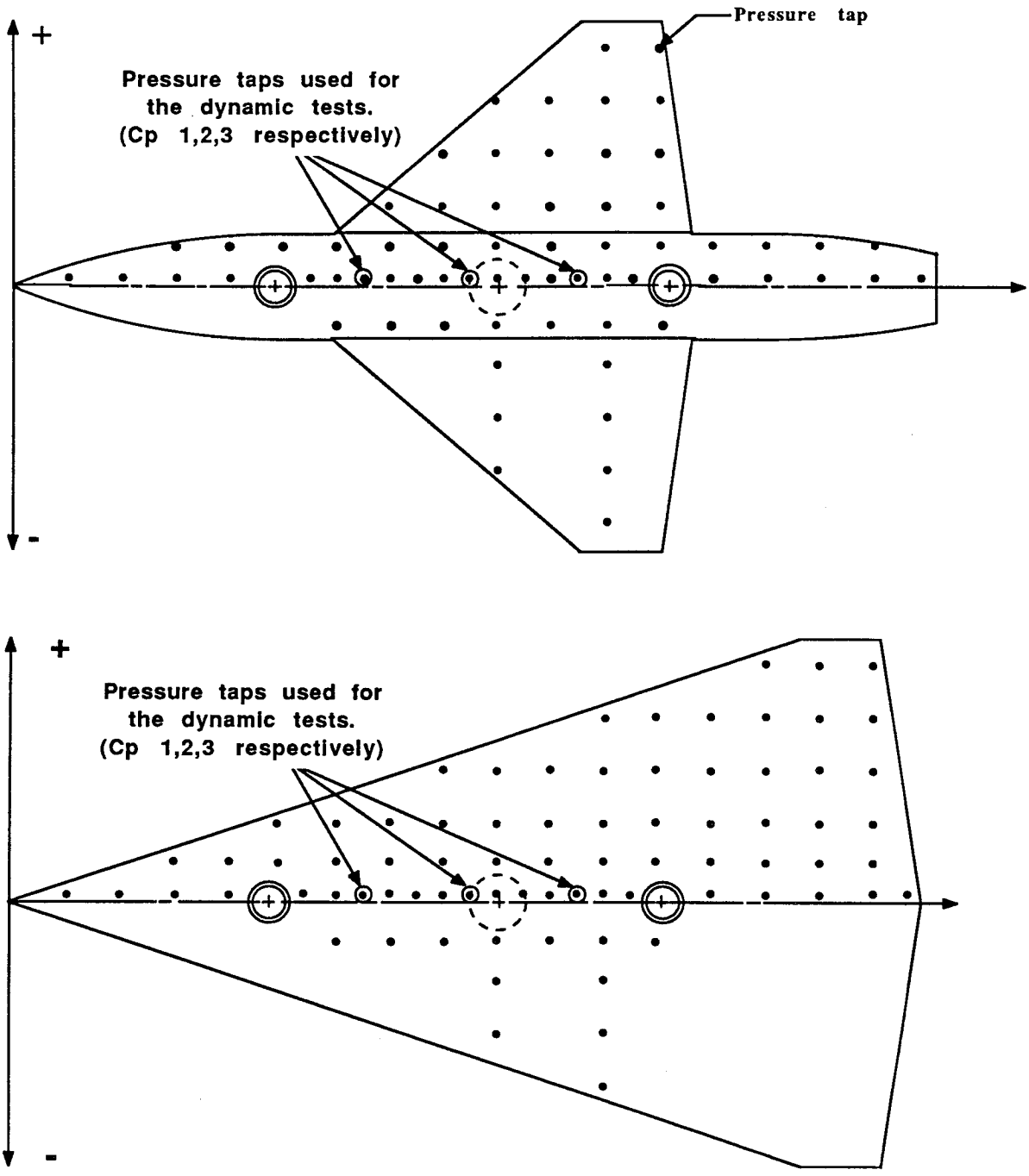

Figure 6. Flat plate wing/body and delta wing pressure tap locations.

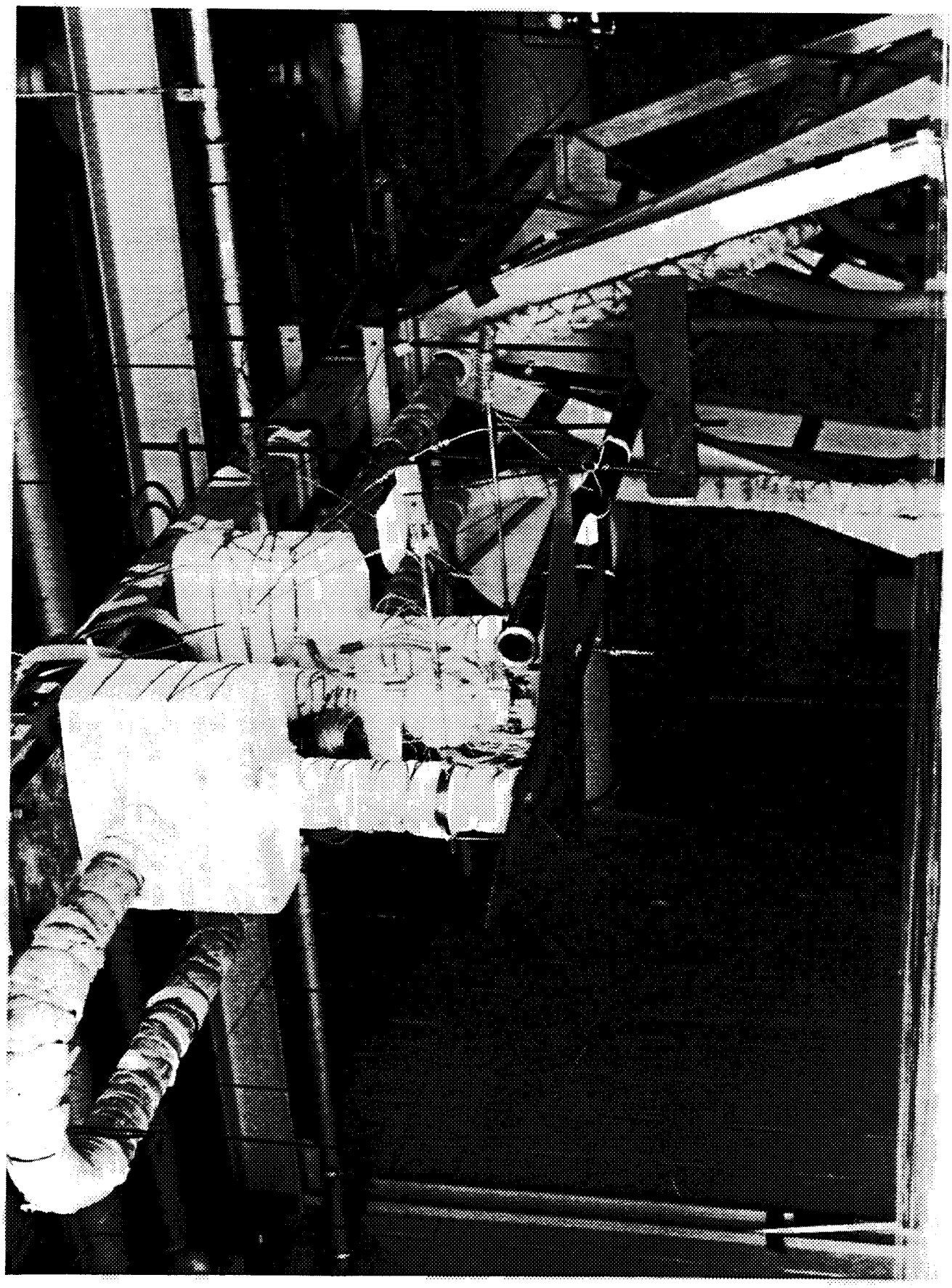

Figure 7. Photograph of the wing/body model installed on the Hover Test Rig.

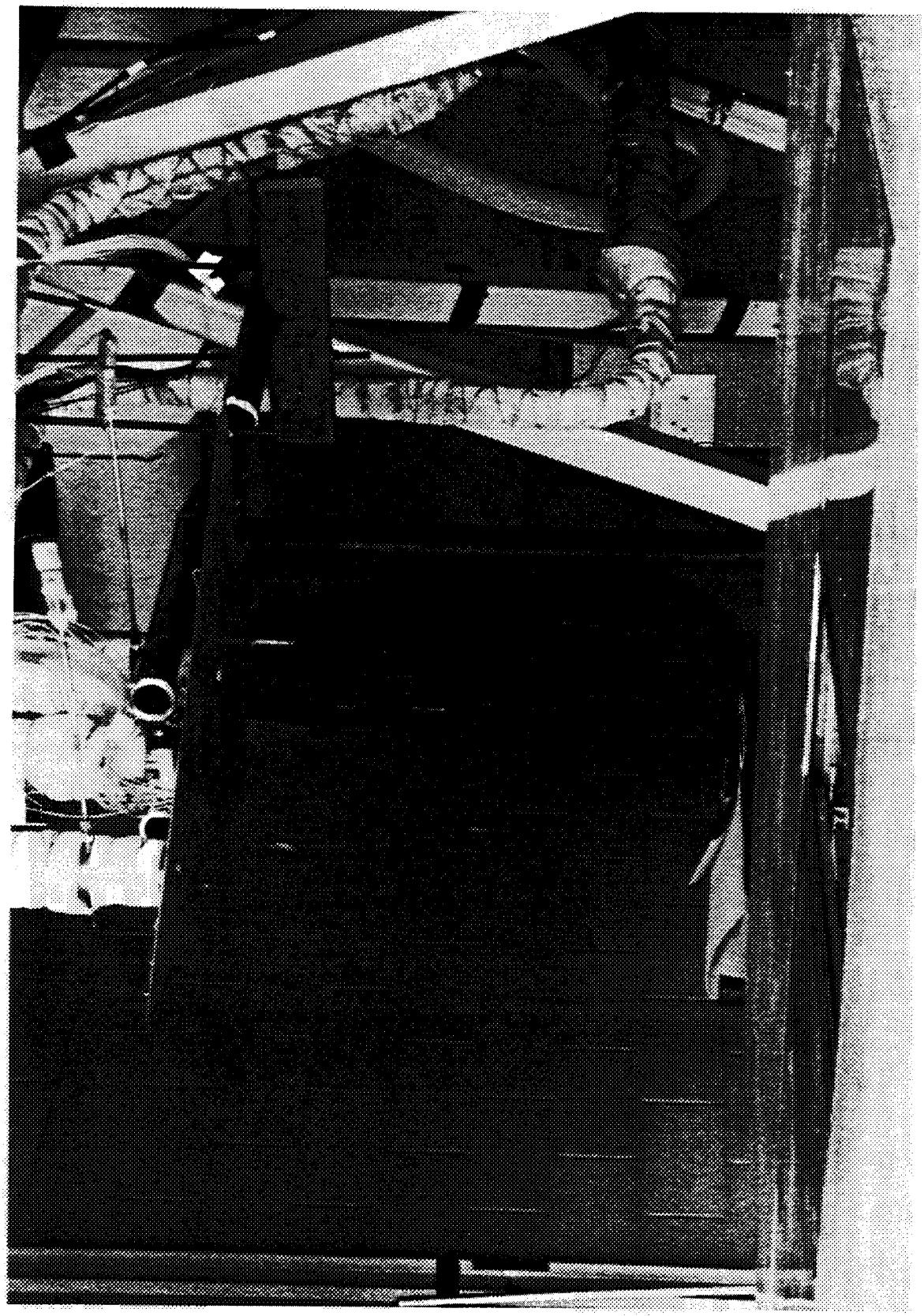

Figure 8. Photograph of the delta wing model installed on the Hover Test Rig.

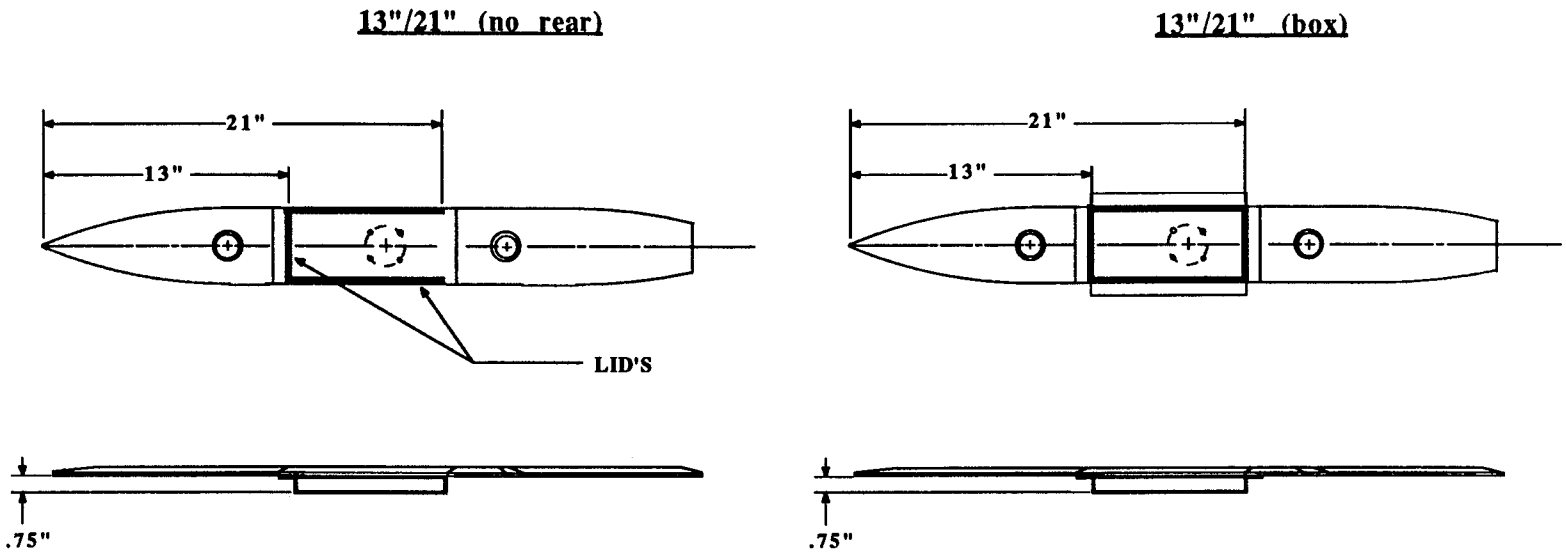

Figure 9. Lift improvement device configurations investigated for the body alone.

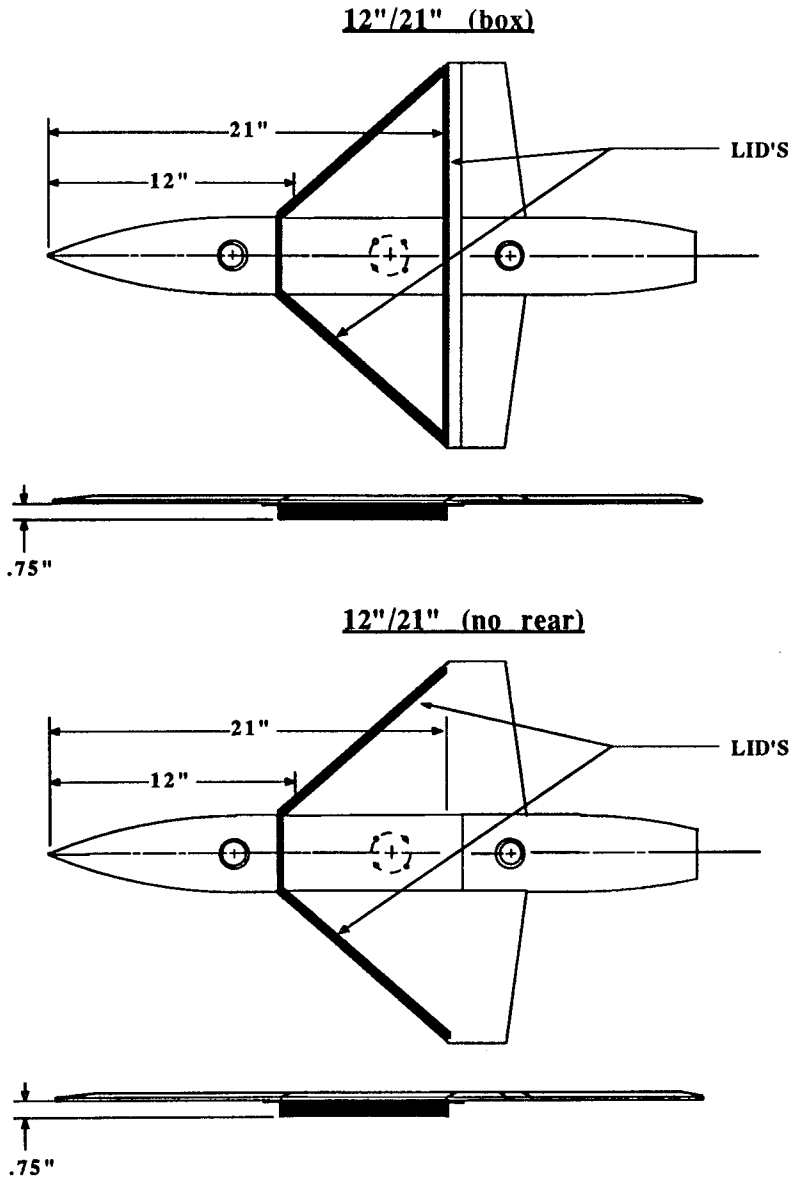

Figure 10. Wing/body lift improvement device configurations.

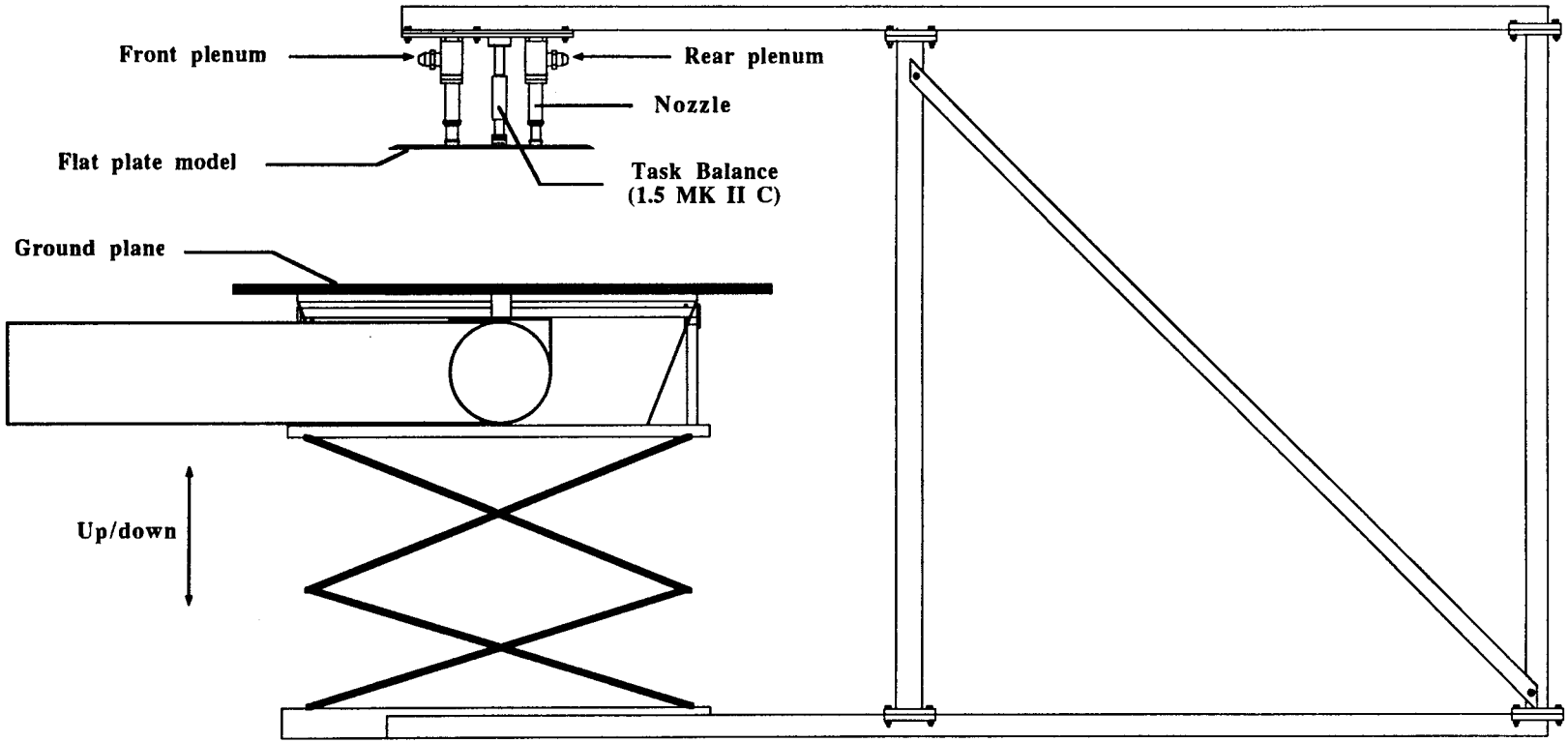

Figure 11. General arrangement of the Hover Test Rig.

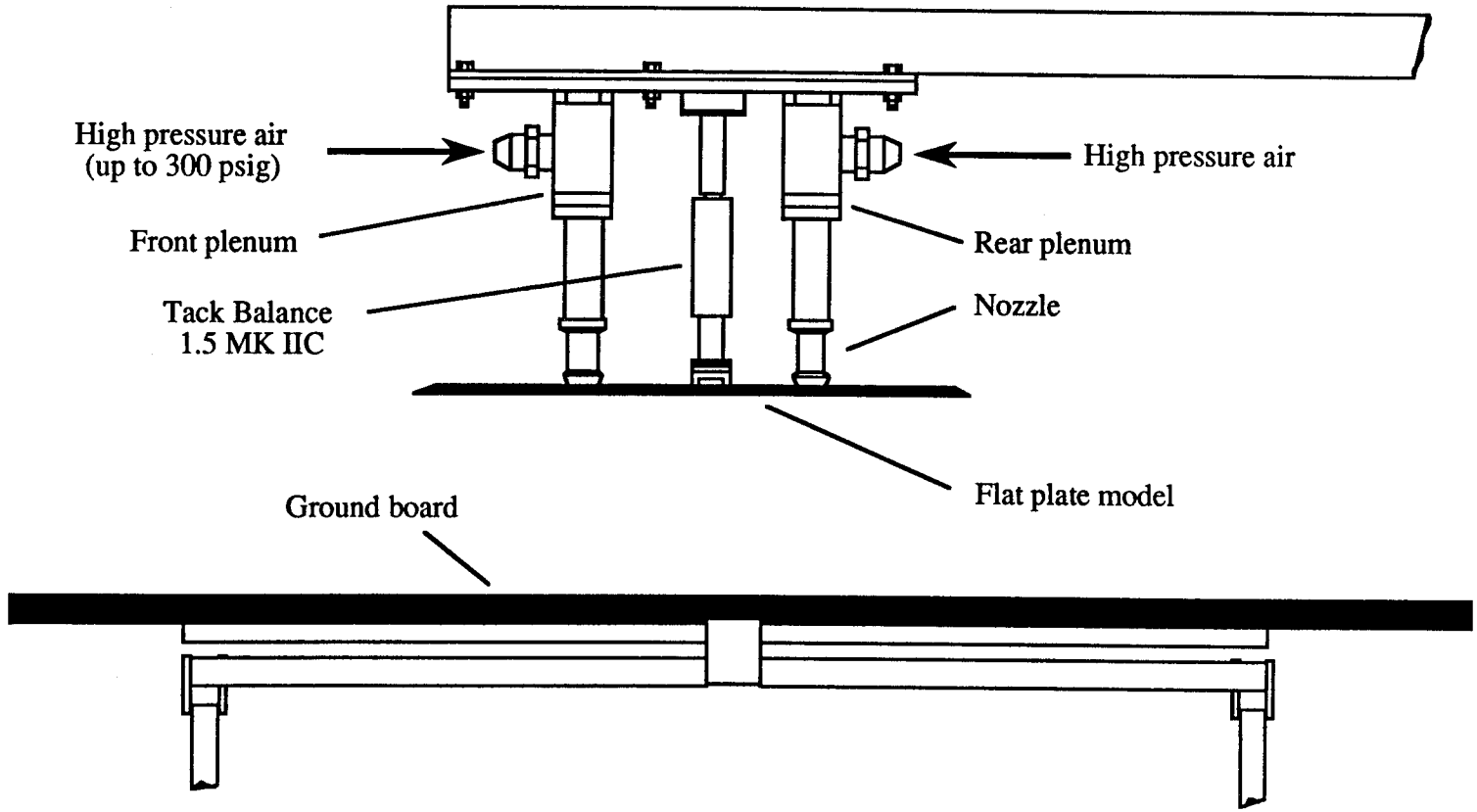

Figure 12. Detail of the model setup on the Hover Test Rig.

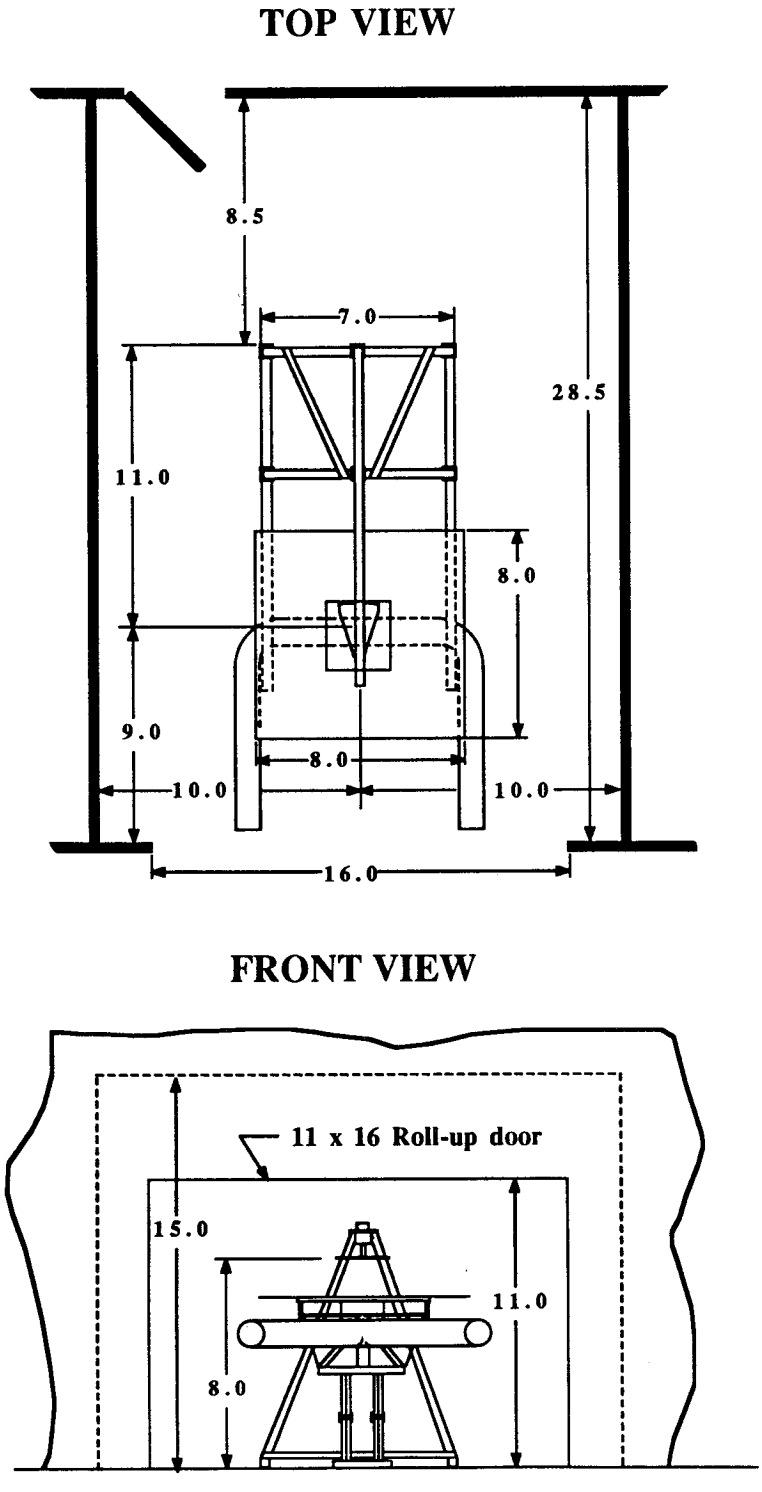

Figure 13. Location of the Hover Test Rig in the Rye Canyon test cell.

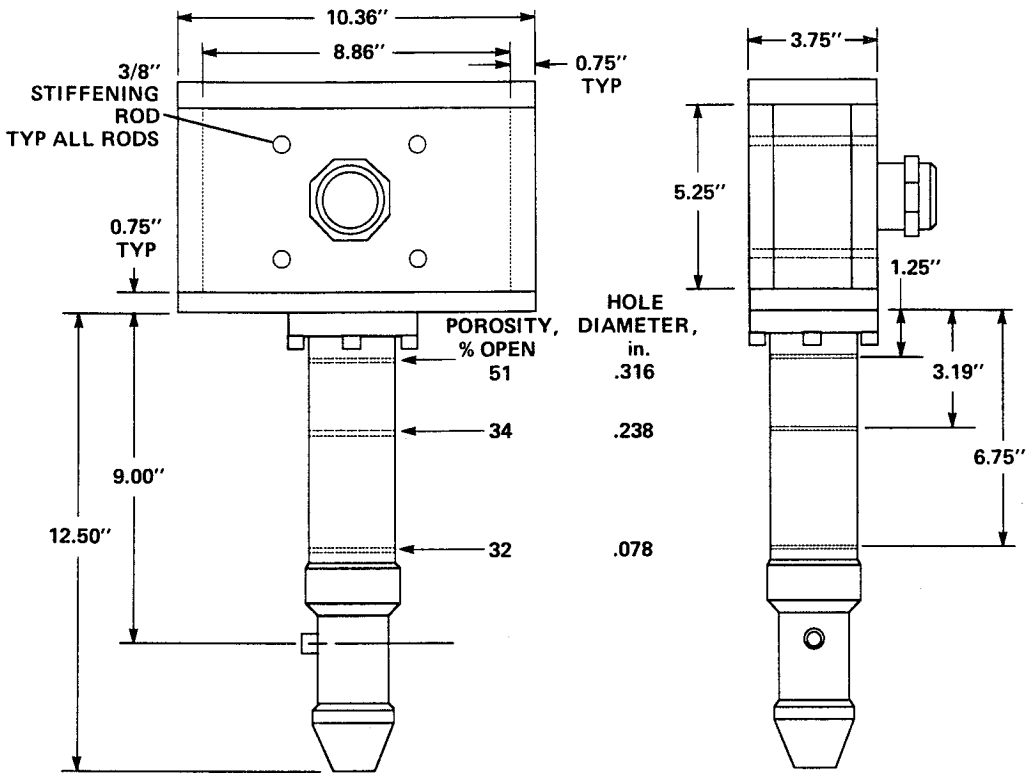

Figure 14. Details of the plenum and nozzle arrangement used in the tests.

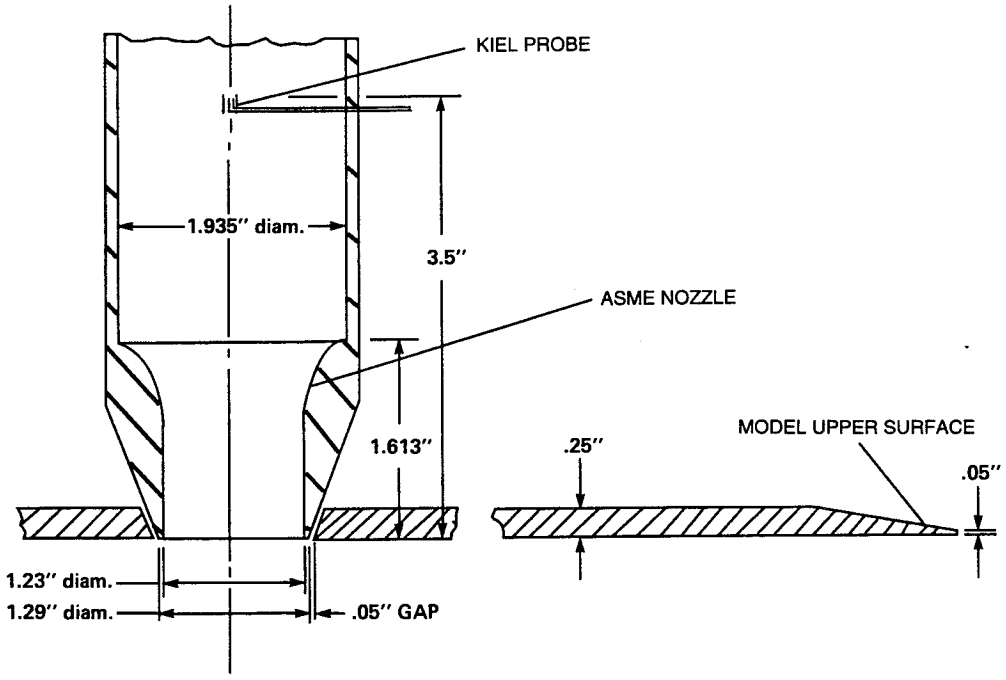

Figure 15. Details of the arrangement between the Kiel probe, nozzle, and model.

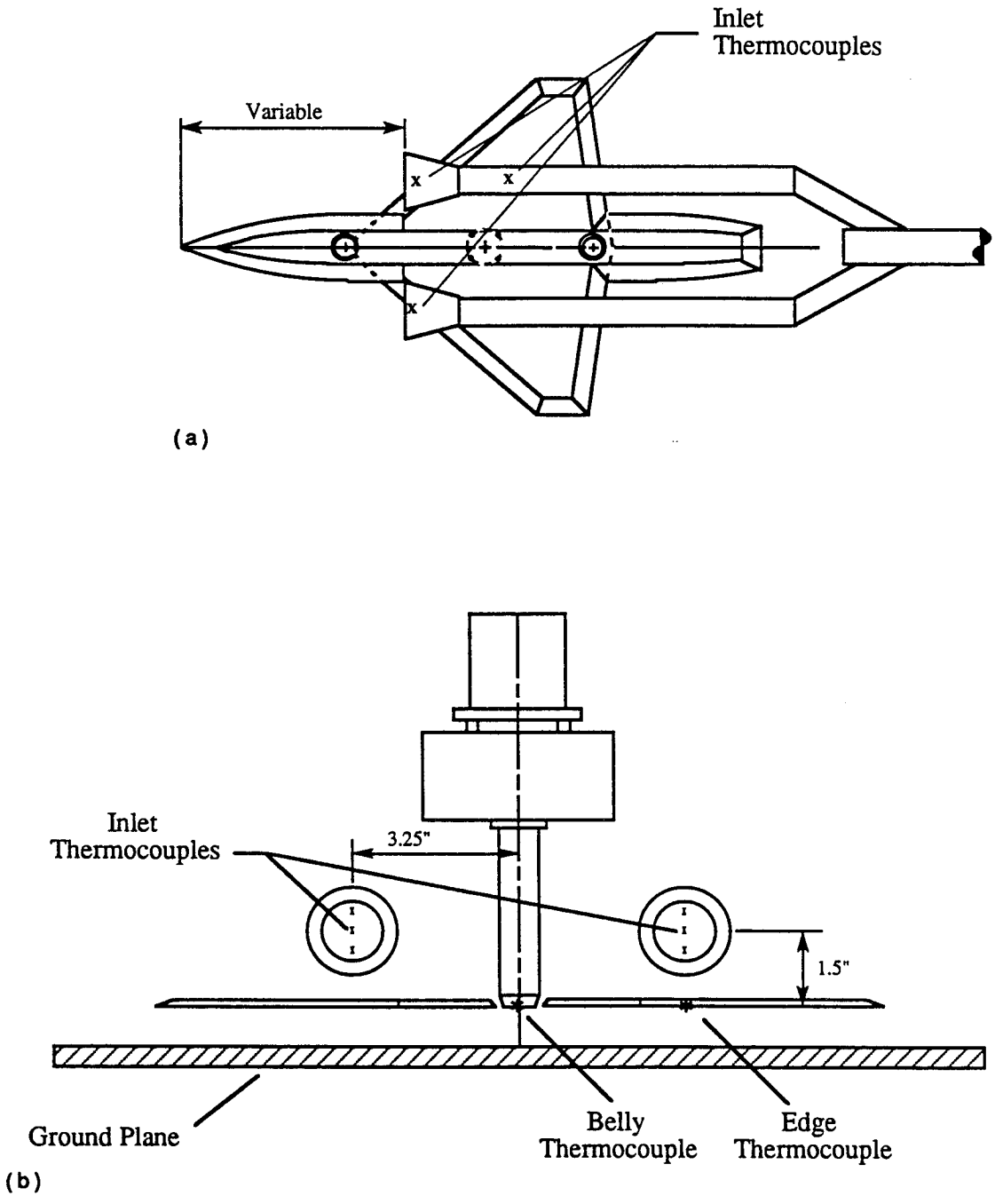

Figure 16(a). Inlet layout with respect to the model and nozzles, top view, (b) inlet layout with respect to the model and nozzles, front view.

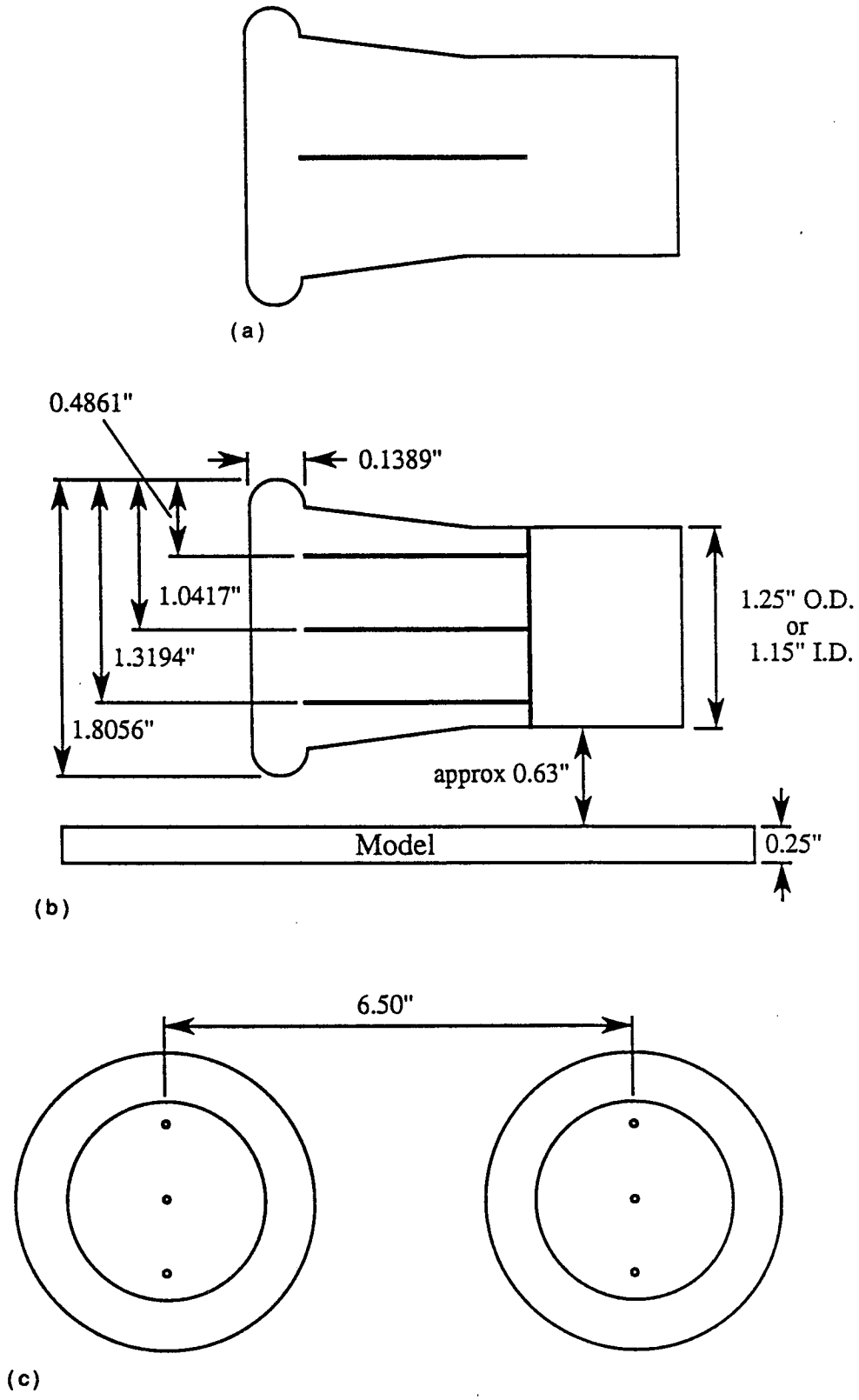

Figure 17(a). Inlet system detail, top view, (b) inlet system detail, side view, (c) inlet system detail, front view.

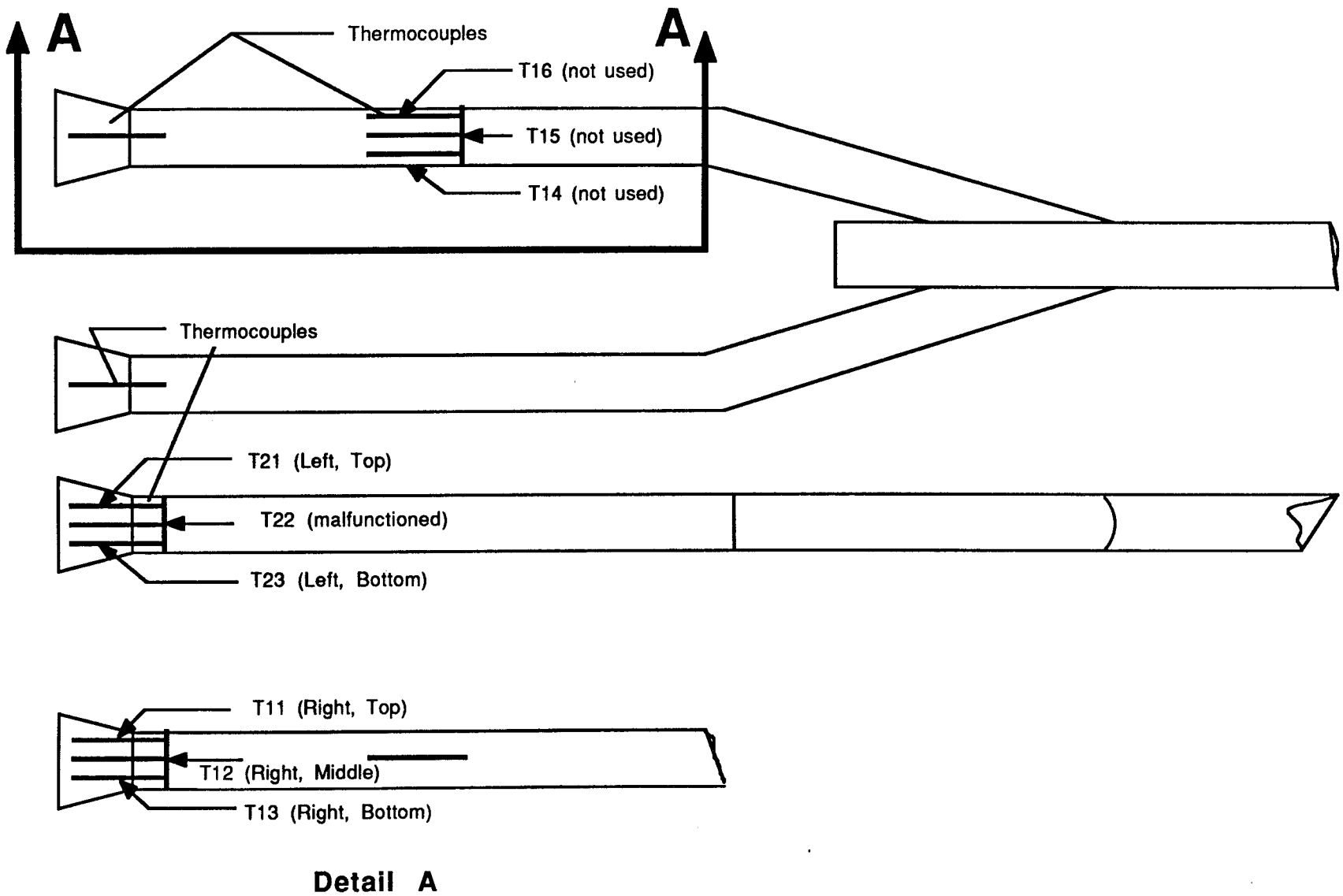

Figure 18. Inlet Thermocouple locations.

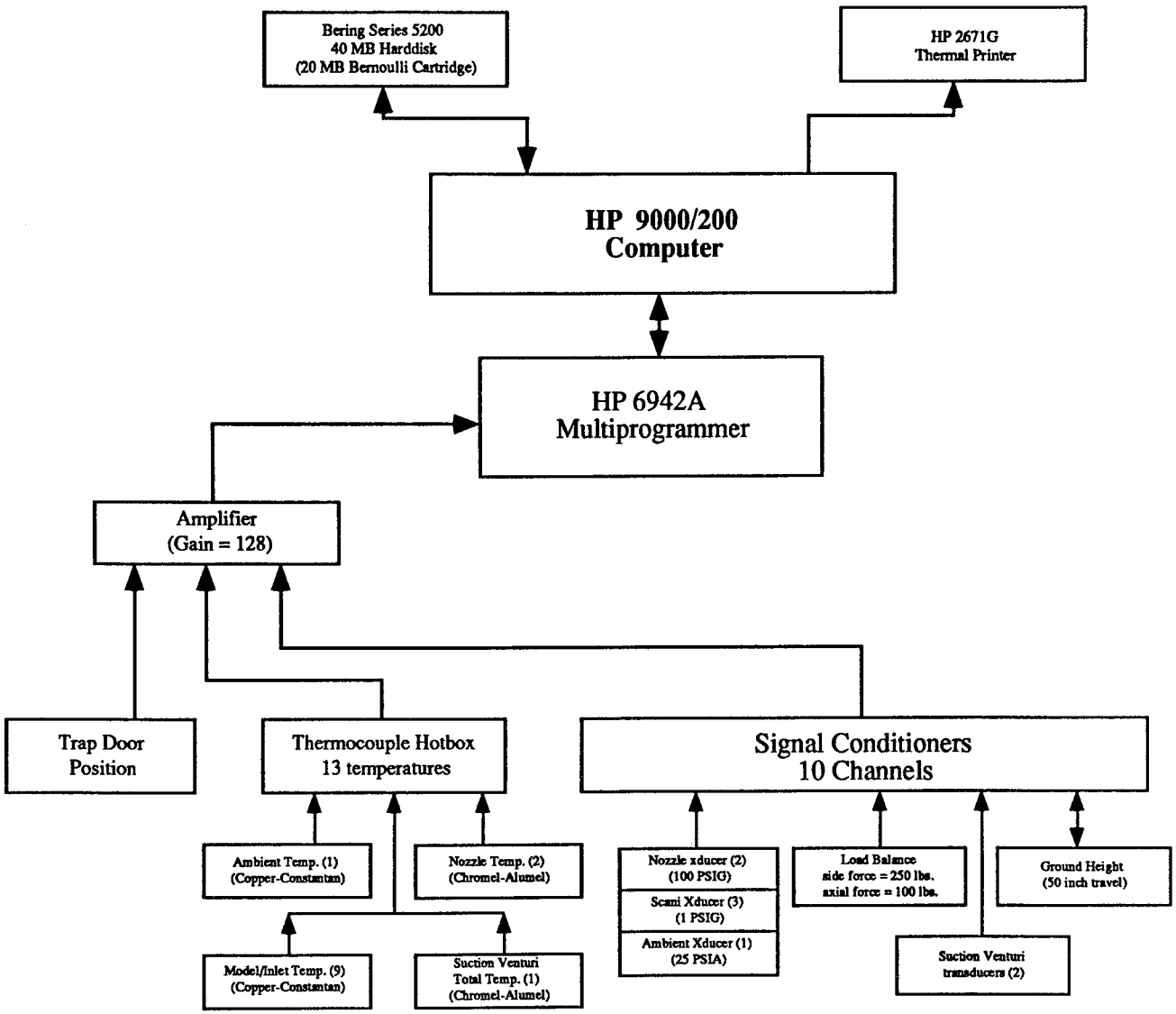

Figure 19. Instrumentation and data acquisition system diagram.

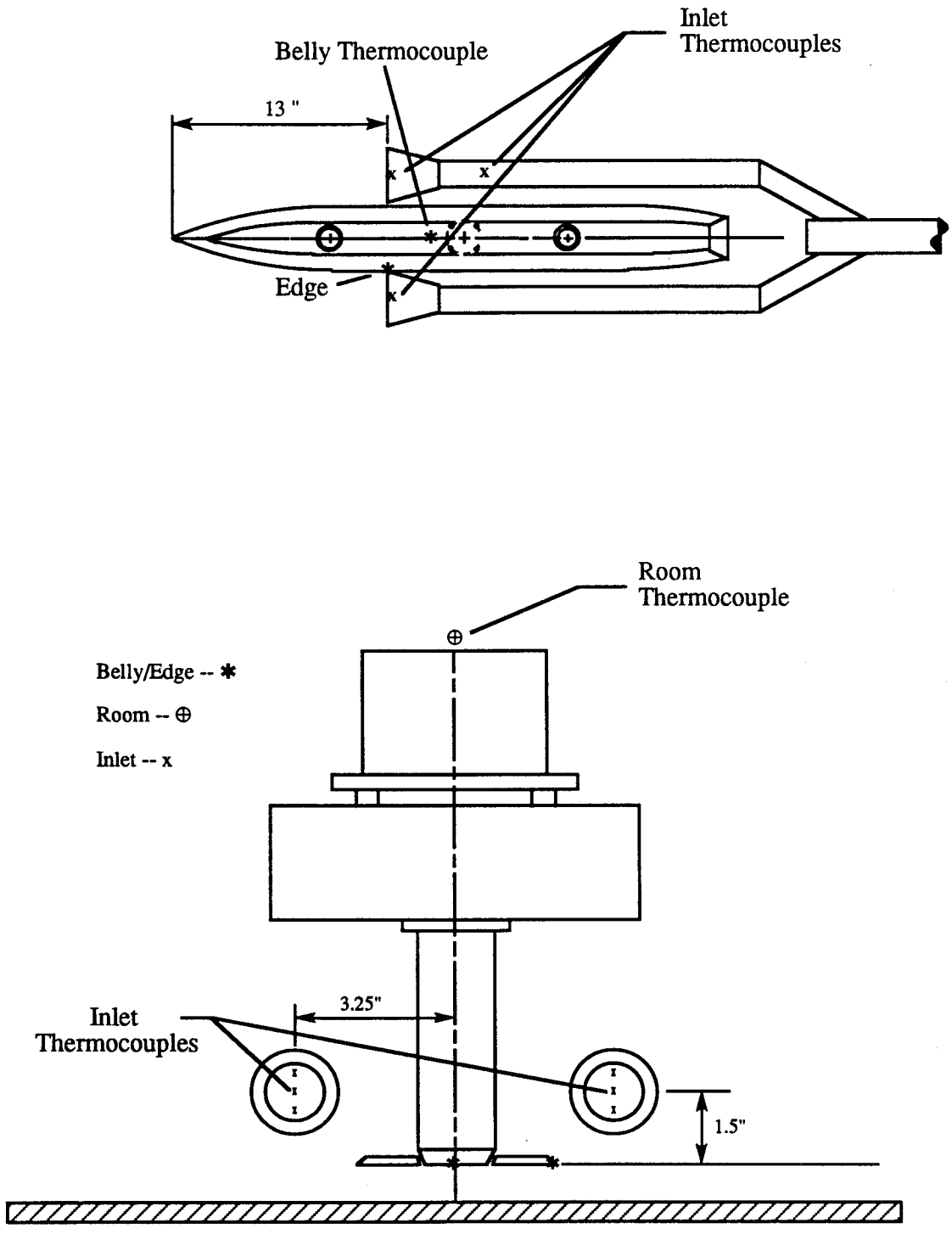

Figure 20. Locations of model thermocouples for data set 1.

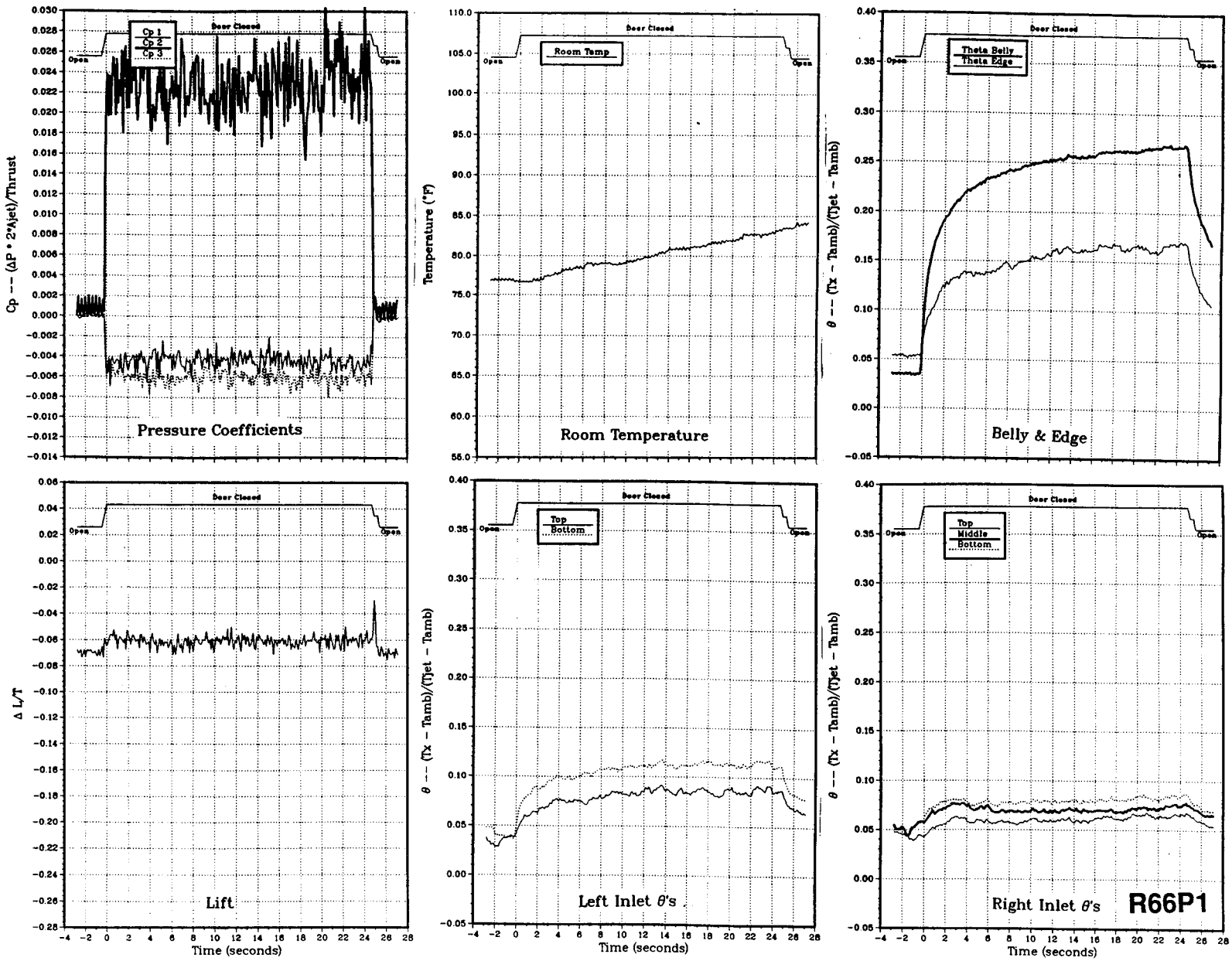

Figure 21(a). Body alone, no LIDs, NPR = 2.0, thrust = 50 lb, height = 4 in., Tjet = 470 °F, inlet position = 13 in., no field temperatures.

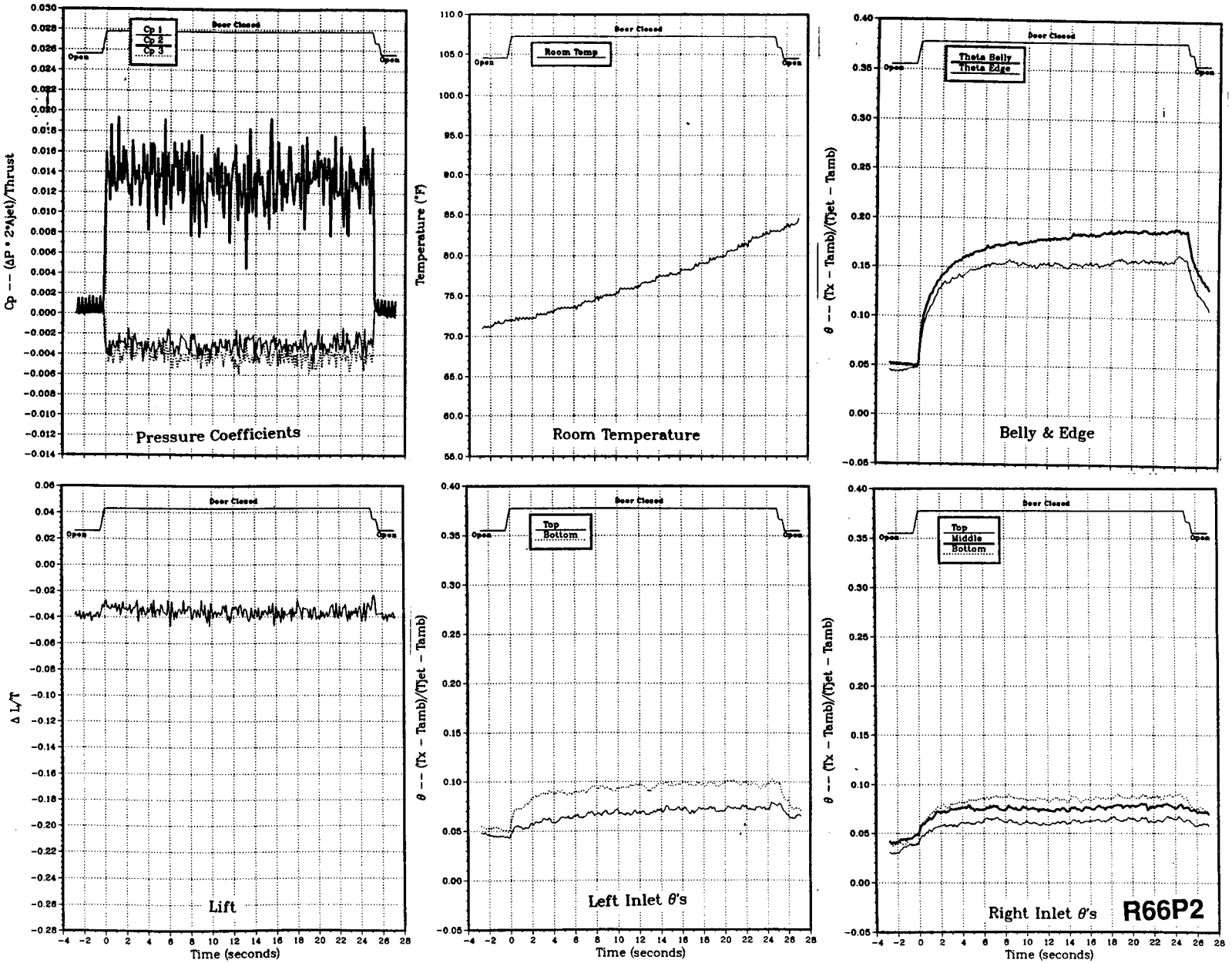

Figure 21(b). Body alone, no LIDs, NPR = 2.0, thrust = 50 lb, height = 6 in., Tjet = 475 °F, inlet position = 13 in., no field temperatures.

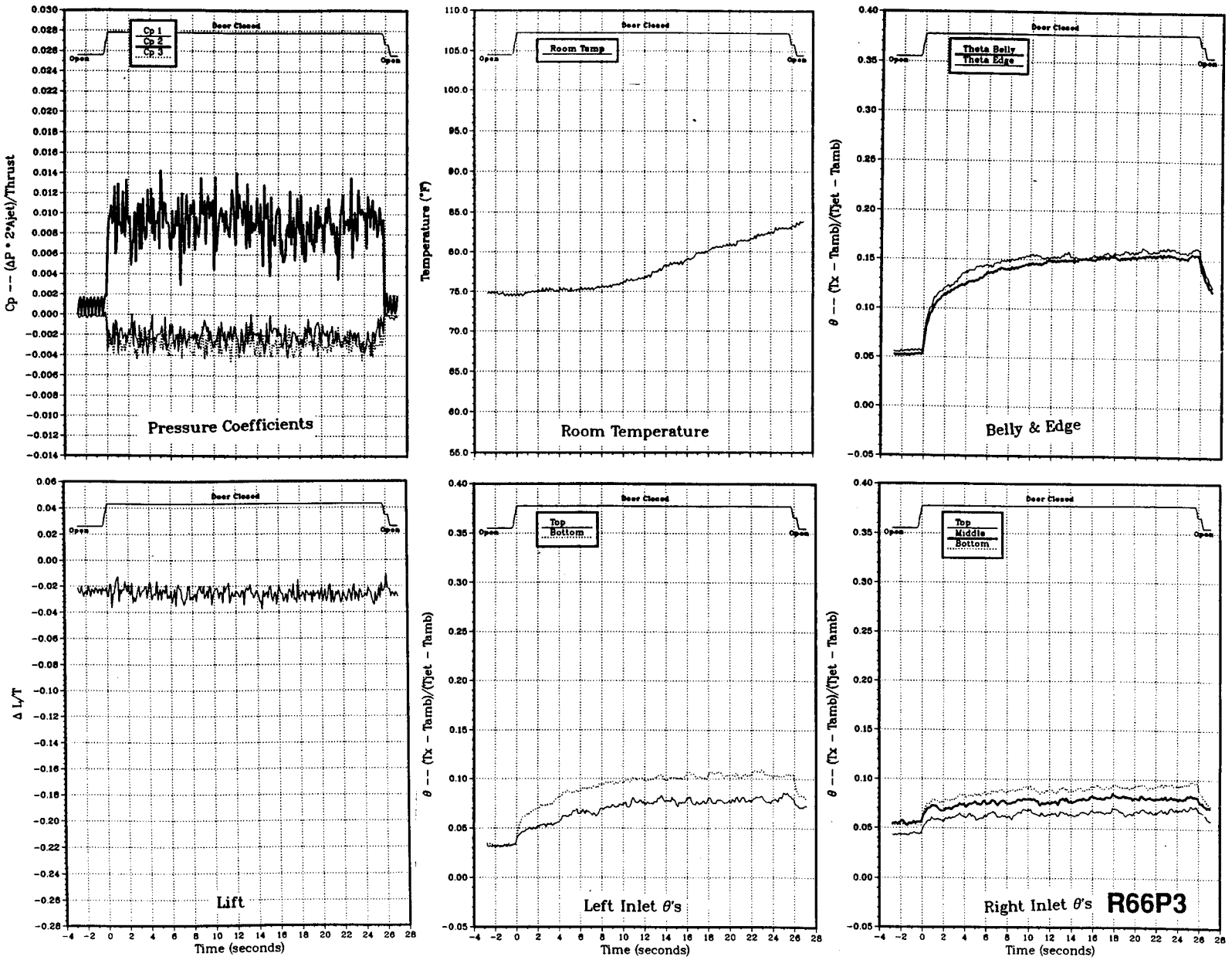

Figure 21(c). Body alone, no LIDs, NPR = 2.0, thrust = 50 lb, height = 8 in., Tjet = 480 °F, inlet position = 13 in., no field temperatures.

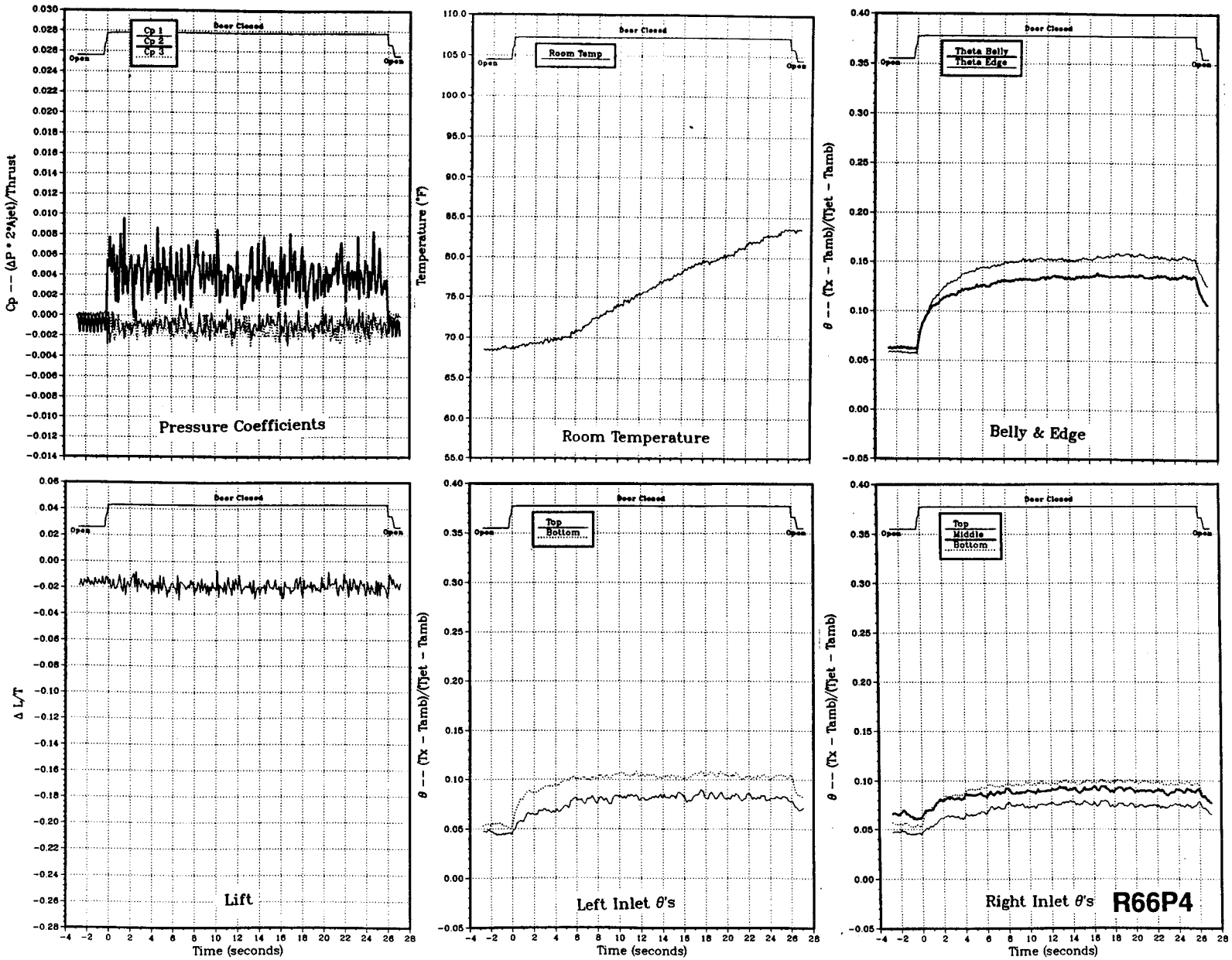

Figure 21(d). Body alone, no LIDs, NPR = 2.0, thrust = 50 lb, height = 10 in., Tjet = 490 °F, inlet position = 13 in., no field temperatures.

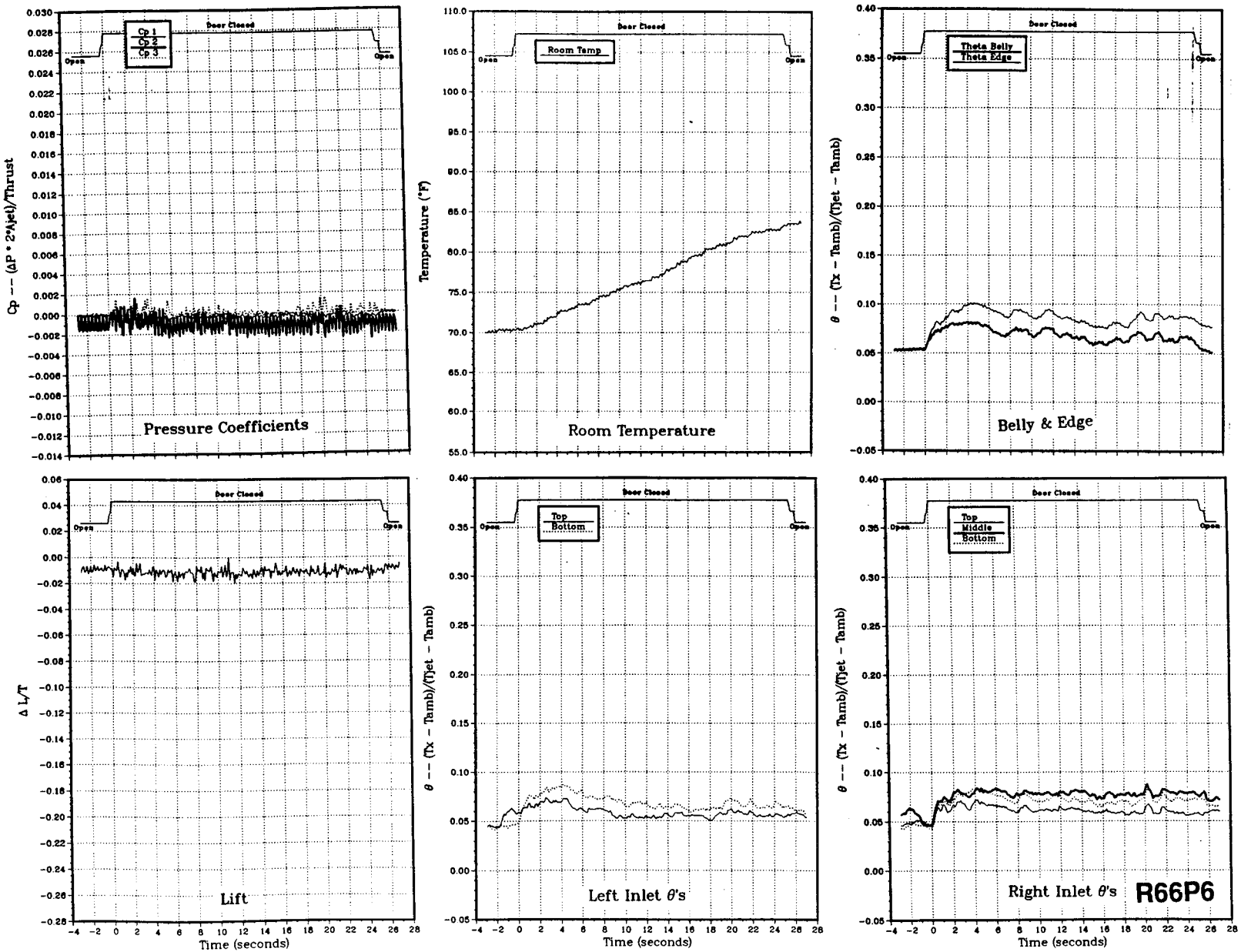

Figure 21(e). Body alone, no LIDs, NPR = 2.0, thrust = 50 lb, height = 20 in., Tjet = 500 °F, inlet position = 13 in., no field temperatures.

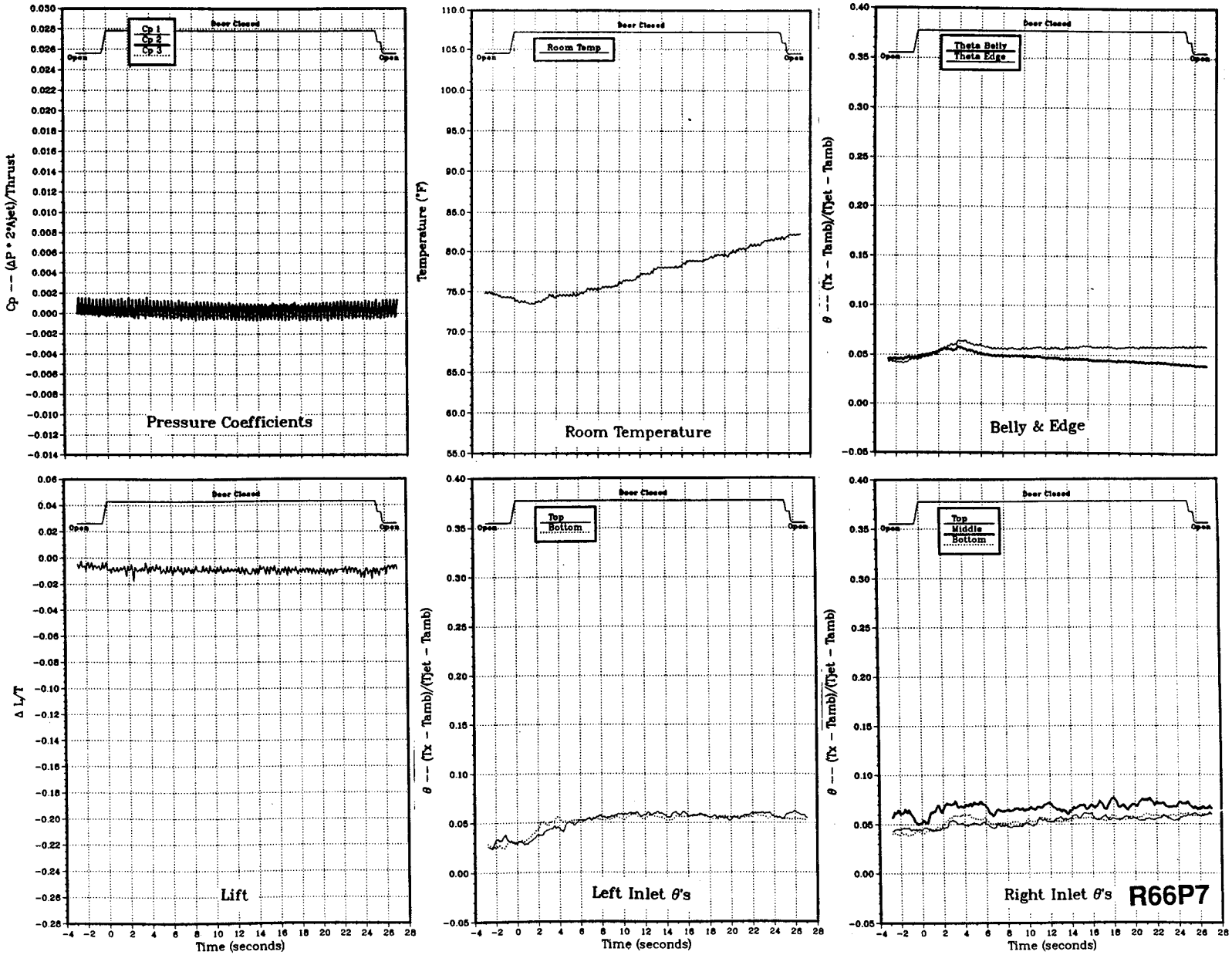

Figure 21(f). Body alone, no LIDs, NPR = 2.0, thrust = 50 lb, height = 30 in., Tjet = 500 °F, inlet position = 13 in., no field temperatures.

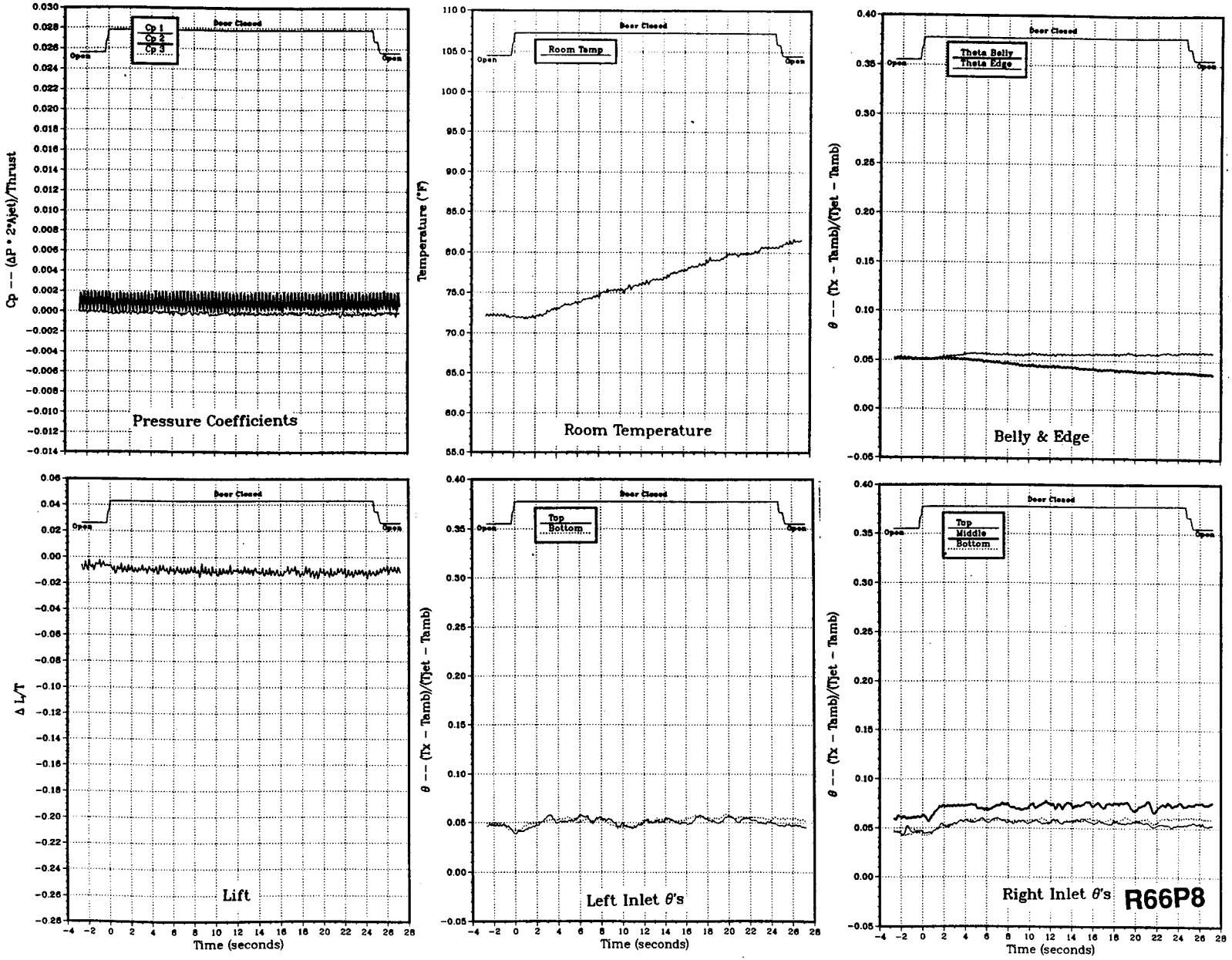

Figure 21(g). Body alone, no LIDs, NPR = 2.0, thrust = 50 lb, height = 40 in., Tjet = 505 °F, inlet position = 13 in., no field temperatures.

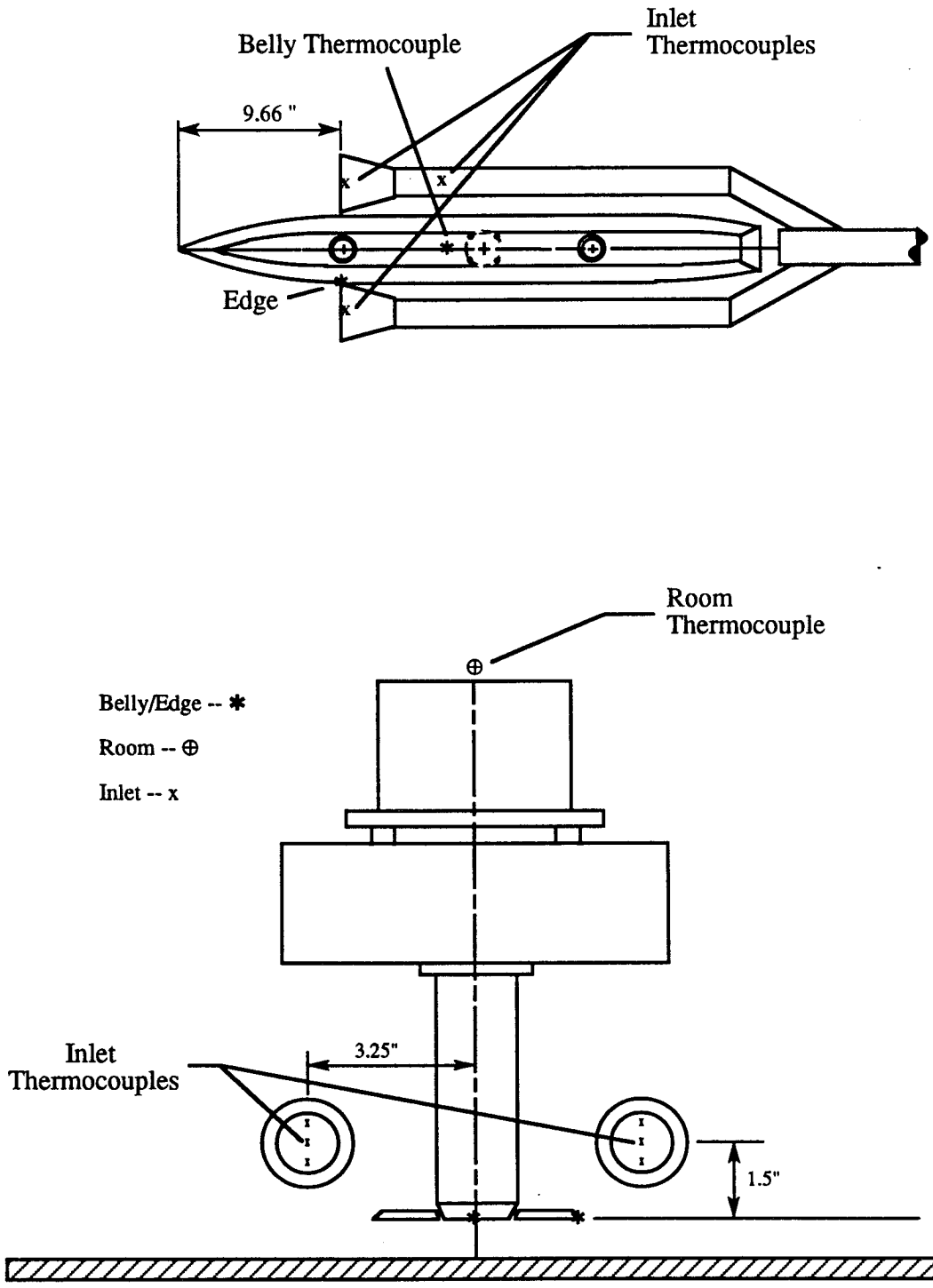

Figure 22. Locations of model thermocouples for data set 2.

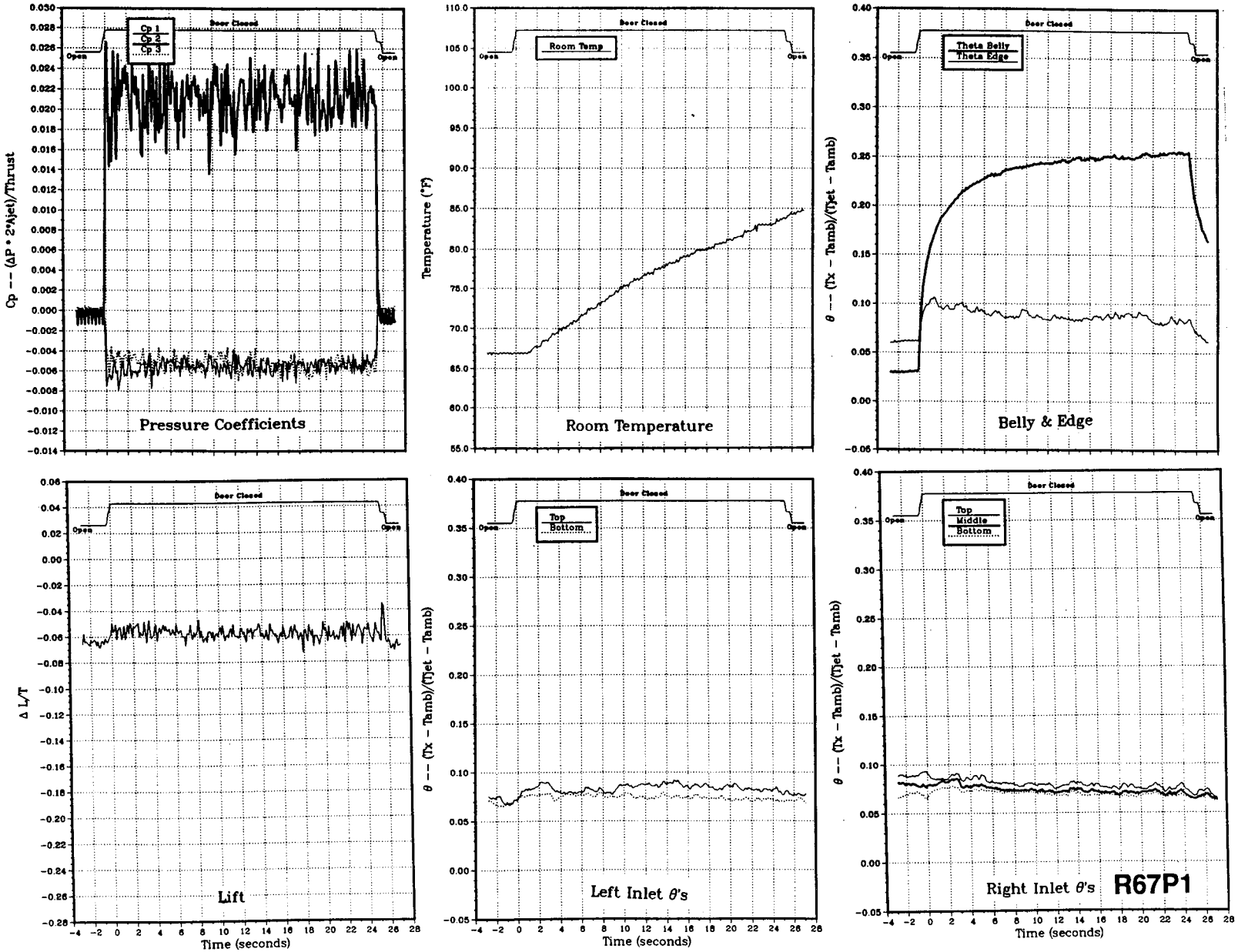

Figure 23(a). Body alone, no LIDs, NPR = 2.0, thrust = 50 lb, height = 4 in., Tjet = 485 °F, inlet position = 9.66 in., no field temperatures.

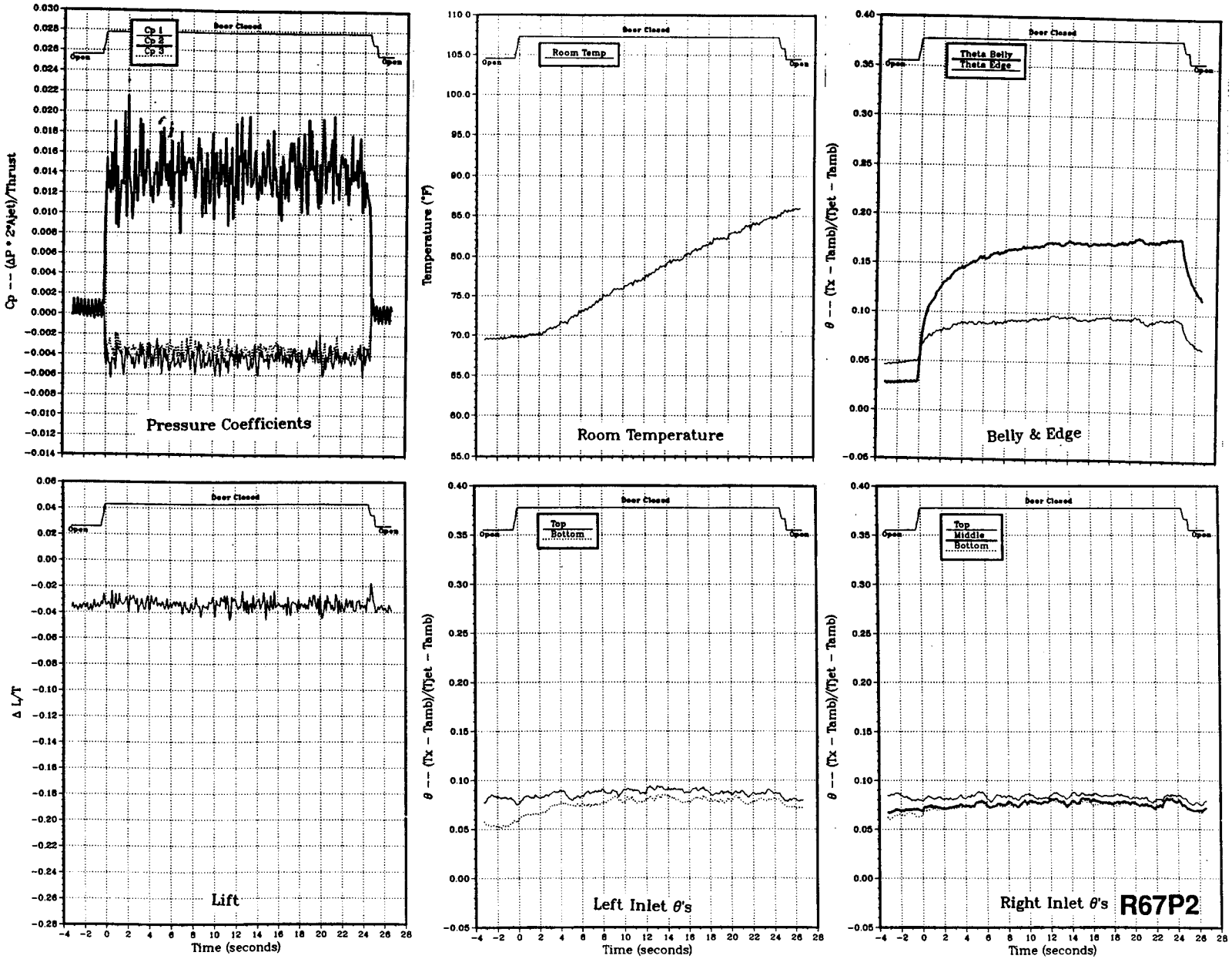

Figure 23(b). Body alone, no LIDs, NPR = 2.0, thrust = 50 lb, height = 6 in., Tjet = 500 °F, inlet position = 9.66 in., no field temperatures.

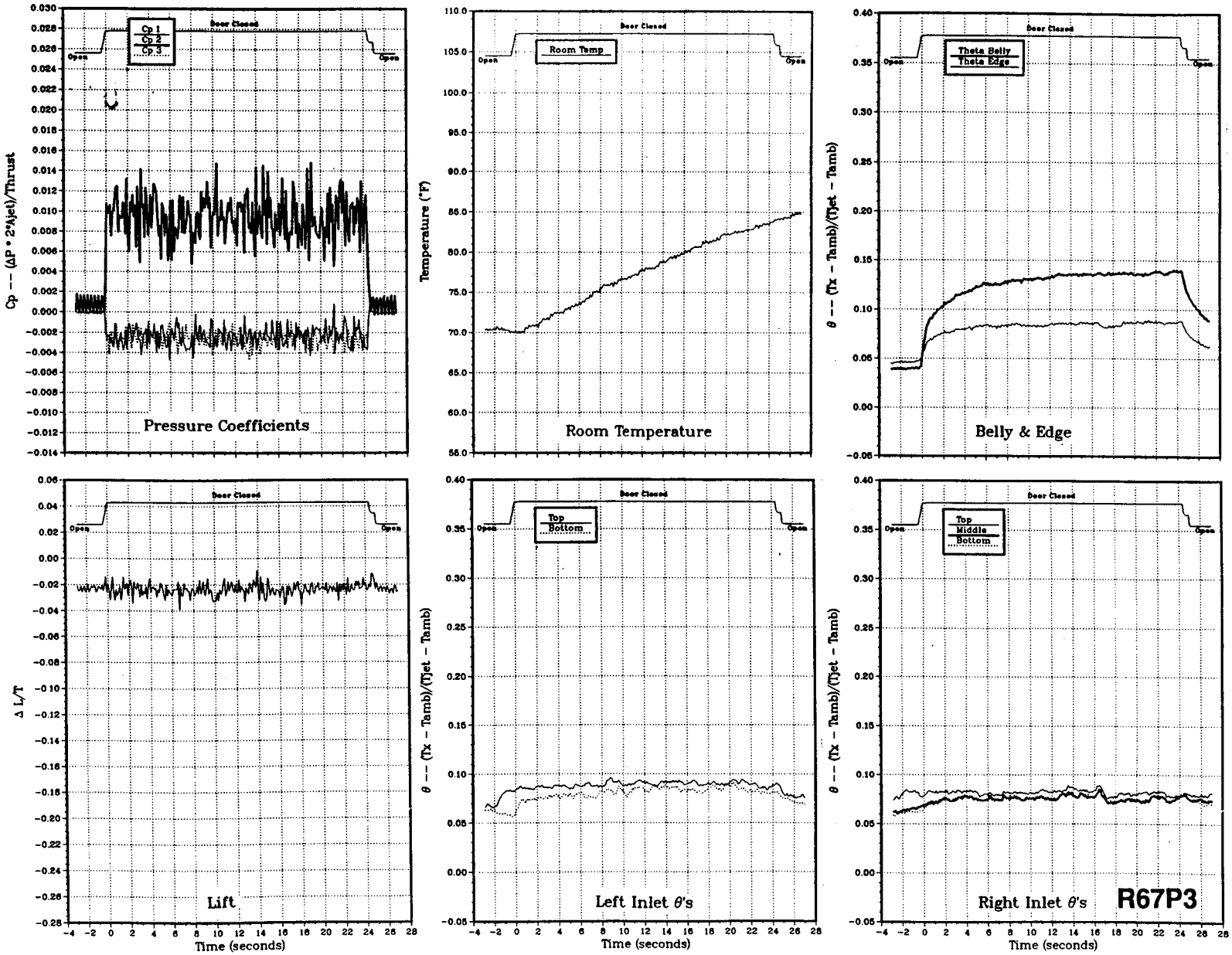

Figure 23(c). Body alone, no LIDs, NPR = 2.0, thrust = 50 lb, height = 8 in., Tjet = 505 °F, inlet position = 9.66 in., no field temperatures.

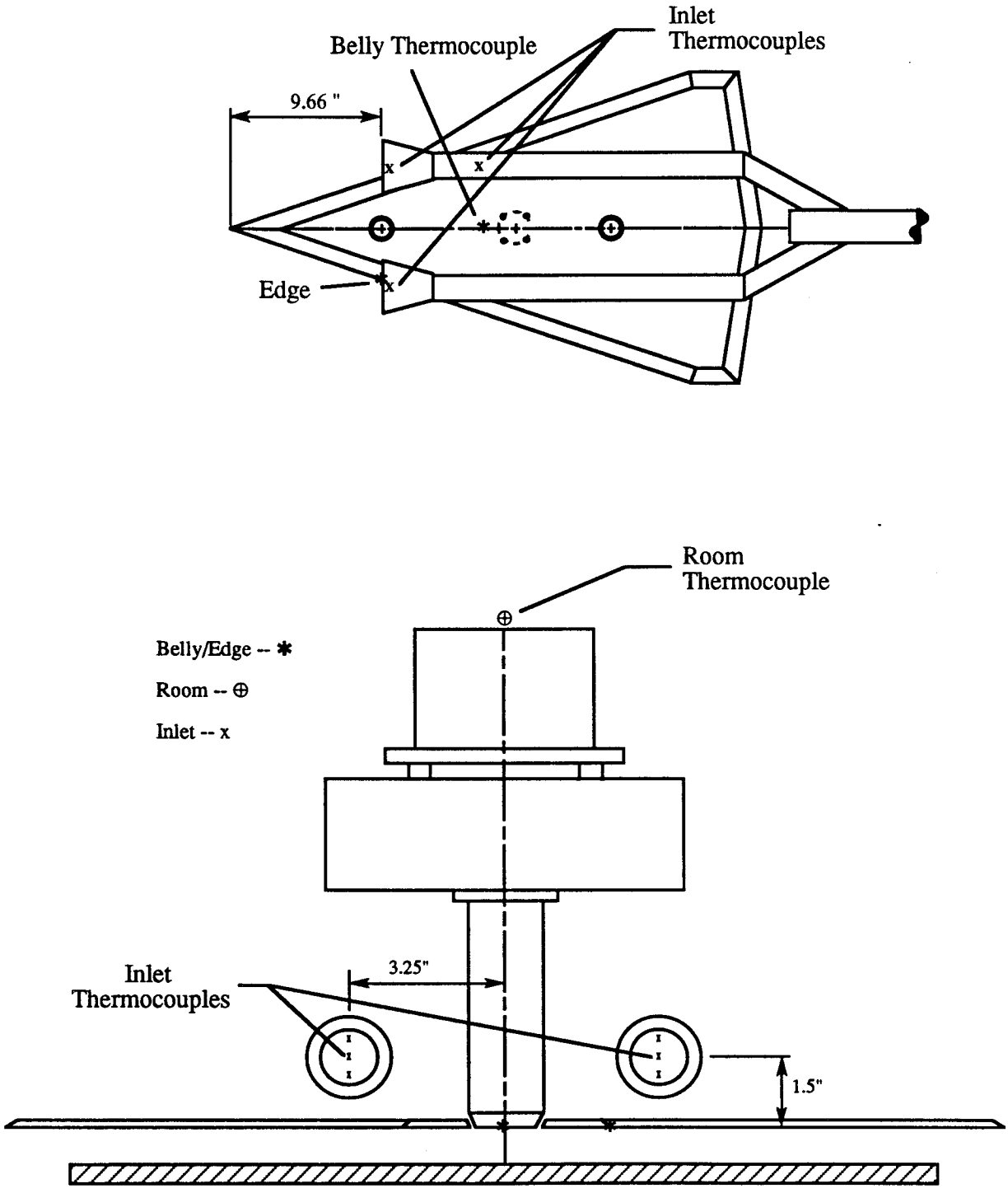

Figure 24. Locations of model thermocouple for data set 3.

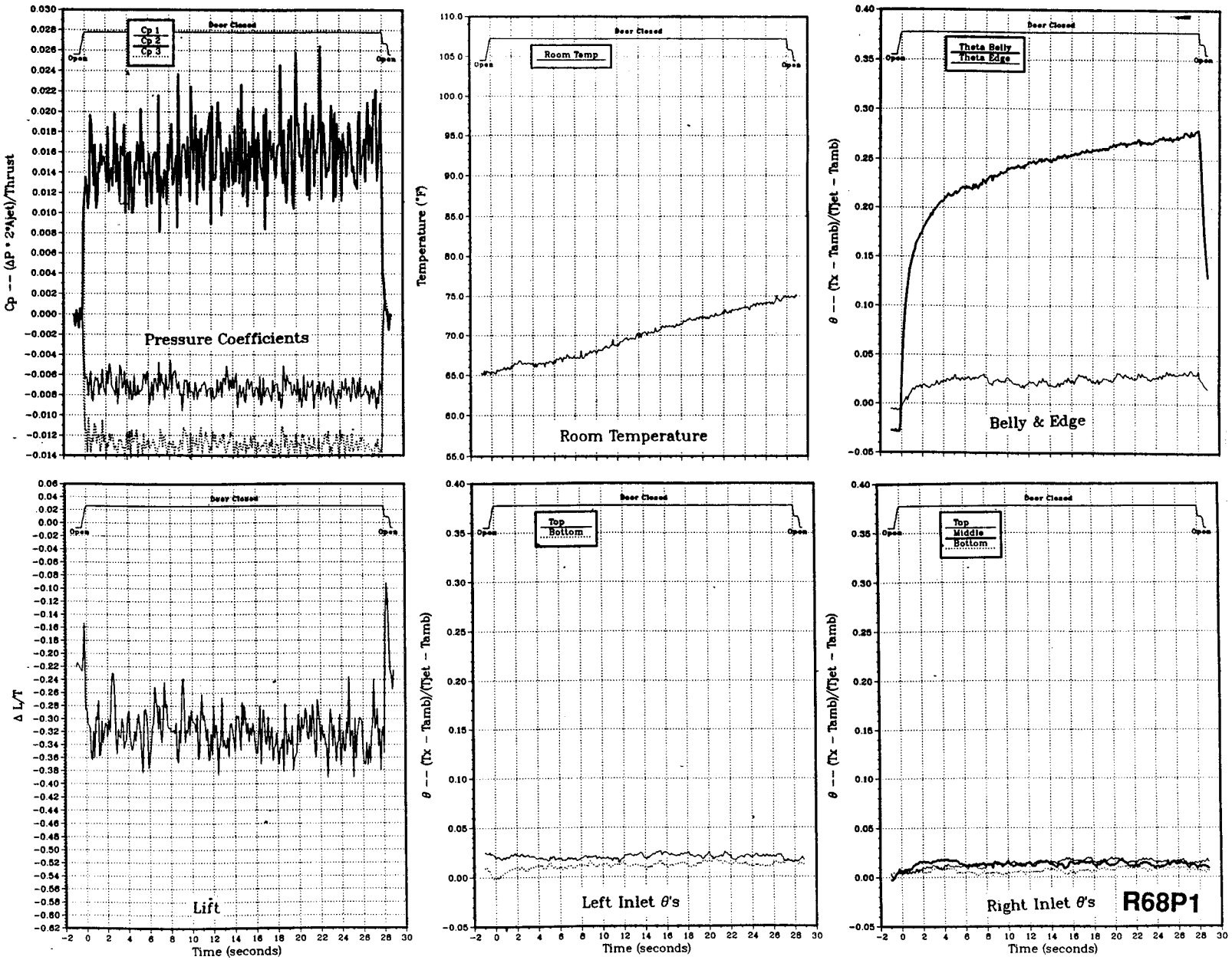

Figure 25(a). Delta wing, no LIDs, NPR = 2.0, thrust = 50 lb, height = 4 in., Tjet = 400 °F, inlet position = 9.66 in., no field temperatures.

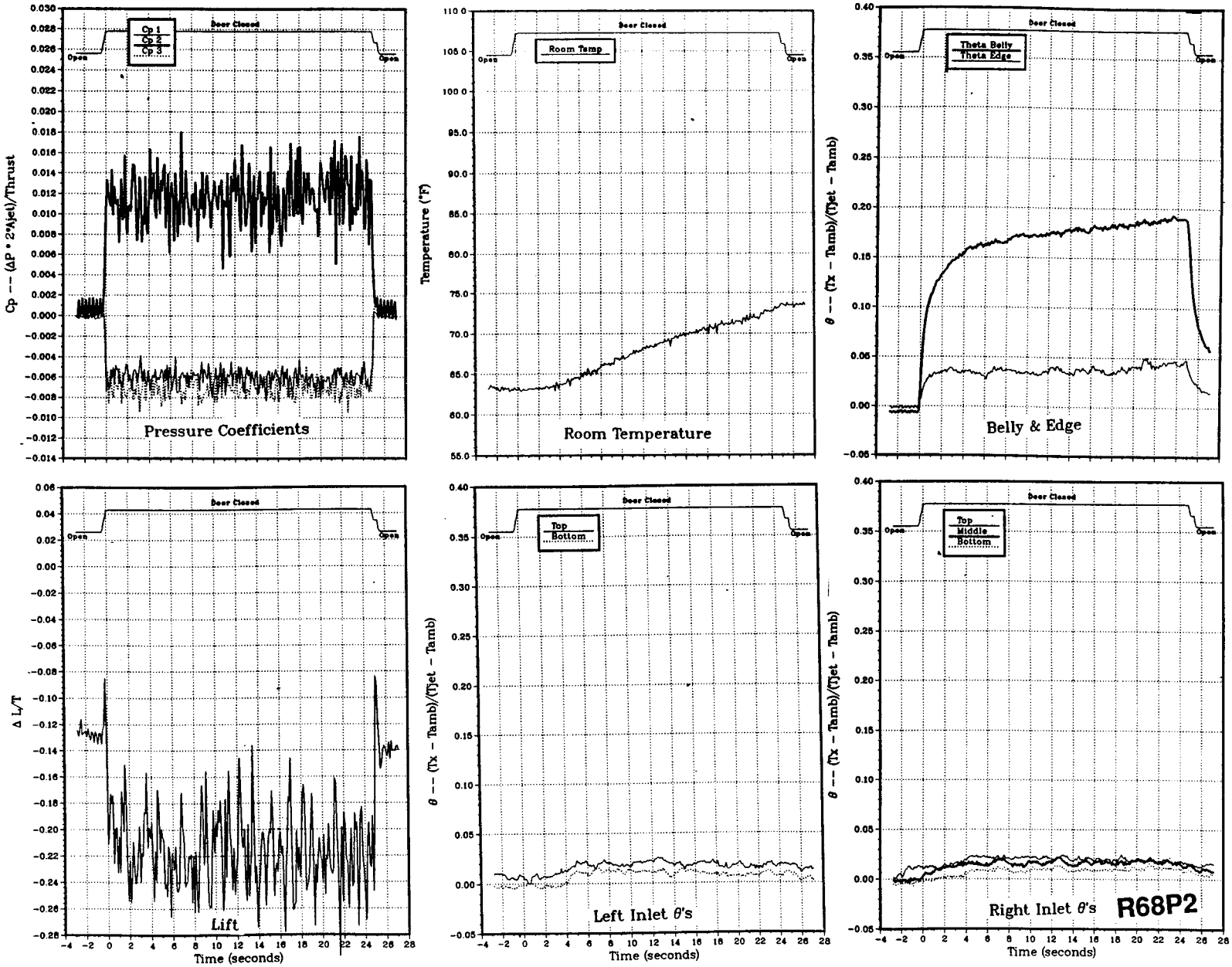

Figure 25(b). Delta wing, no LIDs, NPR = 2.0, thrust = 50 lb, height = 6 in., Tjet = 419 °F, inlet position = 9.66 in., no field temperatures.

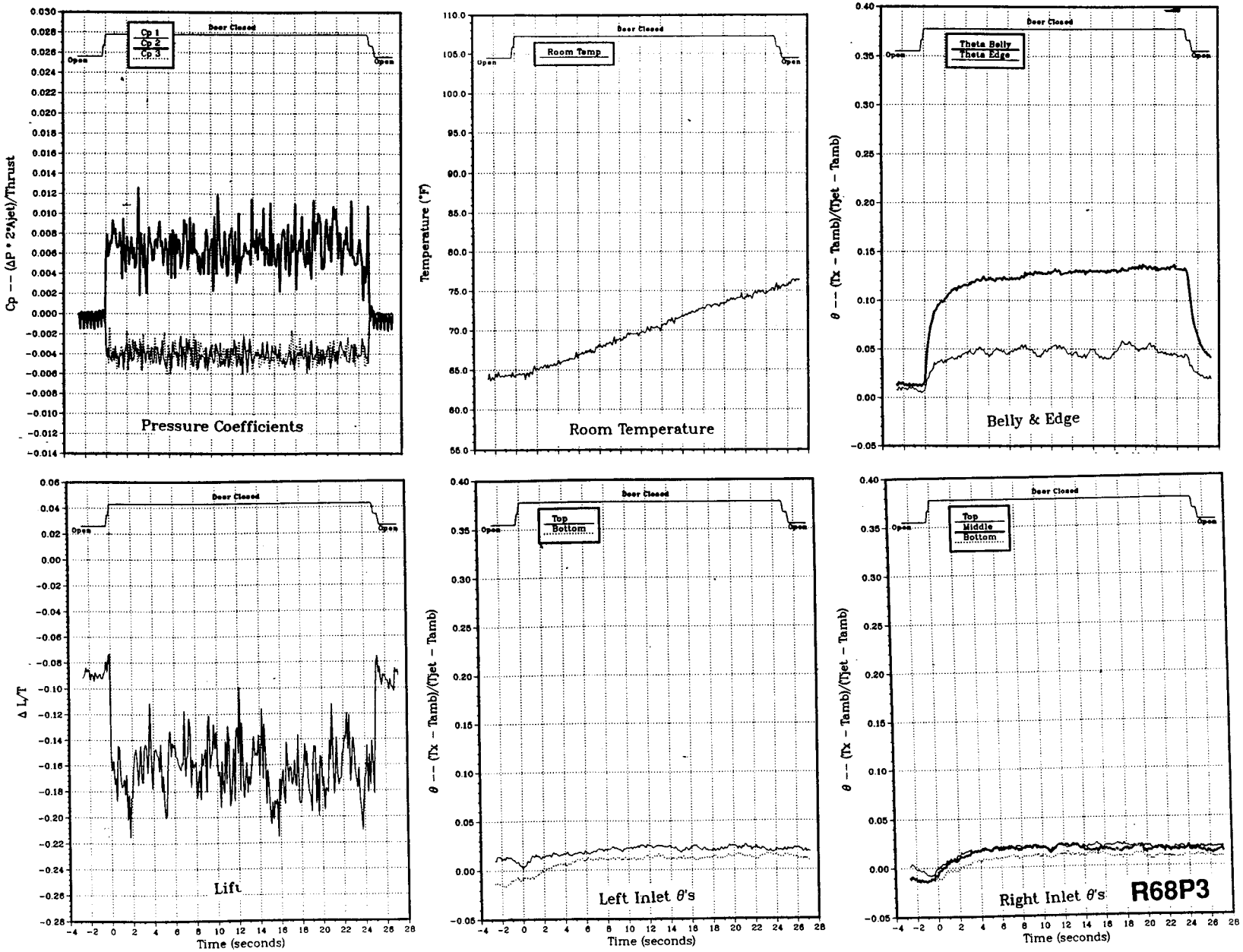

Figure 25(c). Delta wing, no LIDs, NPR = 2.0, thrust = 50 lb, height = 8 in., Tjet = 433 °F, inlet position = 9.66 in., no field temperatures.

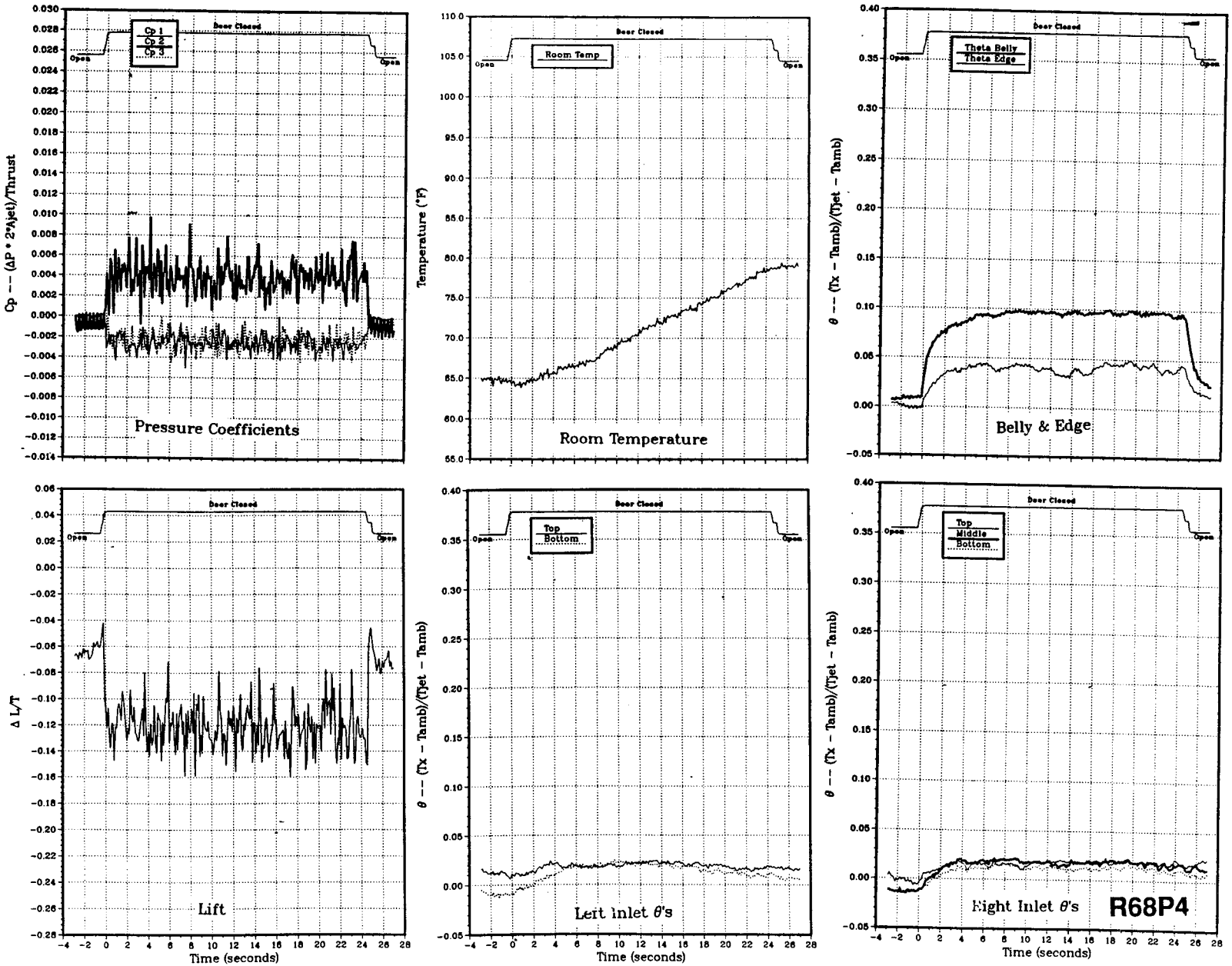

Figure 25(d). Delta wing, no LIDs, NPR = 2.0, thrust = 50 lb, height = 10 in., Tjet = 445 °F, inlet position = 9.66 in., no field temperatures.

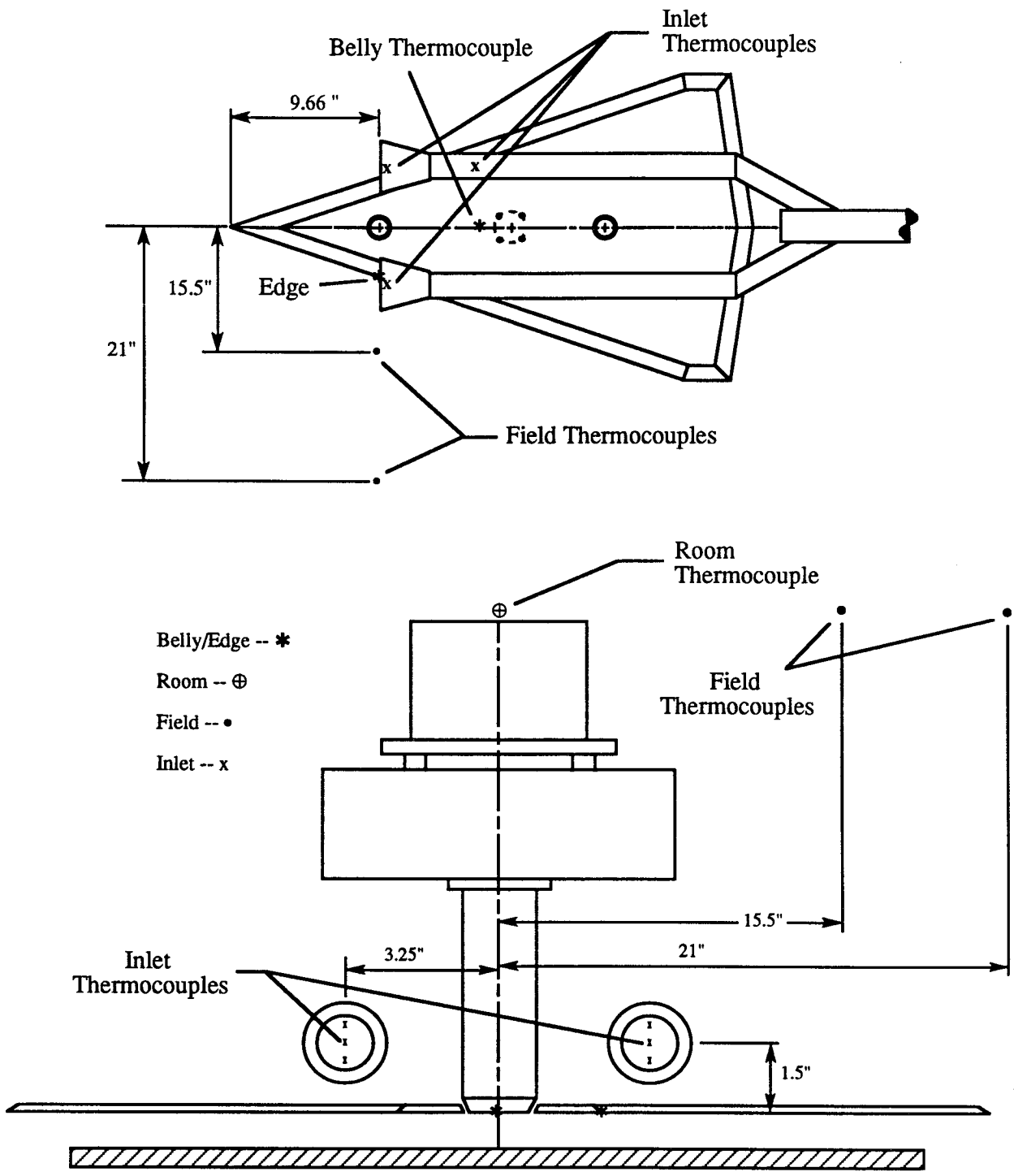

Figure 26. Locations of model and field thermocouples for data set 4.

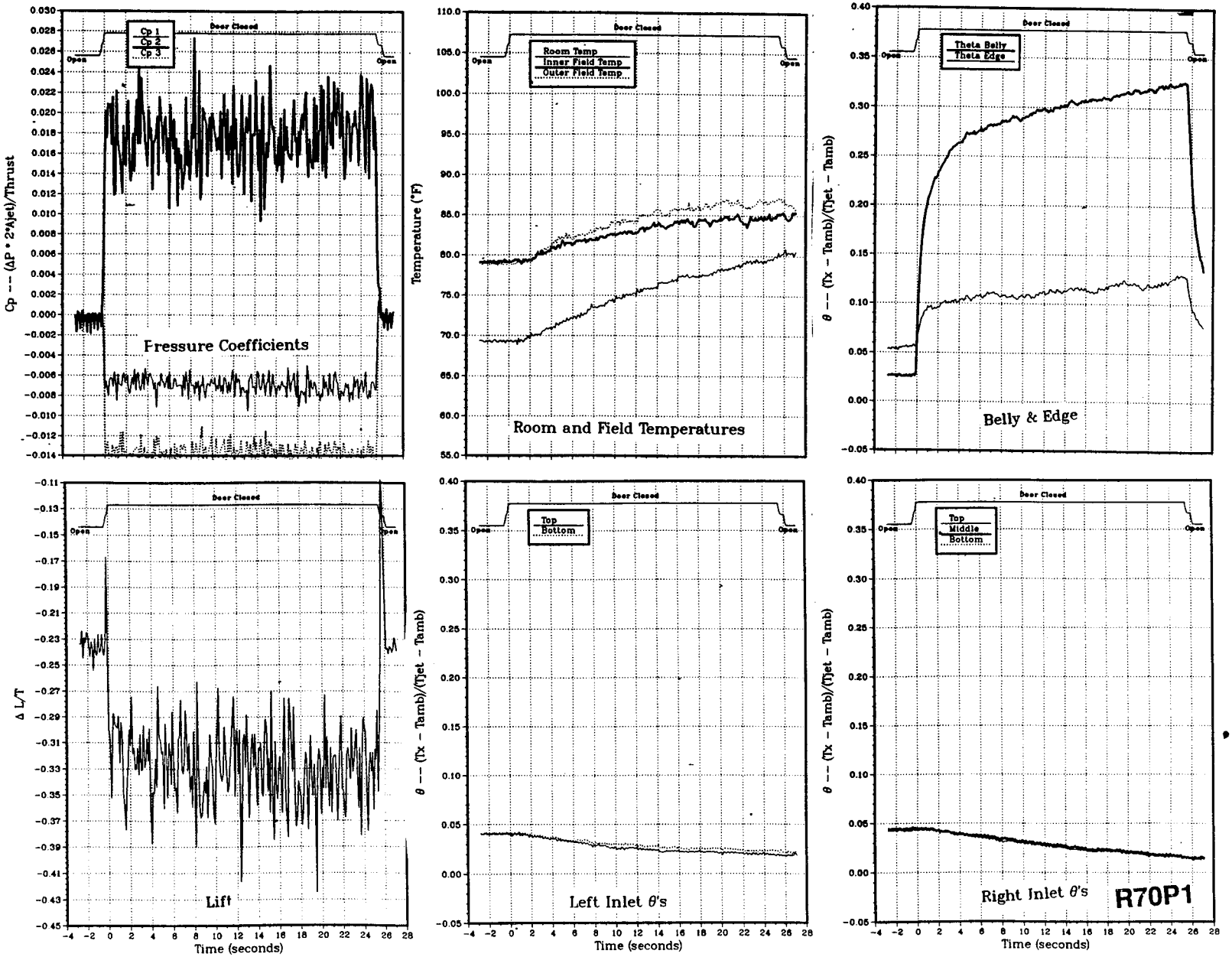

Figure 27(a). Delta wing, no LIDs, NPR = 2.0, thrust = 50 lb, height = 4 in., Tjet = 415 °F, inlet position = 9.66 in., no inlet suction.

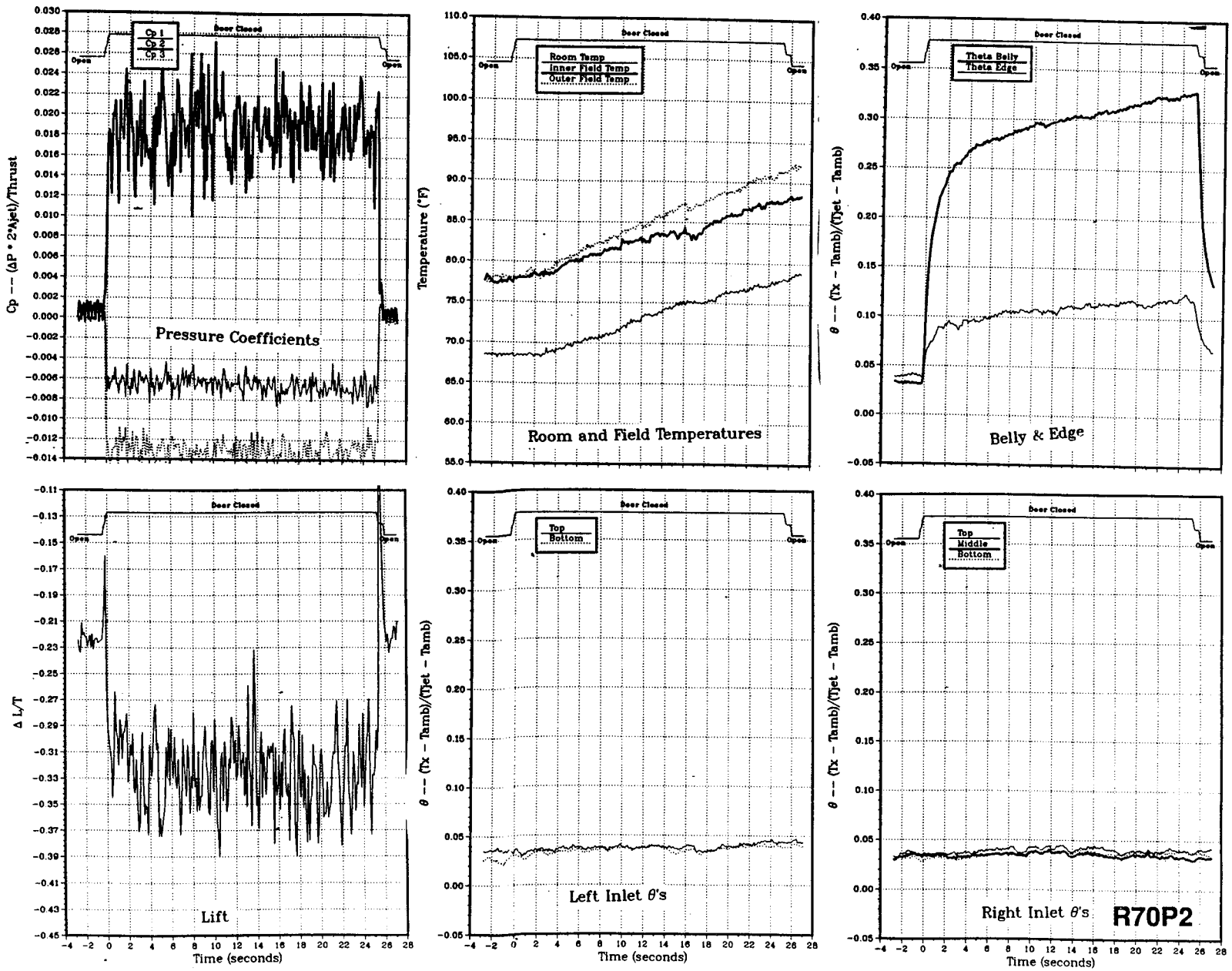

Figure 27(b). Delta wing, no LIDs, NPR = 2.0, thrust = 50 lb, height = 4 in., Tjet = 440 °F, inlet position = 9.66 in., max suction = 0.551 lb/sec.

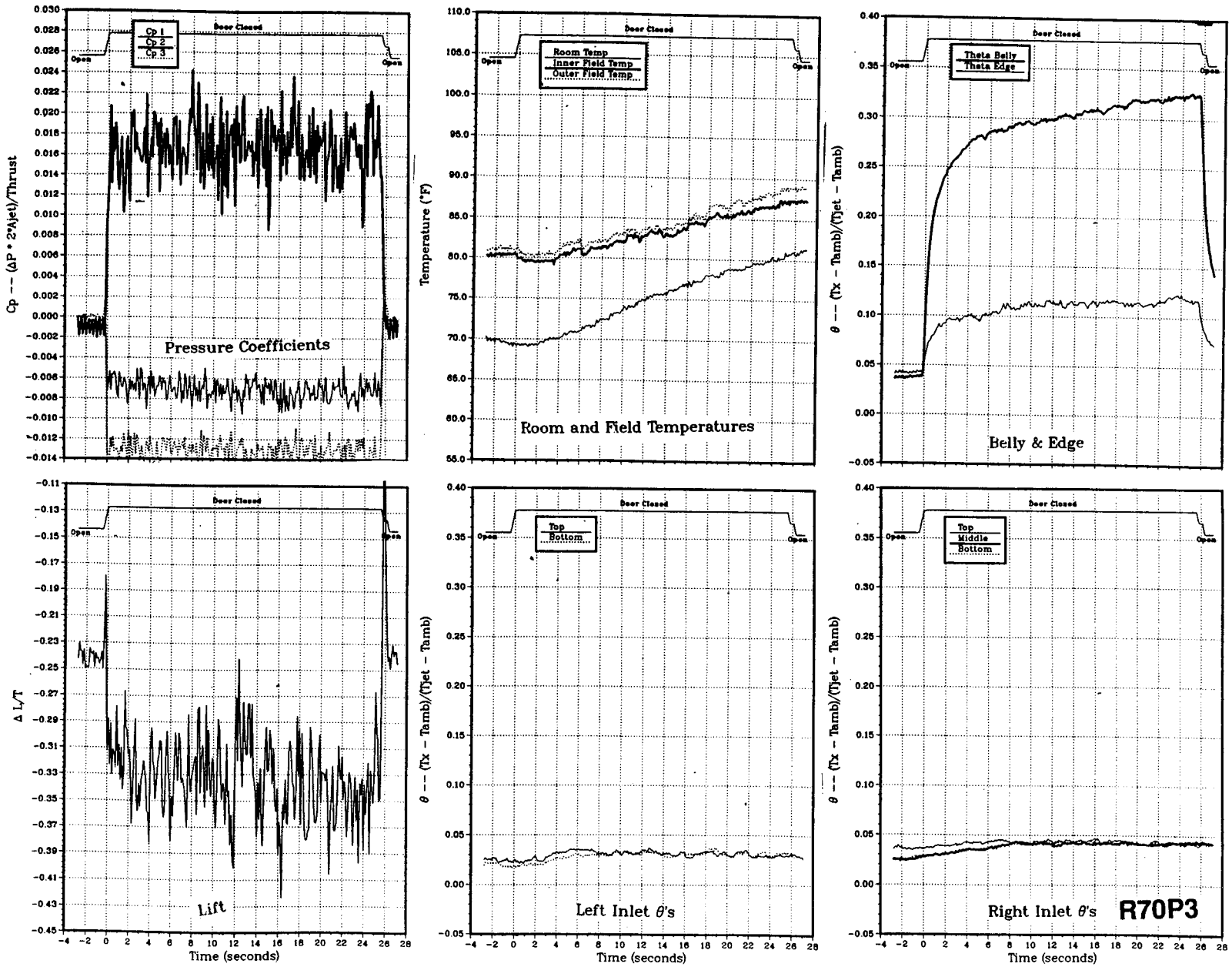

Figure 27(c). Delta wing, no LIDs, NPR = 2.0, thrust = 50 lb, height = 4 in., Tjet = 453 °F, inlet position = 9.66 in., suction = 0.437 lb/sec.

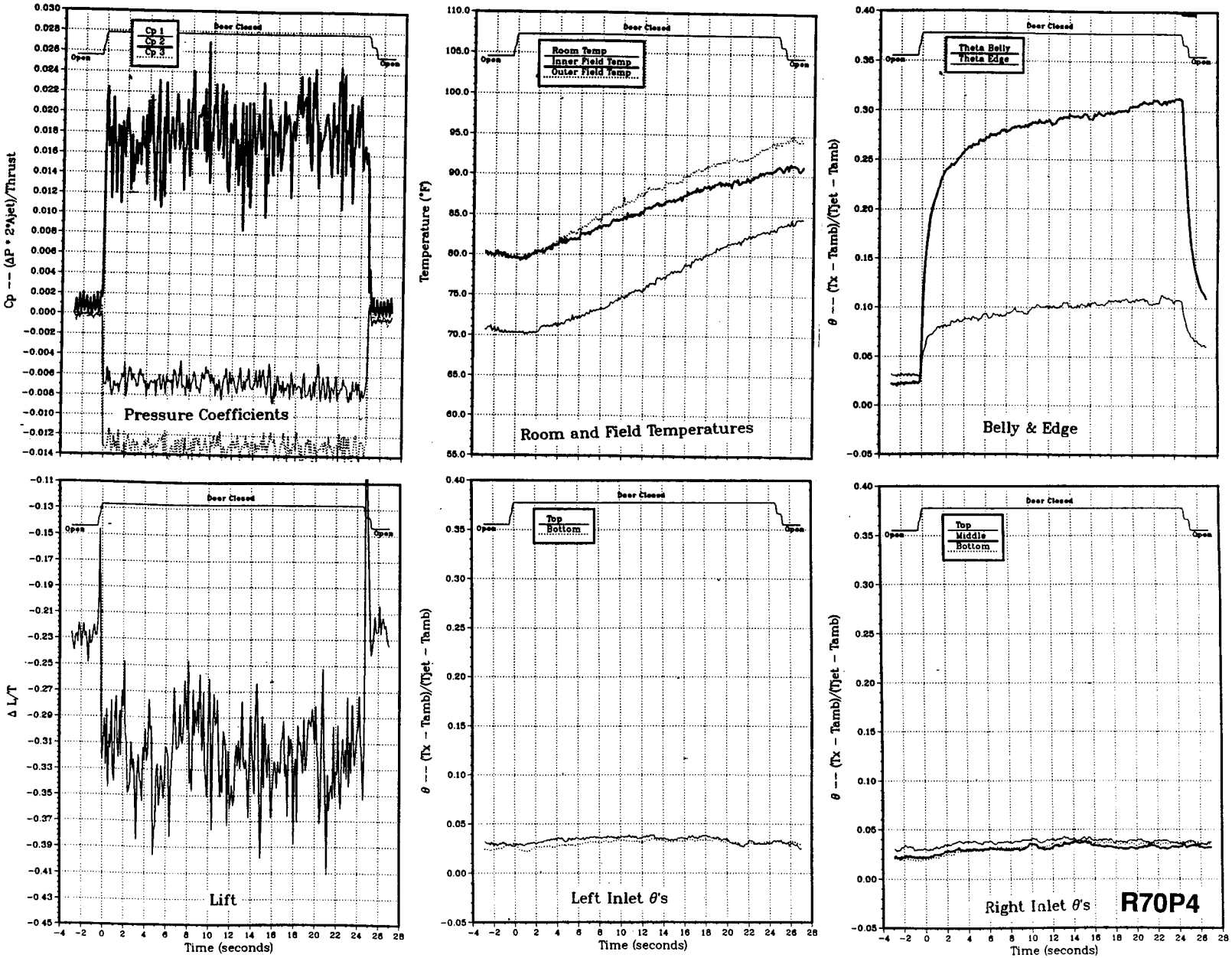

Figure 27(d). Delta wing, no LIDs, NPR = 2.0, thrust = 50 lb, height = 4 in., Tjet = 499 °F, inlet position = 9.66 in., suction = 0.347 lb/sec.

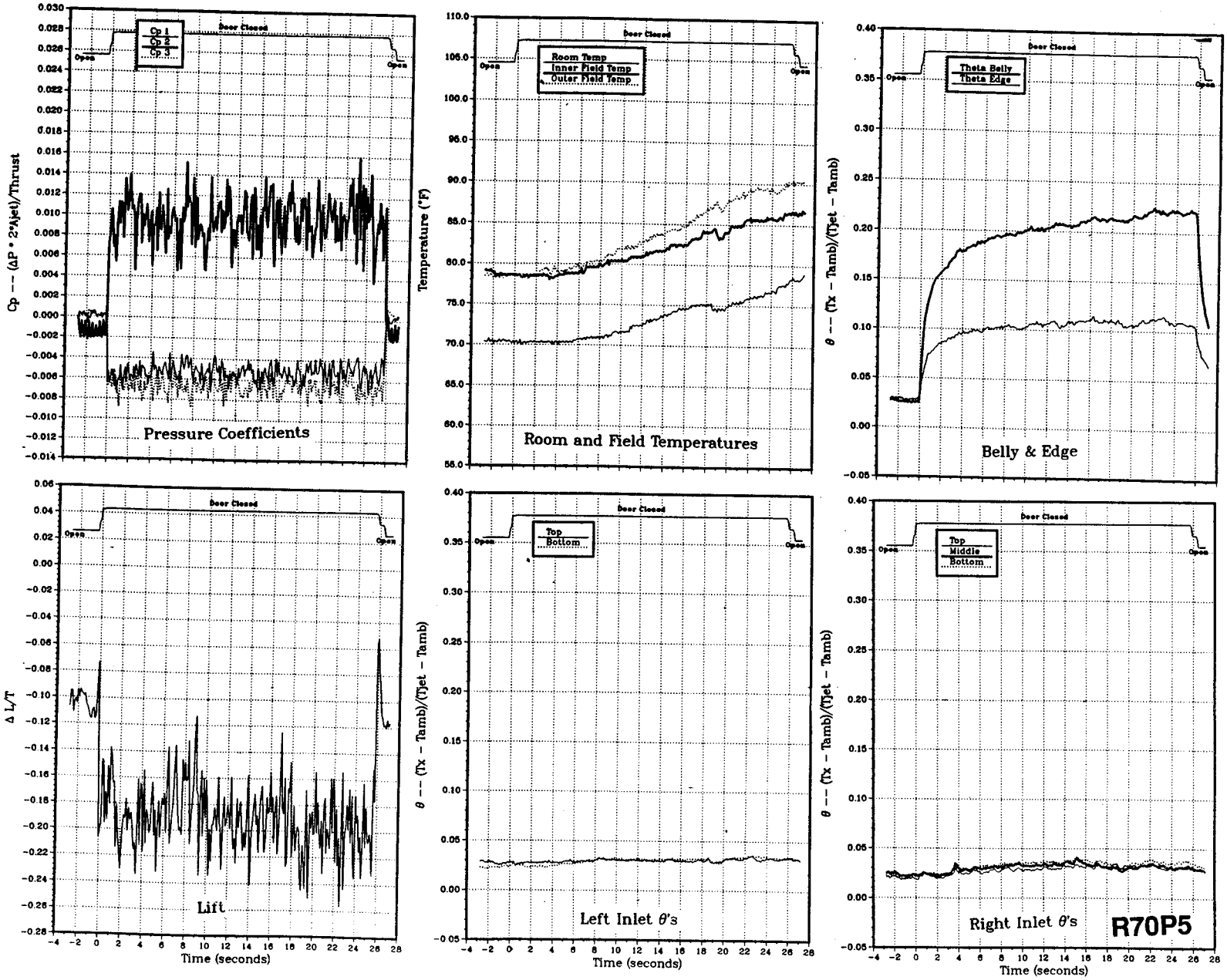

Figure 27(e). Delta wing, no LIDs, NPR = 2.0, thrust = 50 lb, height = 6 in., Tjet = 503 °F, inlet position = 9.66 in., max suction = 0.551 lb/sec.

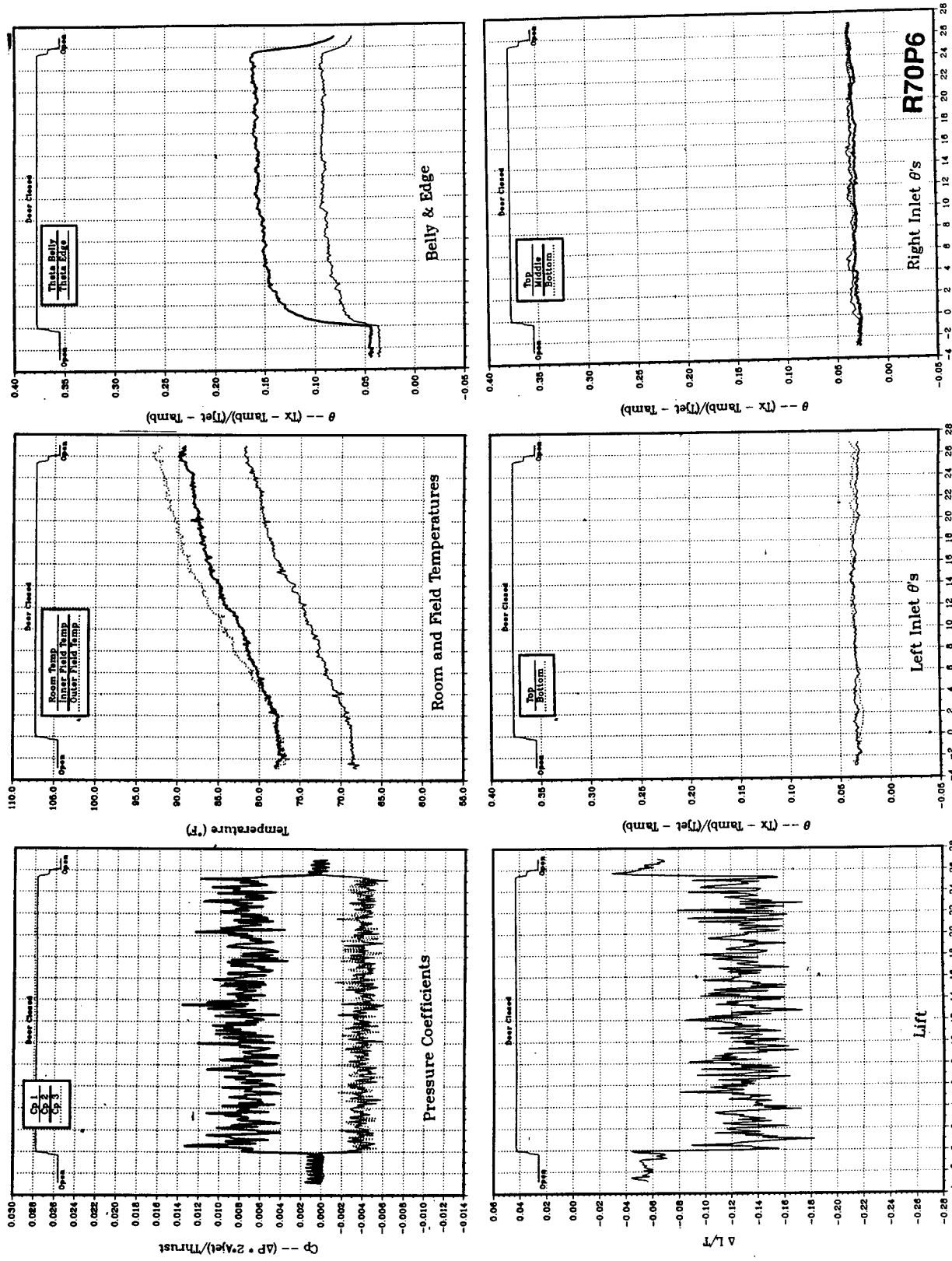

Figure 27(f). Delta wing, no LIDs, NPR = 2.0, thrust = 50 lb, height = 8 in., Tjet = 506 °F, inlet position = 9.66 in.

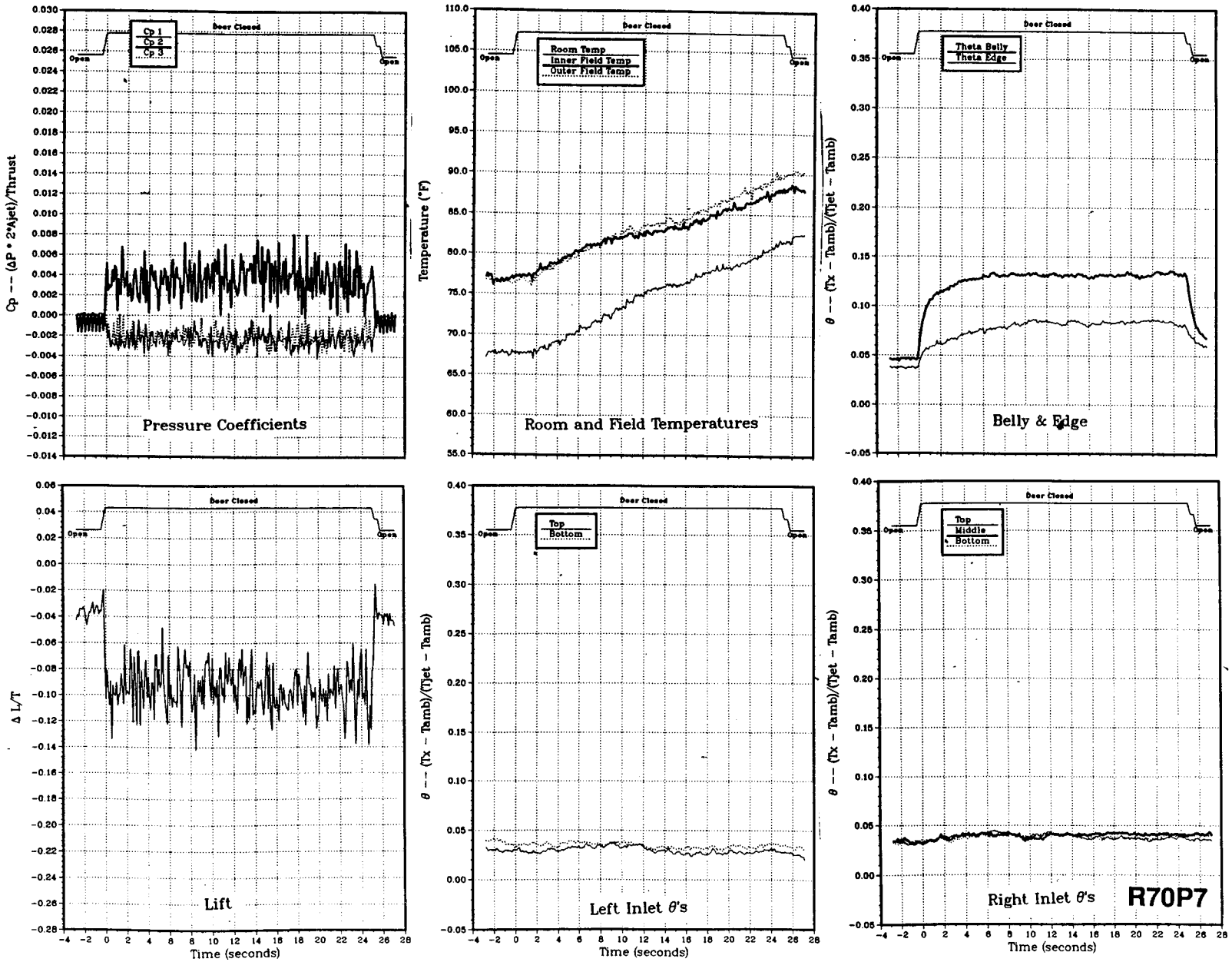

Figure 27(g). Delta wing, no LIDs, NPR = 2.0, thrust = 50 lb, height = 10 in., Tjet = 508 °F, inlet position = 9.66 in.

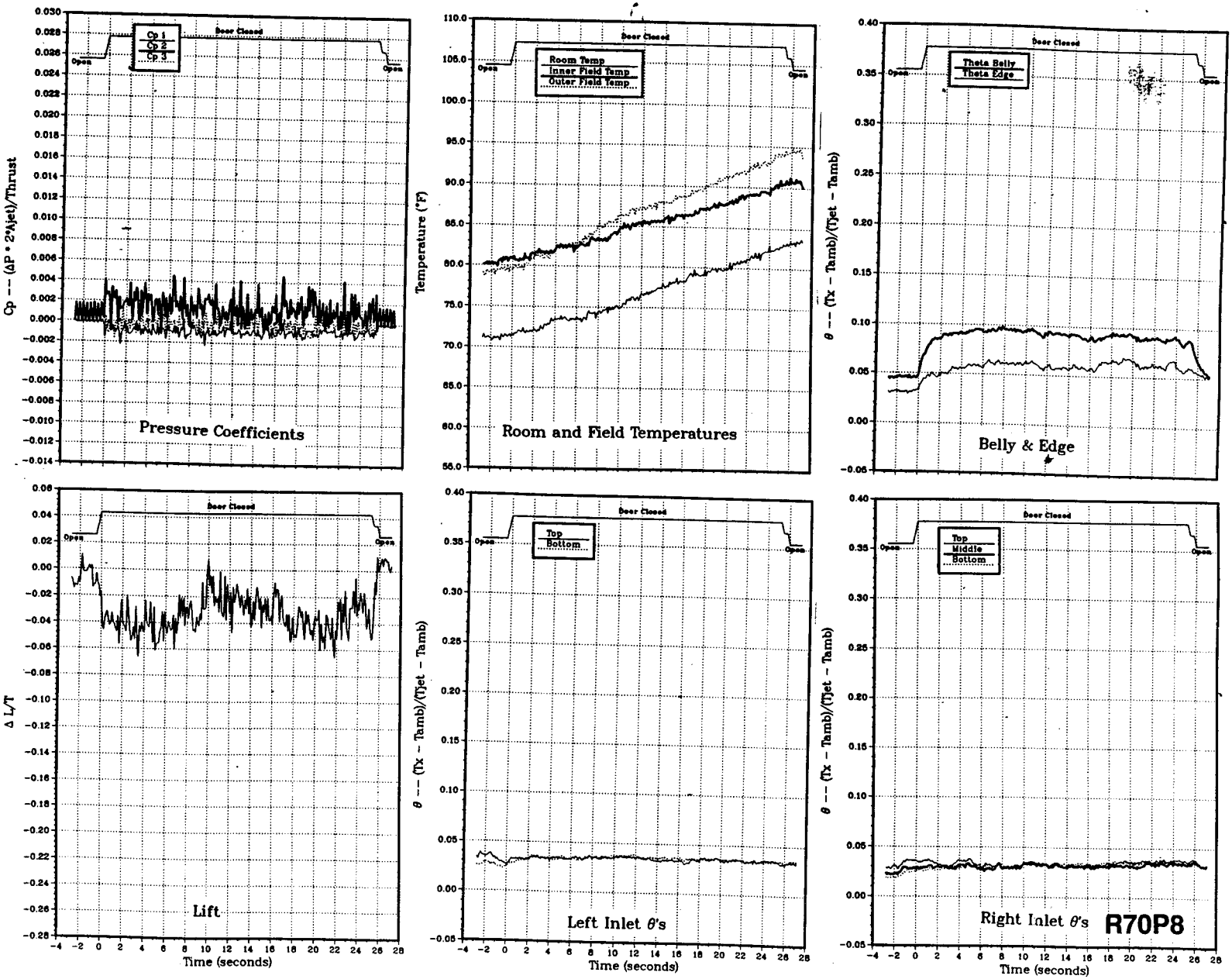

Figure 27(h). Delta wing, no LIDs, NPR = 2.0, thrust = 50 lb, height = 15 in., Tjet = 510 °F, inlet position = 9.66 in.

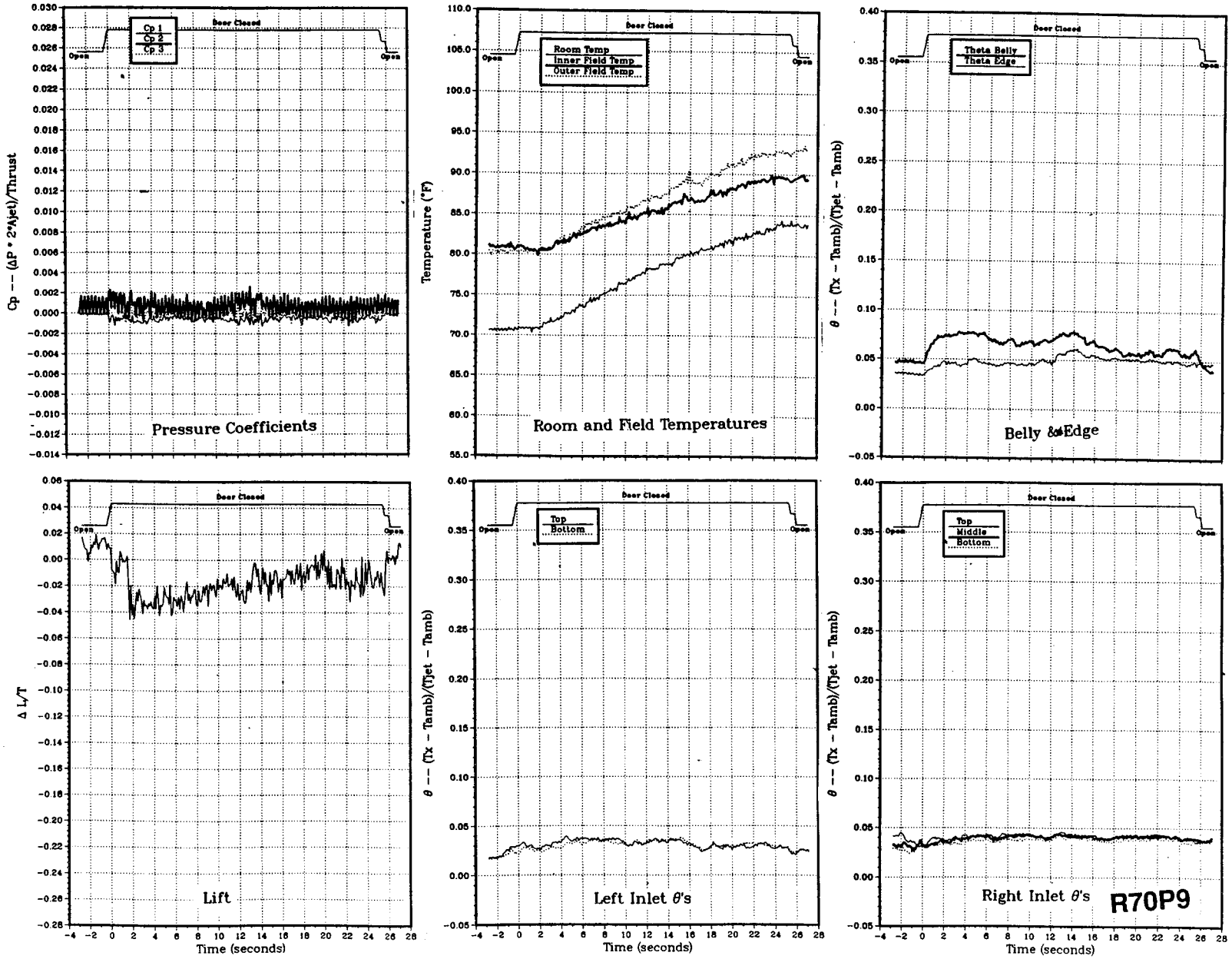

Figure 27(i). Delta wing, no LIDs, NPR = 2.0, thrust = 50 lb, height = 20 in., Tjet = 511 °F, inlet position = 9.66 in.

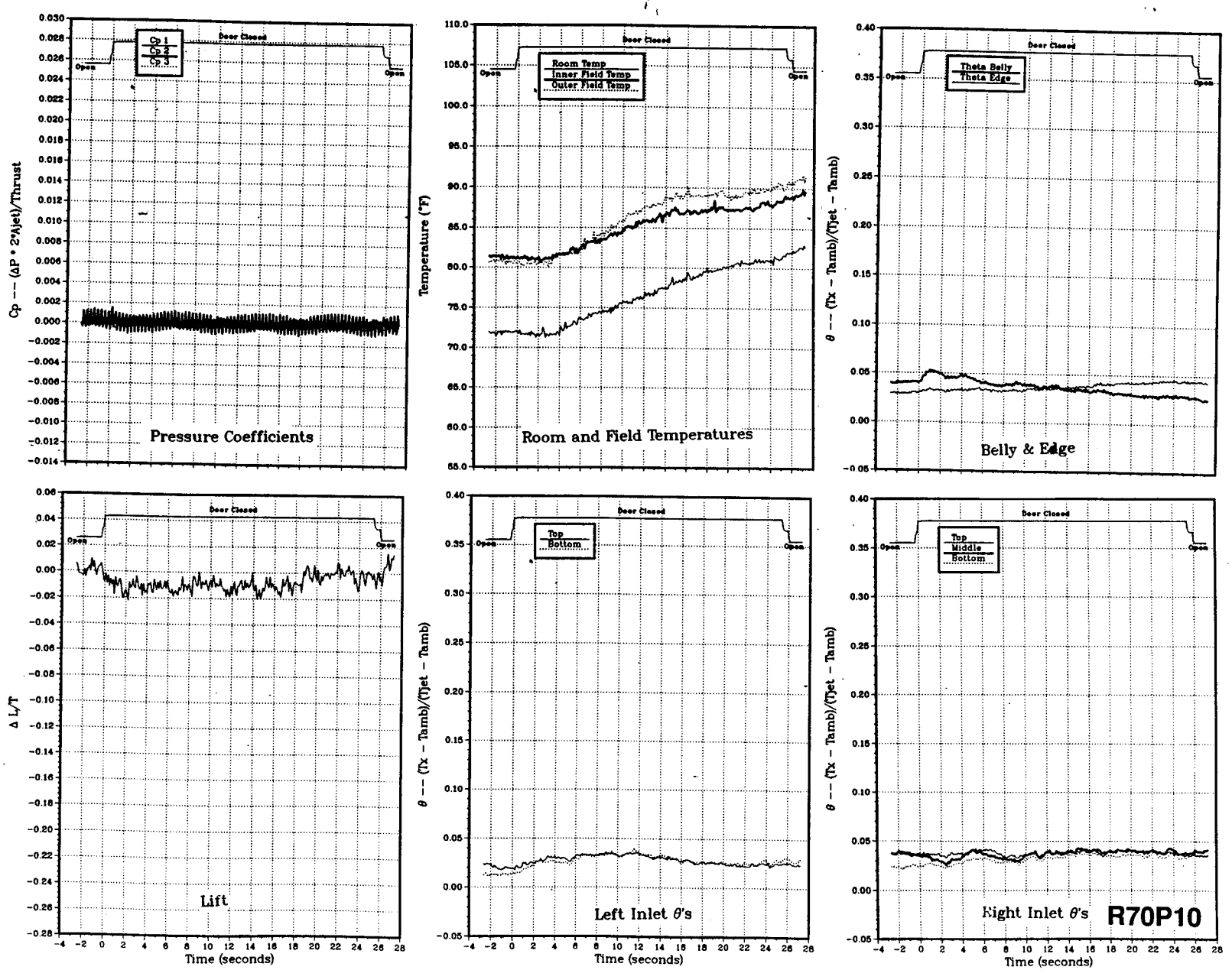

Figure 27(j). Delta wing, no LIDs, NPR = 2.0, thrust = 50 lb, height = 30 in., Tjet = 512 °F, inlet position = 9.66 in.

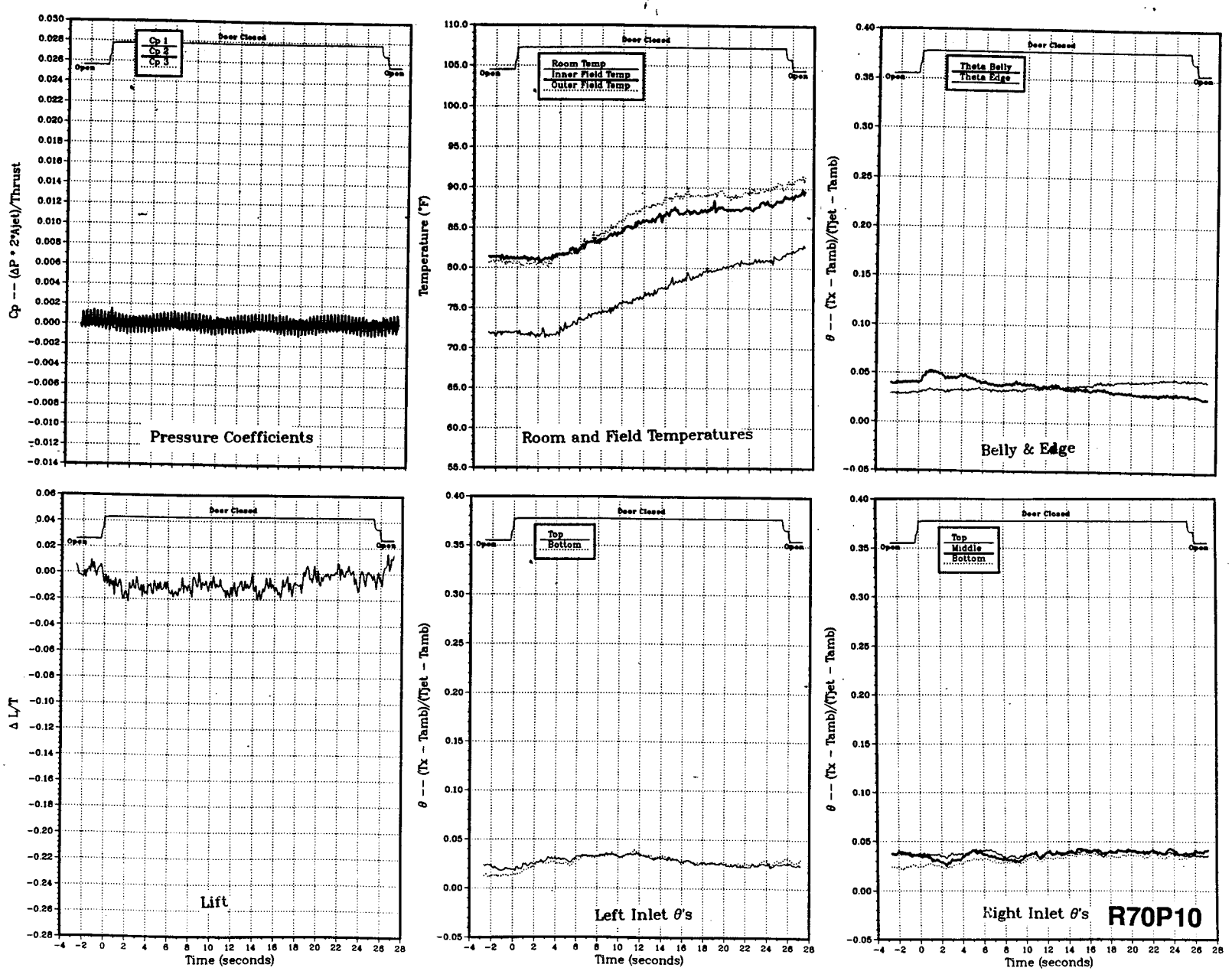

Figure 27(j). Delta wing, no LIDs, NPR = 2.0, thrust = 50 lb, height = 30 in., Tjet = 512 °F, inlet position = 9.66 in.

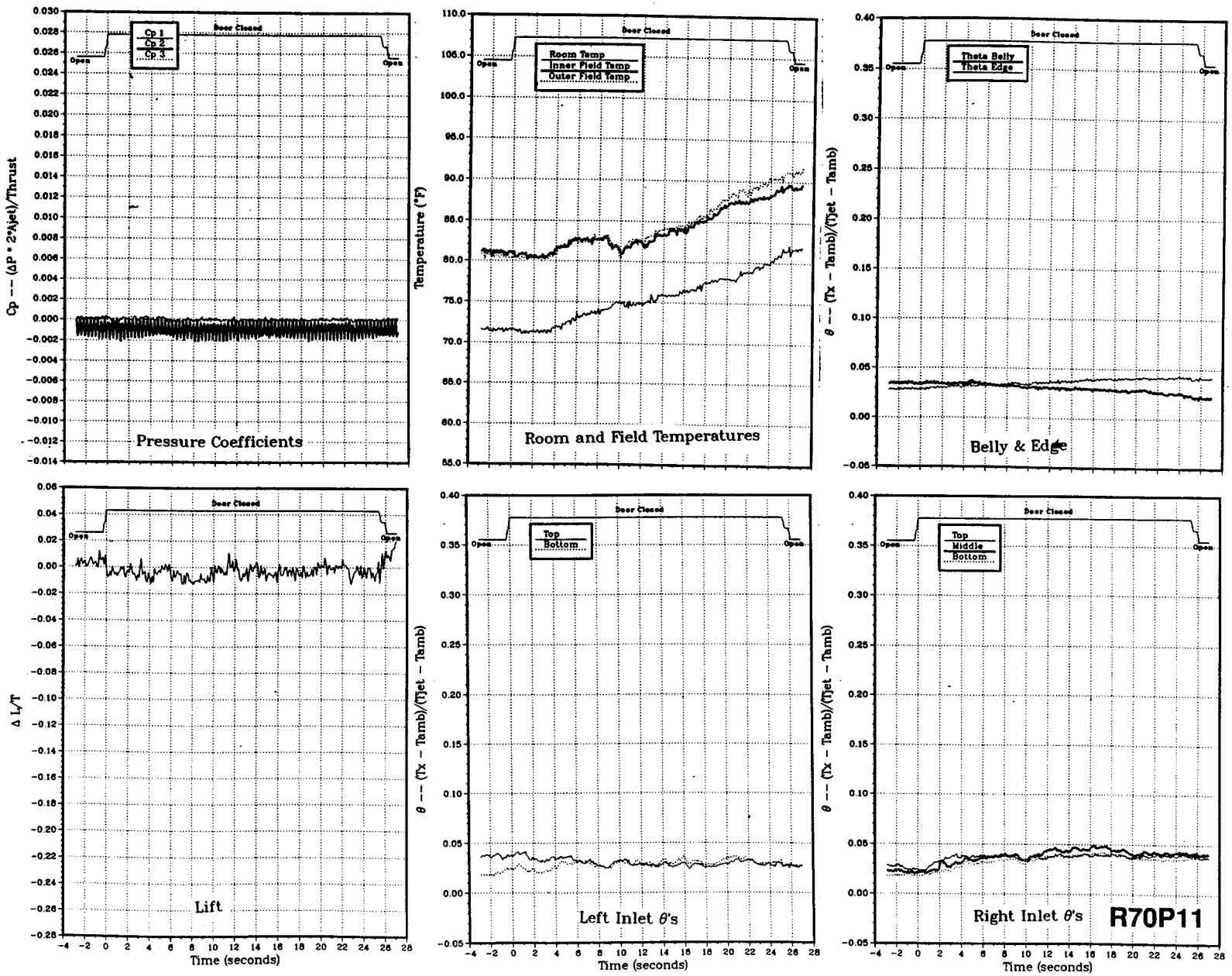

Figure 27(k). Delta wing, no LIDs, NPR = 2.0, thrust = 50 lb, height = 40 in., Tjet = 514 °F, inlet position = 9.66 in.

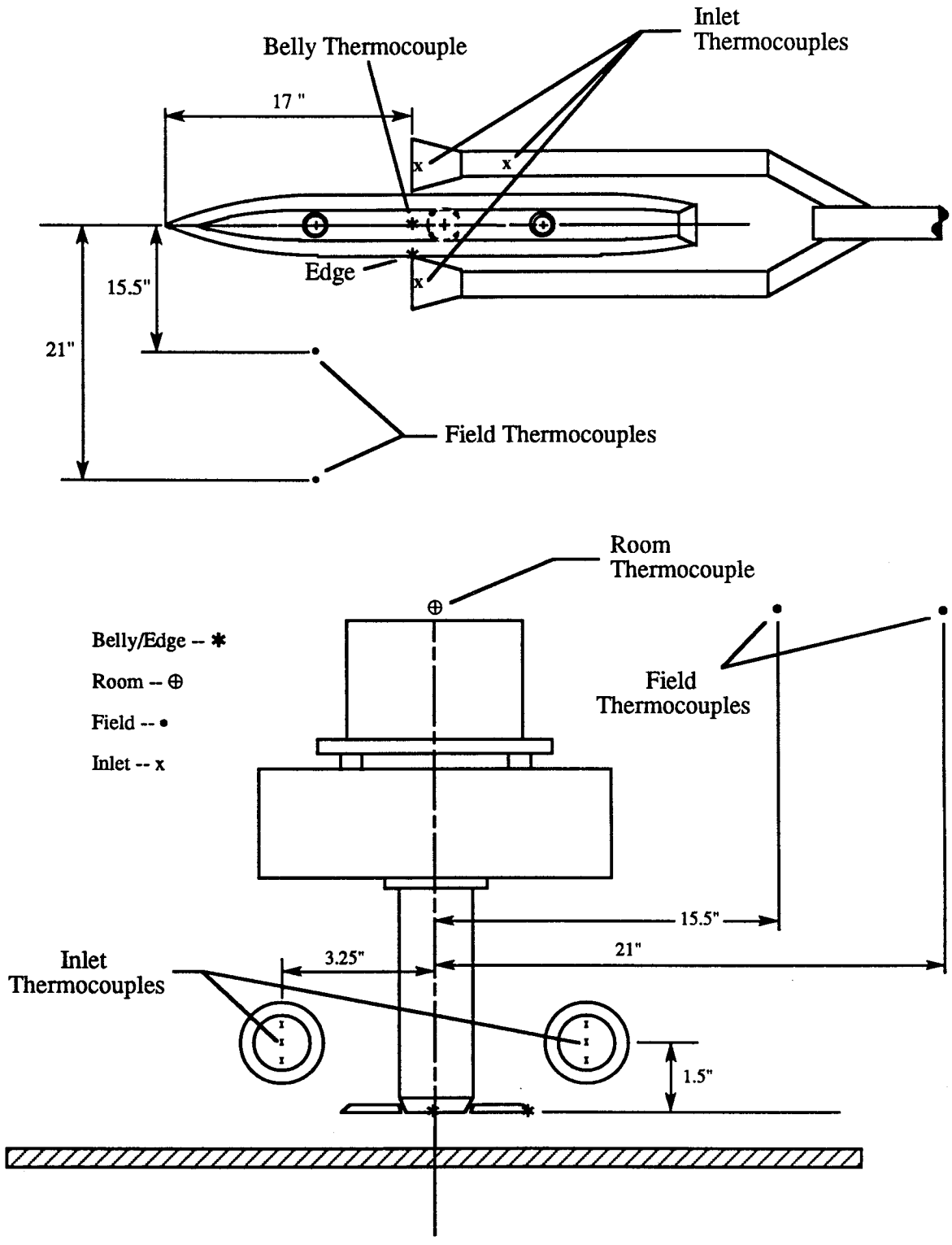

Figure 28. Locations of model and field thermocouples for data set 5.

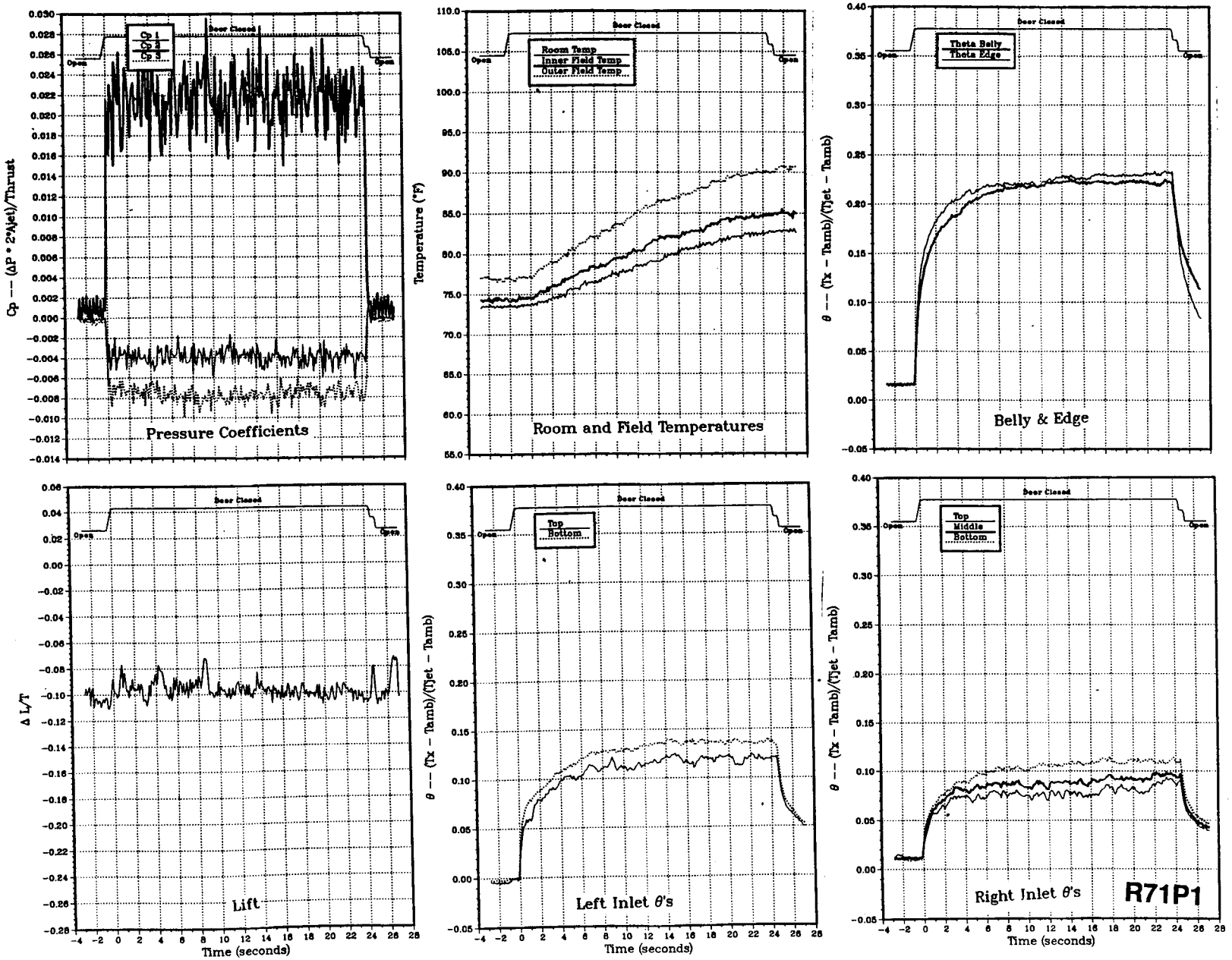

Figure 29(a). Body alone, no LIDs, NPR = 2.0, thrust = 50 lb, height = 4 in., Tjet = 469 °F, inlet position = 17 in., max suction = 0.532 lb/sec.

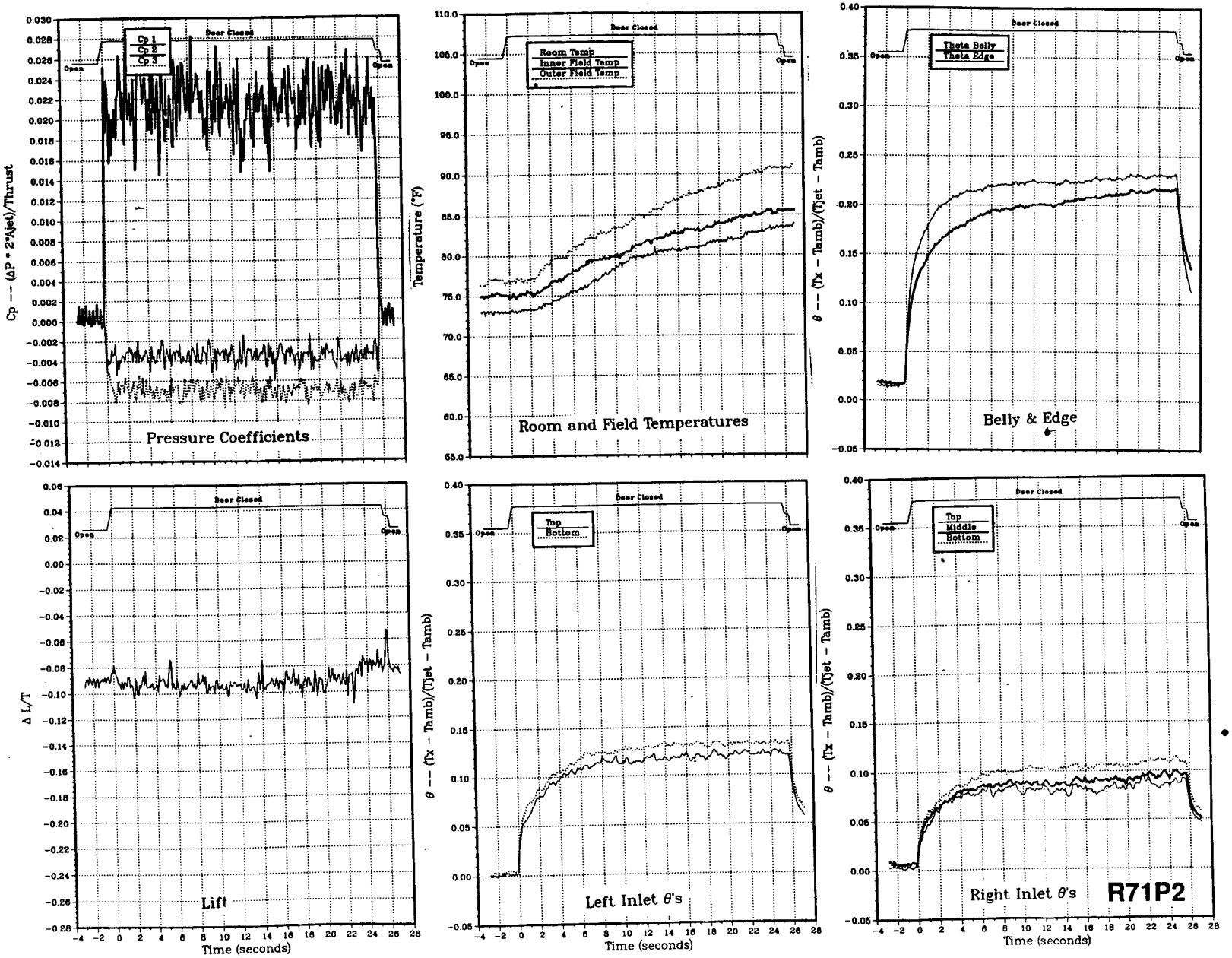

Figure 29(b). Body alone, no LIDs, NPR = 2.0, thrust = 50 lb, height = 4 in., Tjet = 480 °F, inlet position = 17 in., suction = 0.425 lb/sec.

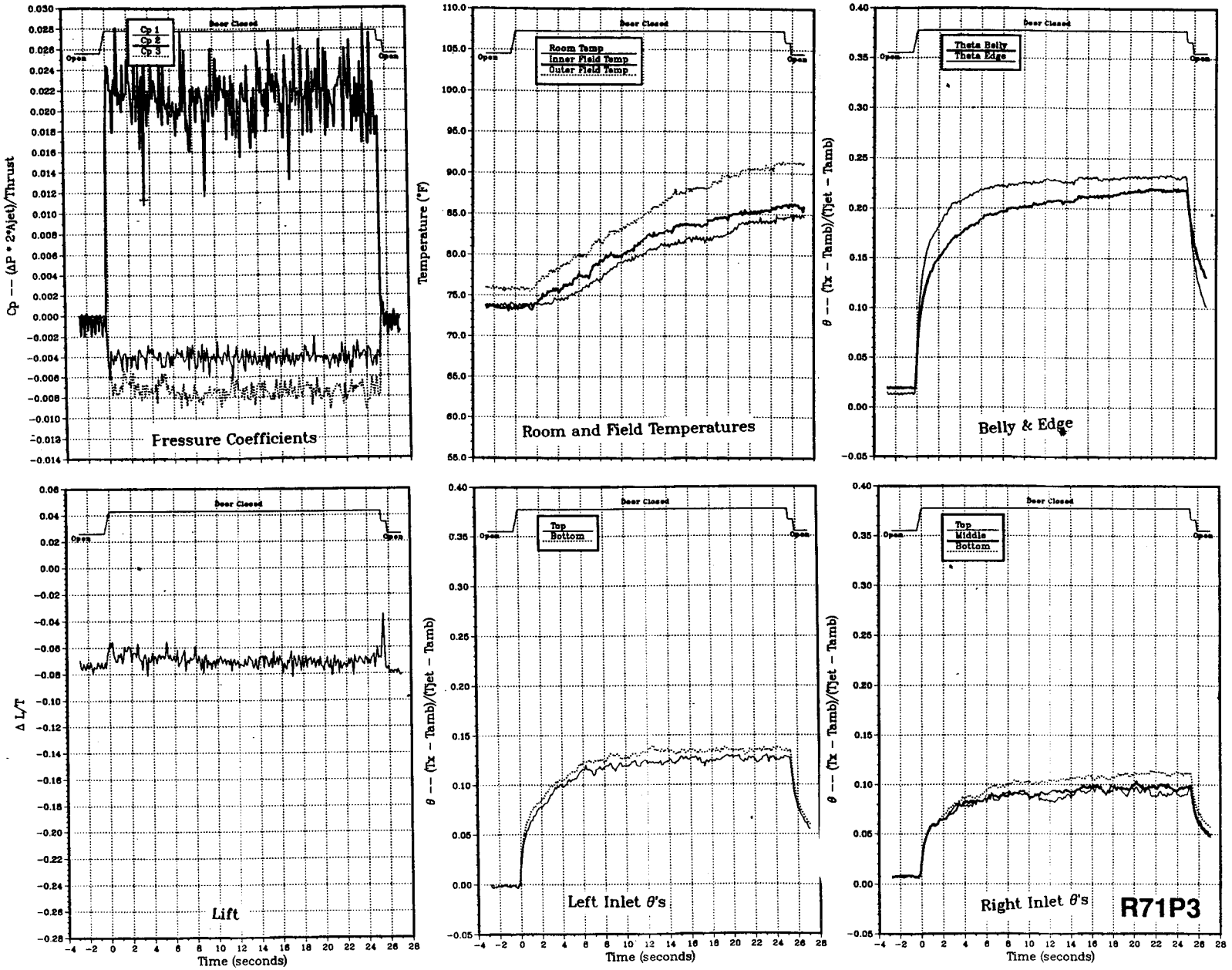

Figure 29(c). Body alone, no LIDs, NPR = 2.0, thrust = 50 lb, height = 4 in., Tjet = 486 °F, inlet position = 17 in., suction = 0.346 lb/sec.

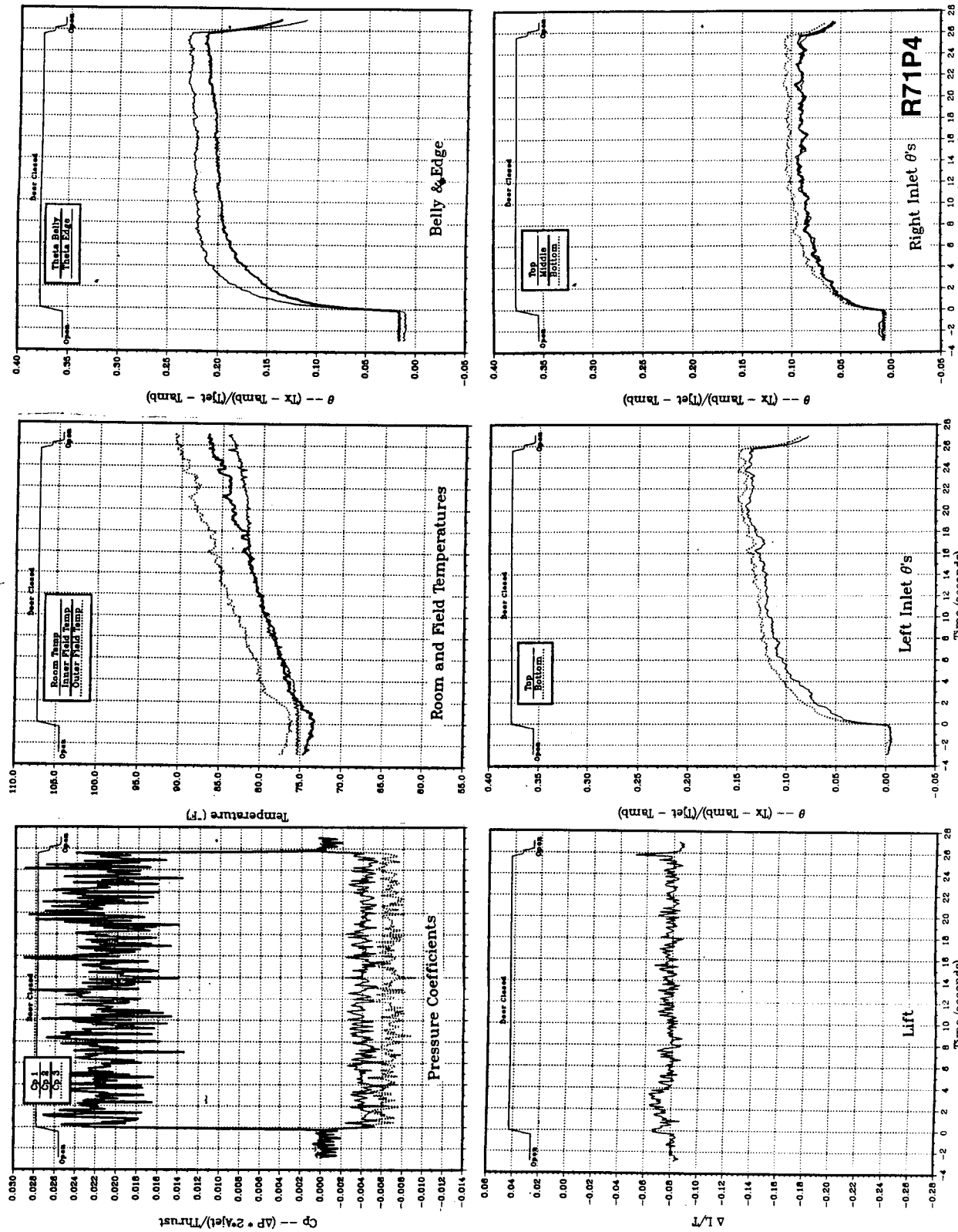

Figure 29(d). Body alone, no LIDs, NPR = 2.0, thrust = 50 lb, height = 4 in., Tjet = 492 °F, inlet position = 17 in., suction = 0.245 lb/sec.

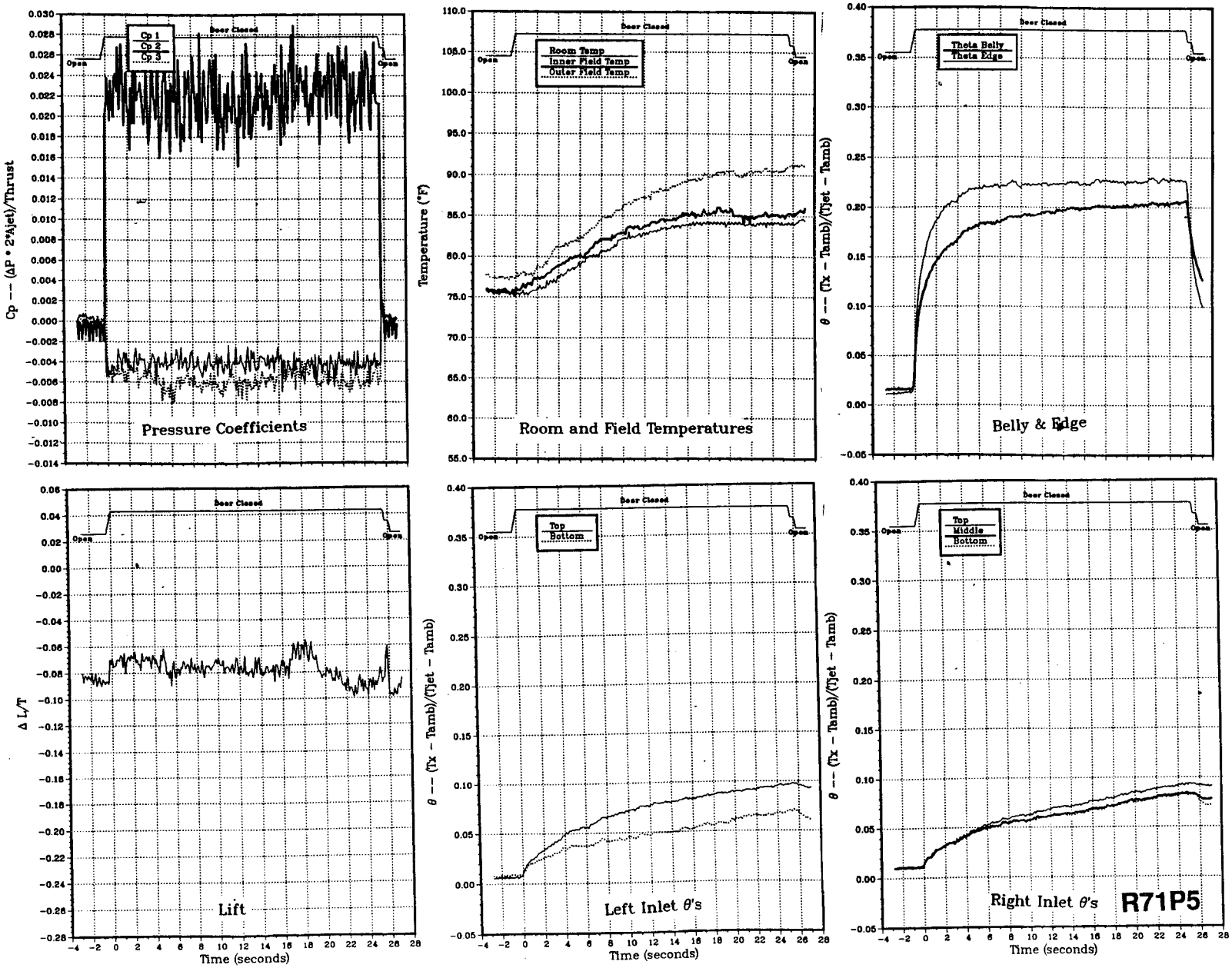

Figure 29(e). Body alone, no LIDs, NPR = 2.0, thrust = 50 lb, height = 4 in., Tjet = 497 °F, inlet position = 17 in., no inlet suction.

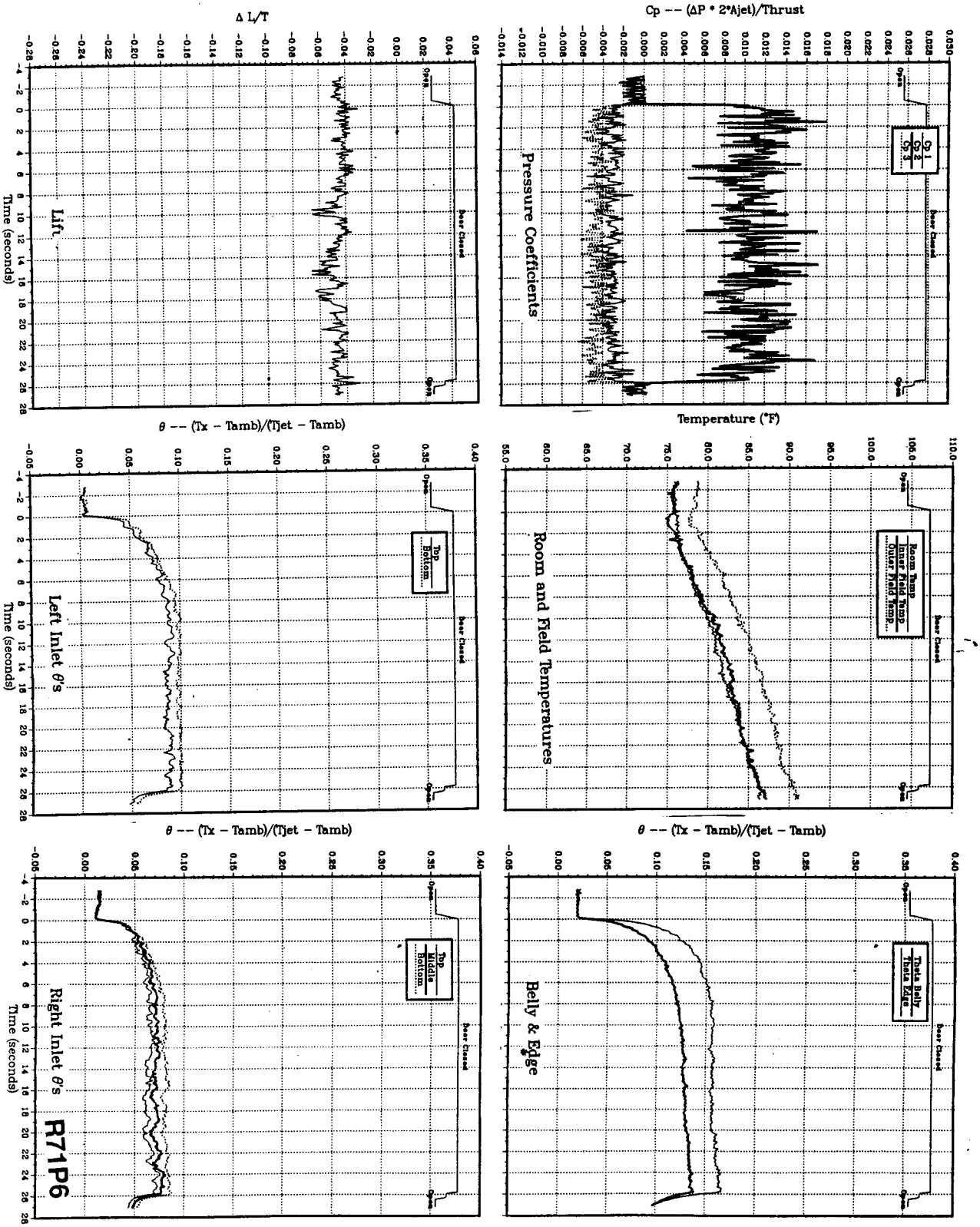

Figure 29(f). Body alone, no LIDs, NPR = 2.0, thrust = 50 lb, height = 6 in., Tjet = 502 °F, inlet position = 17 in.

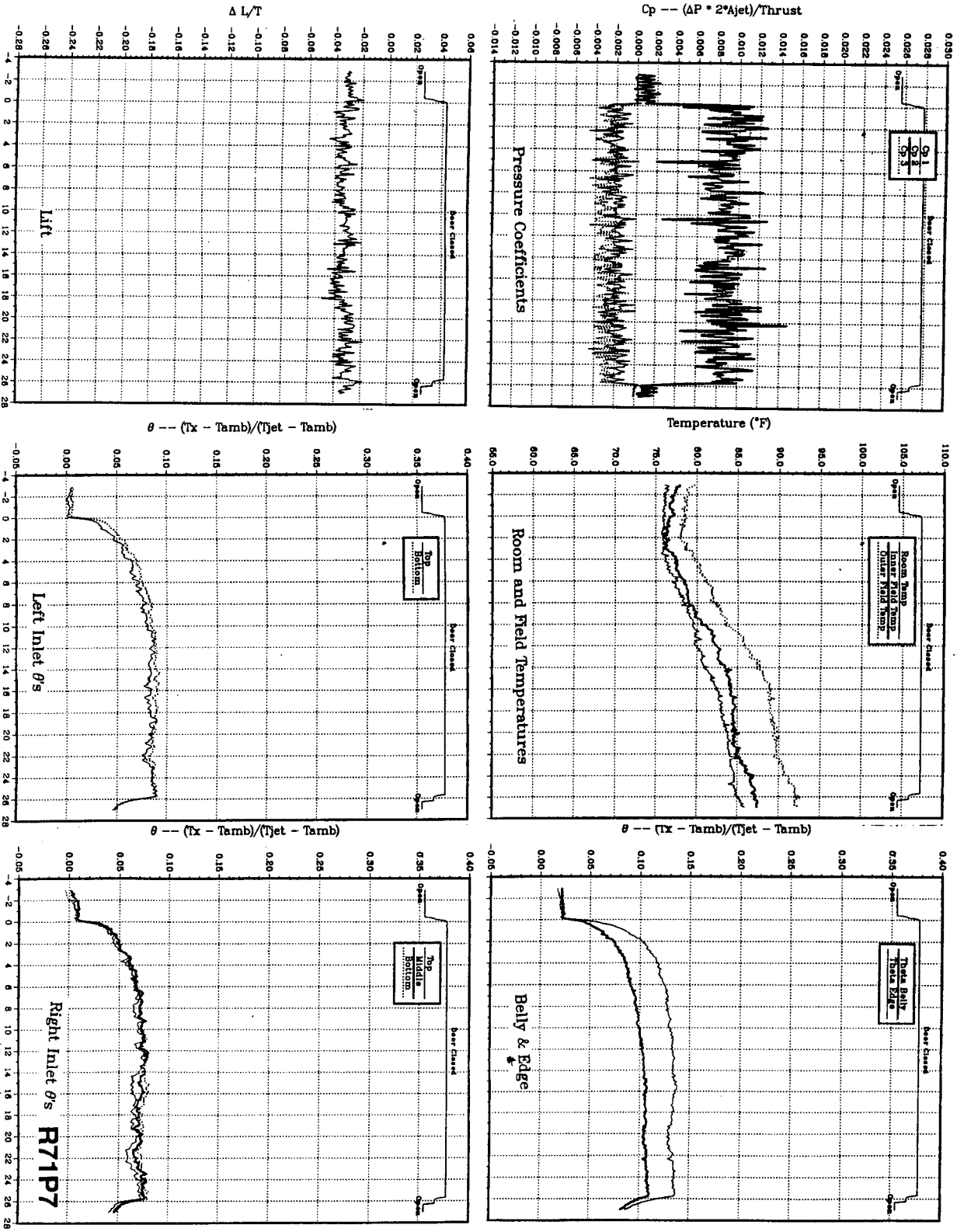

Figure 29(g). Body alone, no LIDs, NPR = 2.0, thrust = 50 lb, height = 8 in., Tjet = 505 °F, inlet position = 17 in.

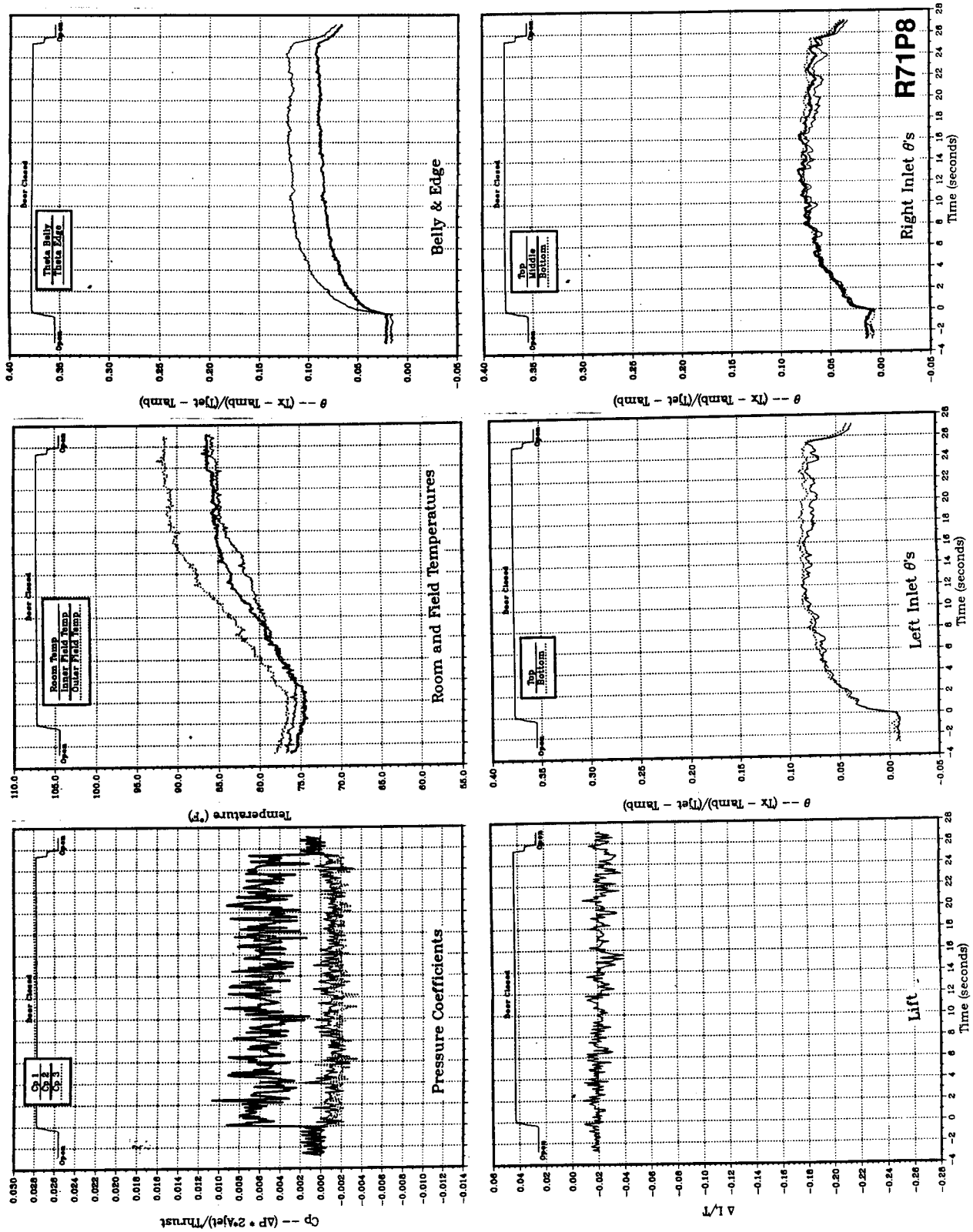

Figure 29(h). Body alone, no LIDs, NPR = 2.0, thrust = 50 lb, height = 10 in., Tjet = 507 °F, inlet position = 17 in.

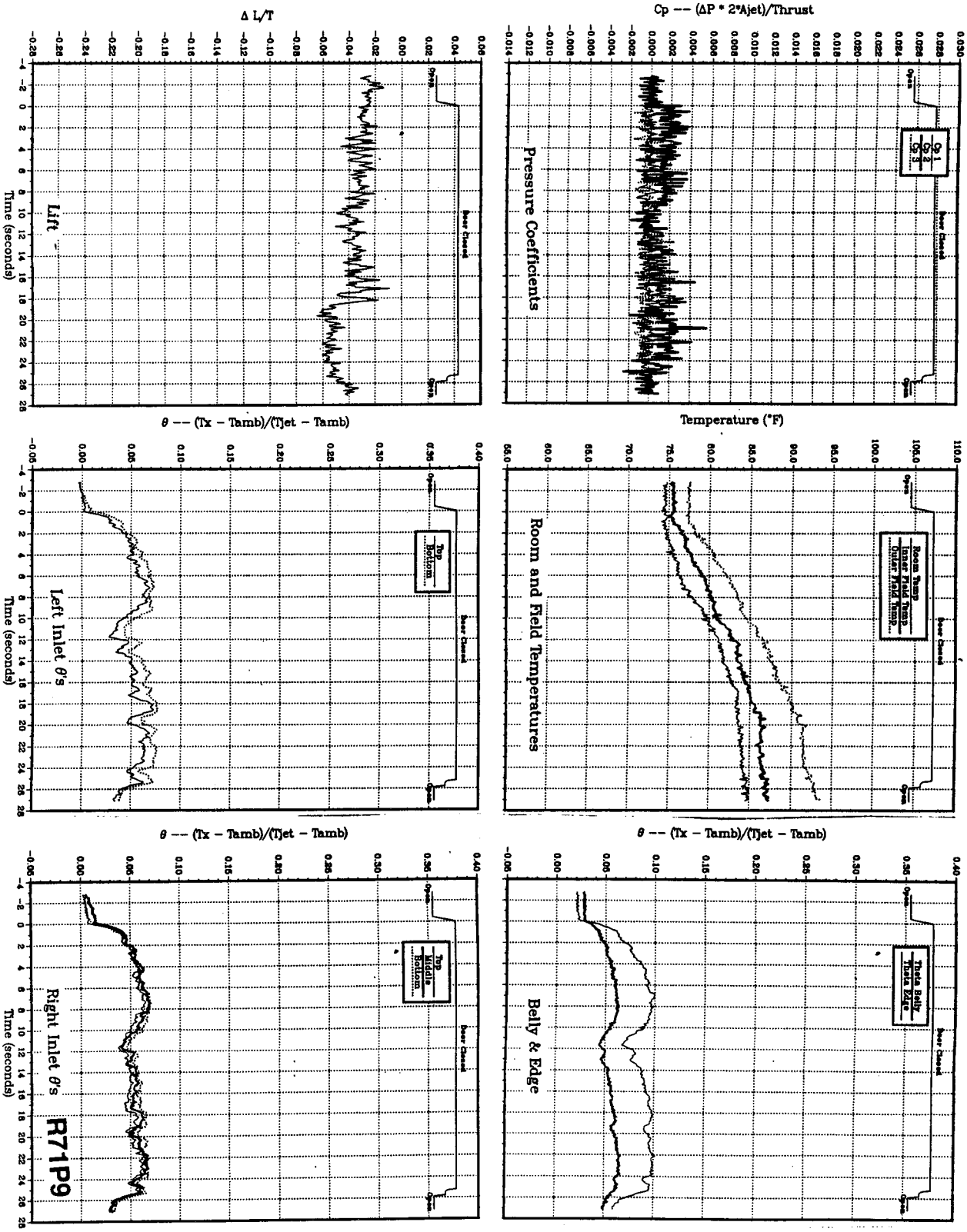

Figure 29(i). Body alone, no LIDs, NPR = 2.0, thrust = 50 lb, height = 15 in., Tjet = 510 °F, inlet position = 17 in.

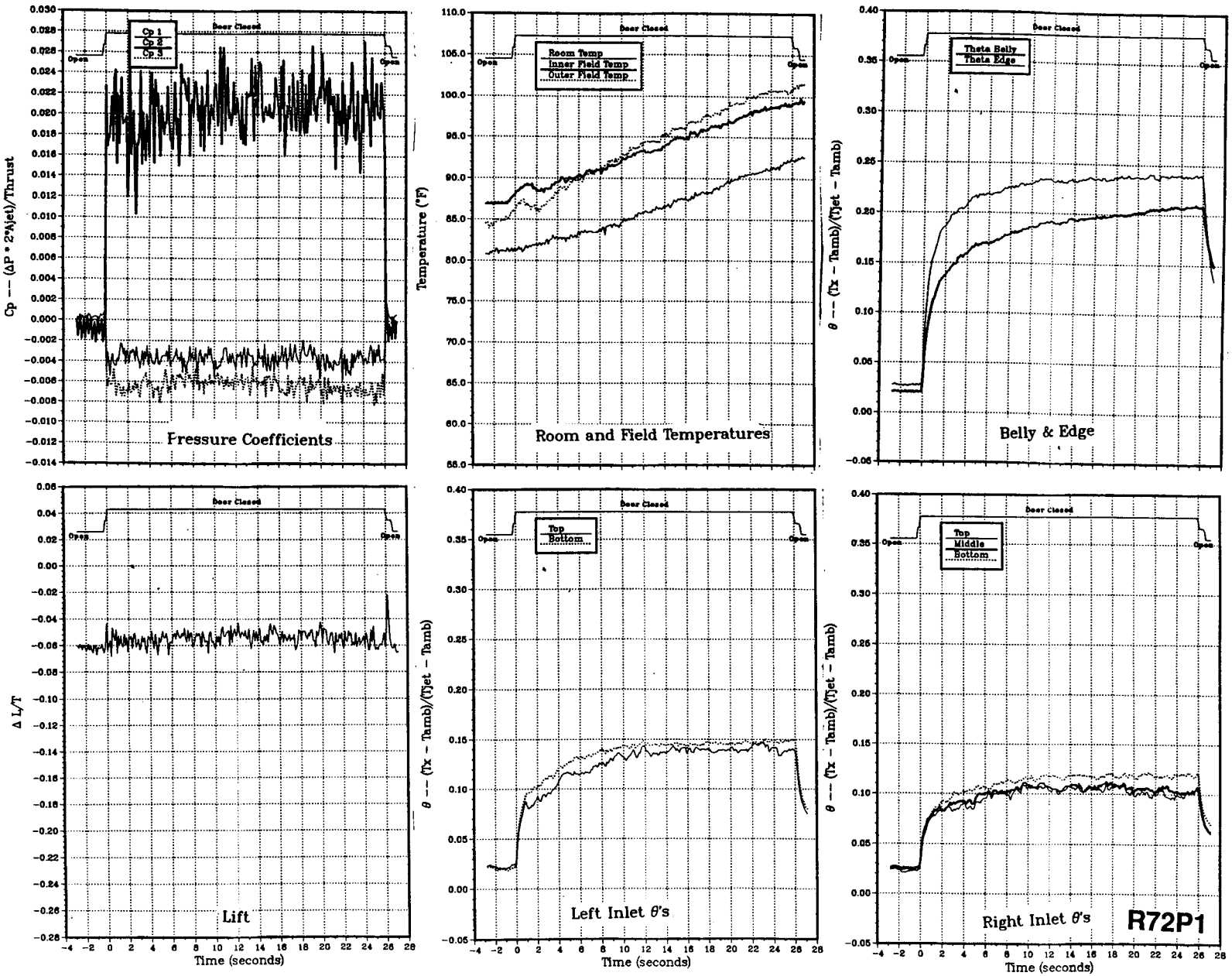

Figure 30(a). Body alone, no LIDs, NPR = 2.0, thrust = 50 lb, height = 4 in., Tjet = 671 °F, inlet position = 17 in.

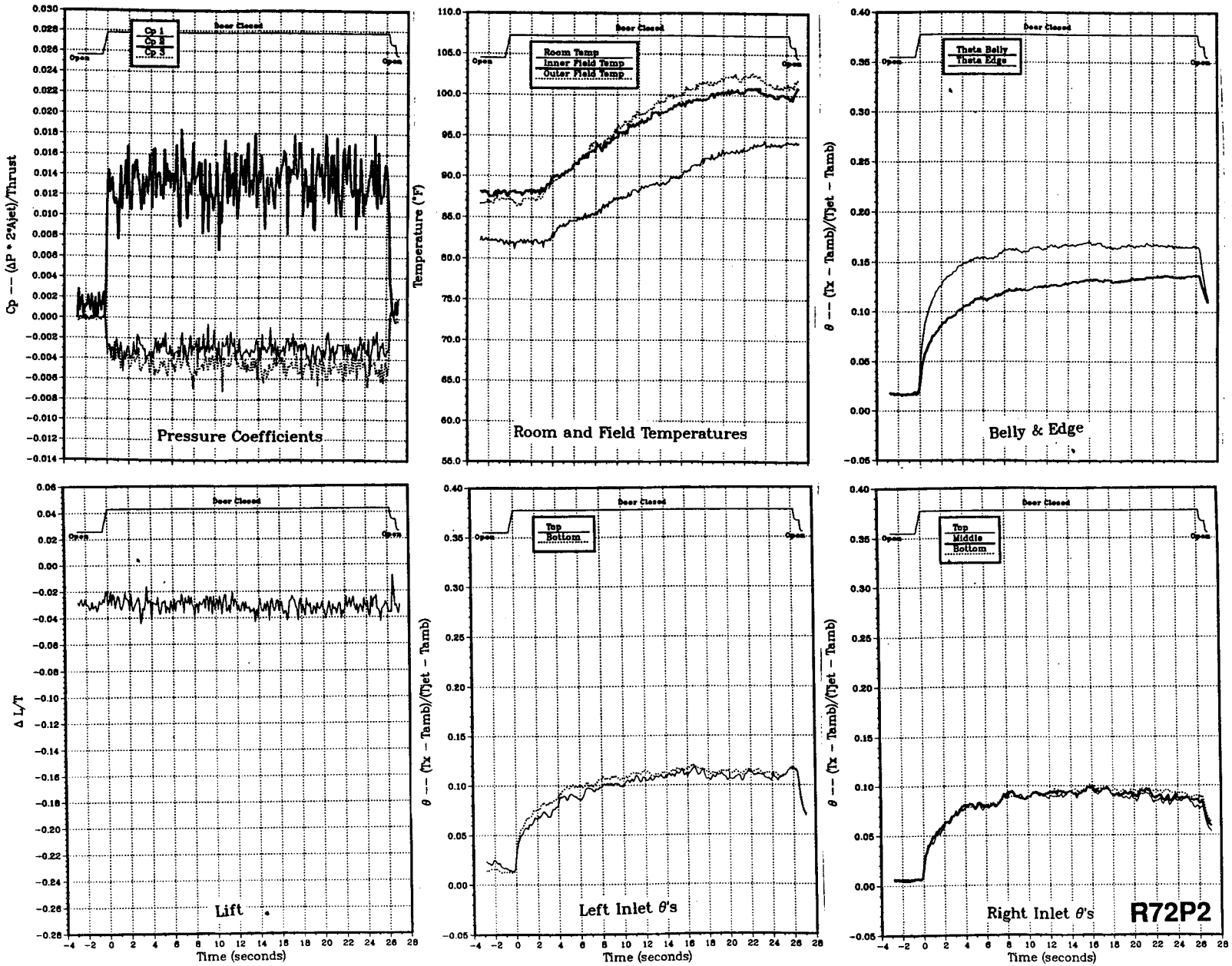

Figure 30(b). Body alone, no LIDs, NPR = 2.0, thrust = 50 lb, height = 6 in., Tjet = 696 °F, inlet position = 17 in.

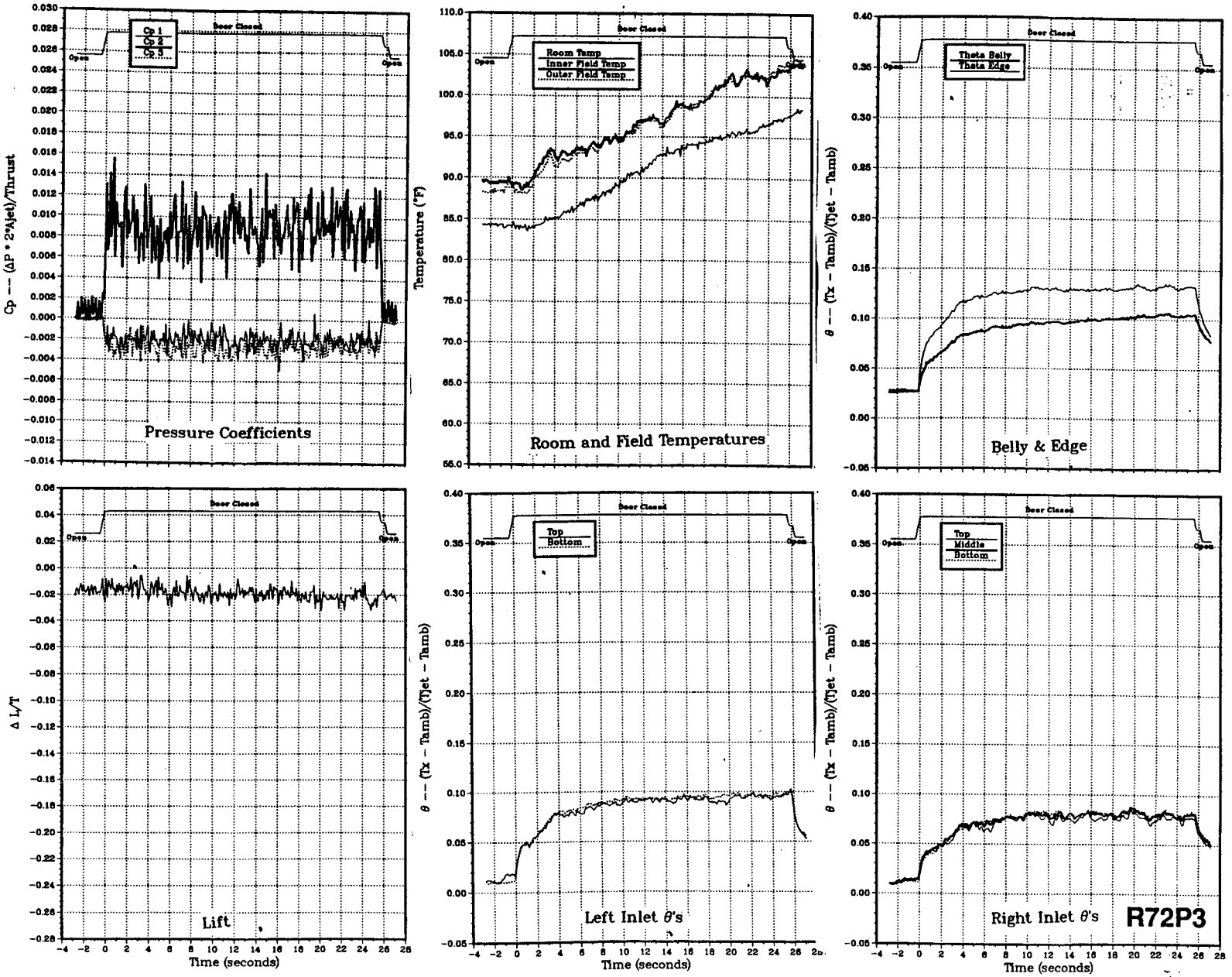

Figure 30(c). Body alone, no LIDs, NPR = 2.0, thrust = 50 lb, height = 8 in., Tjet = 698 °F, inlet position = 17 in.

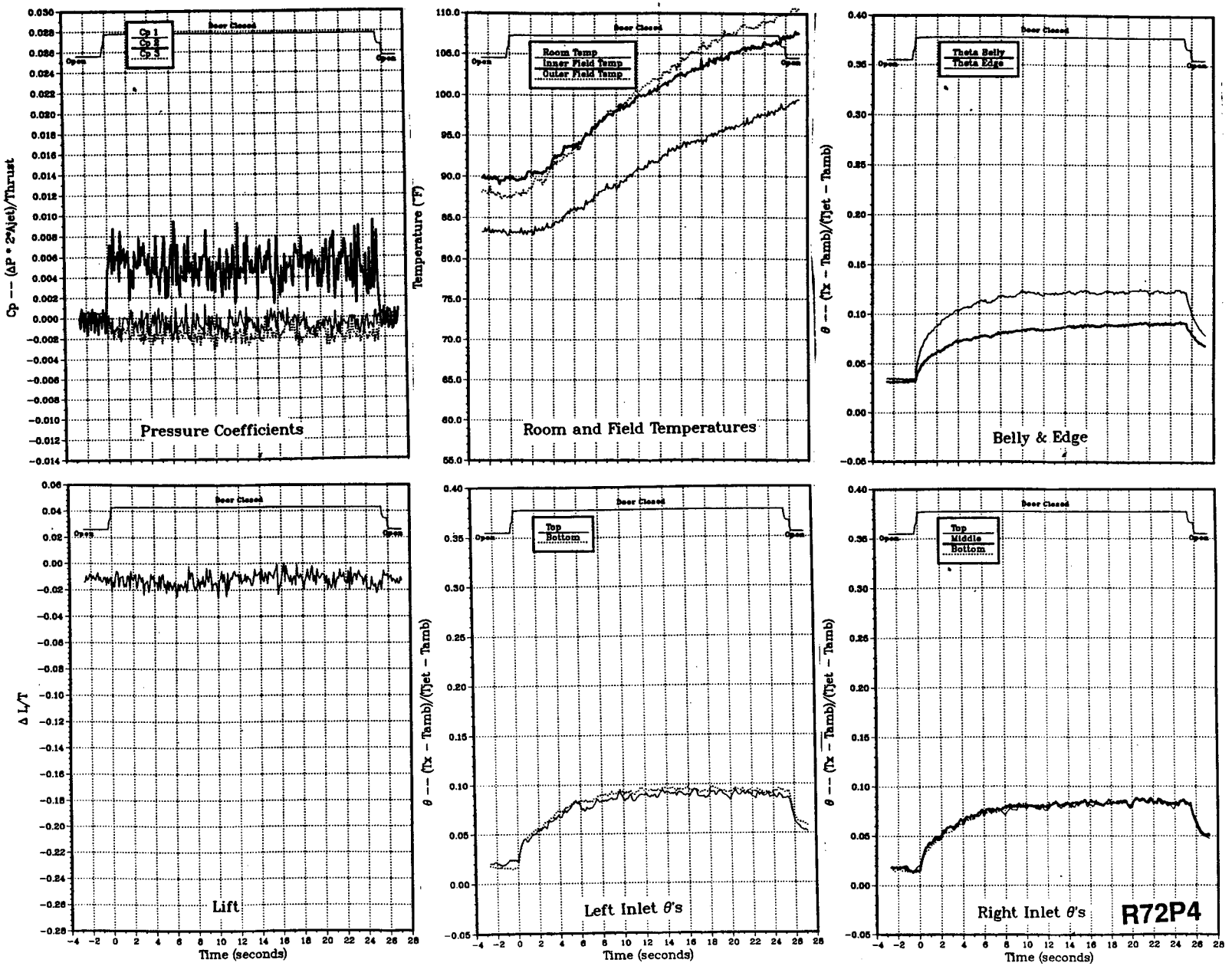

Figure 30(d). Body alone, no LIDs, NPR = 2.0, thrust = 50 lb, height = 10 in., Tjet = 699 °F, inlet position = 17 in.

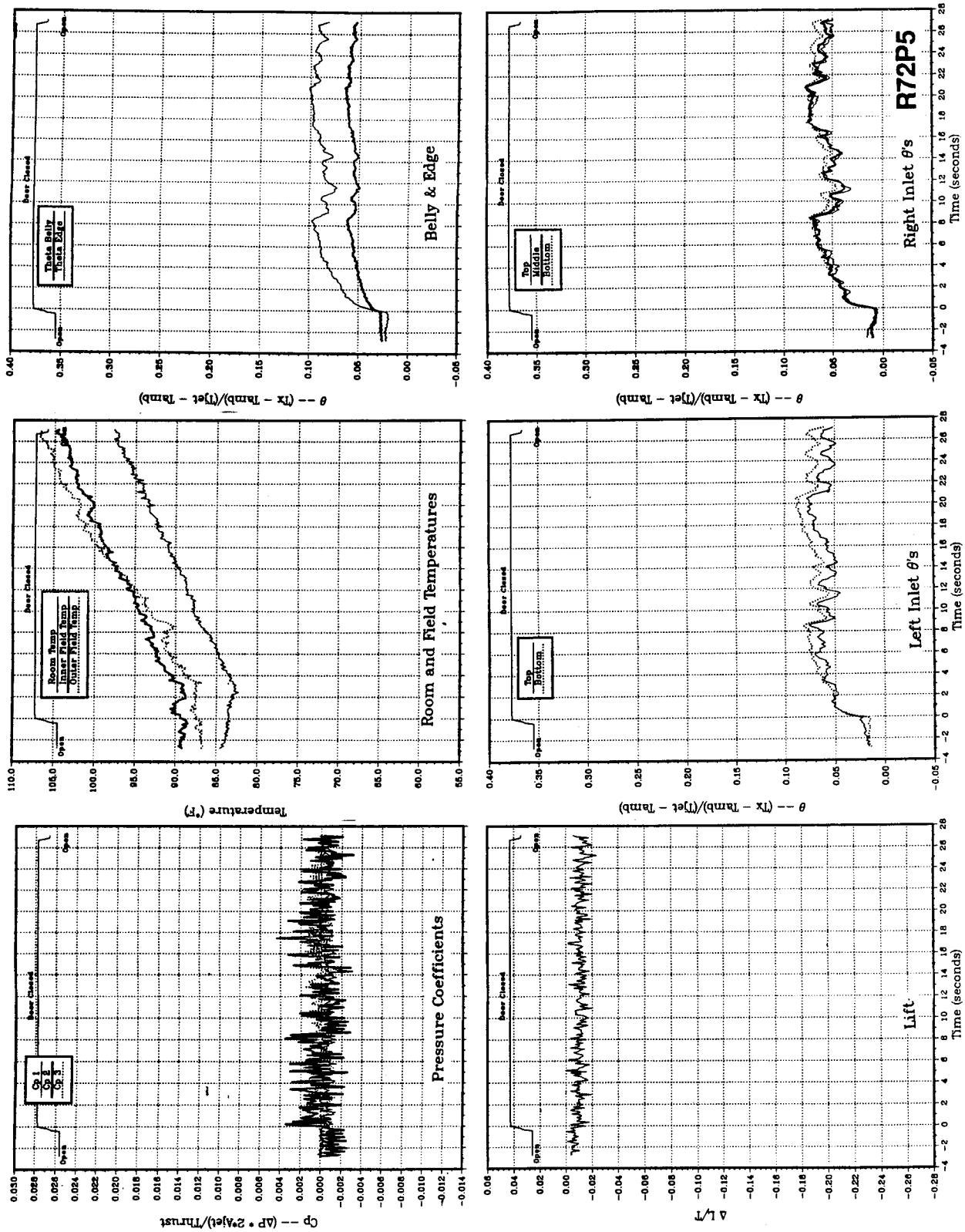

Figure 30(e). Body alone, no LIDs, NPR = 2.0, thrust = 50 lb, height = 15 in., Tjet = 699 °F, inlet position = 17 in.

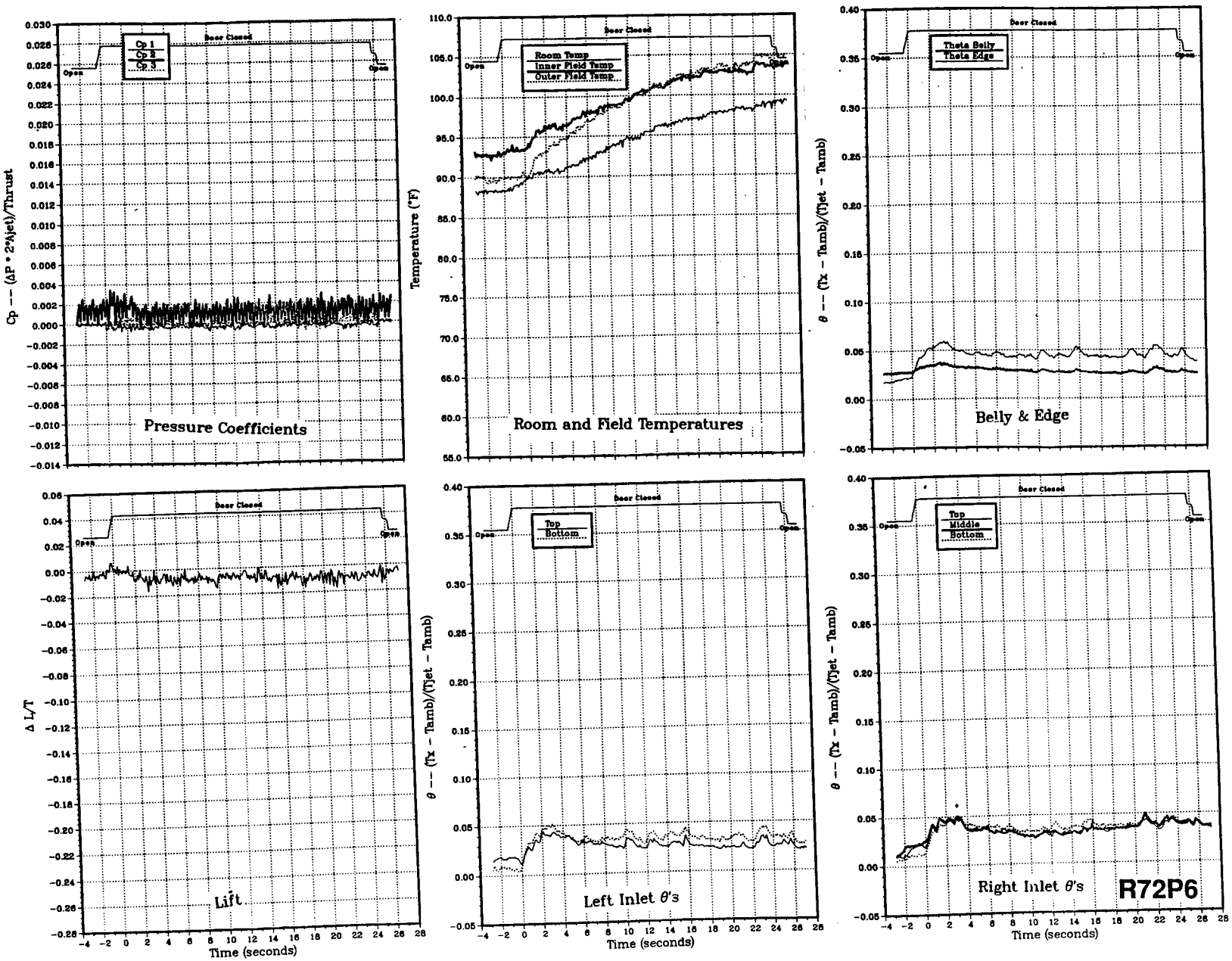

Figure 30(f). Body alone, no LIDs, NPR = 2.0, thrust = 50 lb, height = 20 in., Tjet = 701 °F, inlet position = 17 in.

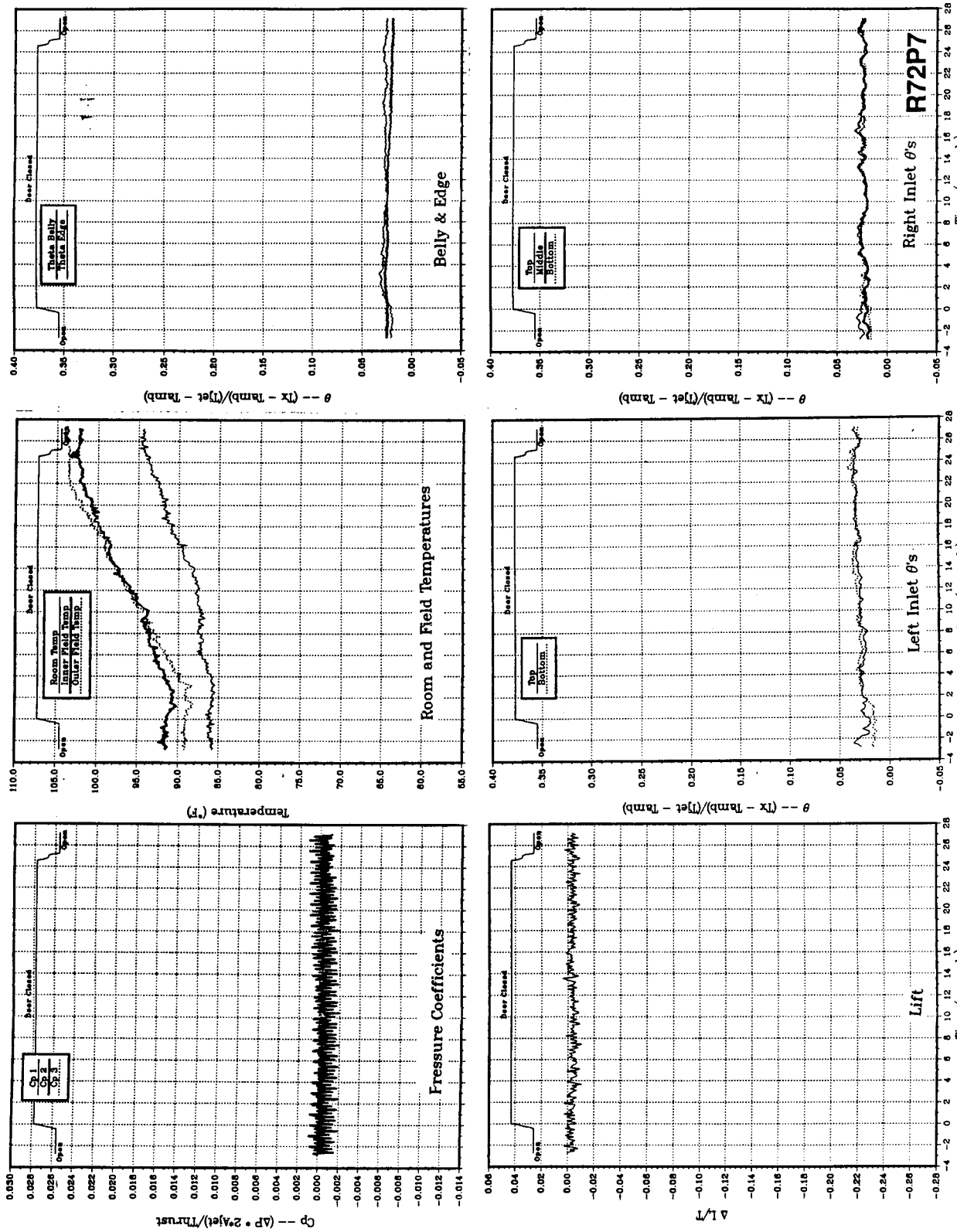

Figure 30(g). Body alone, no LIDs, NPR = 2.0, thrust = 50 lb, height = 30 in., Tjet = 702 °F, inlet position = 17 in.

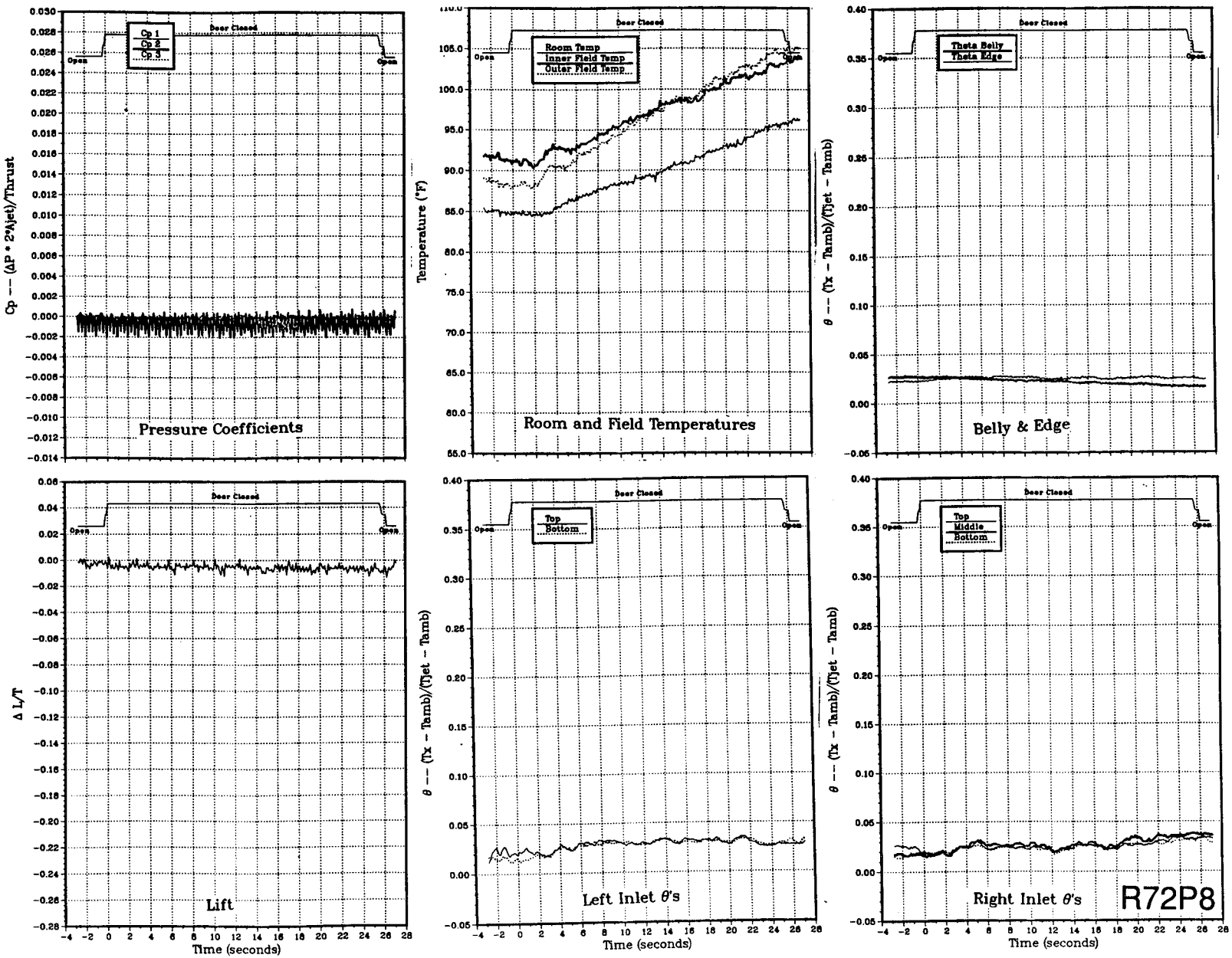

Figure 30(h). Body alone, no LIDs, NPR = 2.0, thrust = 50 lb, height = 40 in., Tjet = 703 °F, inlet position = 17 in.

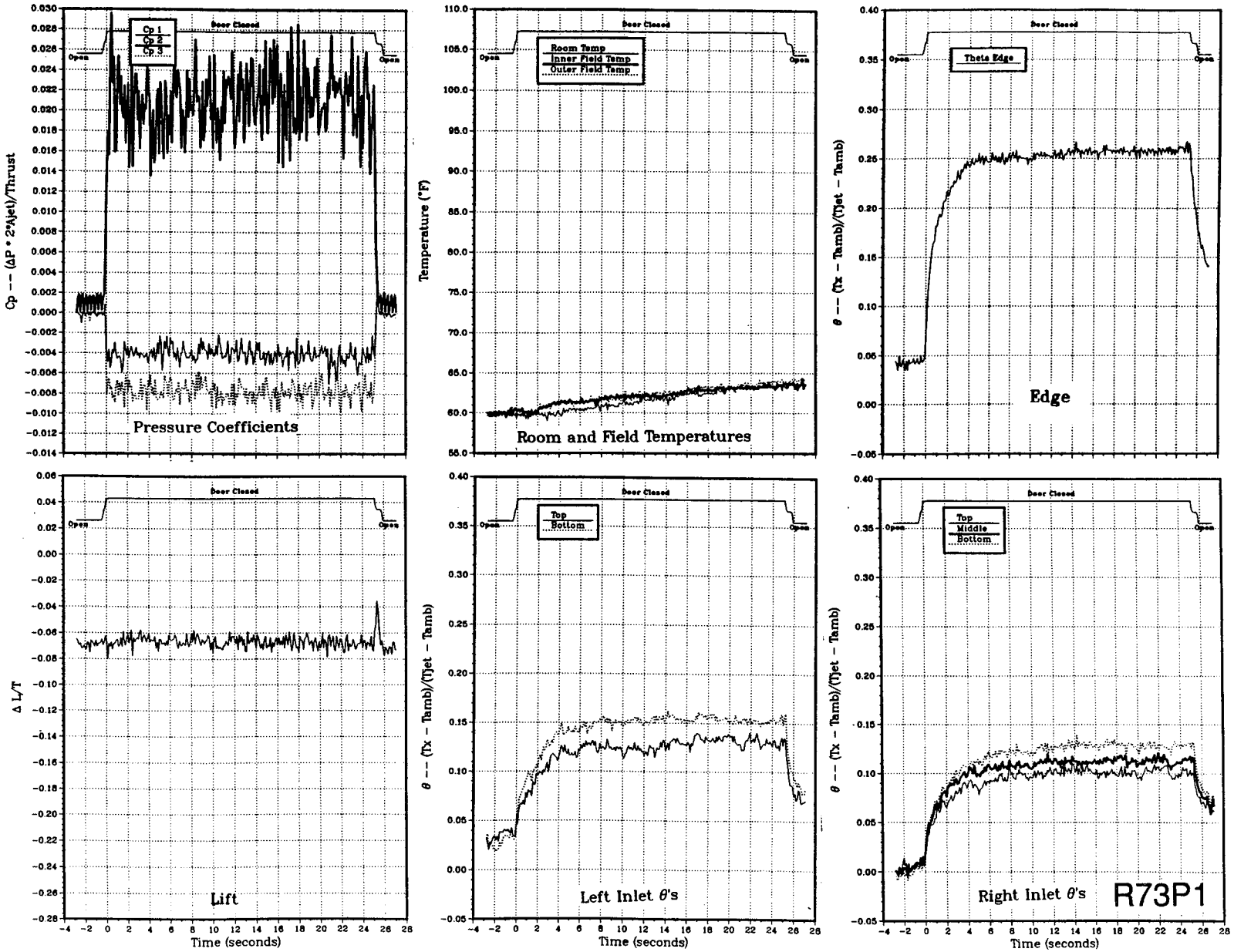

Figure 31(a). Body alone, no LIDs, NPR = 2.0, thrust = 50 lb, height = 4 in., Tjet = 174 °F, inlet position = 17 in.

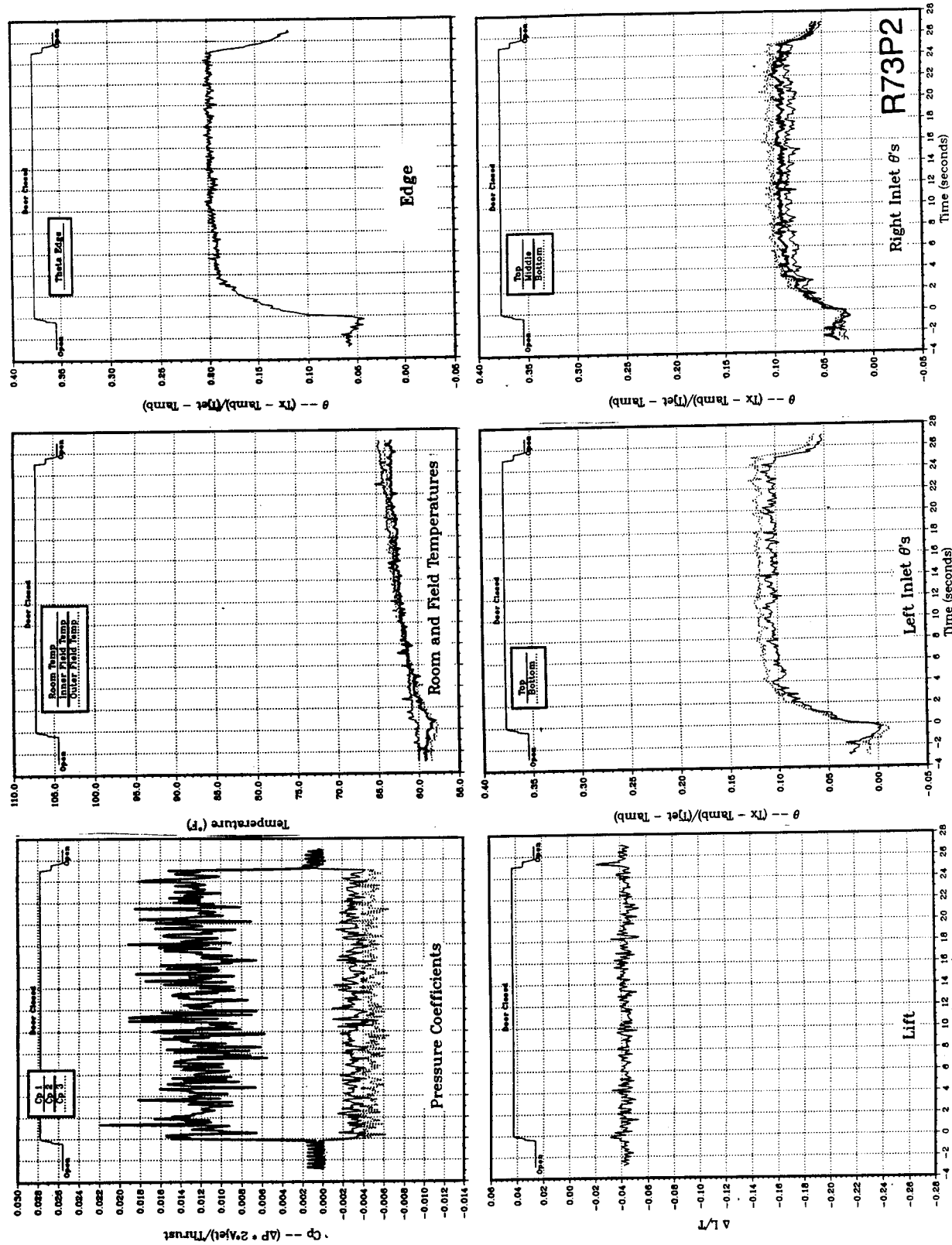

Figure 31(b). Body alone, no LIDs, NPR = 2.0, thrust = 50 lb, height = 6 in., Tjet = 188 °F, inlet position = 17 in.

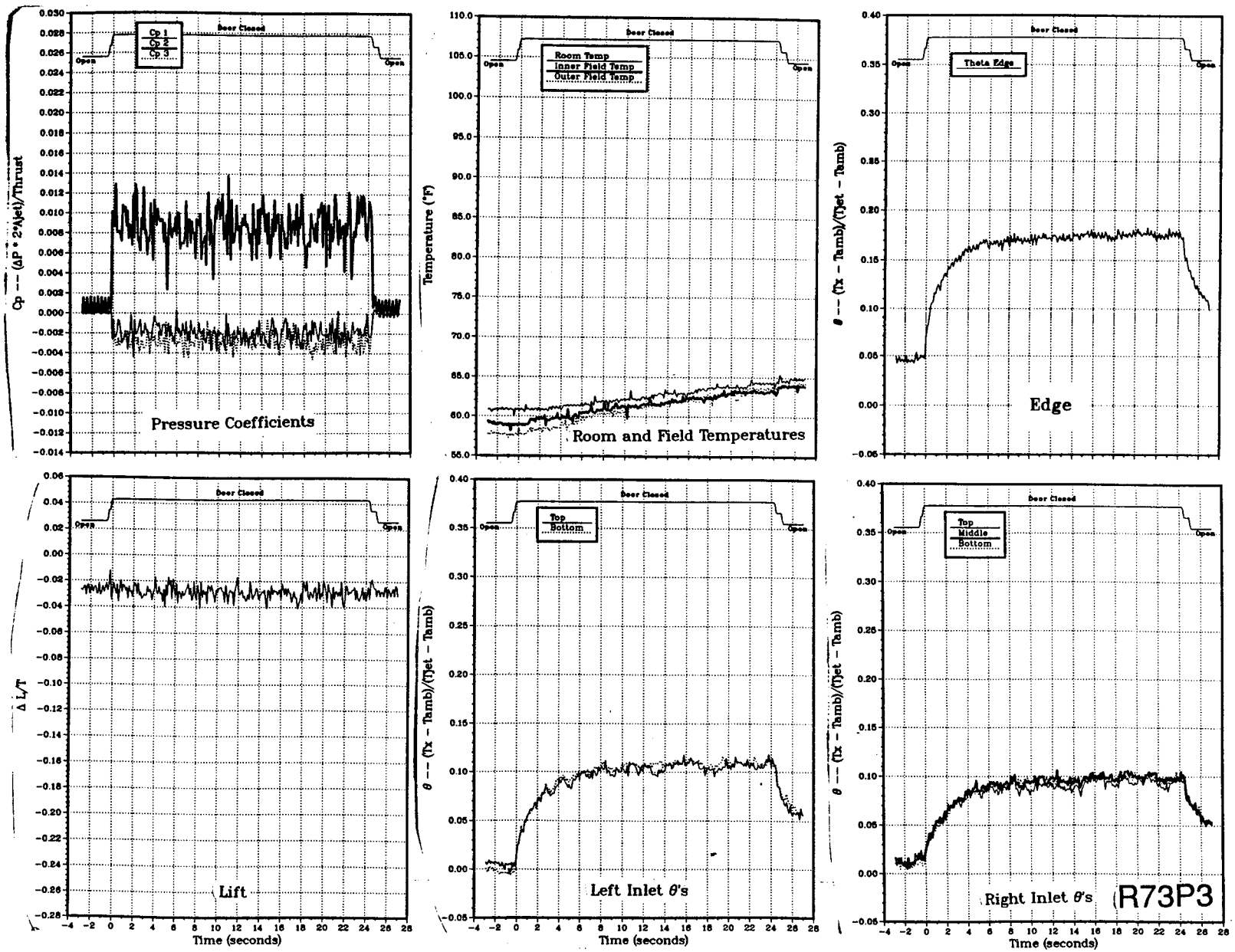

Figure 31(c). Body alone, no LIDs, NPR = 2.0, thrust = 50 lb, height = 8 in., Tjet = 192 °F, inlet position = 17 in.

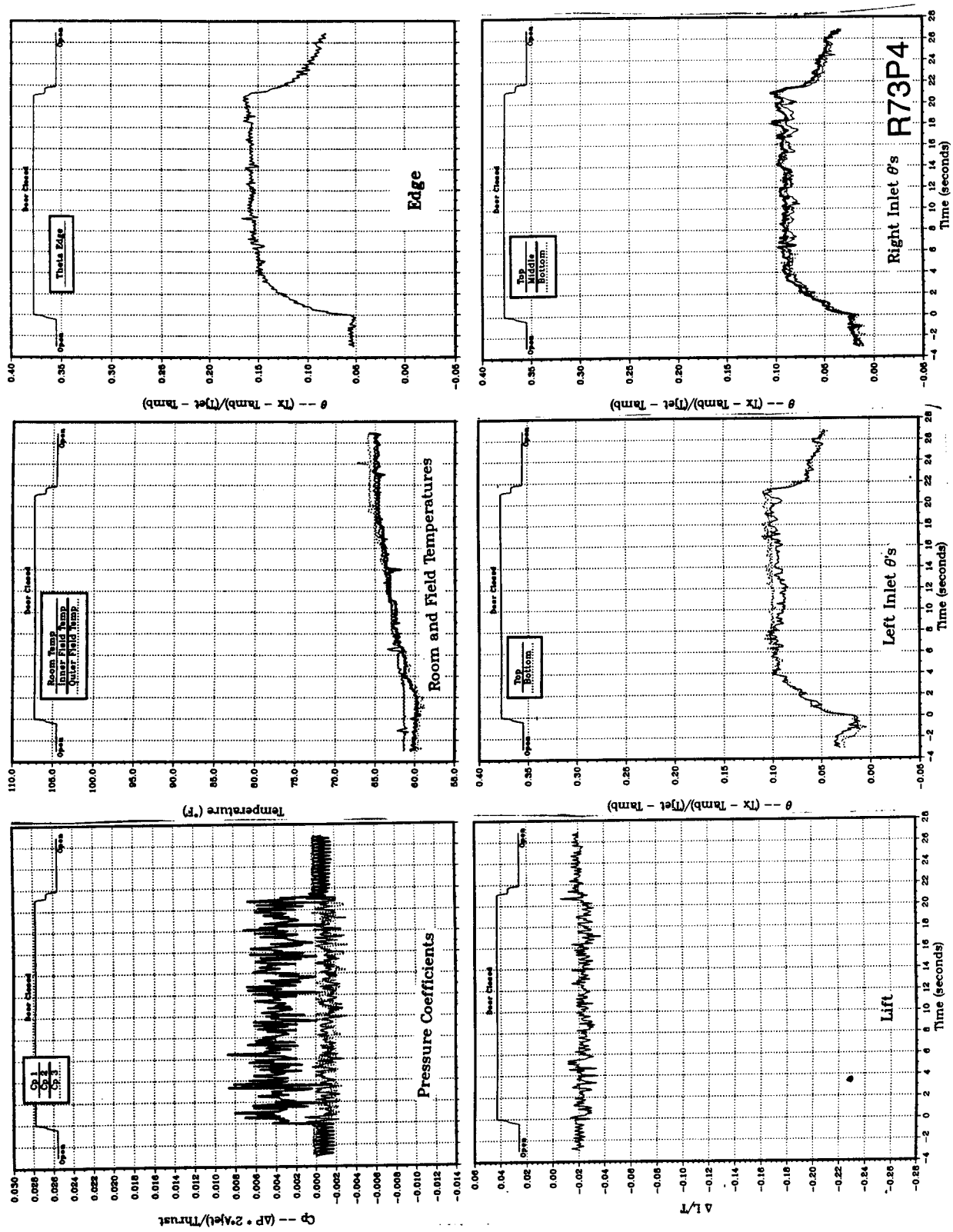

Figure 31(d). Body alone, no LIDs, NPR = 2.0, thrust = 50 lb, height = 10 in., Tjet = 201 °F, inlet position = 17 in.

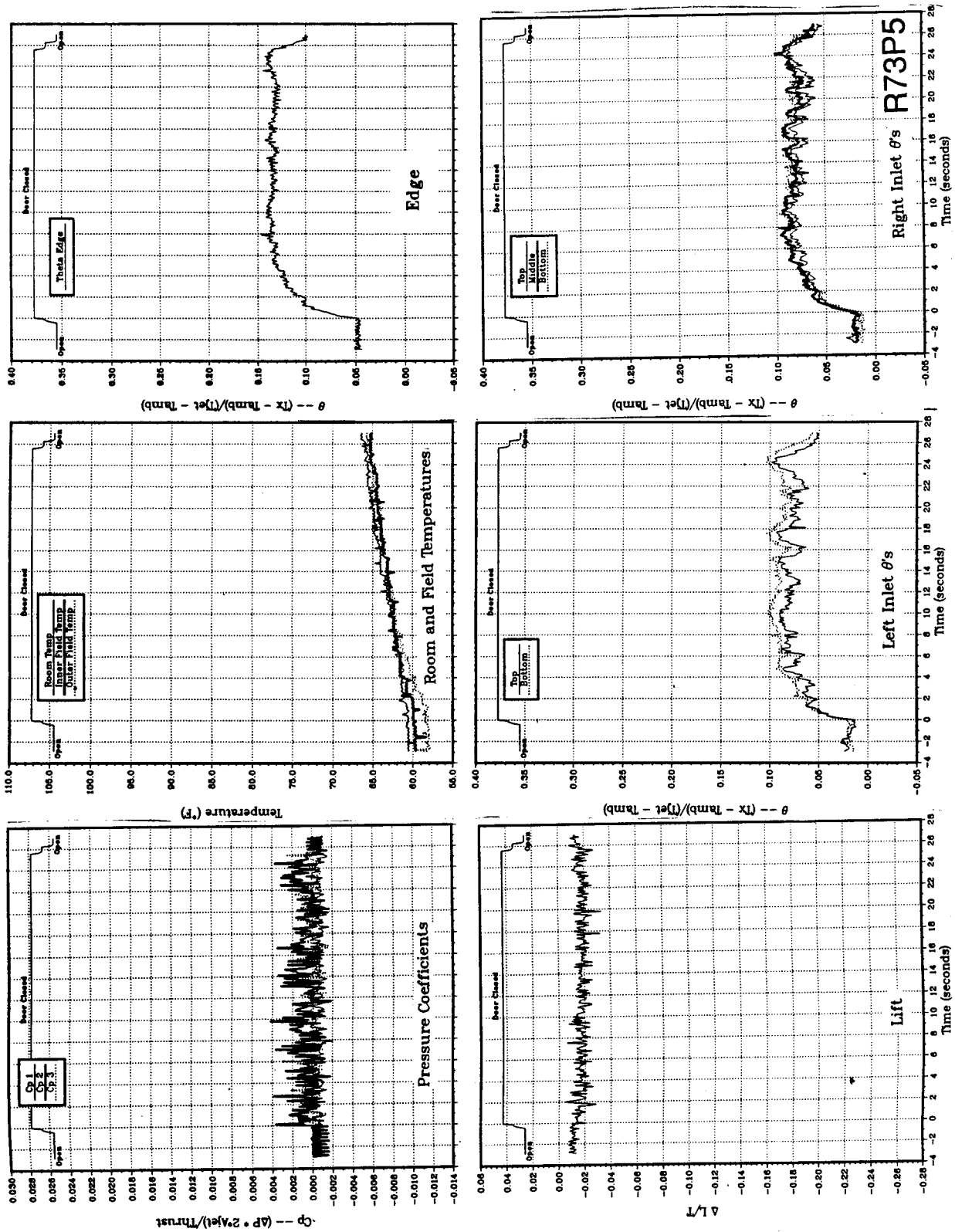

Figure 31(e). Body alone, no LIDs, NPR = 2.0, thrust = 50 lb, height = 15 in., Tjet = 204 °F, inlet position = 17 in.

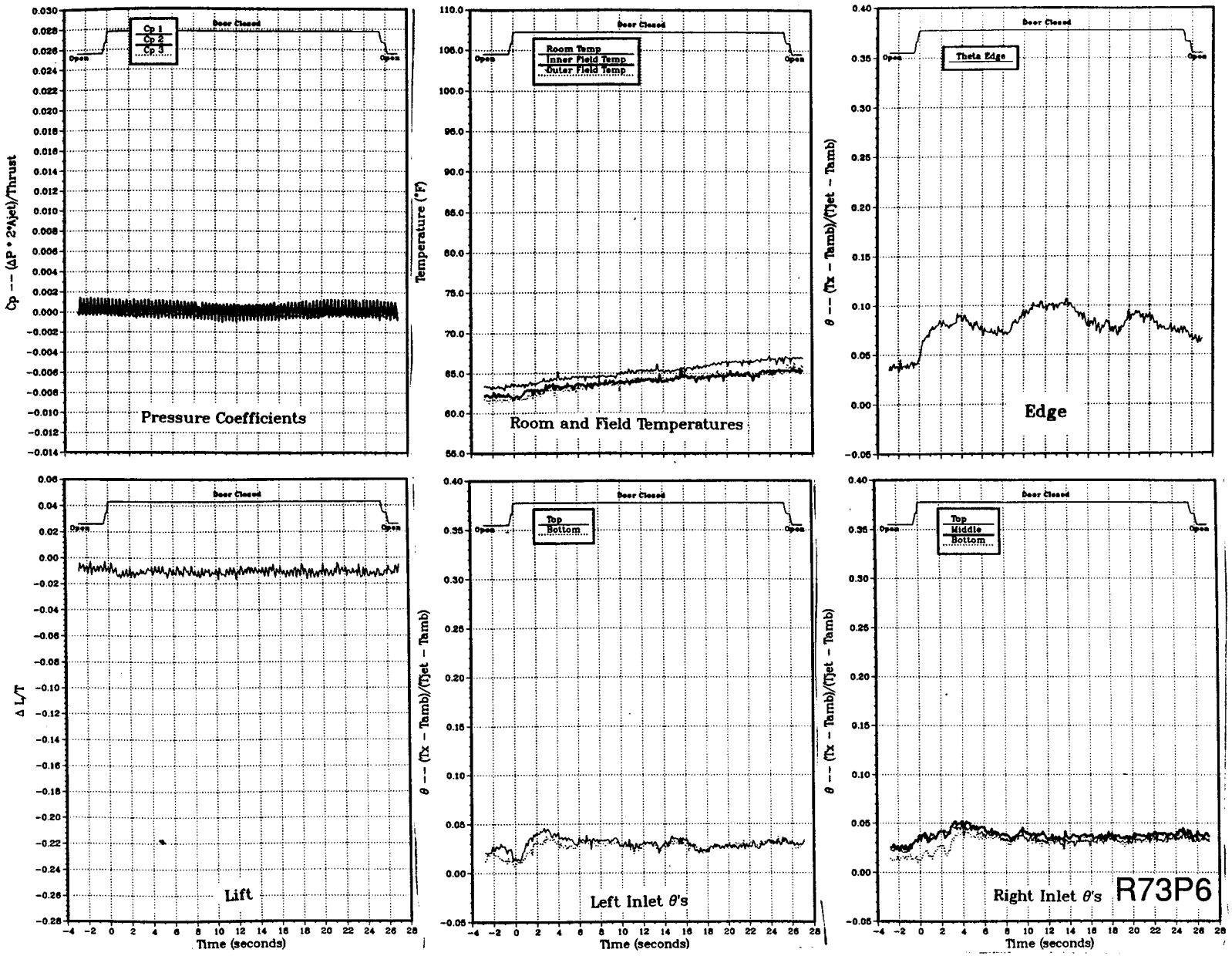

Figure 31(f). Body alone, no LIDs, NPR = 2.0, thrust = 50 lb, height = 20 in., Tjet = 208 °F, inlet position = 17 in.

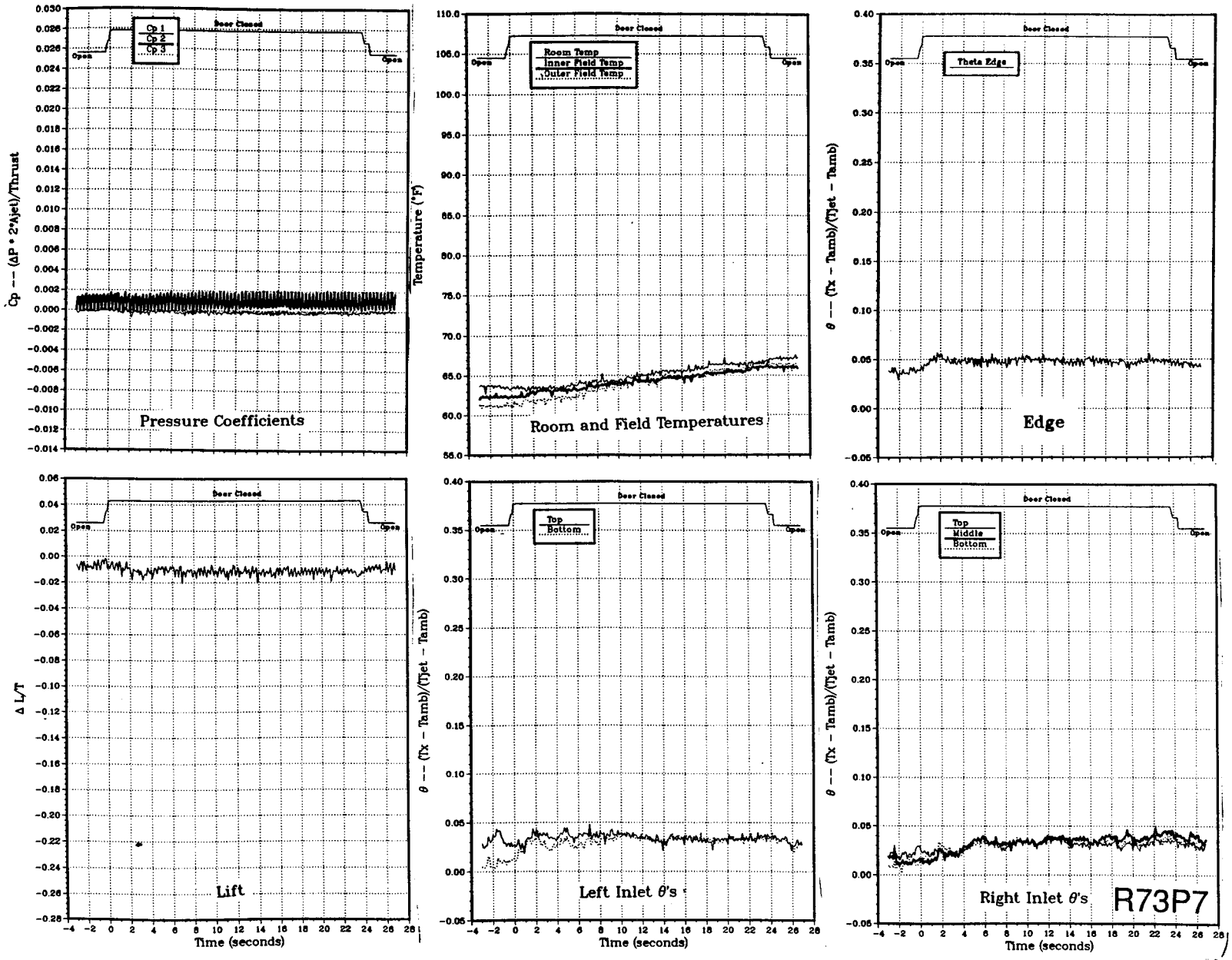

Figure 31(g). Body alone, no LIDs, NPR = 2.0, thrust = 50 lb, height = 30 in., Tjet = 210 °F, inlet position = 17 in.

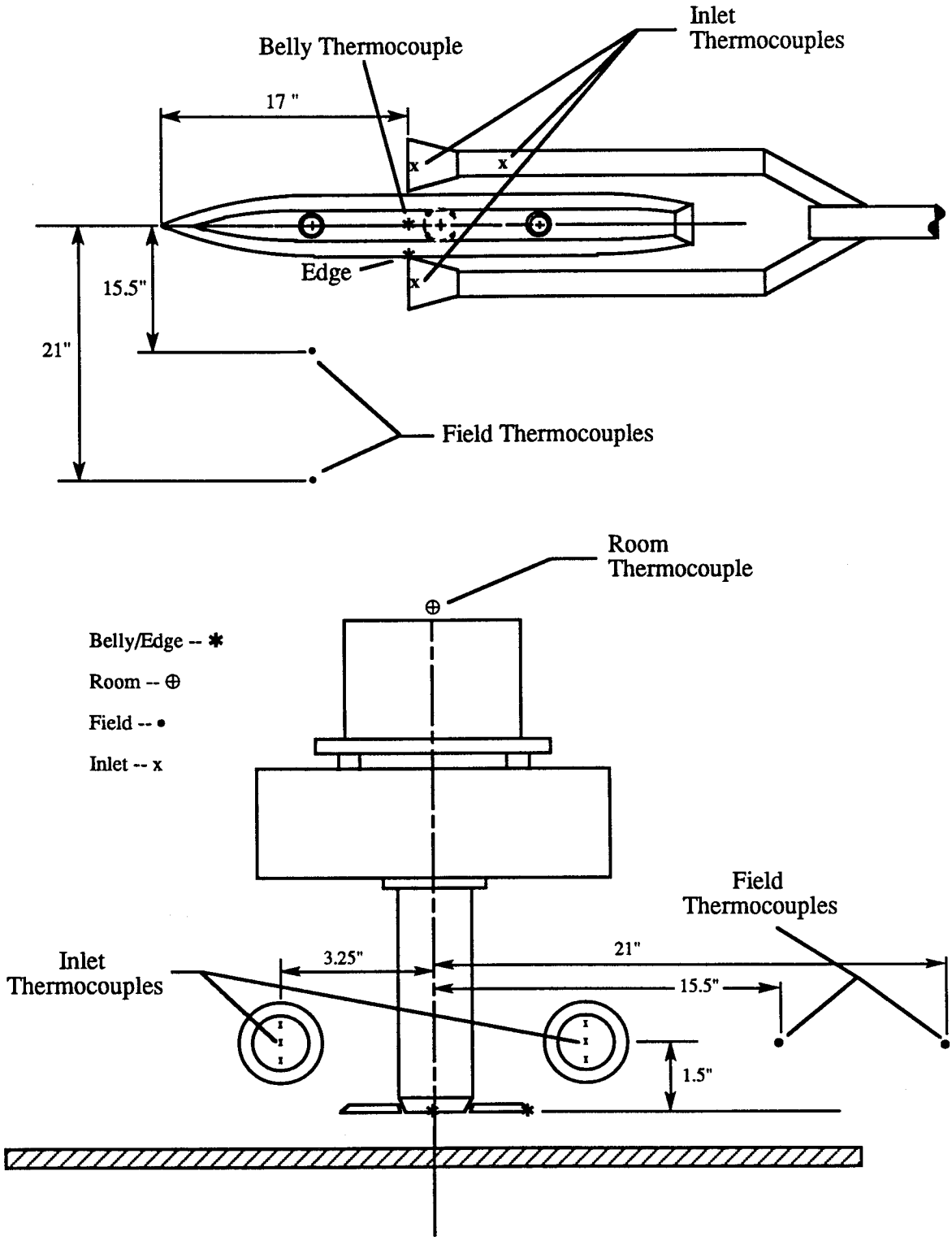

Figure 32. Locations of model and field thermocouples for data set 6.

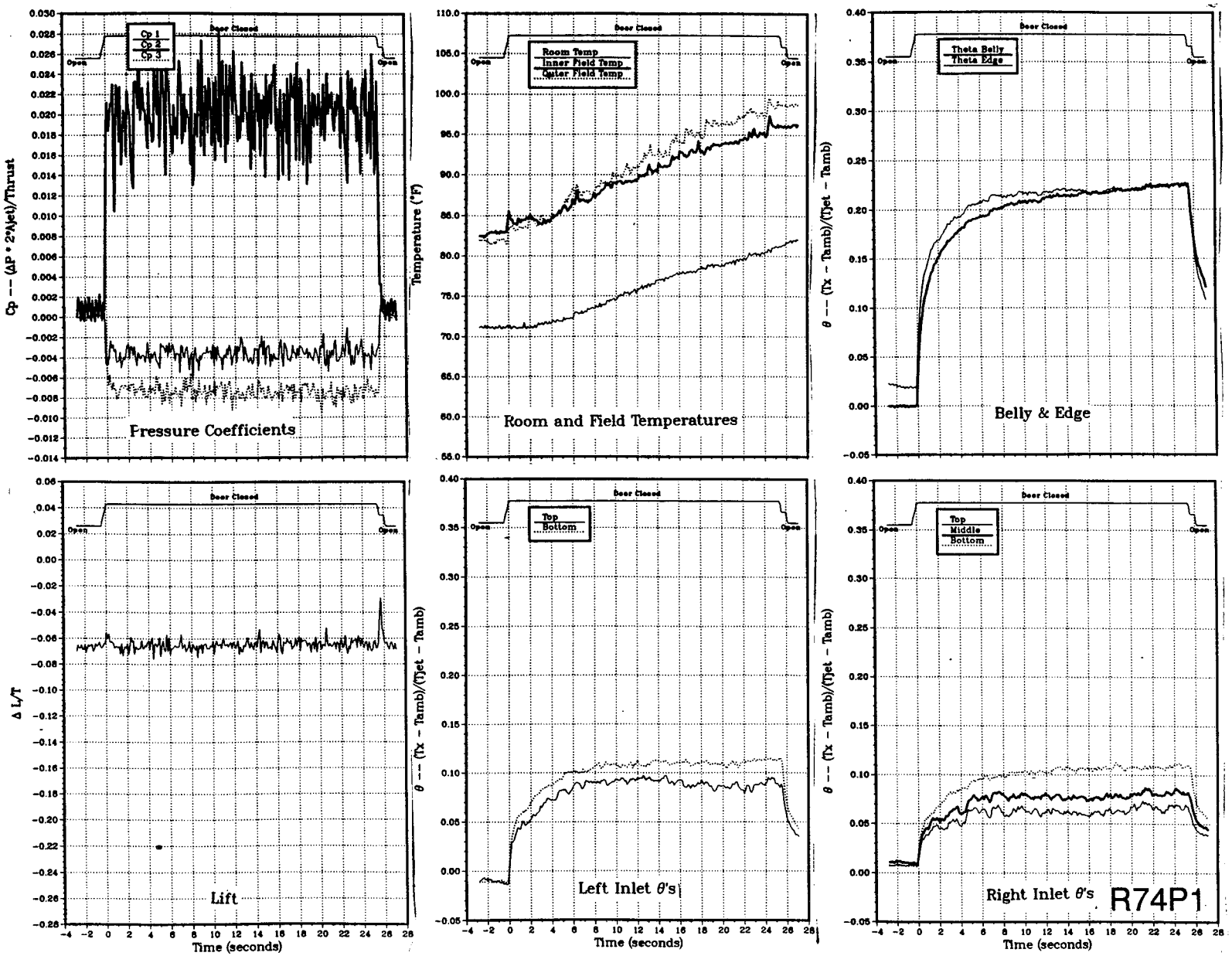

Figure 33(a). Body alone, no LIDs, NPR = 2.0, thrust = 50 lb, height = 4 in., Tjet = 480 °F, inlet position = 17 in.

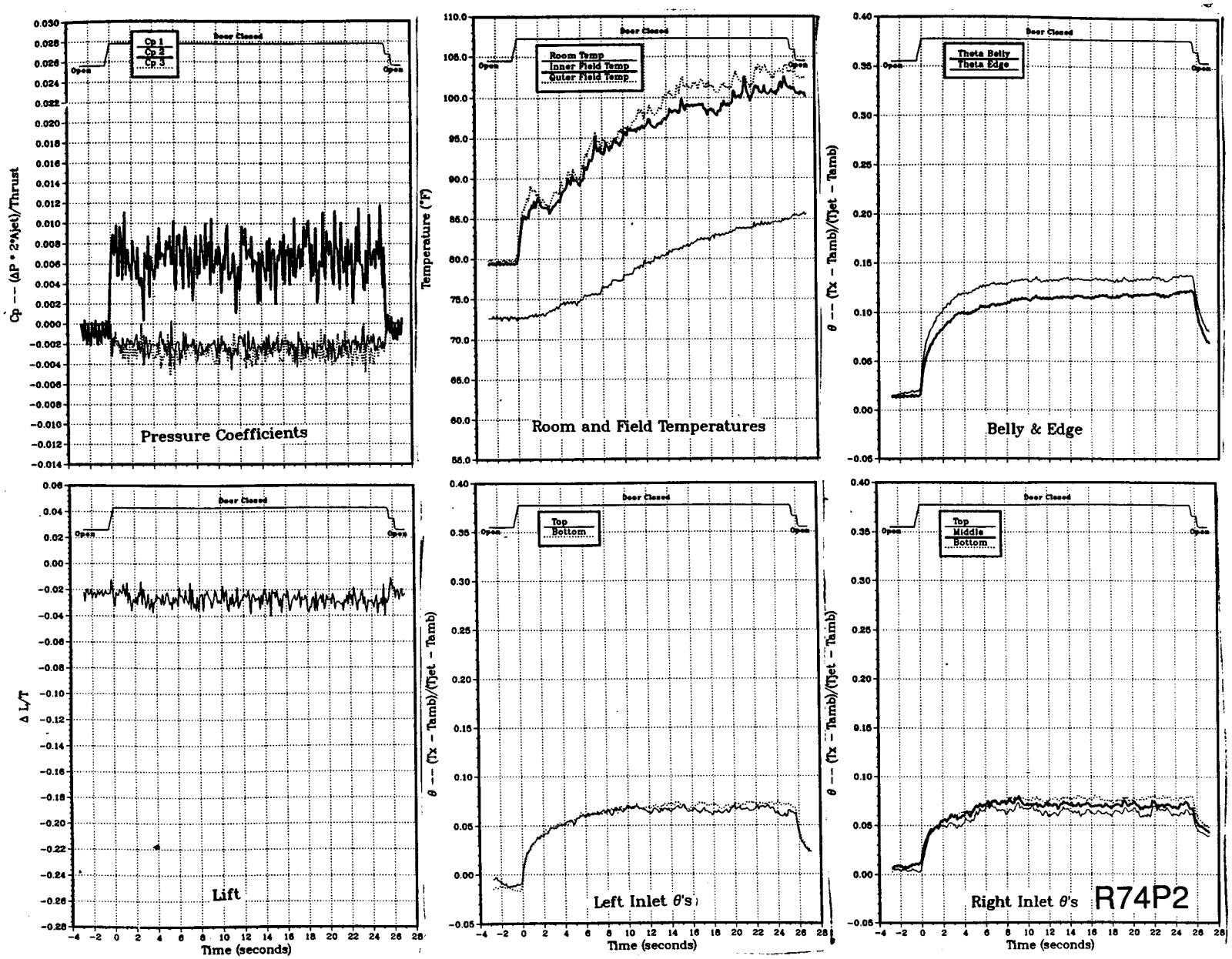

Figure 33(b). Body alone, no LIDs, NPR = 2.0, thrust = 50 lb, height = 8 in., Tjet = 485 °F, inlet position = 17 in.

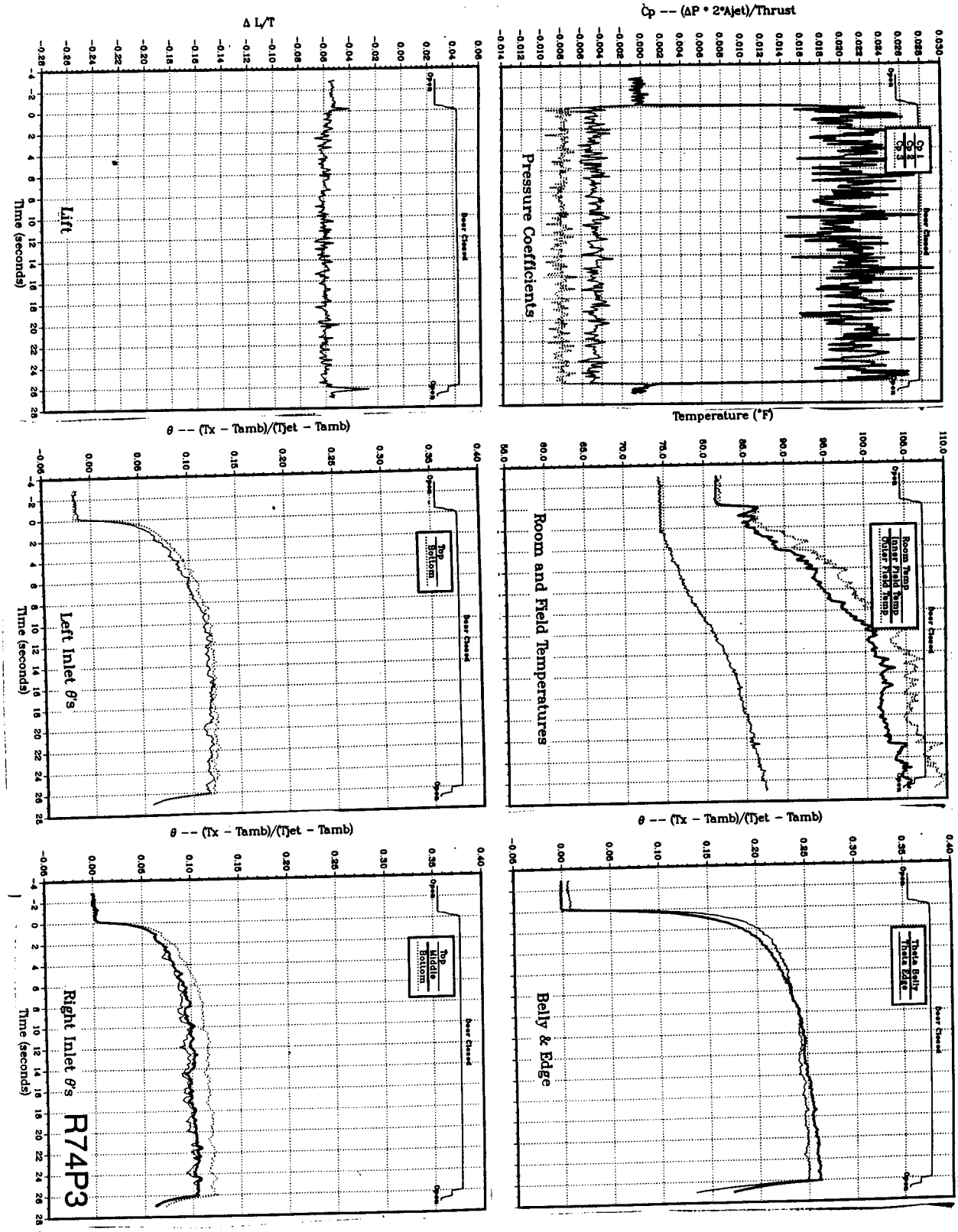

Figure 33(c). Body alone, no LIDs, NPR = 3.0, thrust = 92 lb, height = 4 in., Tjet = 500 °F, inlet position = 17 in.

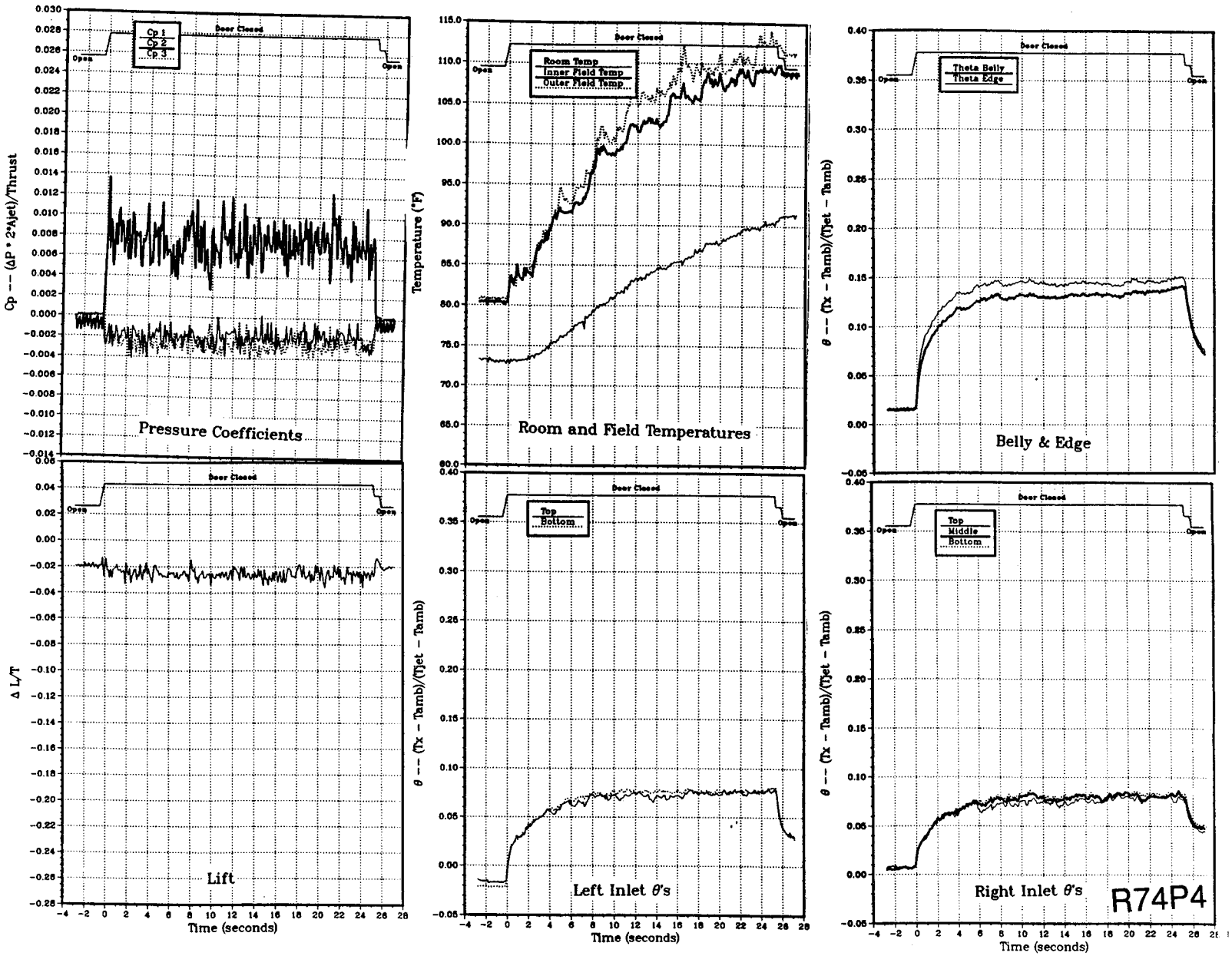

Figure 33(d). Body alone, no LIDs, NPR = 3.0, thrust = 92 lb, height = 8 in., Tjet = 509 °F, inlet position = 17 in.

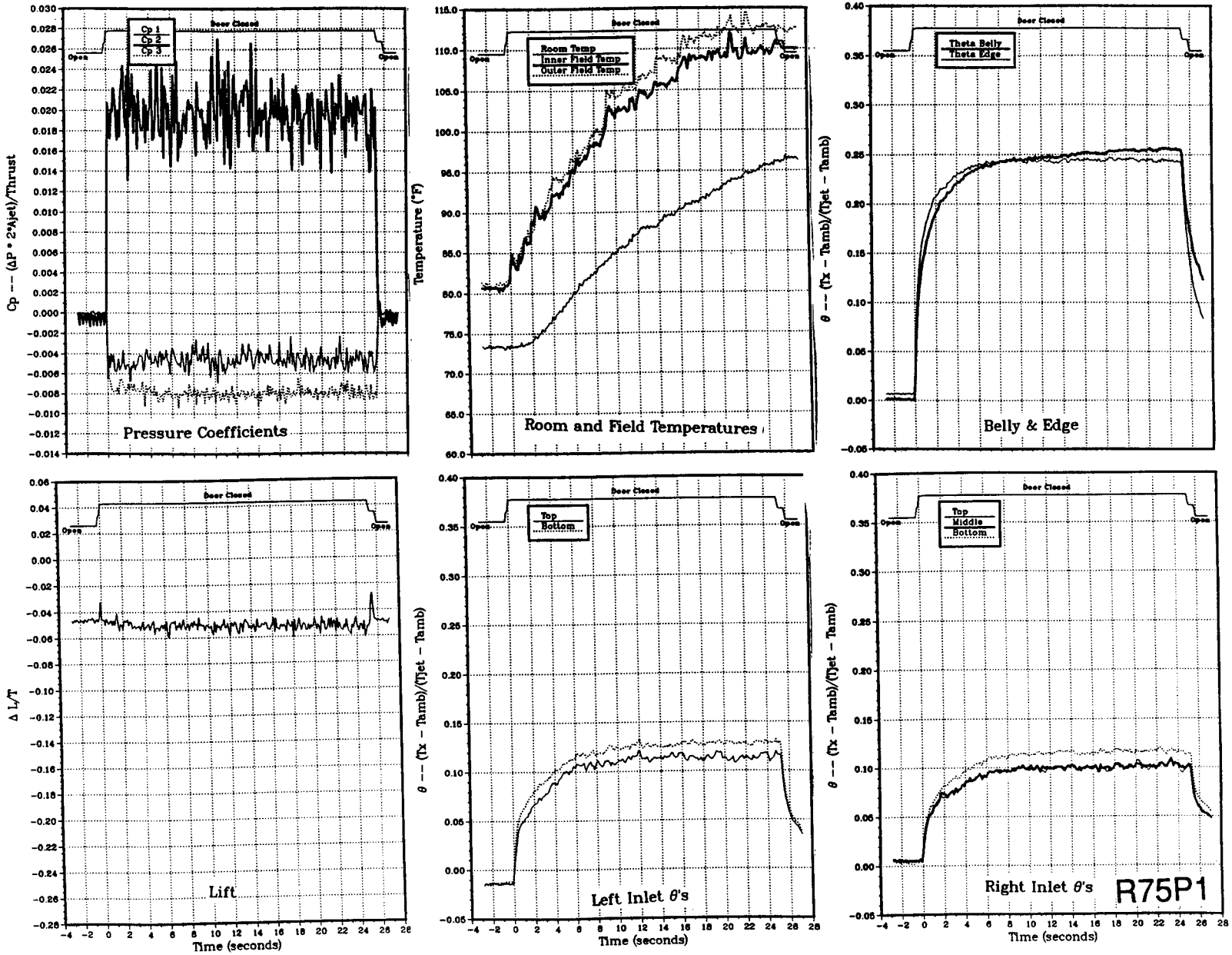

Figure 34(a). Body alone, no LIDs, NPR = 4.0, thrust = 133 lb, height = 4 in., Tjet = 525 °F, inlet position = 17 in.

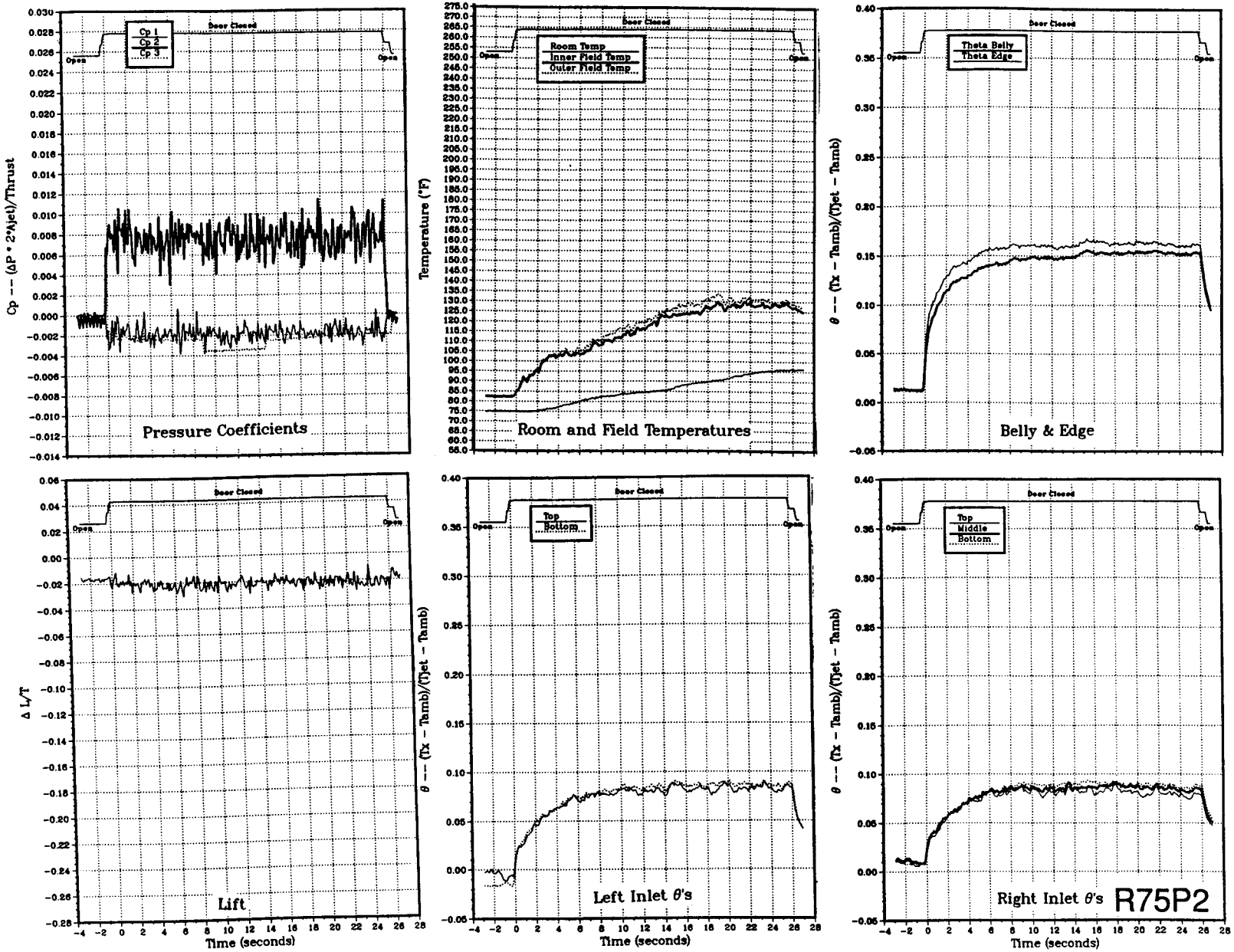

Figure 34(b). Body alone, no LIDs, NPR = 4.0, thrust = 133 lb, height = 8 in., Tjet = 533 °F, inlet position = 17 in.

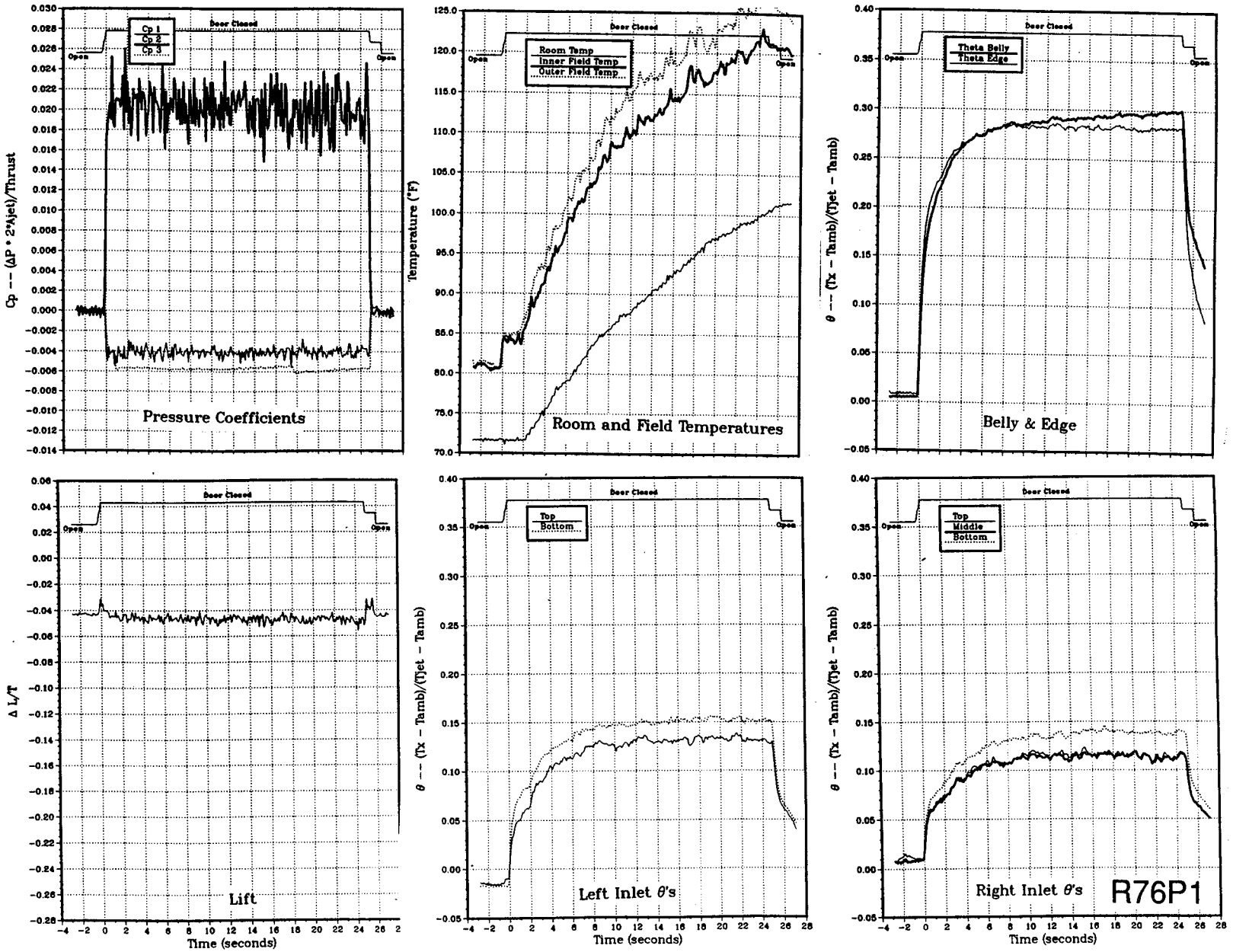

Figure 35(a). Body alone, no LIDs, NPR = 5.0, thrust = 176 lb, height = 4 in., Tjet = 545 °F, inlet position = 17 in.

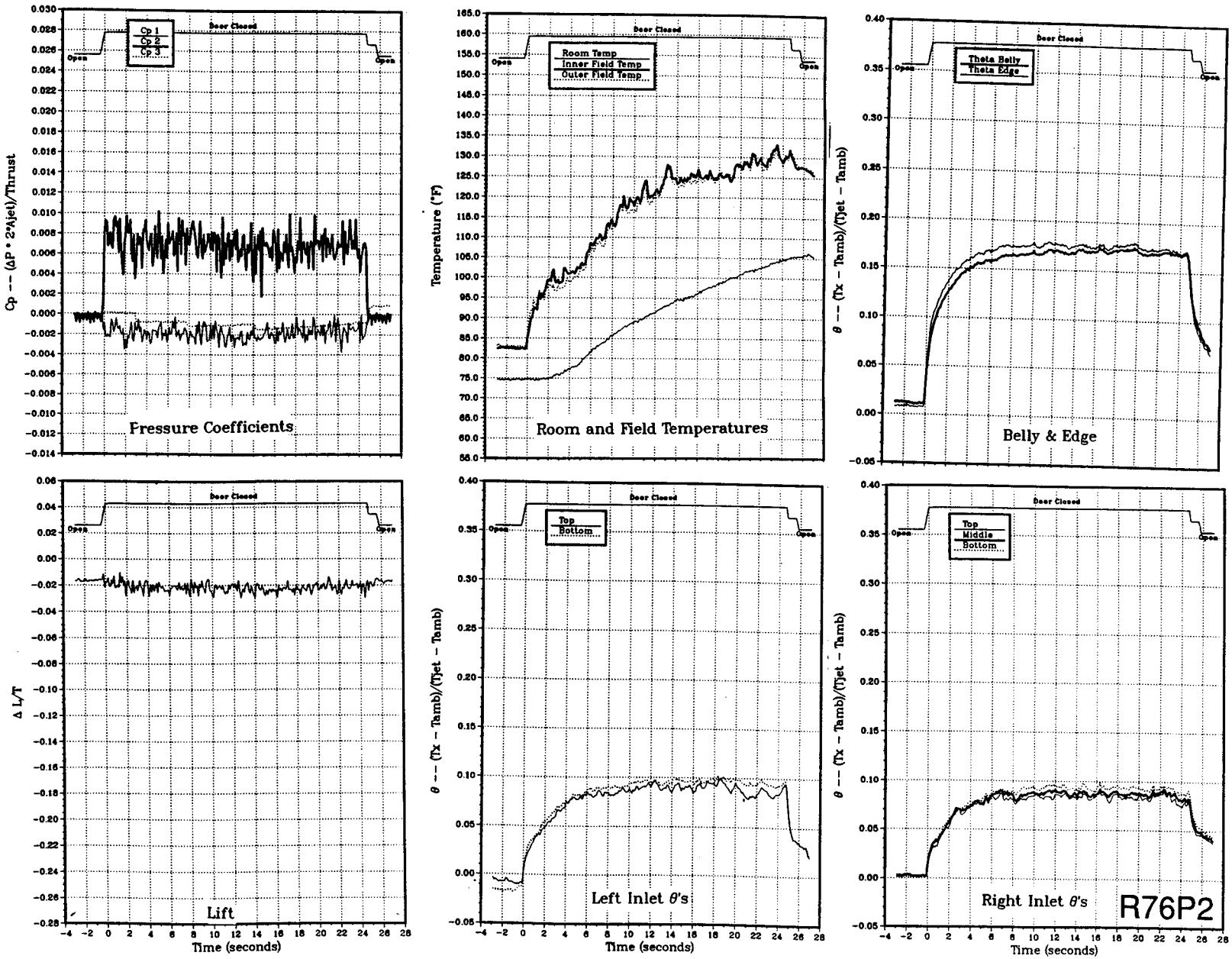

Figure 35(b). Body alone, no LIDs, NPR = 5.0, thrust = 176 lb, height = 8 in., Tjet = 550 °F, inlet position = 17 in.

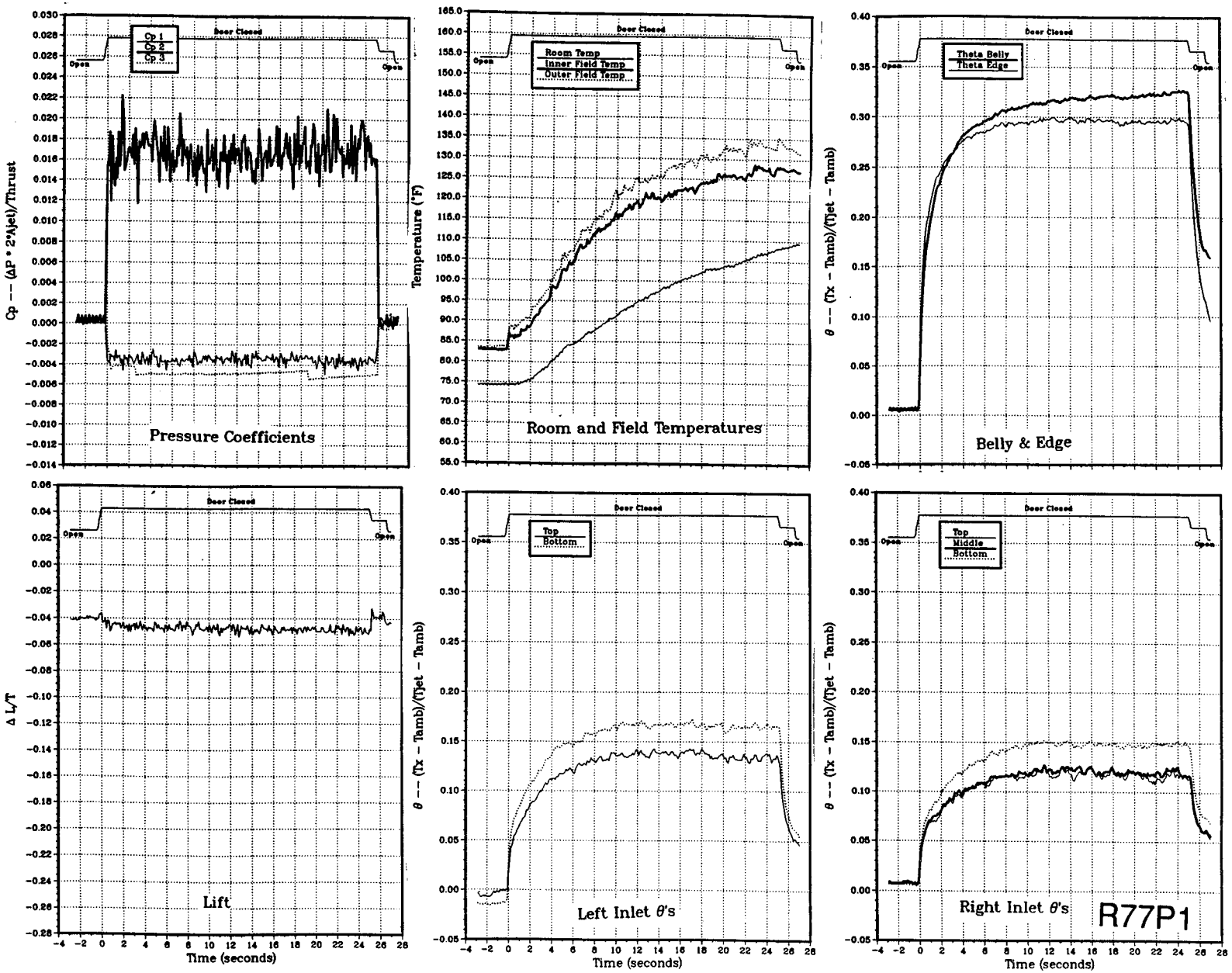

Figure 36(a). Body alone, no LIDs, NPR = 6.0, thrust = 219 lb, height = 4 in., Tjet = 560 °F, inlet position = 17 in.

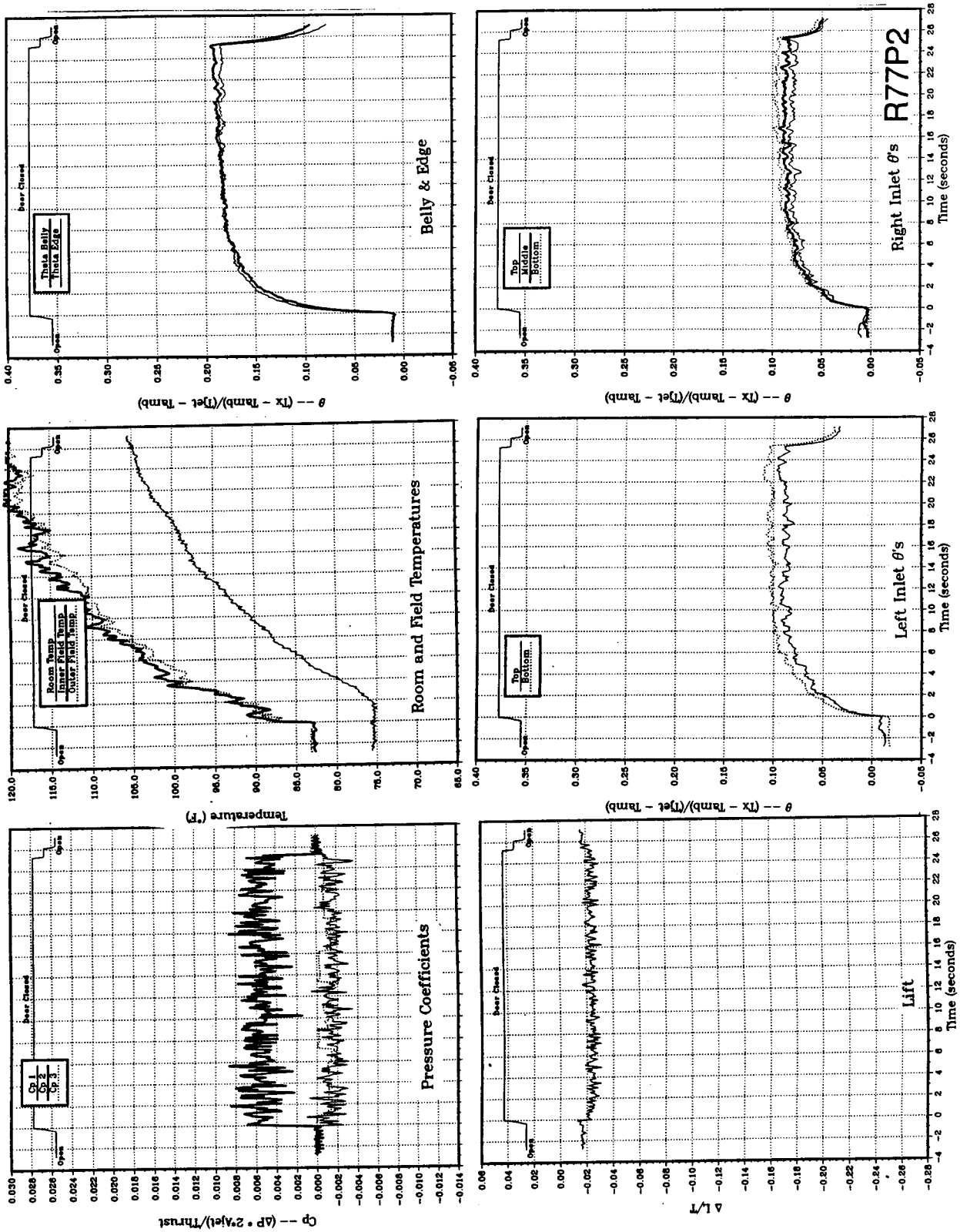

Figure 36(b). Body alone, no LIDs, NPR = 6.0, thrust = 219 lb, height = 8 in., Tjet = 562 °F, inlet position = 17 in.

C-2

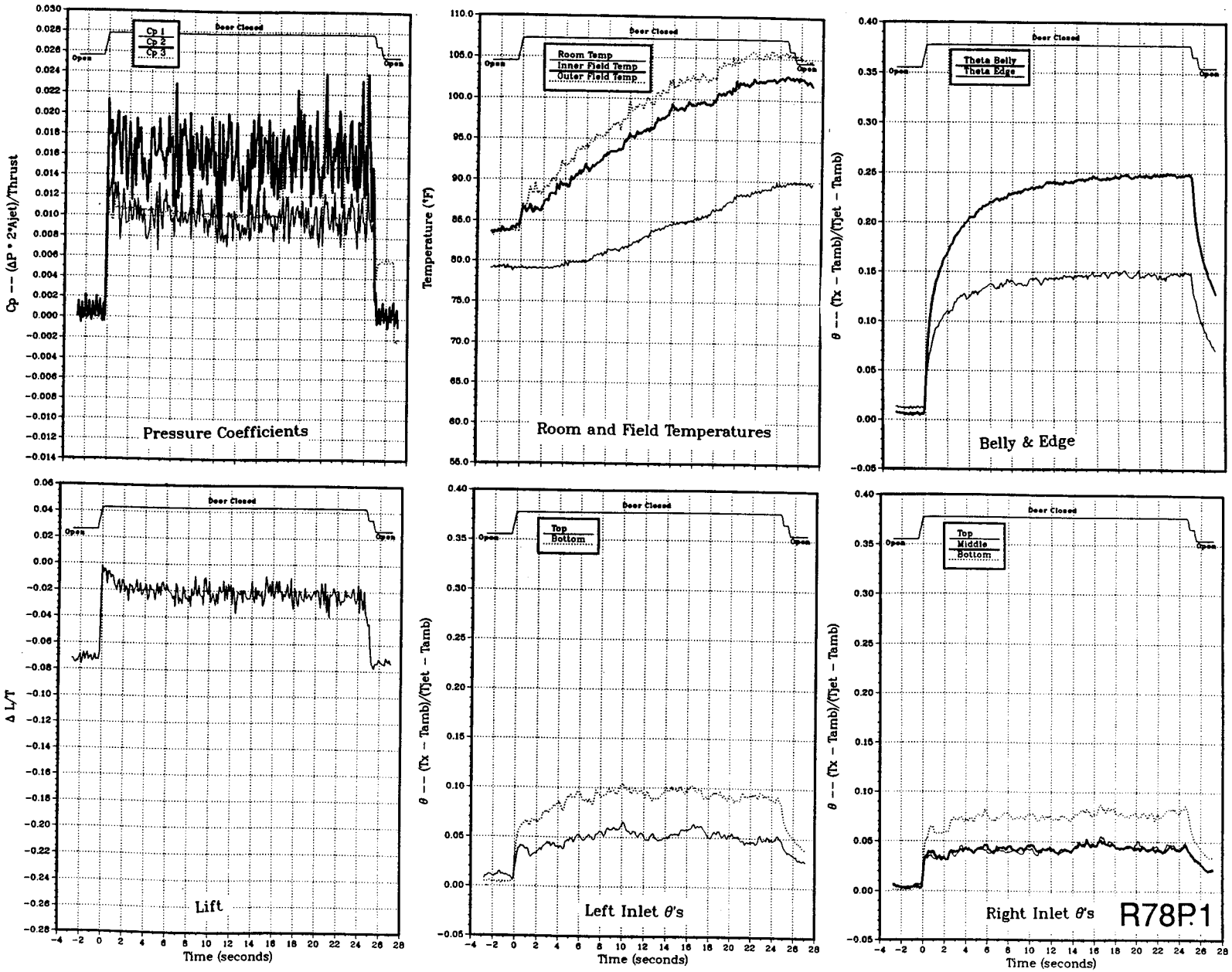

Figure 37(a). Body alone, Box LIDs (13/21), NPR = 2.0, thrust = 50 lb, height = 4 in., Tjet = 482 °F, inlet position = 17 in.

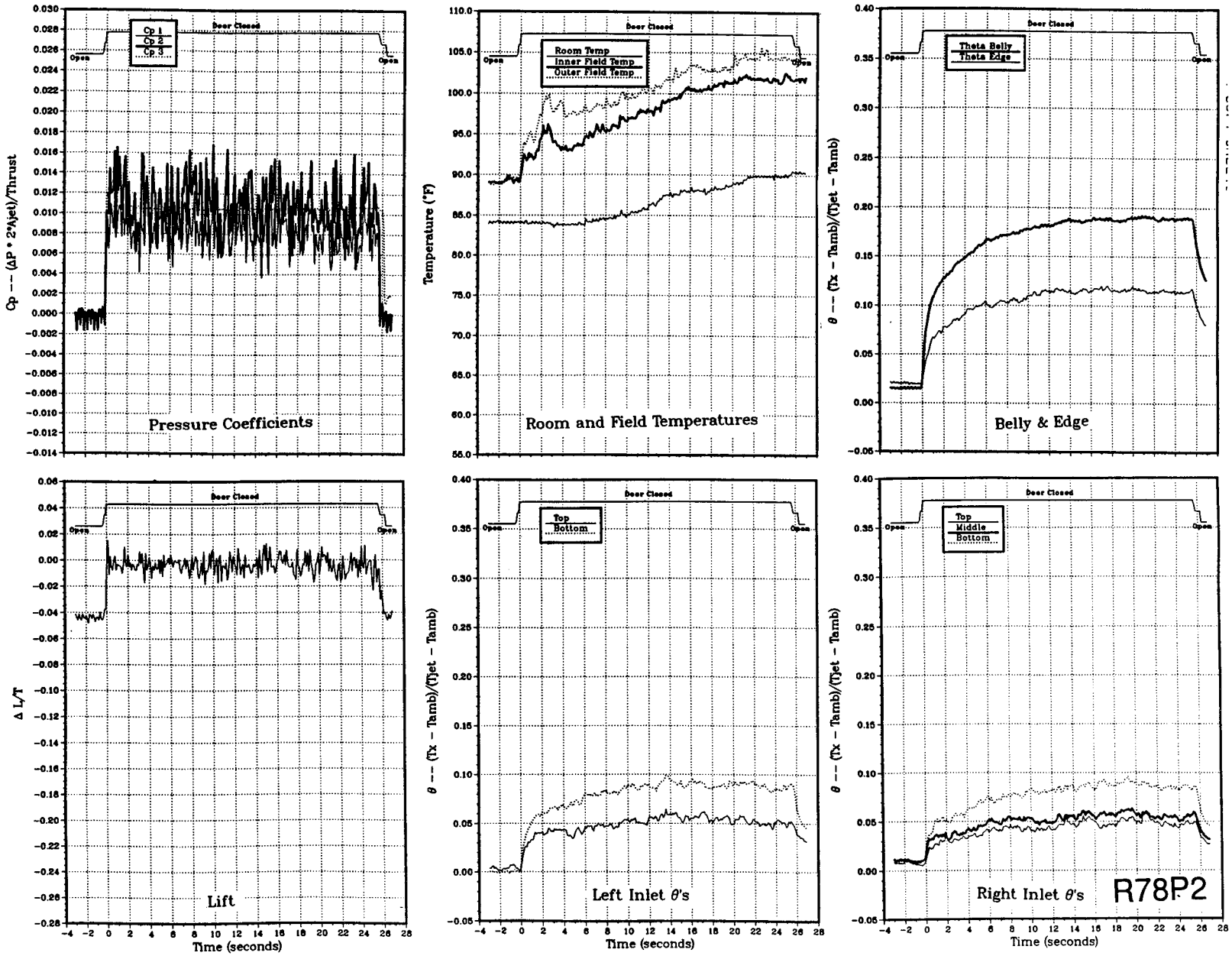

Figure 37(b). Body alone, Box LIDs (13/21), NPR = 2.0, thrust = 50 lb, height = 6 in., Tjet = 488 °F, inlet position = 17 in.

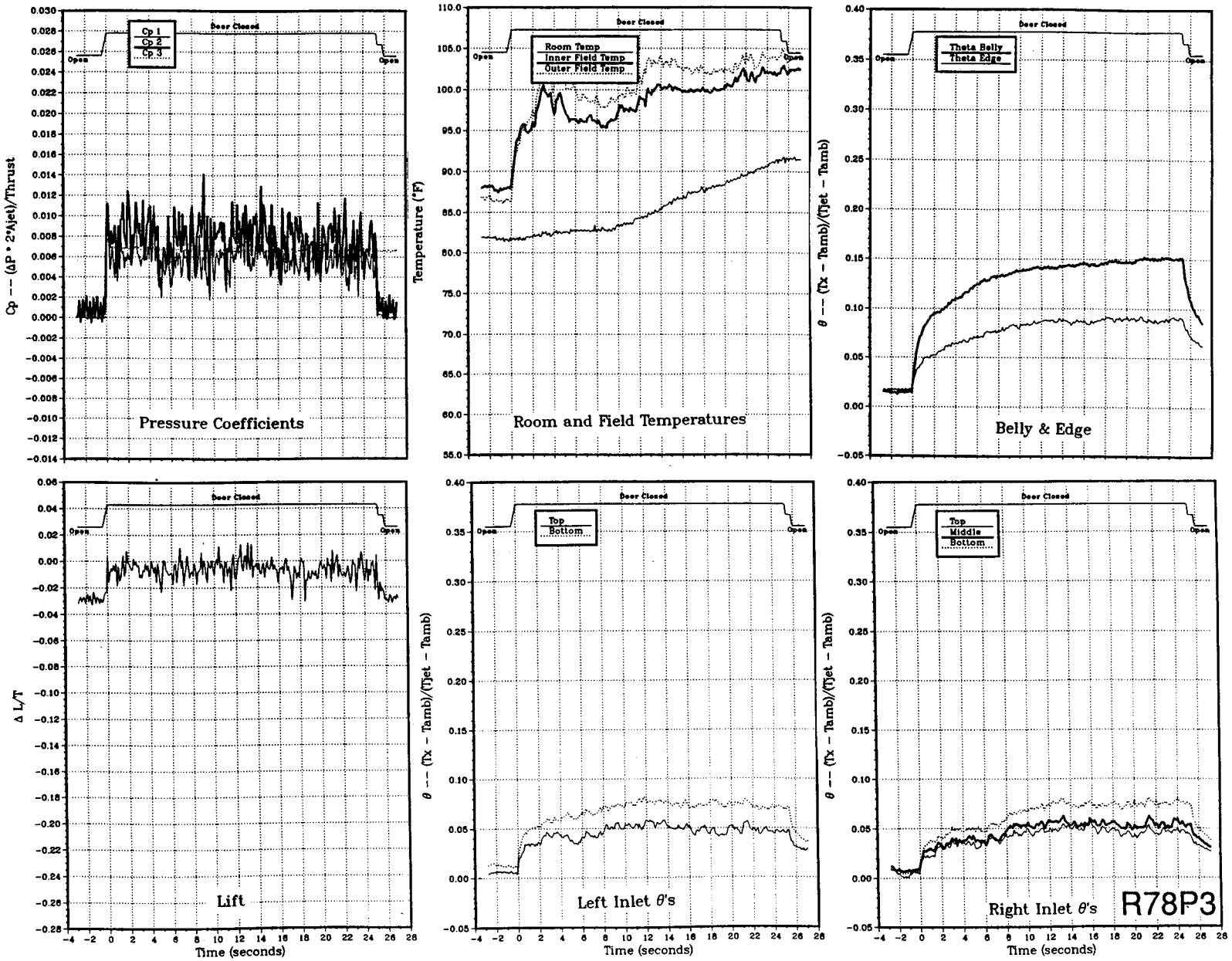

Figure 37(c). Body alone, Box LIDs (13/21), NPR = 2.0, thrust = 50 lb, height = 8 in., Tjet = 493 °F, inlet position = 17 in.

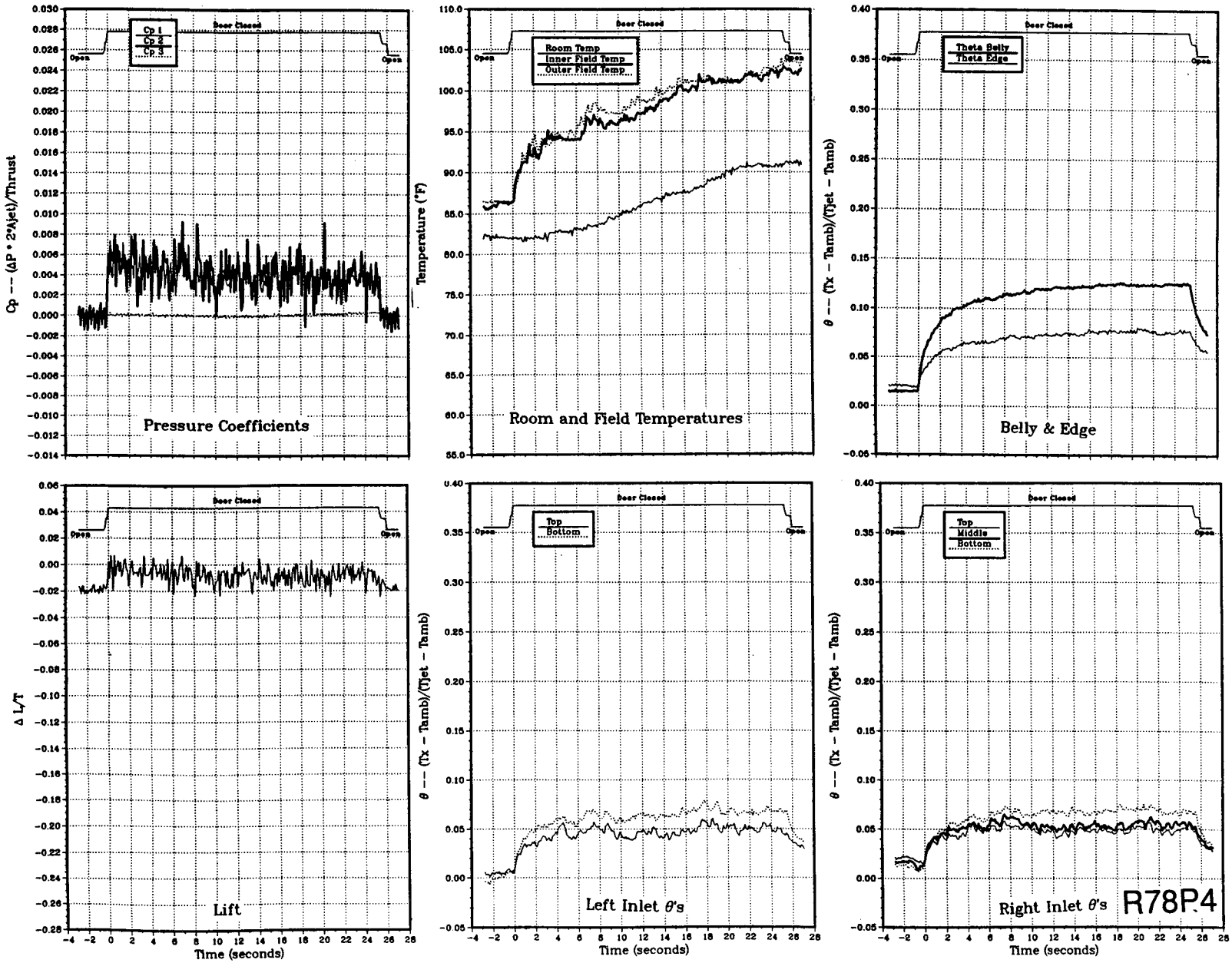

Figure 37(d). Body alone, Box LIDs (13/21), NPR = 2.0, thrust = 50 lb, height = 10 in., Tjet = 498 °F, inlet position = 17 in.

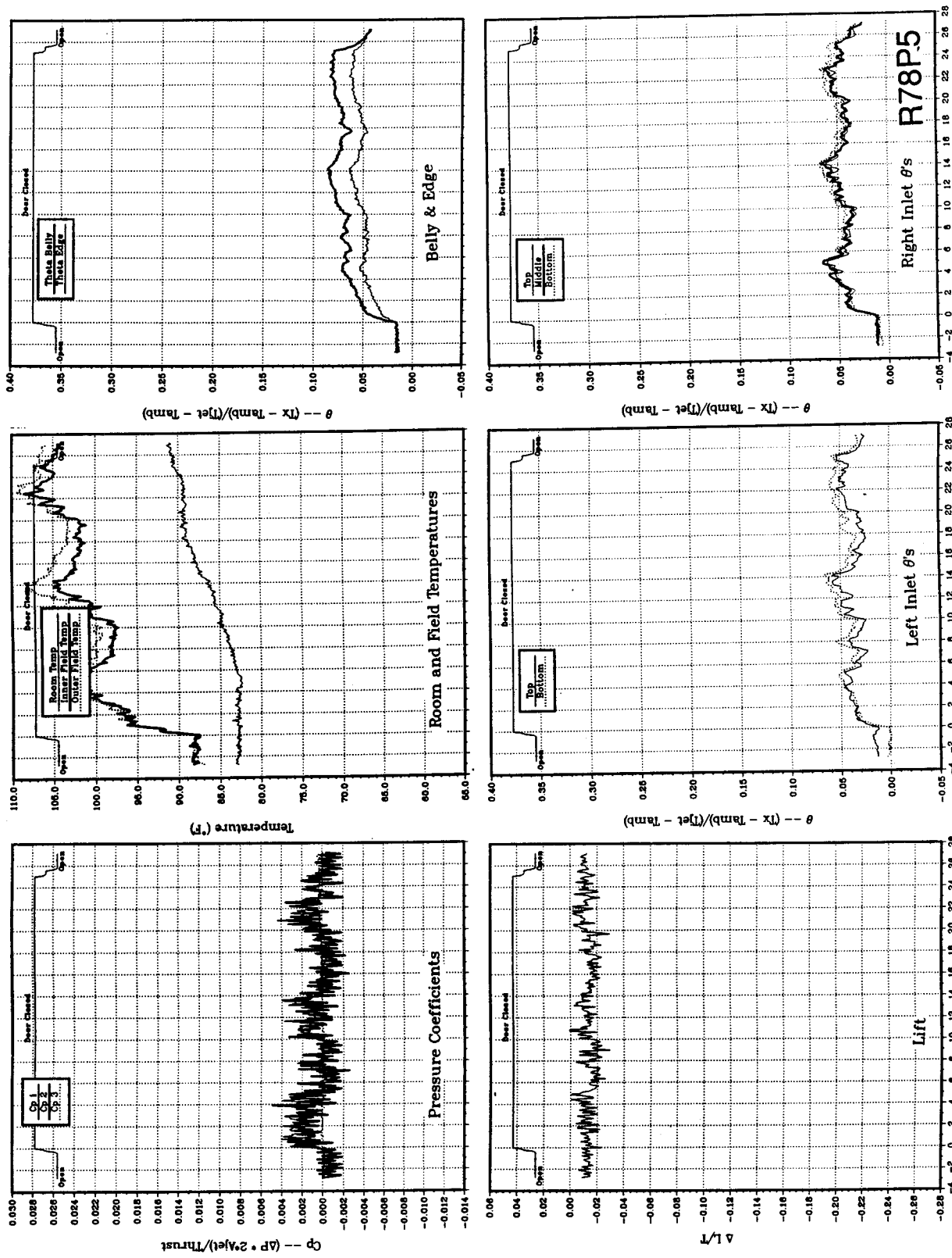

Figure 37(e). Body alone, Box LIDs (13/21), NPR = 2.0, thrust = 50 lb, height = 15 in., Tjet = 502 °F, inlet position = 17 in.

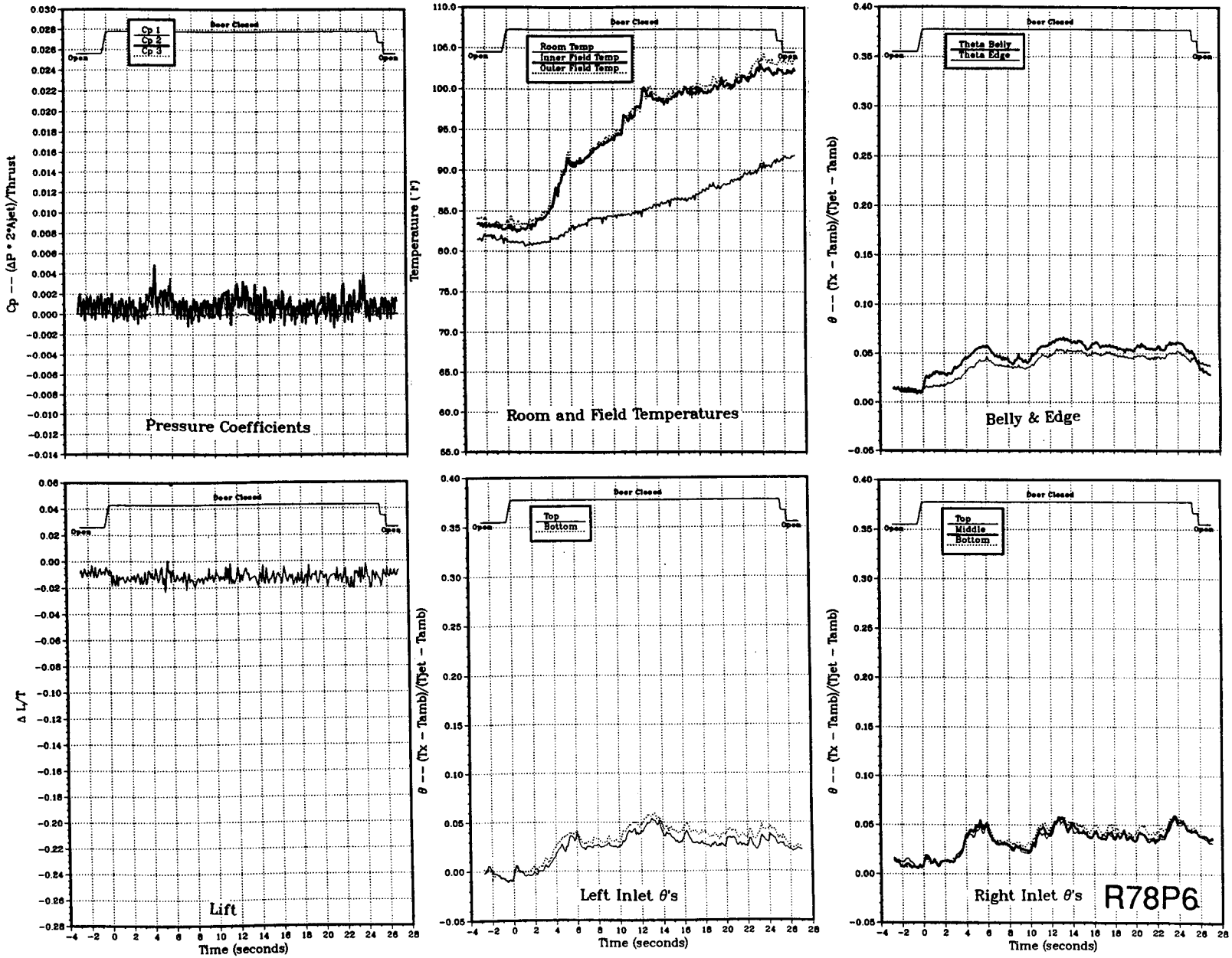

Figure 37(f). Body alone, Box LIDs (13/21), NPR = 2.0, thrust = 50 lb, height = 17 in., Tjet = 505 °F, inlet position = 17 in.

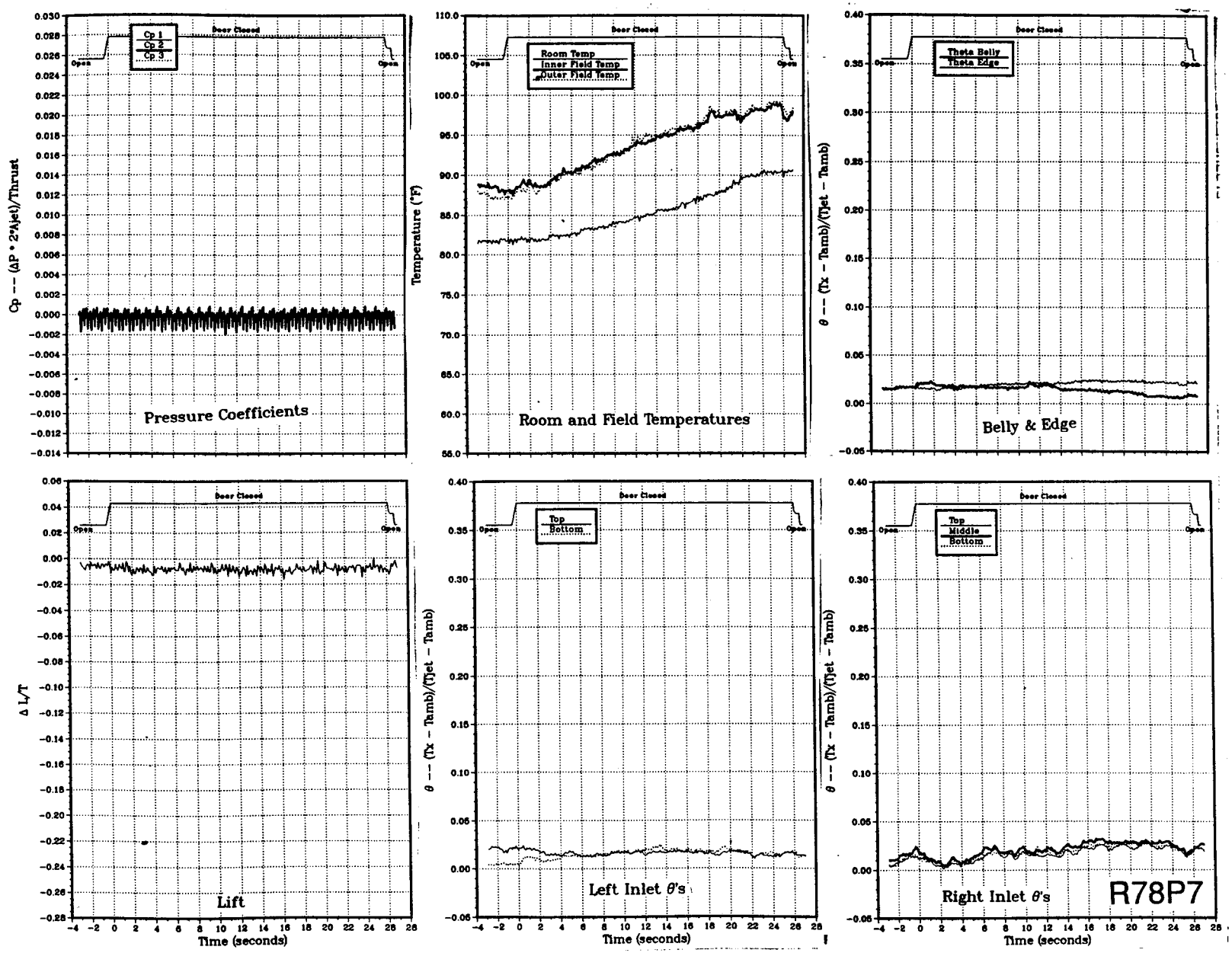

Figure 37(g). Body alone, Box LIDs (13/21), NPR = 2.0, thrust = 50 lb, height = 20 in., Tjet = 508 °F, inlet position = 17 in.

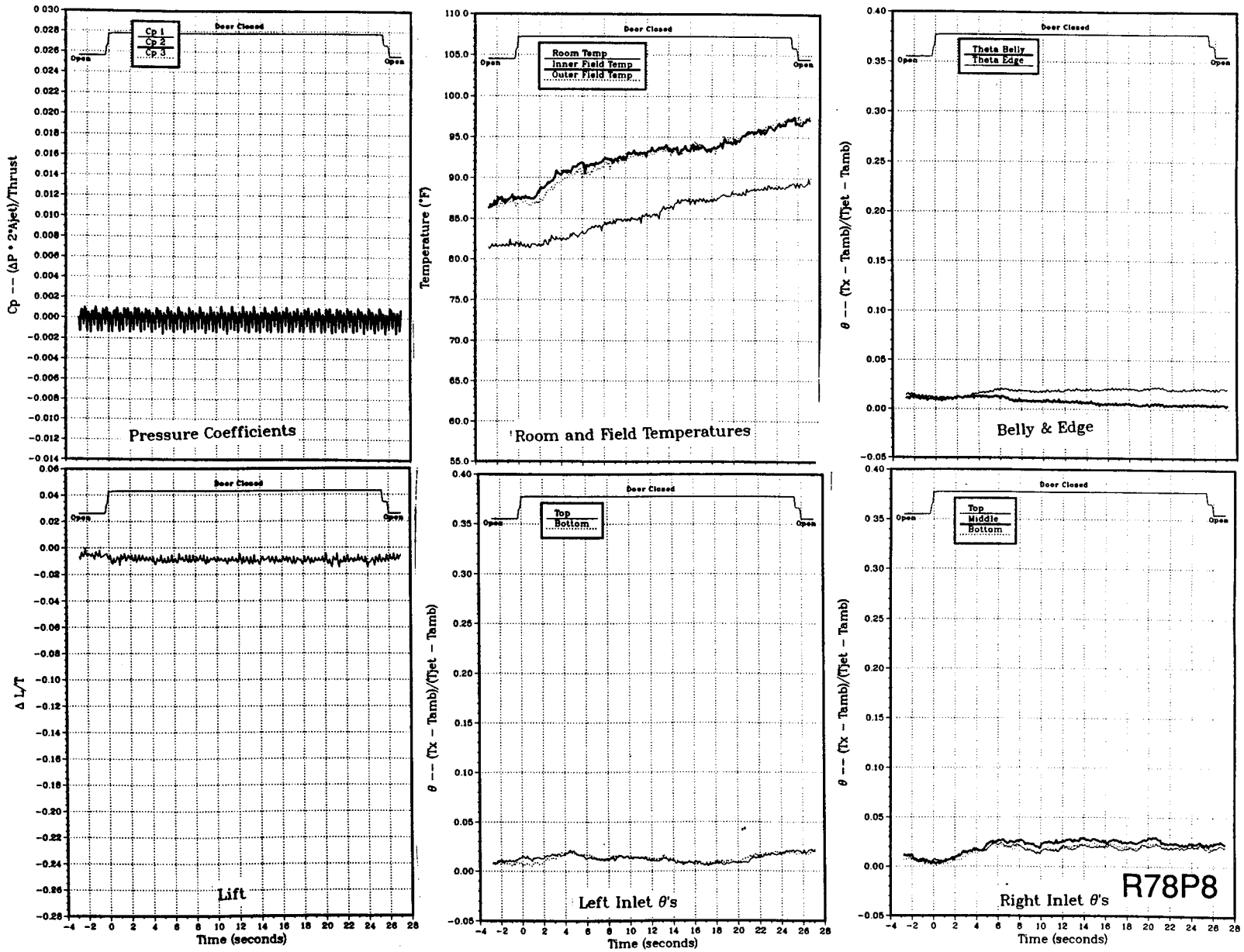

Figure 37(h). Body alone, Box LIDs (13/21), NPR = 2.0, thrust = 50 lb, height = 40 in., Tjet = 511 °F, inlet position = 17 in.

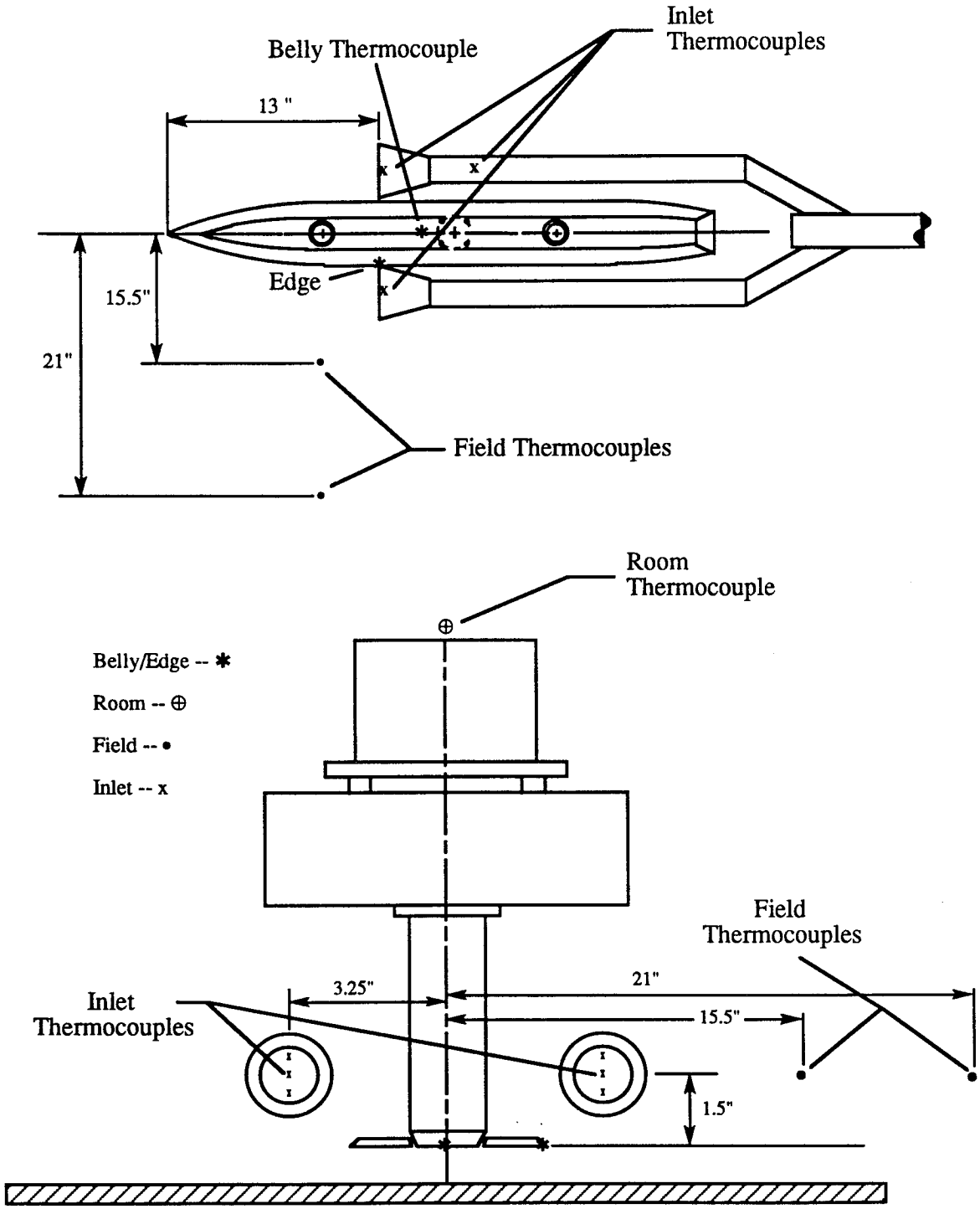

Figure 38. Locations of model and field thermocouples for data set 7.

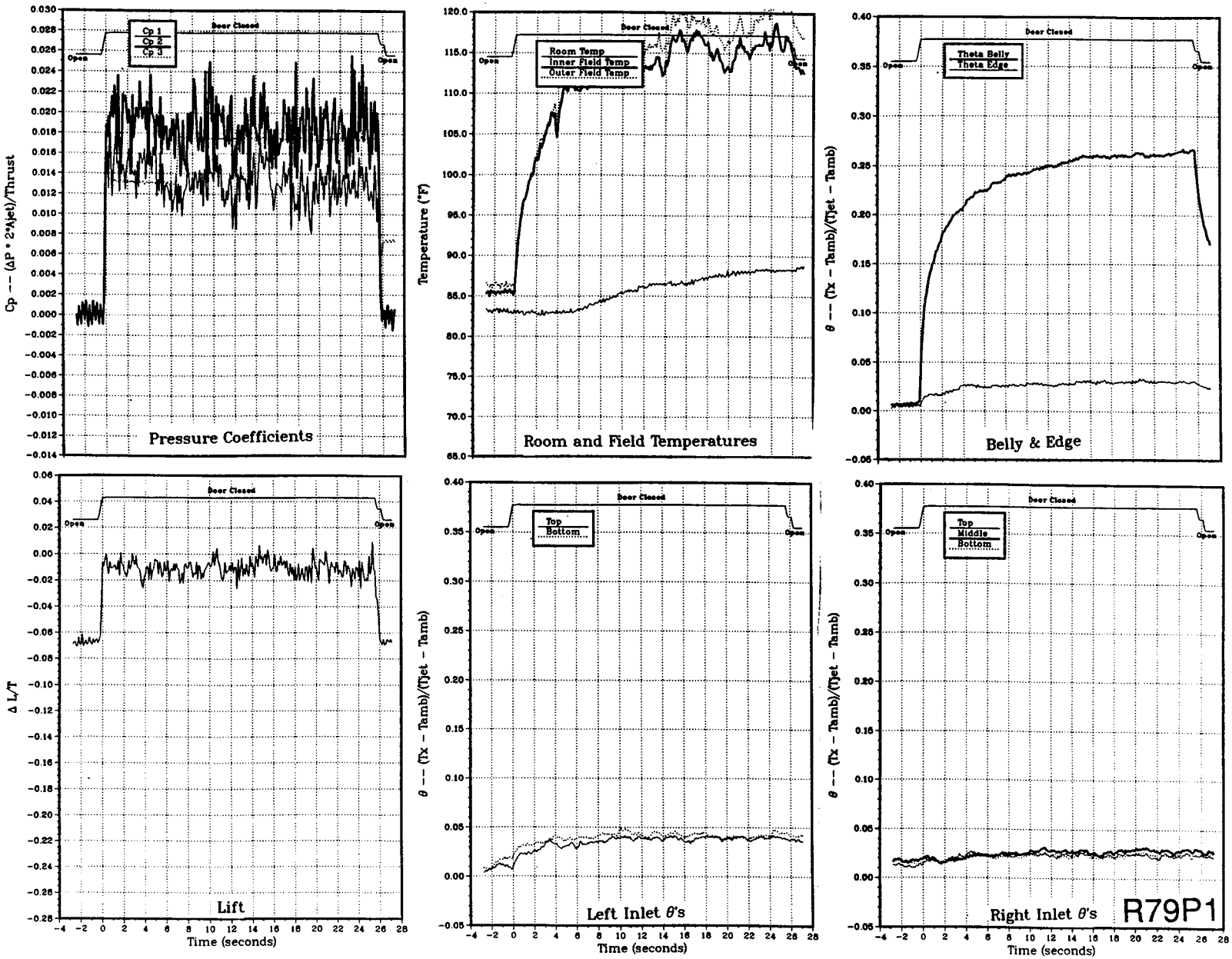

Figure 39(a). Body alone, Box LIDs (13/21), NPR = 2.0, thrust = 50 lb, height = 4 in., Tjet = 497 °F, inlet position = 13 in.

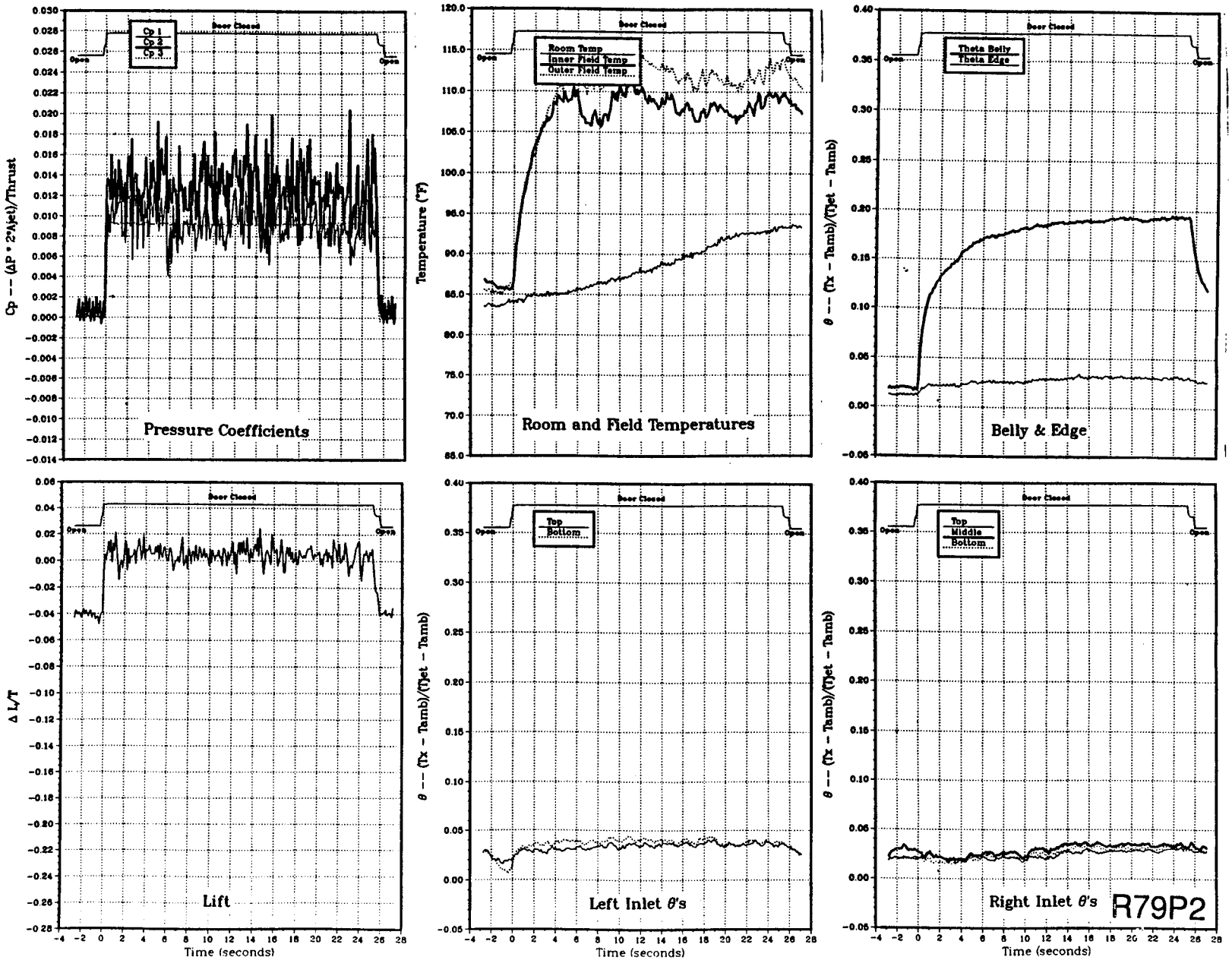

Figure 39(b). Body alone, Box LIDs (13/21), NPR = 2.0, thrust = 50 lb, height = 6 in., Tjet = 501 °F, inlet position = 13 in.

Figure 39(c). Body alone, Box LIDs (13/21), NPR = 2.0, thrust = 50 lb, height = 8 in., Tjet = 505 °F, inlet position = 13 in.

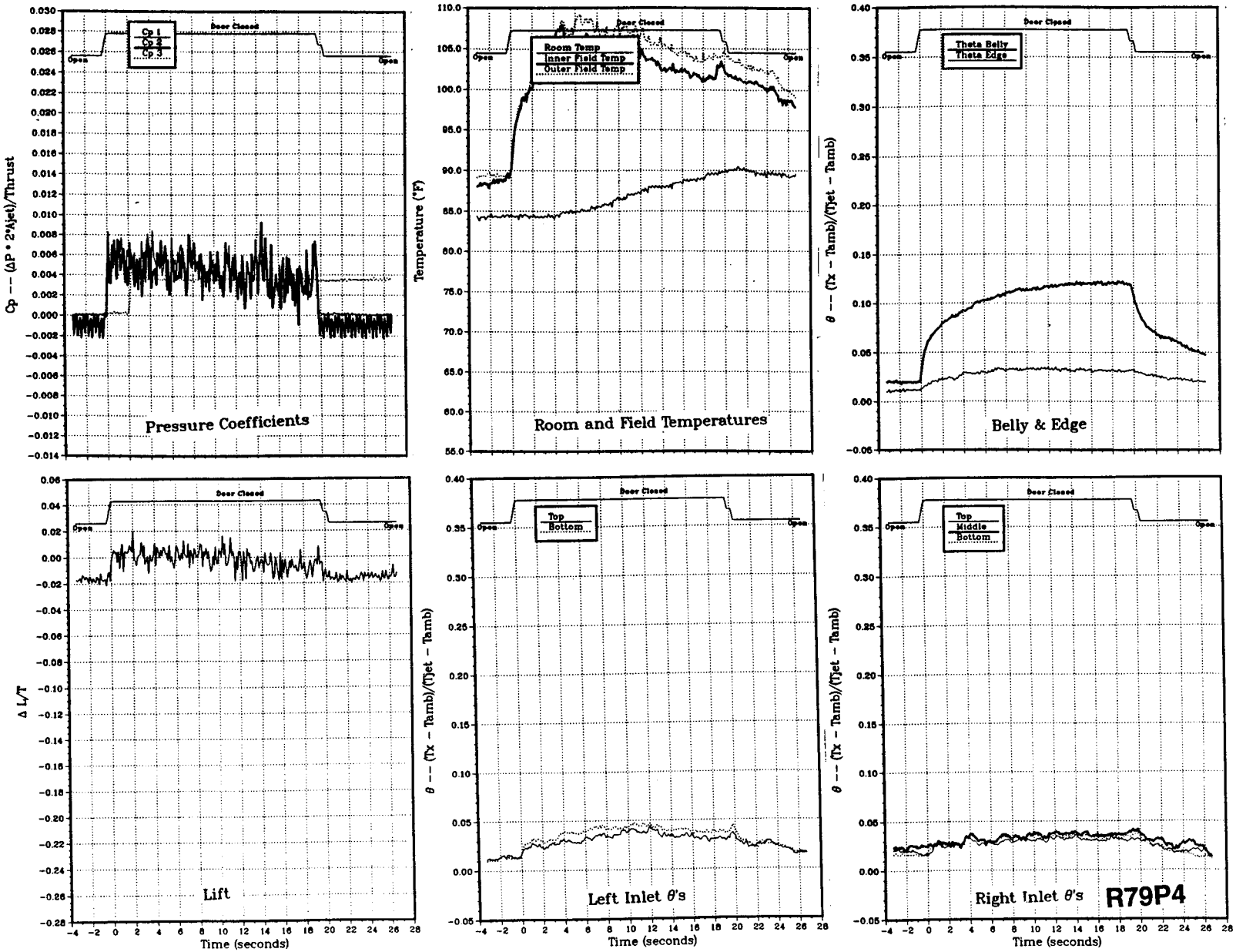

Figure 39(d). Body alone, Box LIDs (13/21), NPR = 2.0, thrust = 50 lb, height = 10 in., Tjet = 508 °F, inlet position = 13 in.

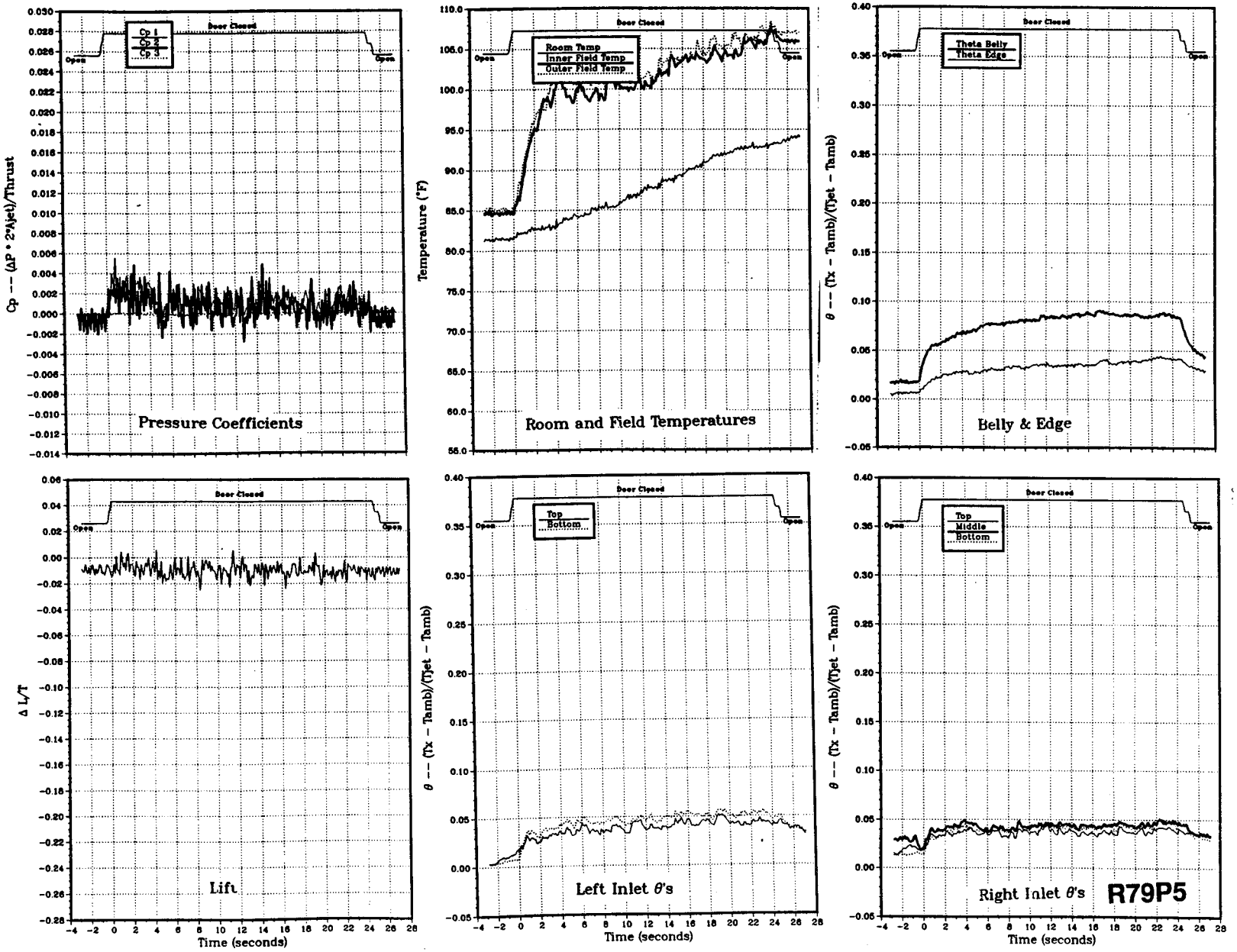

Figure 39(e). Body alone, Box LIDs (13/21), NPR = 2.0, thrust = 50 lb, height = 15 in., Tjet = 511 °F, inlet position = 13 in.

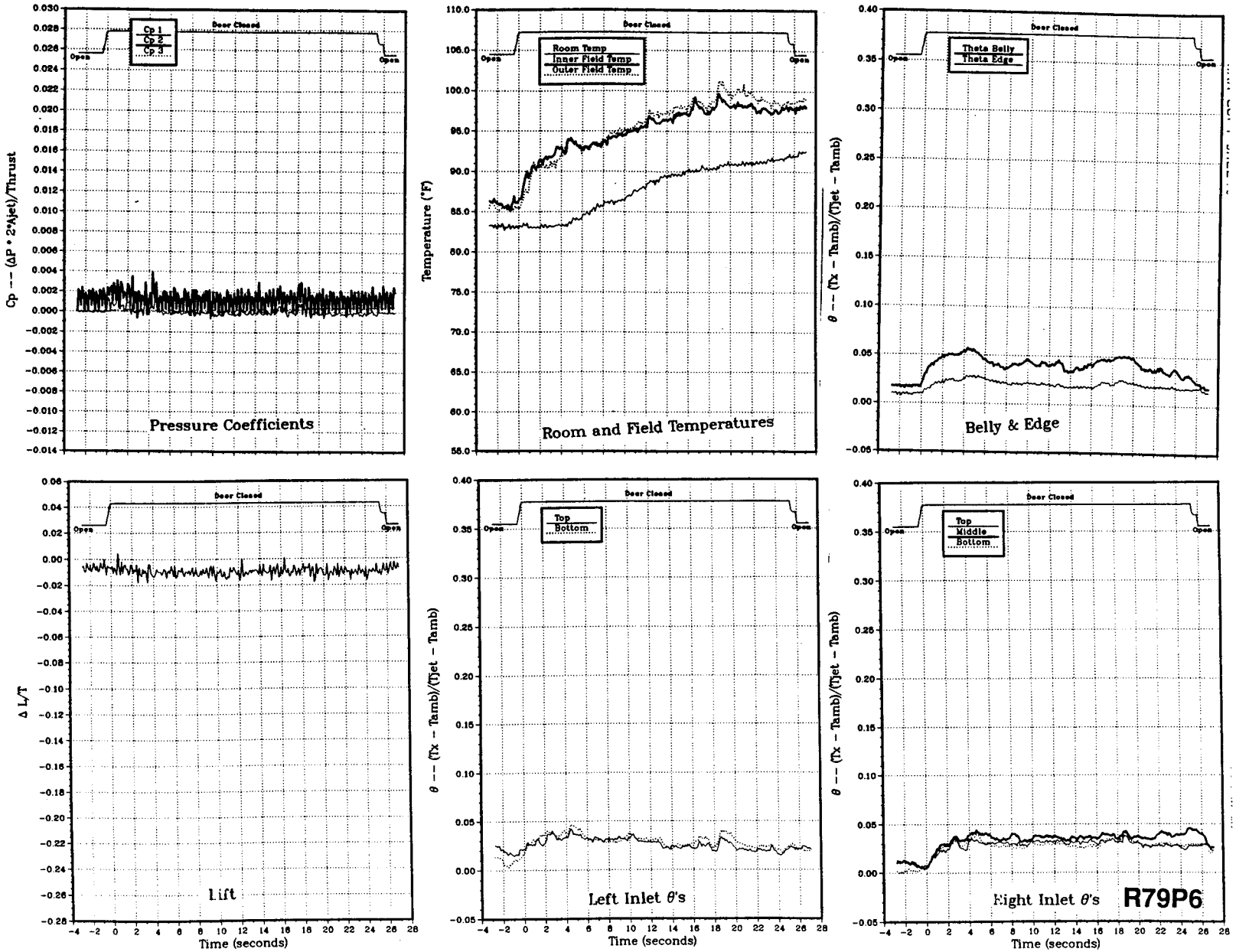

Figure 39(f). Body alone, Box LIDs (13/21), NPR = 2.0, thrust = 50 lb, height = 20 in., Tjet = 514 °F, inlet position = 13 in.

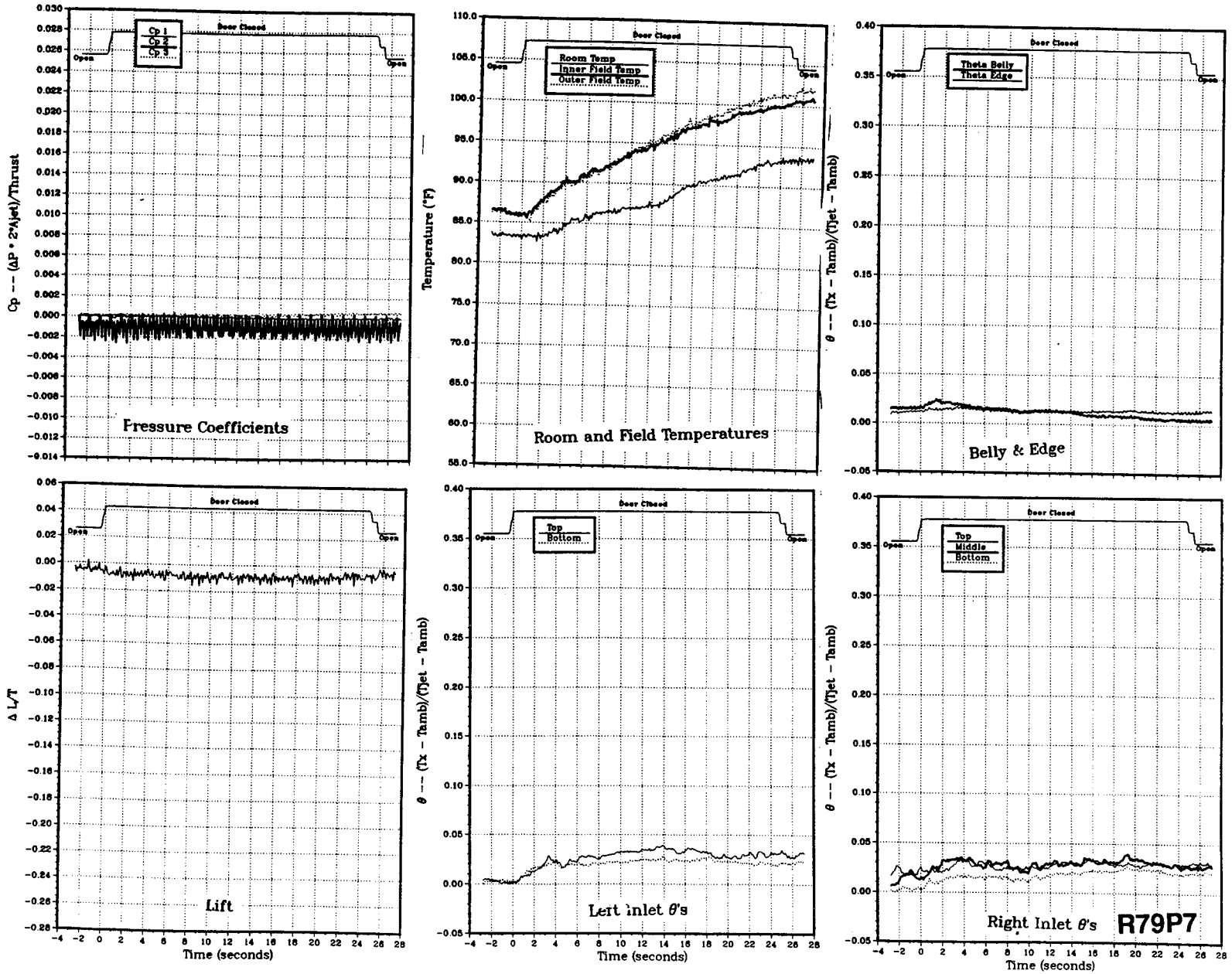

Figure 39(g). Body alone, Box LIDs (13/21), NPR = 2.0, thrust = 50 lb, height = 30 in., Tjet = 515 °F, inlet position = 13 in.

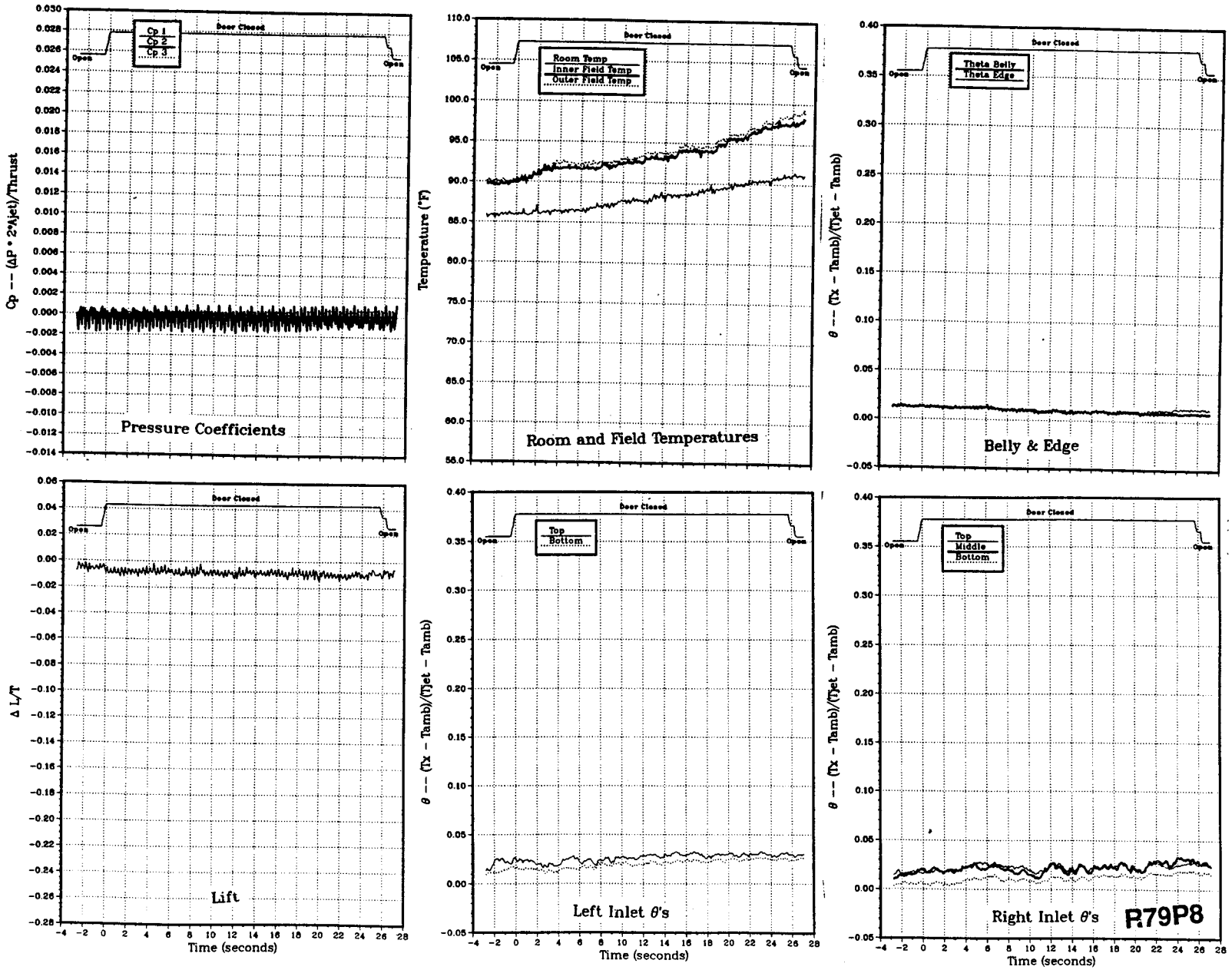

Figure 39(h). Body alone, Box LIDs (13/21), NPR = 2.0, thrust = 50 lb, height = 40 in., Tjet = 517 °F, inlet position = 13 in.

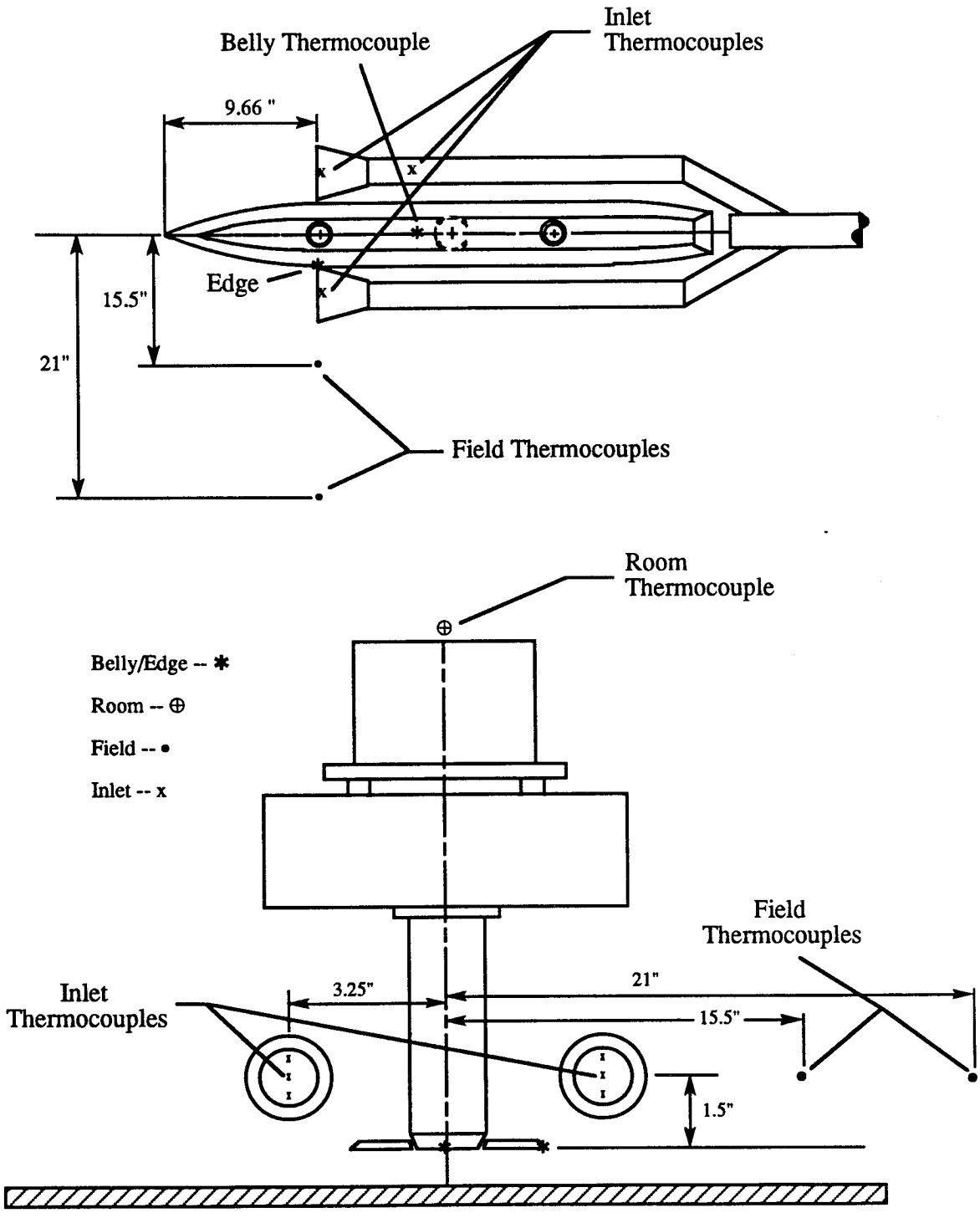

Figure 40. Locations of model and field thermocouples for data set 8.

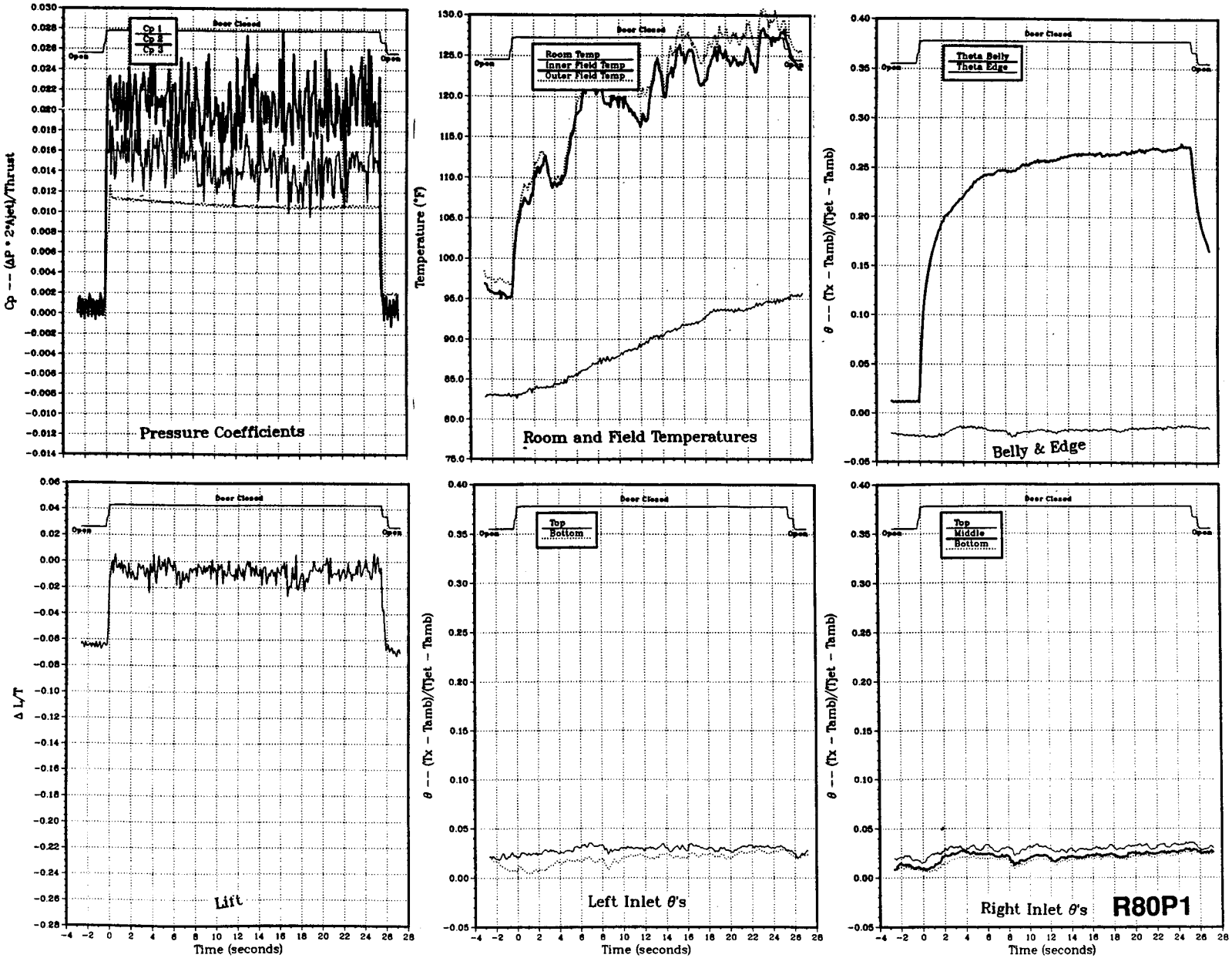

Figure 41(a). Body alone, Box LIDs (13/21), NPR = 2.0, thrust = 50 lb, height = 4 in., Tjet = 500 °F, inlet position = 9.66 in.

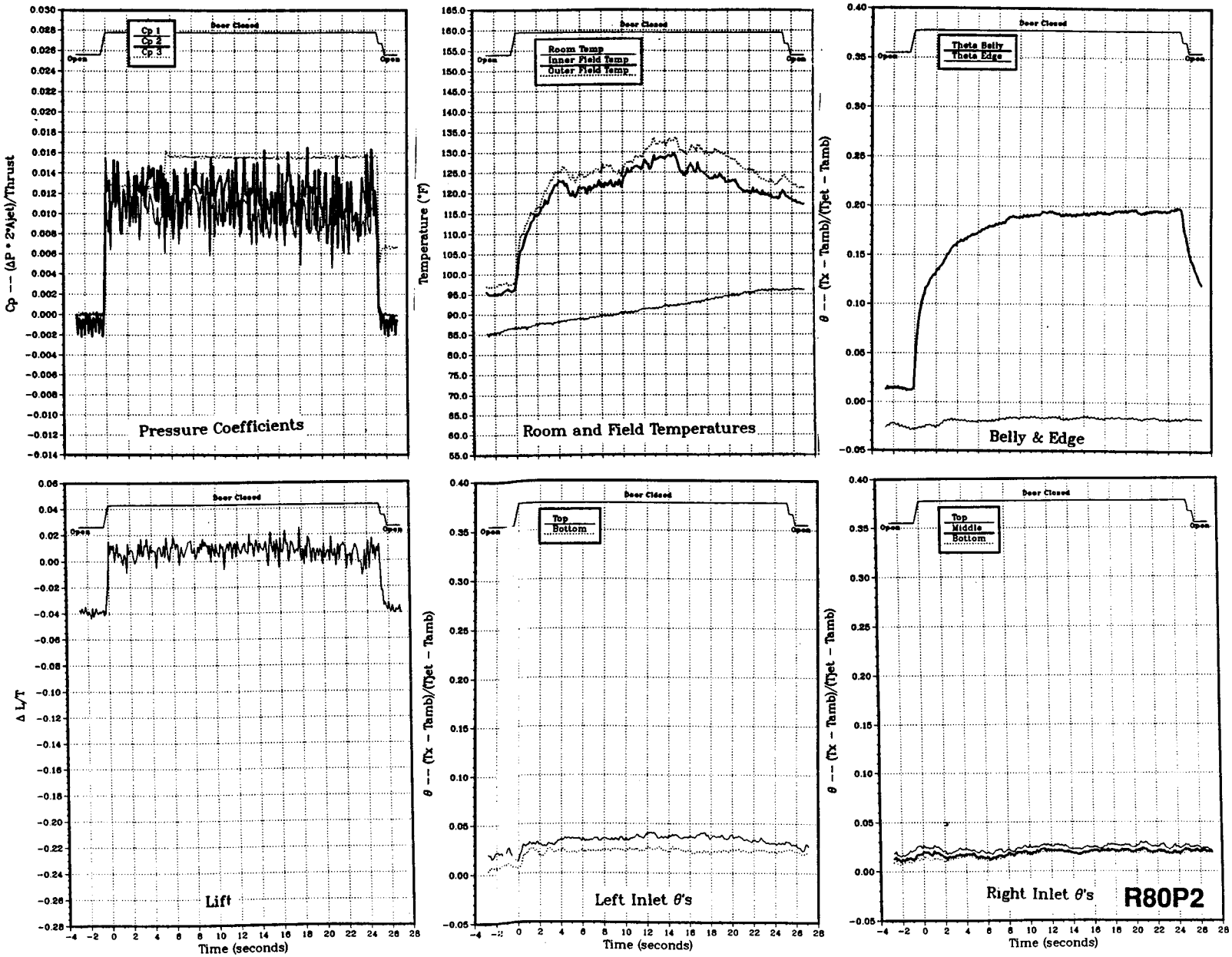

Figure 41(b). Body alone, Box LIDs (13/21), NPR = 2.0, thrust = 50 lb, height = 6 in., Tjet = 506 °F, inlet position = 9.66 in.

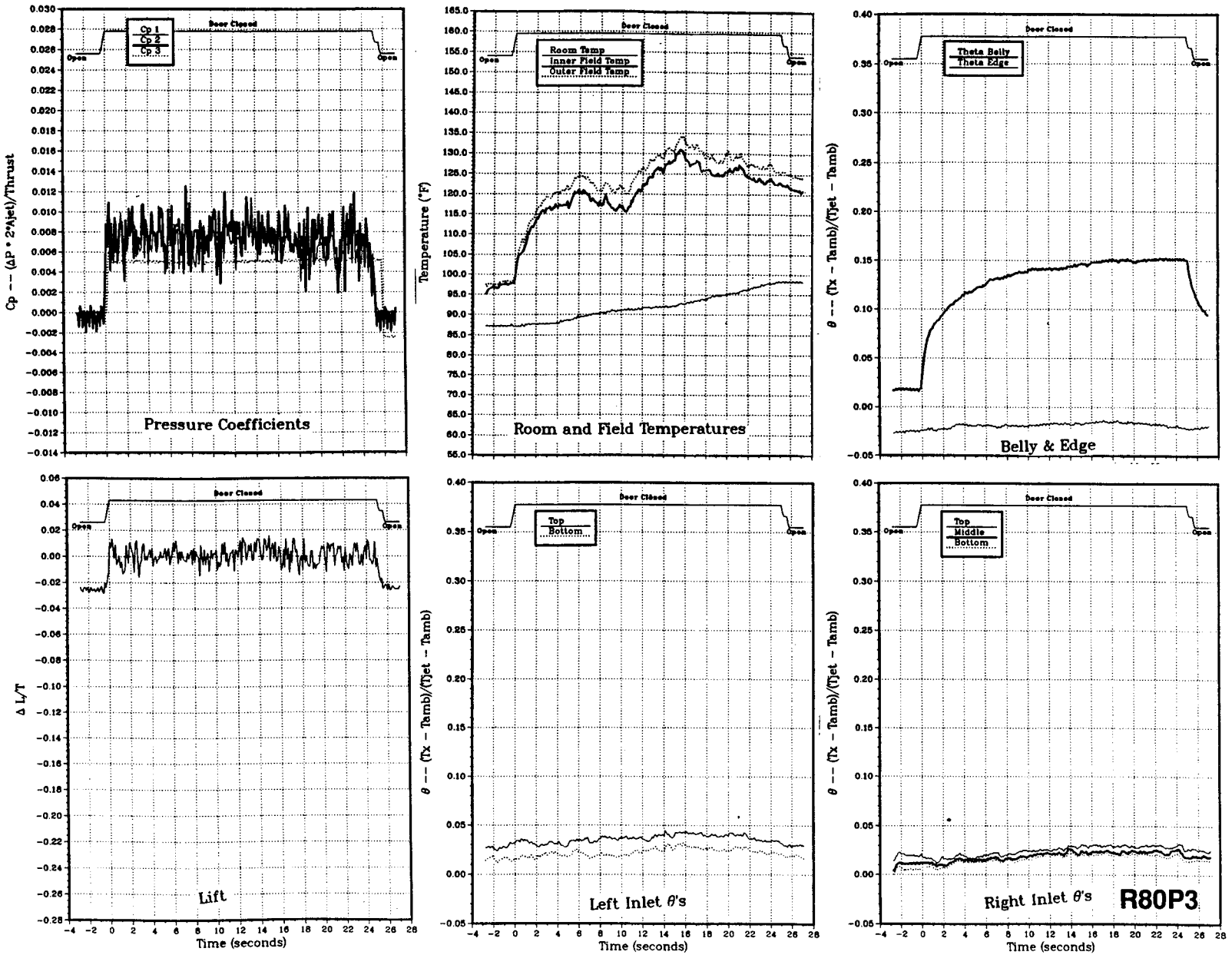

Figure 41(c). Body alone, Box LIDs (13/21), NPR = 2.0, thrust = 50 lb, height = 8 in., Tjet = 508 °F, inlet position = 9.66 in.

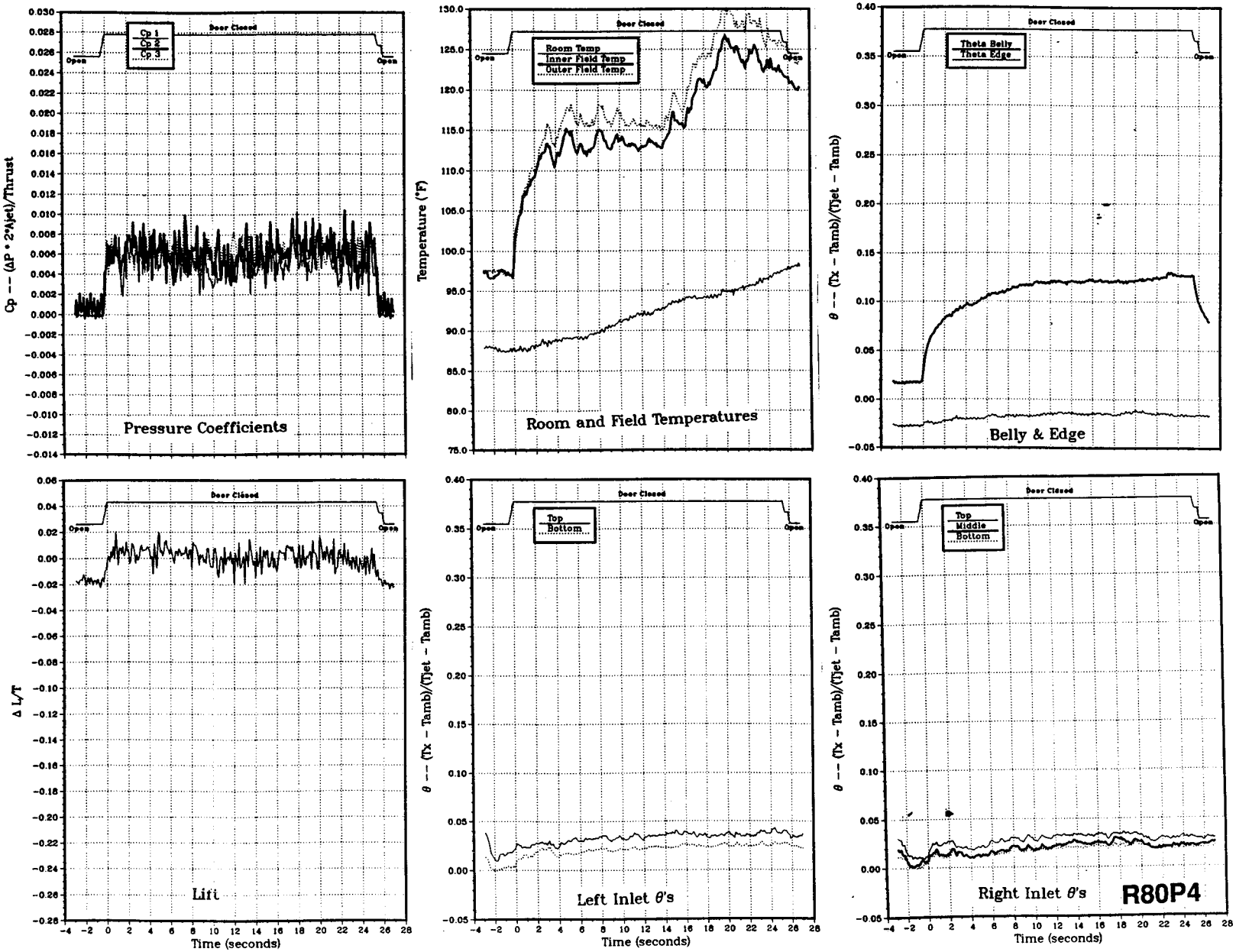

Figure 41(d). Body alone, Box LIDs (13/21), NPR = 2.0, thrust = 50 lb, height = 10 in., Tjet = 510 °F, inlet position = 9.66 in.

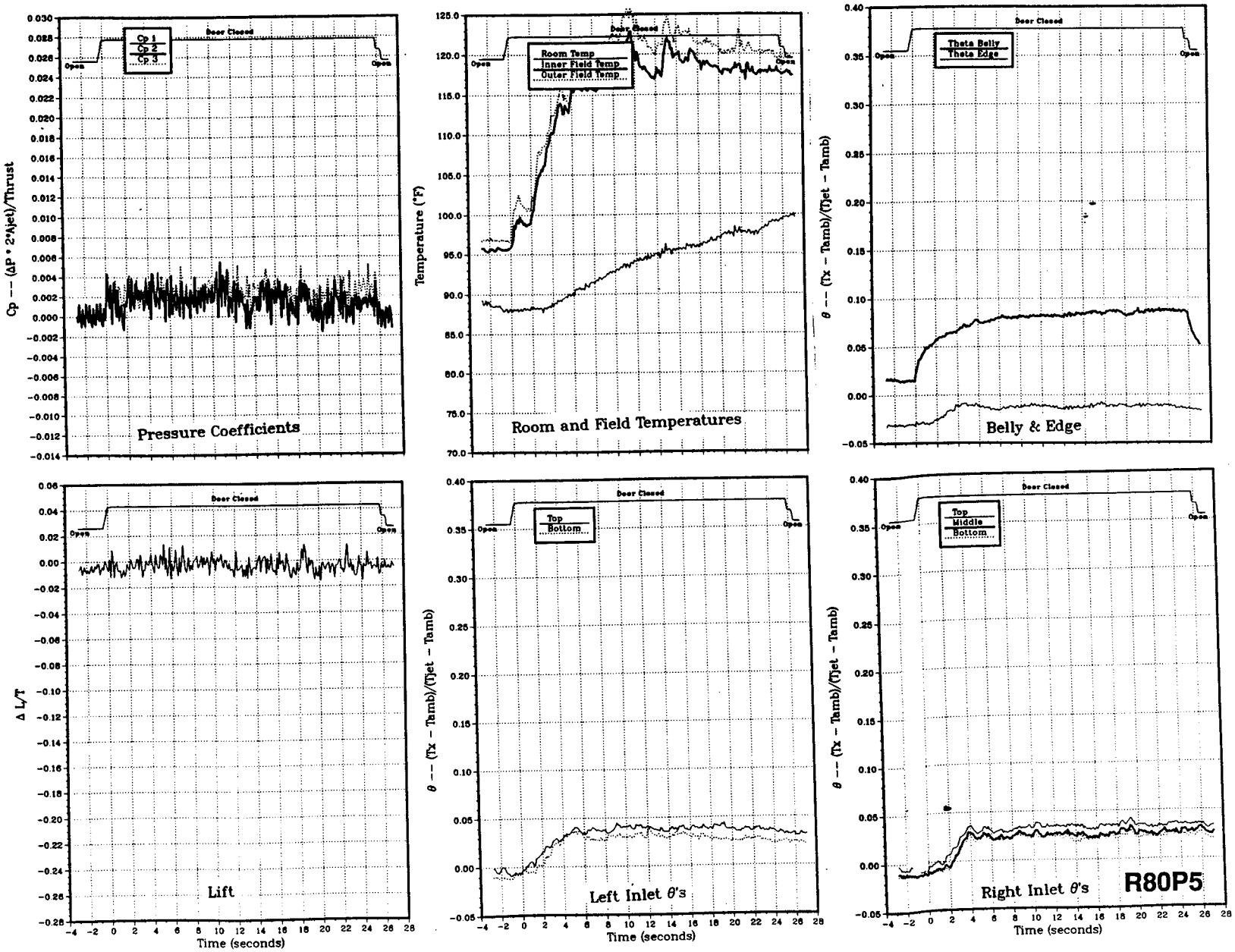

Figure 41(e). Body alone, Box LIDs (13/21), NPR = 2.0, thrust = 50 lb, height = 15 in., Tjet = 512 °F, inlet position = 9.66 in.

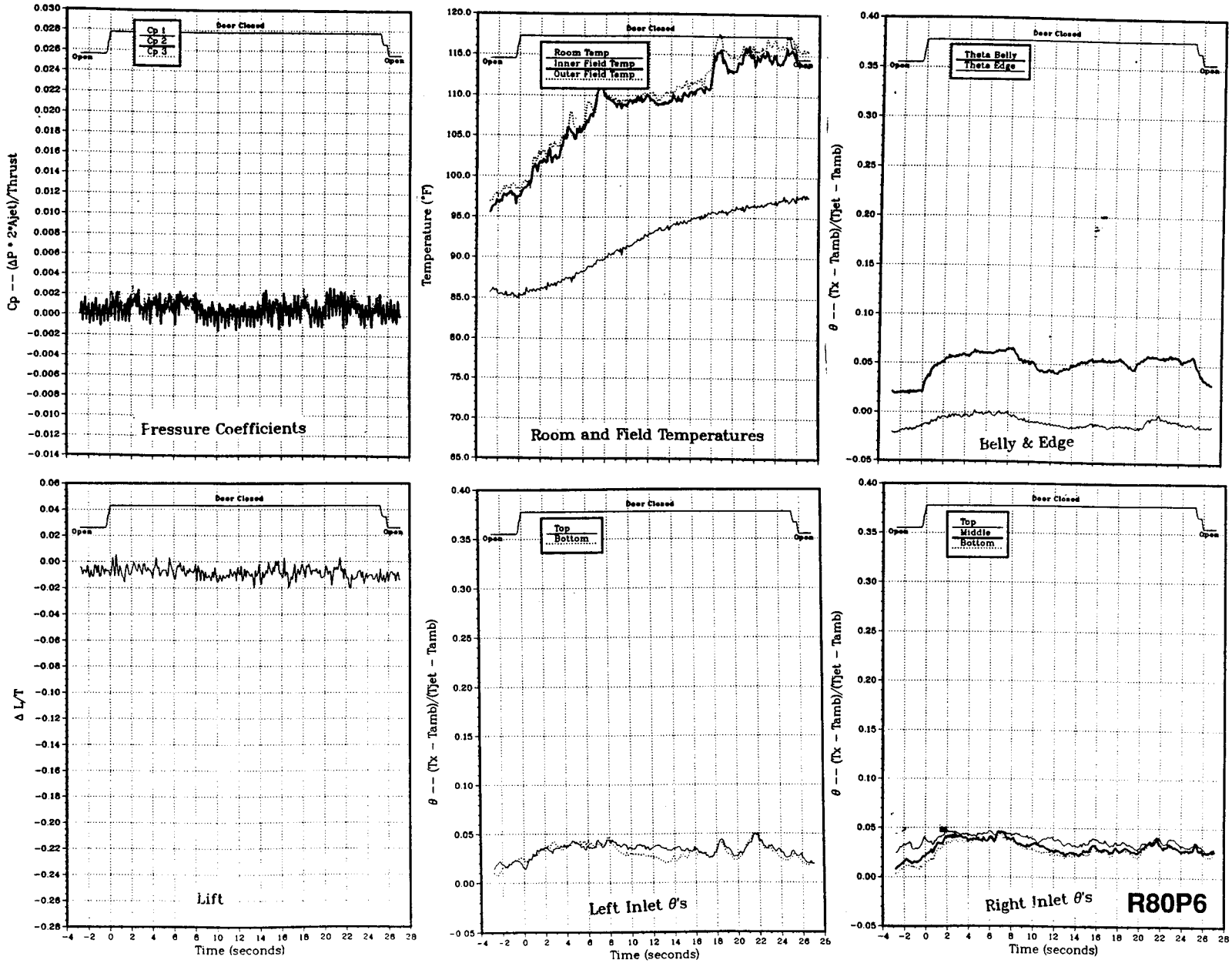

Figure 41(f). Body alone, Box LIDs (13/21), NPR = 2.0, thrust = 50 lb, height = 20 in., Tjet = 514 °F, inlet position = 9.66 in.

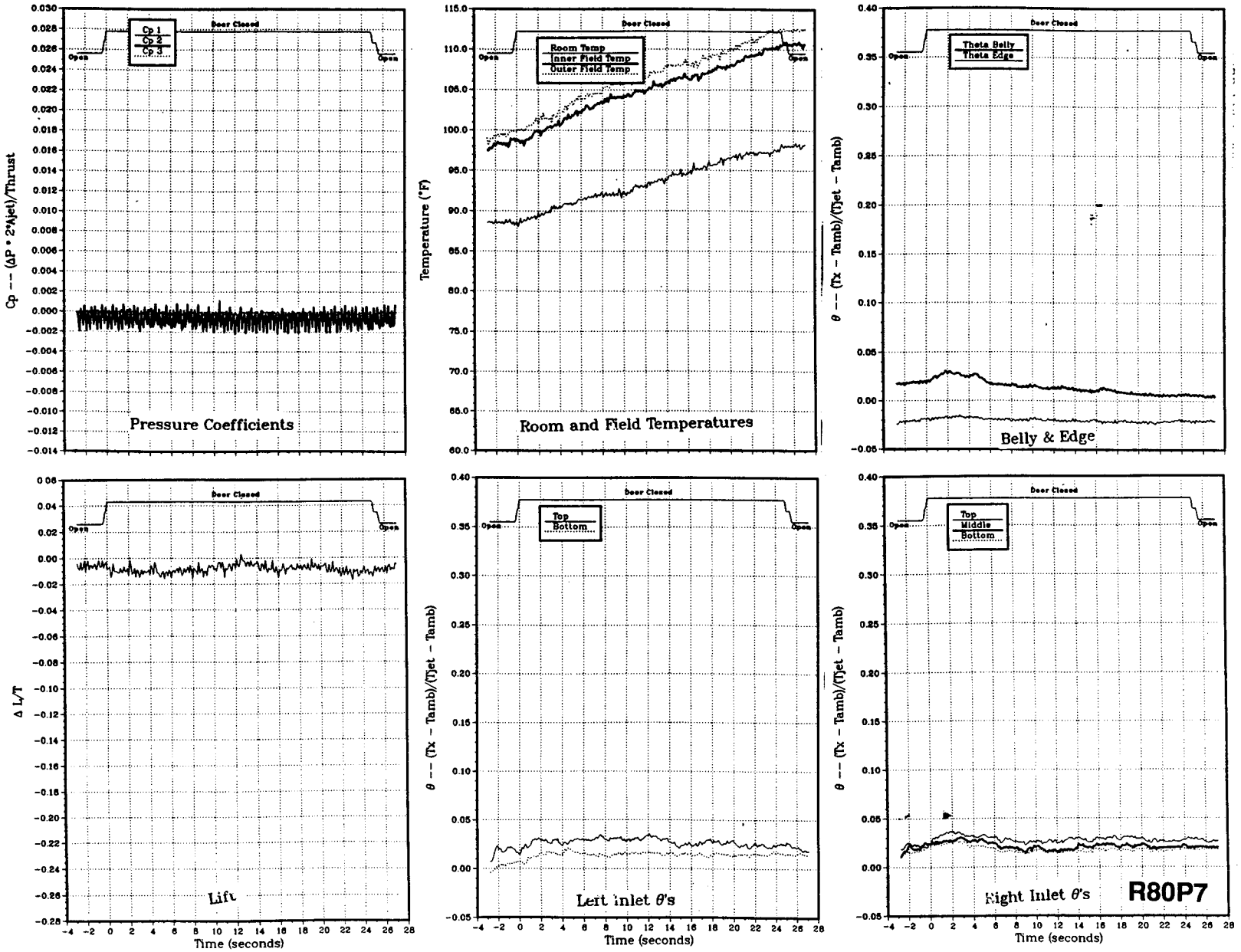

Figure 41(g). Body alone, Box LIDs (13/21), NPR = 2.0, thrust = 50 lb, height = 30 in., Tjet = 516 °F, inlet position = 9.66 in.

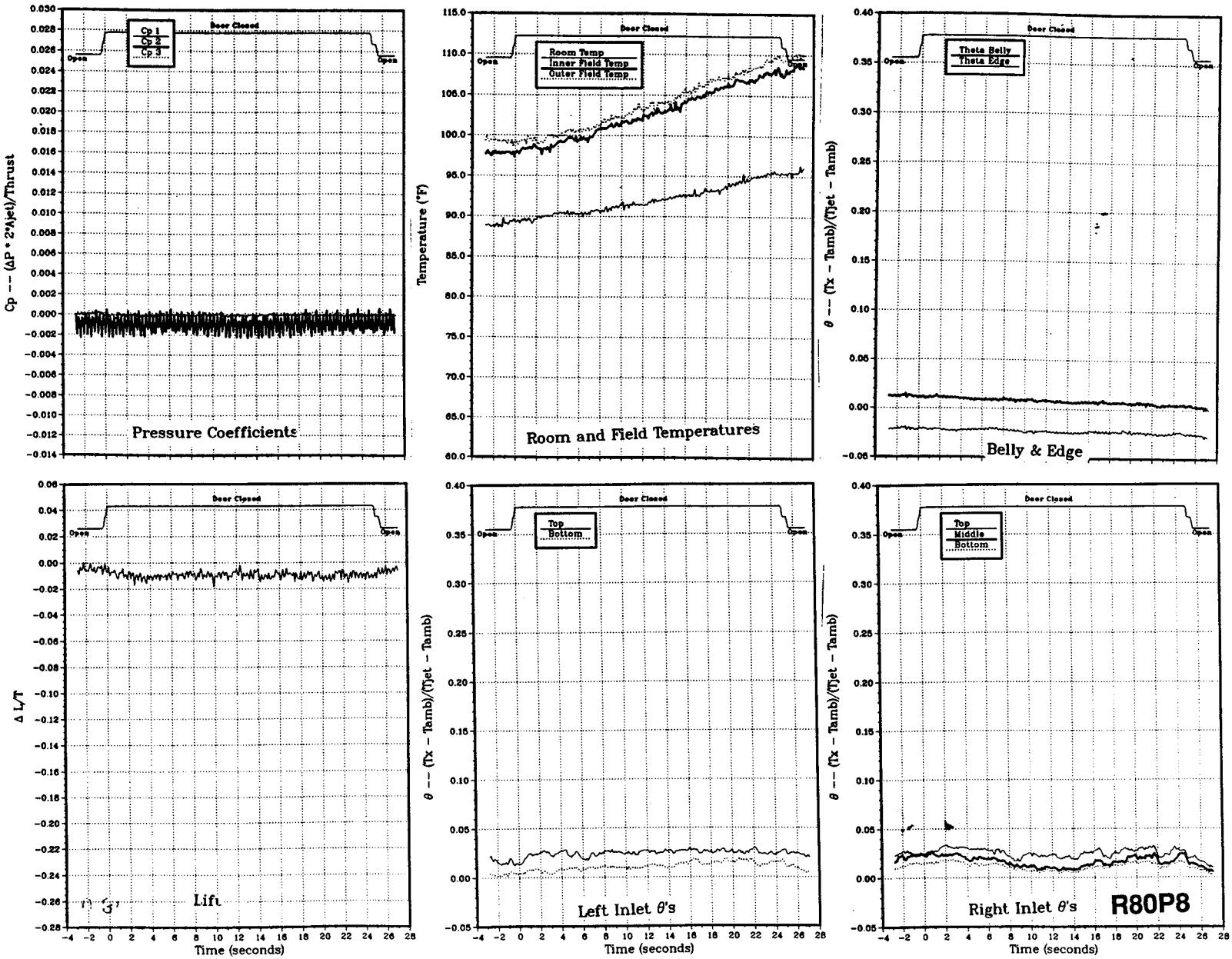

Figure 41(h). Body alone, Box LIDs (13/21), NPR = 2.0, thrust = 50 lb, height = 40 in., Tjet = 517 °F, inlet position = 9.66 in.

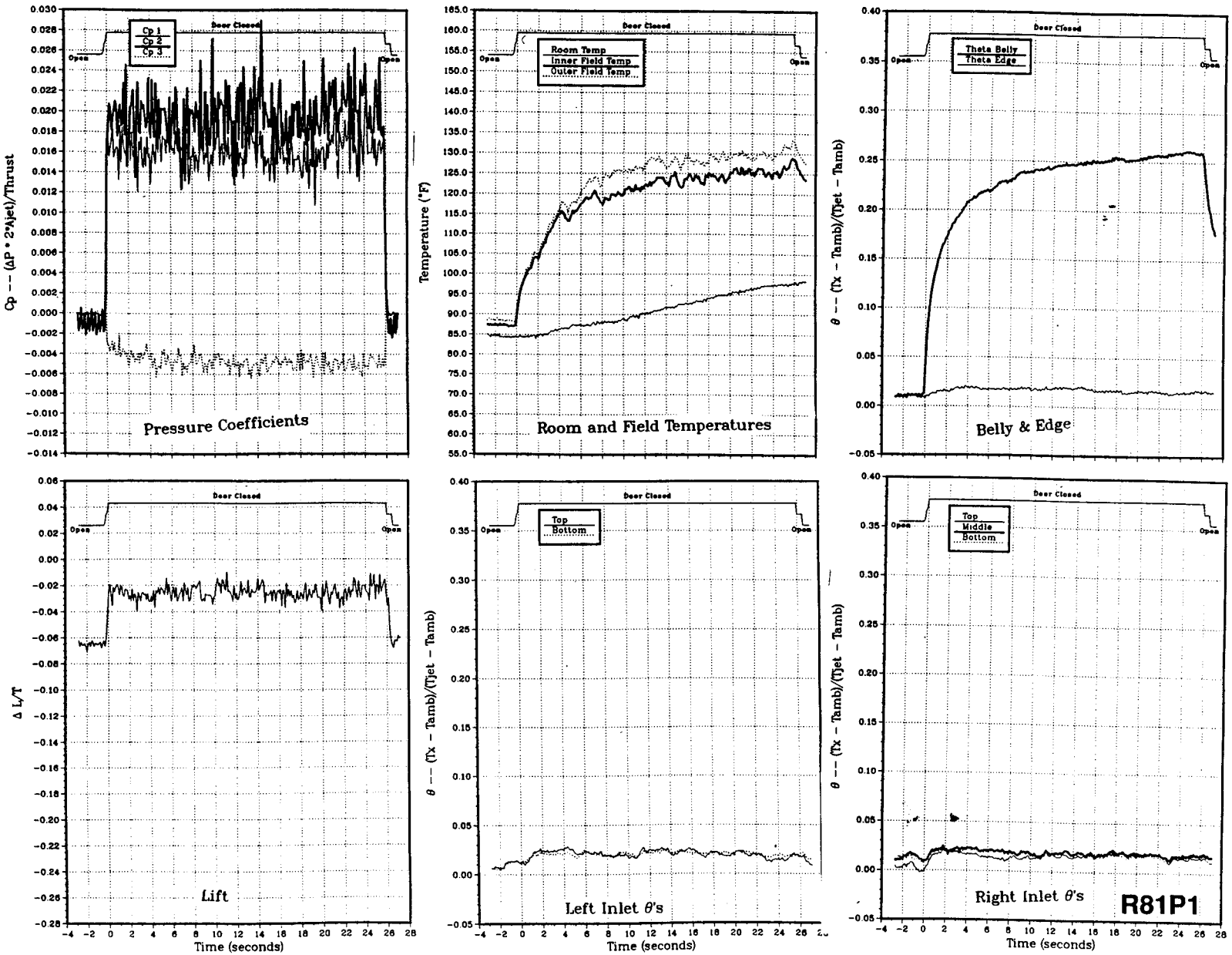

Figure 42(a). Body alone, Box LIDs (13/no rear), NPR = 2.0, thrust = 50 lb, height = 4 in., Tjet = 510 °F, inlet position = 9.66 in.

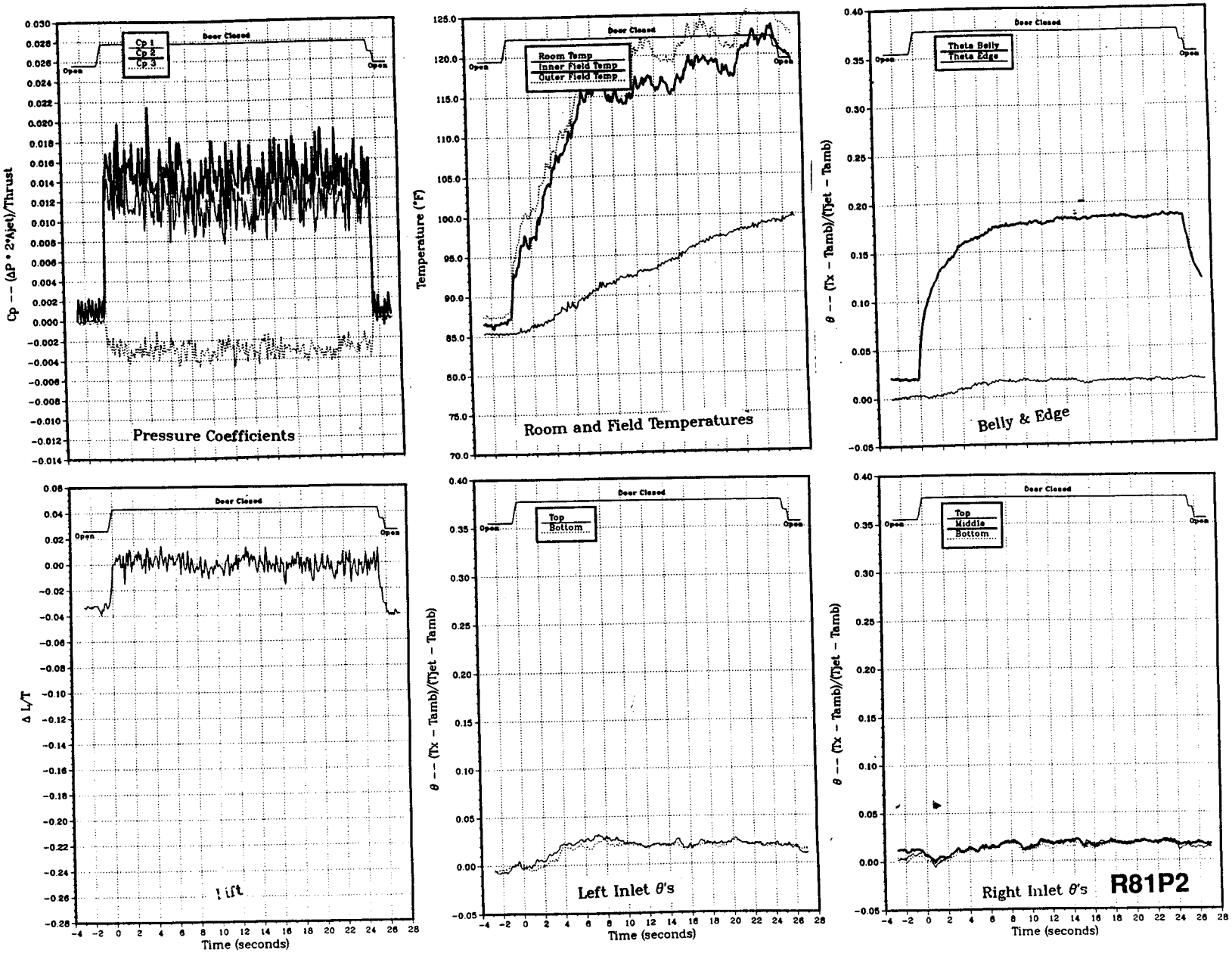

Figure 42(b). Body alone, Box LIDs (13/no rear), NPR = 2.0, thrust = 50 lb, height = 6 in., Tjet = 511 °F, inlet position = 9.66 in.

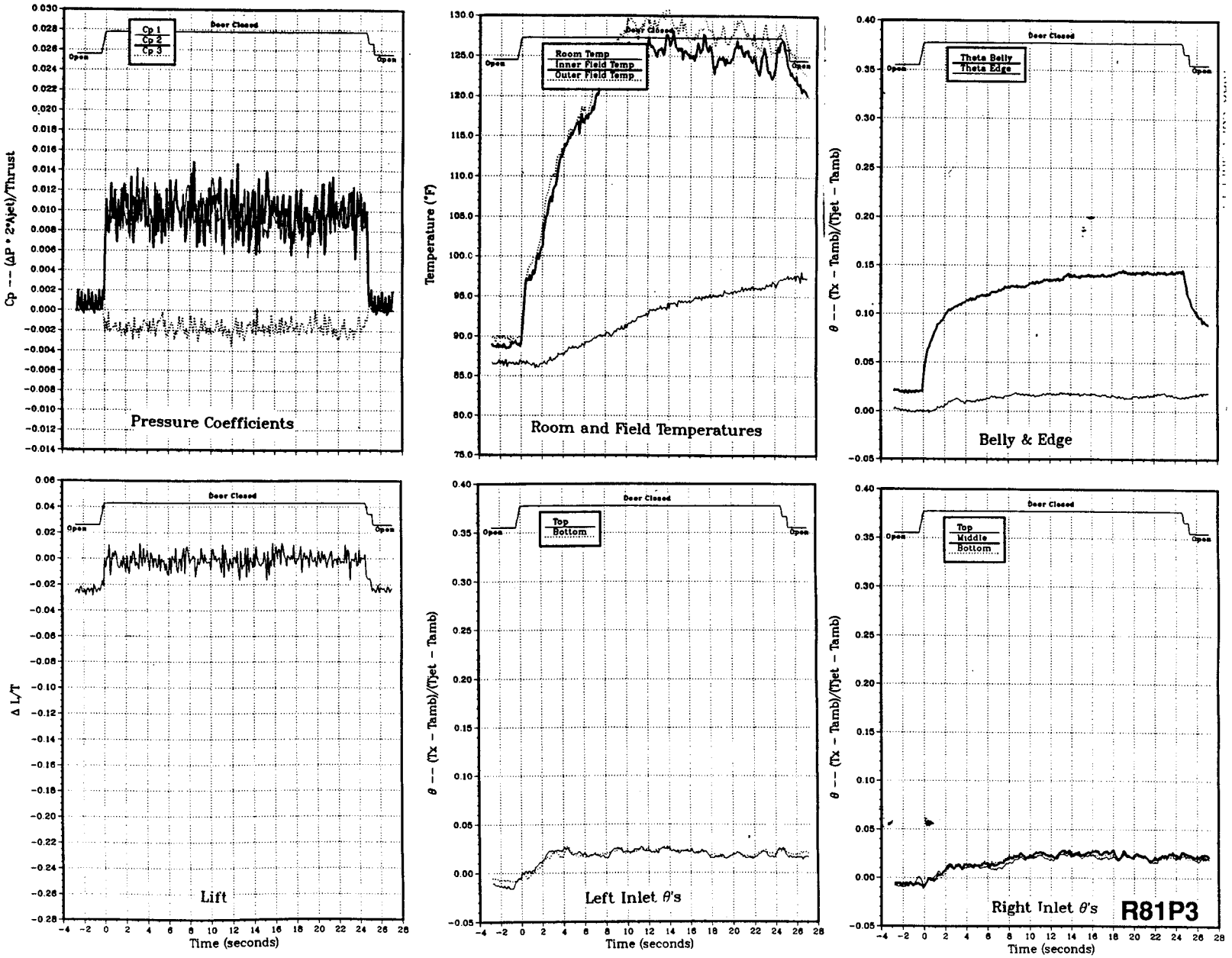

Figure 42(c). Body alone, Box LIDs (13/no rear), NPR = 2.0, thrust = 50 lb, height = 8 in., Tjet = 513 °F, inlet position = 9.66 in.

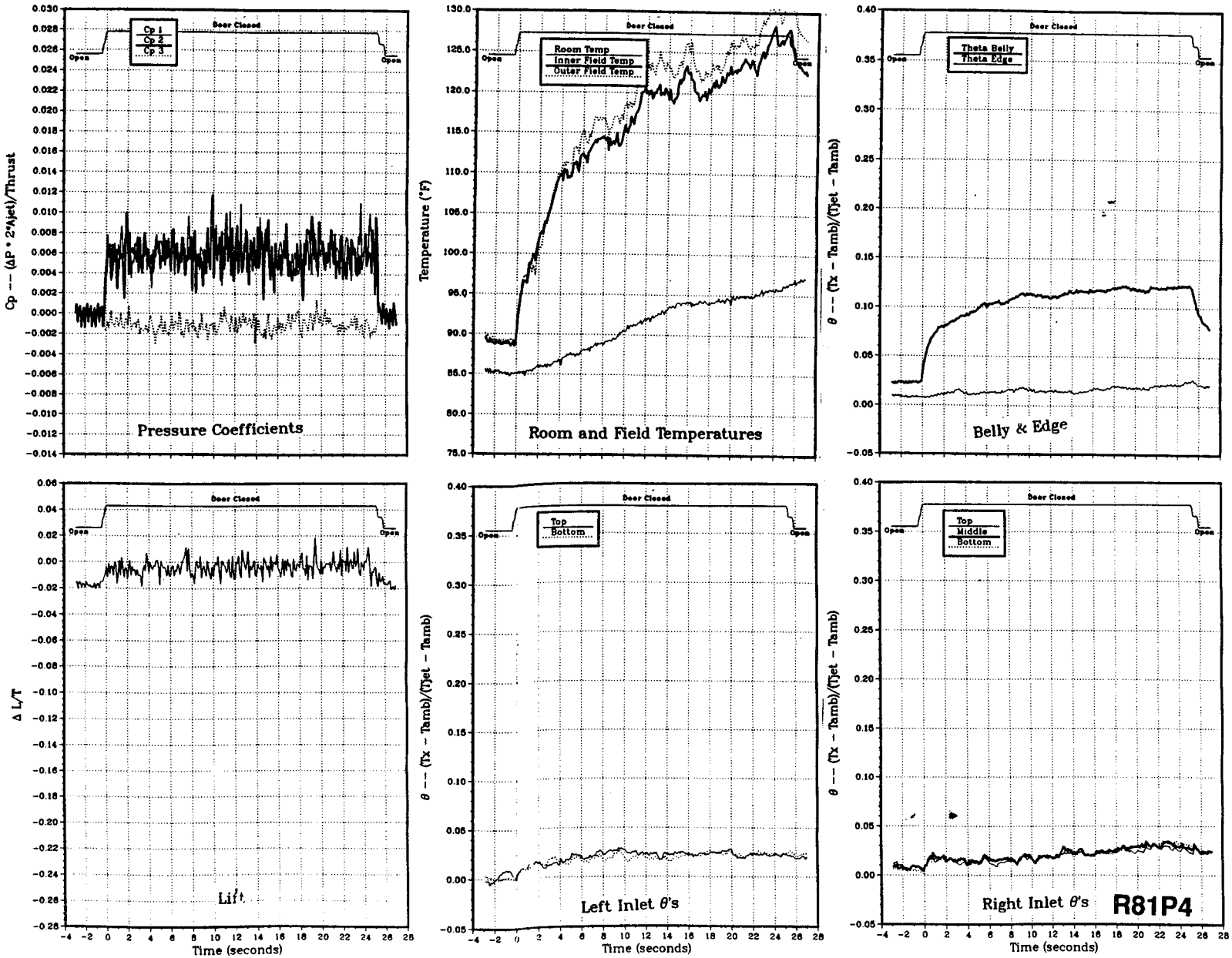

Figure 42(d). Body alone, Box LIDs (13/no rear), NPR = 2.0, thrust = 50 lb, height = 10 in., Tjet = 515 °F, inlet position = 9.66 in.

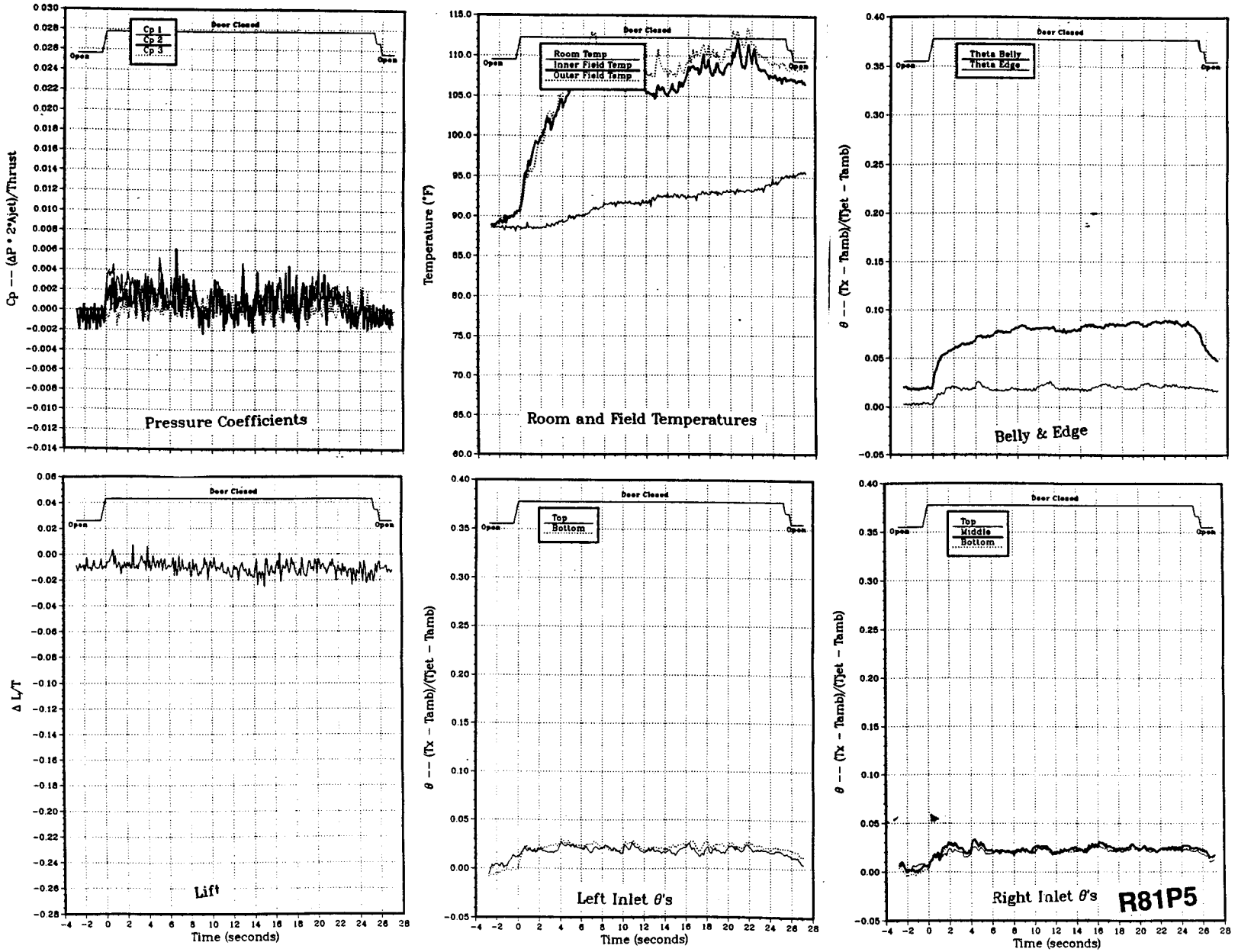

Figure 42(e). Body alone, Box LIDs (13/no rear), NPR = 2.0, thrust = 50 lb, height = 15 in., Tjet = 517 °F, inlet position = 9.66 in.

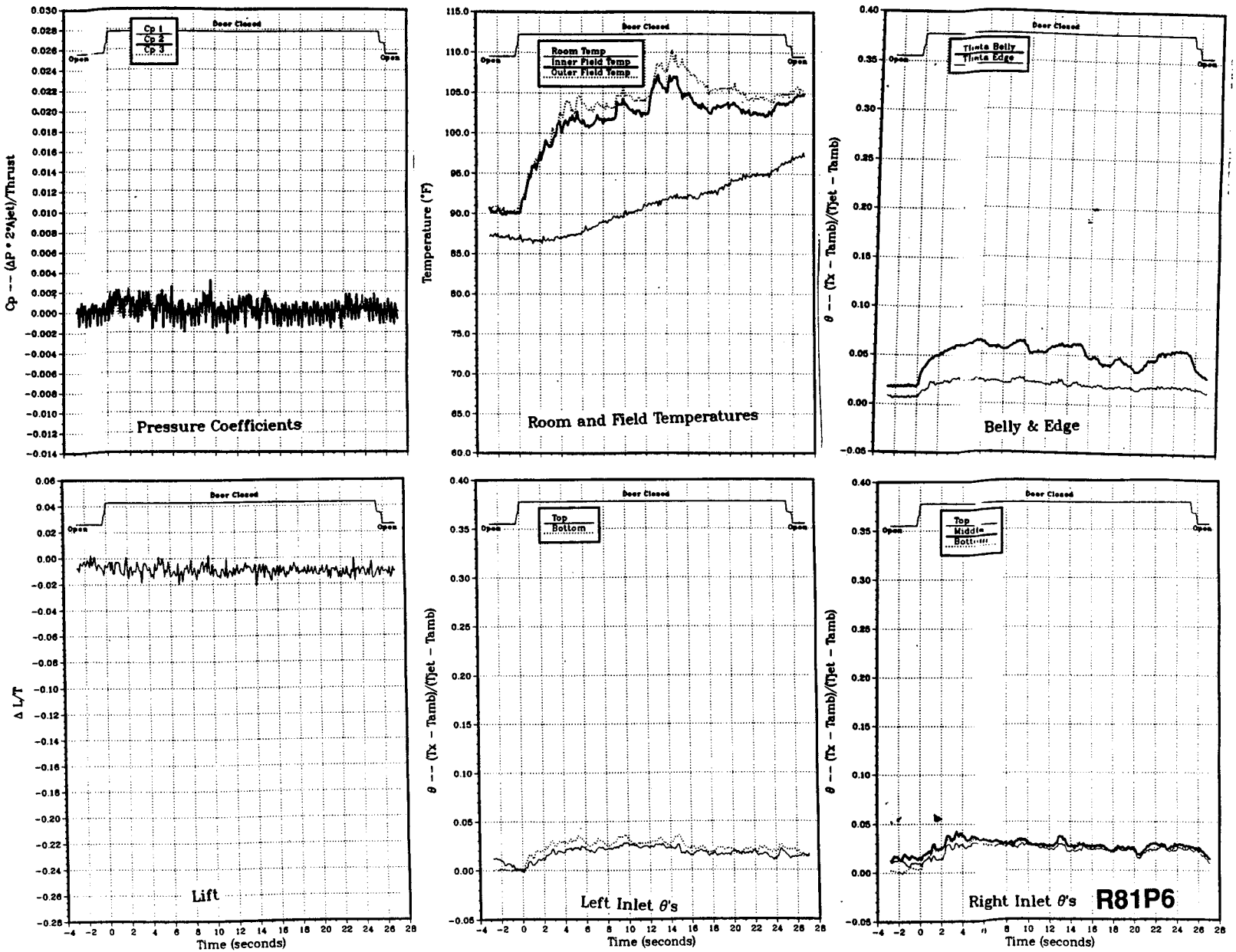

Figure 42(f). Body alone, Box LIDs (13/no rear), NPR = 2.0, thrust = 50 lb, height = 20 in., Tjet = 518 °F, inlet position = 9.66 in.

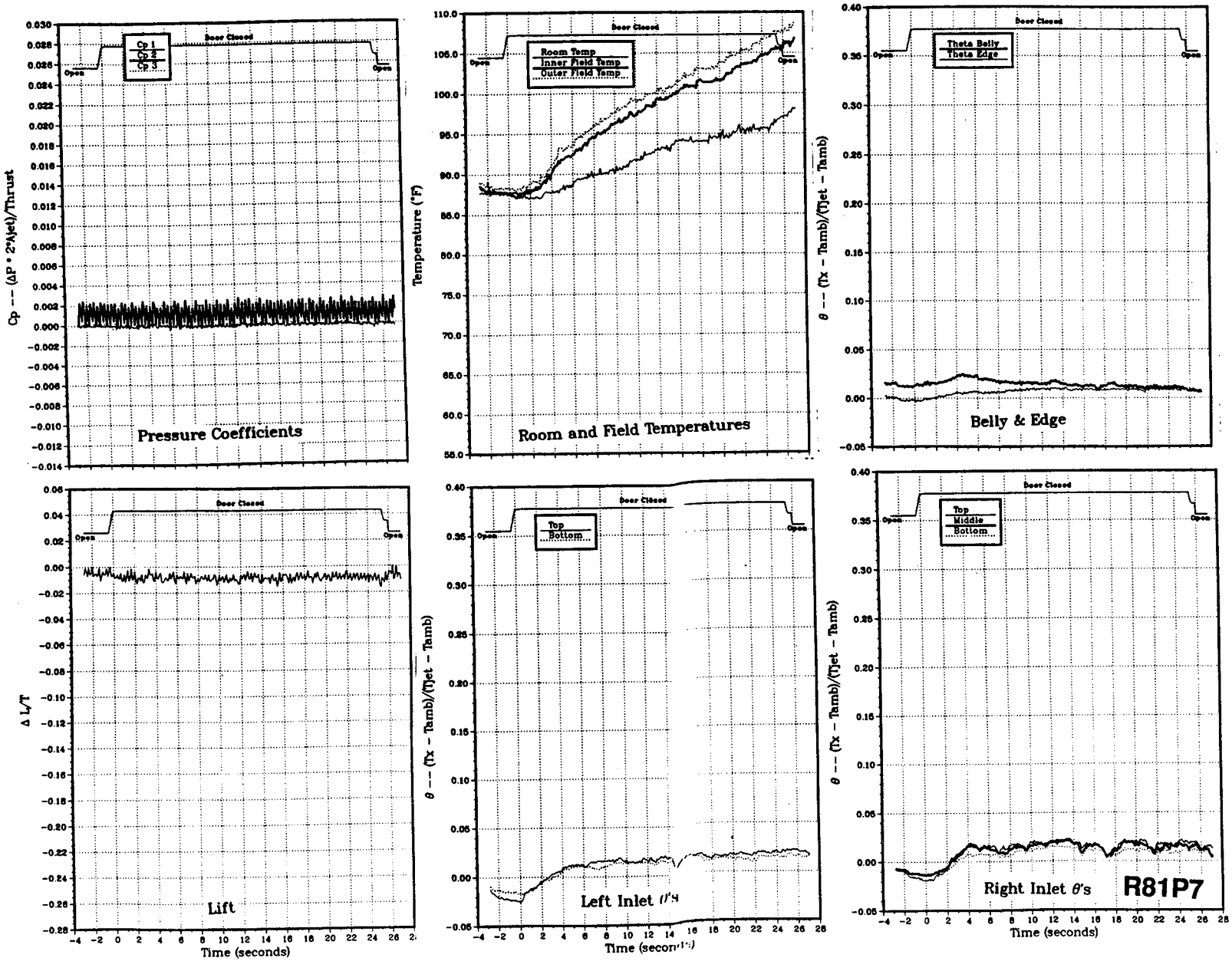

Figure 42(g). Body alone, Box LIDs (13/no rear), NPR = 2.0, thrust = 50 lb, height = 30 in., Tjet = 518 °F, inlet position = 9.66 in.

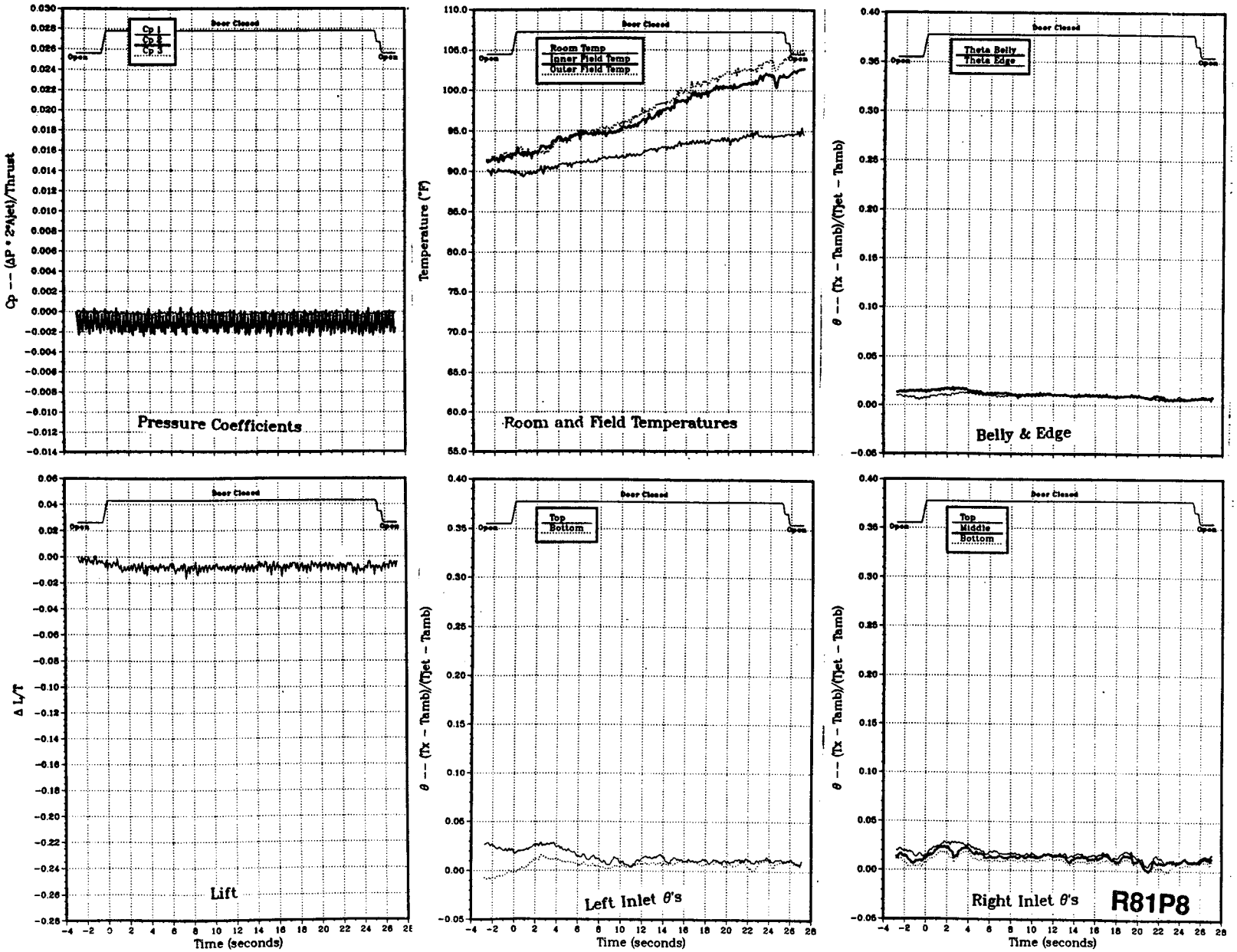

Figure 42(h). Body alone, Box LIDs (13/no rear), NPR = 2.0, thrust = 50 lb, height = 40 in., Tjet = 520 °F, inlet position = 9.66 in.

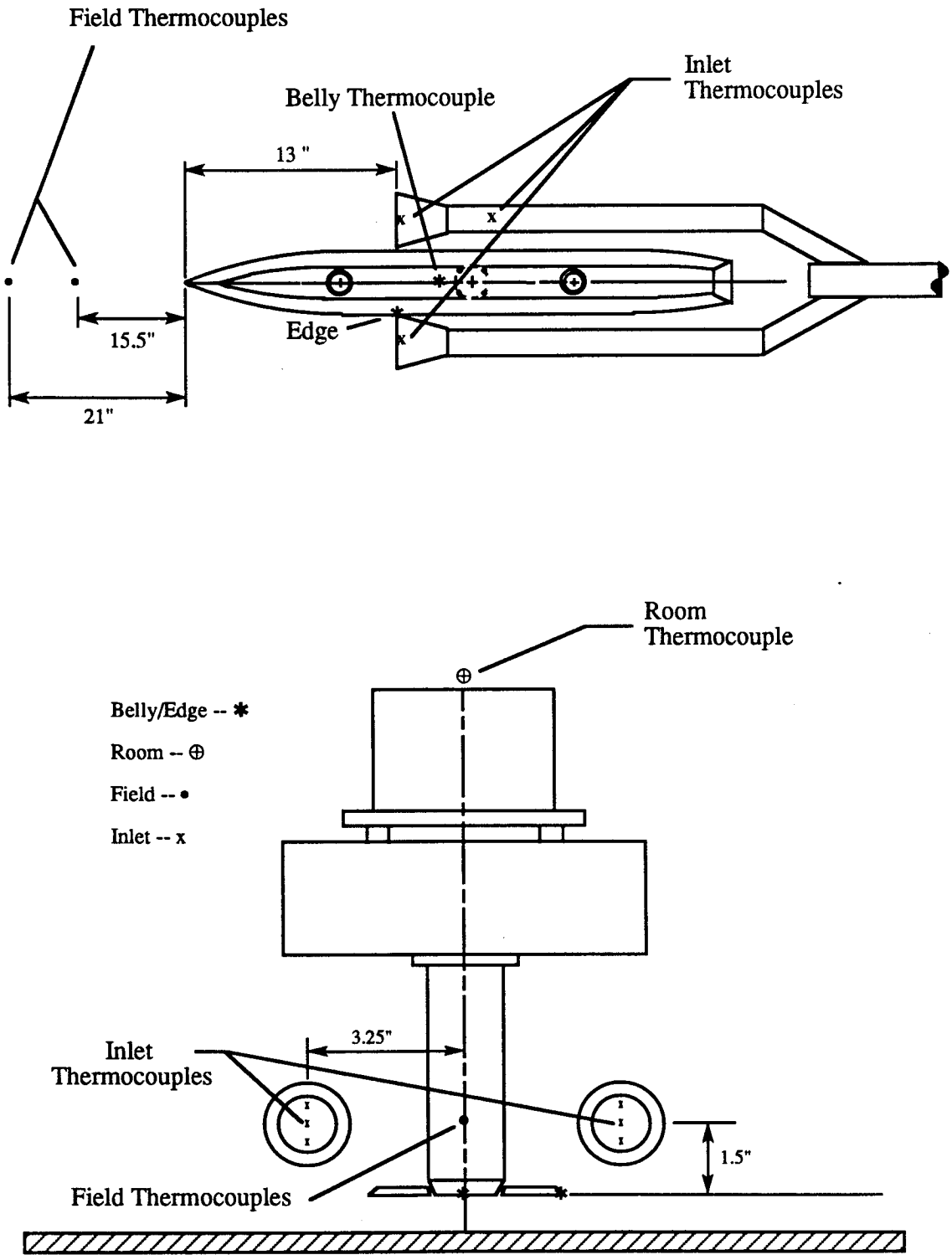

Figure 43. Locations of model and field thermocouples for data set 9.

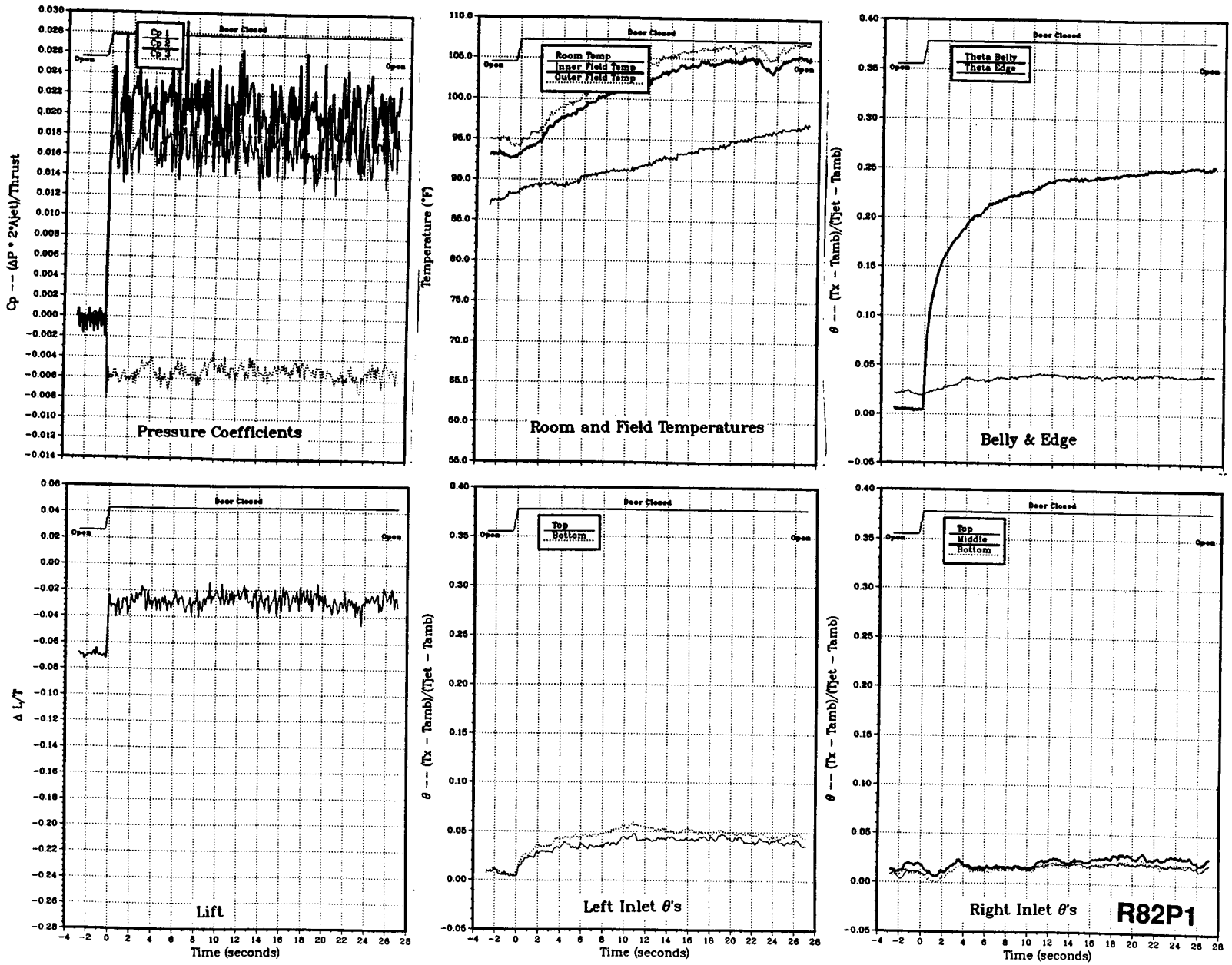

Figure 44(a). Body alone, no LIDs, NPR = 2.0, thrust = 50 lb, height = 4 in., Tjet = 495 °F, inlet position = 13 in.

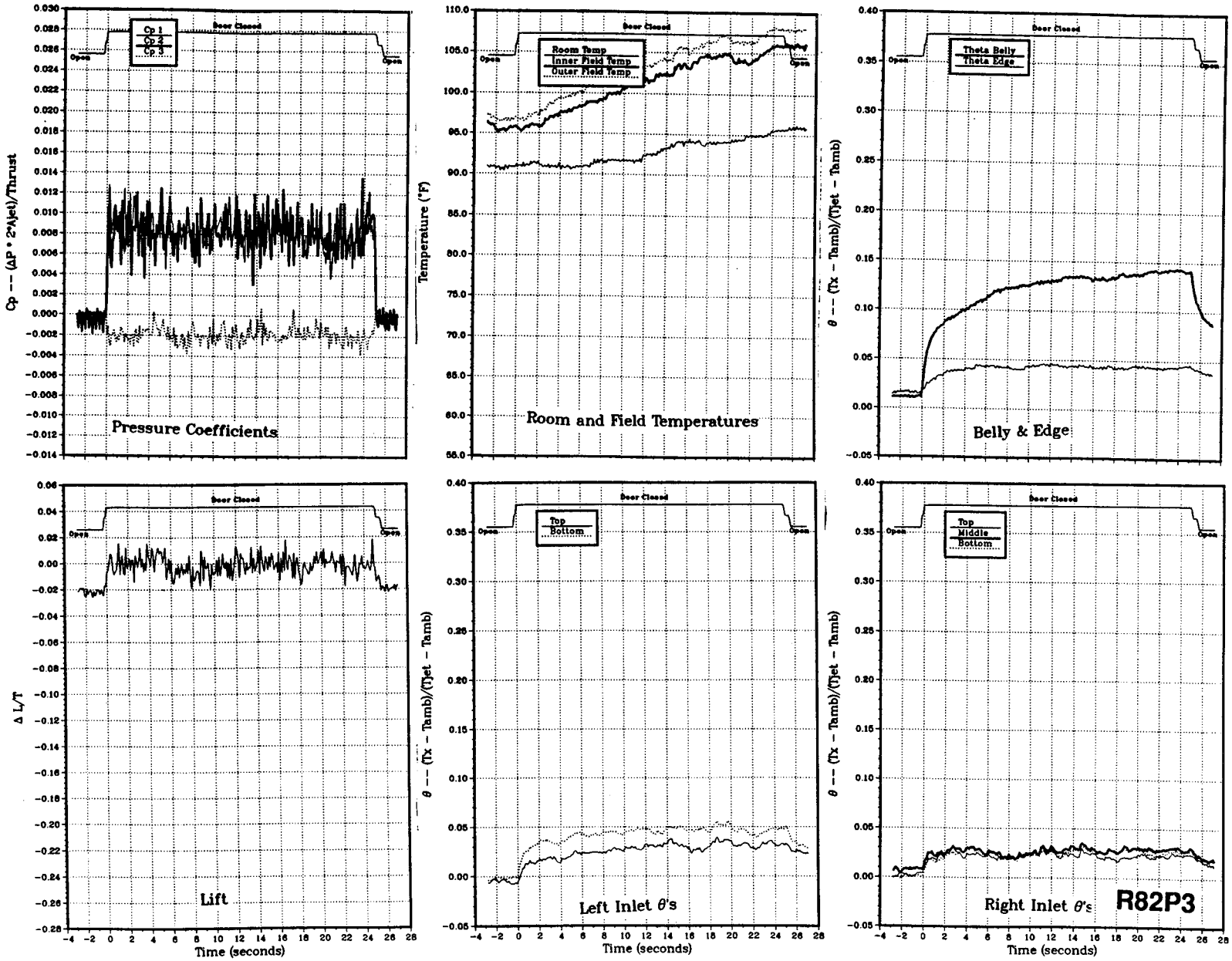

Figure 44(c). Body alone, no LIDs, NPR = 2.0, thrust = 50 lb, height = 8 in., Tjet = 503 °F, inlet position = 13 in.

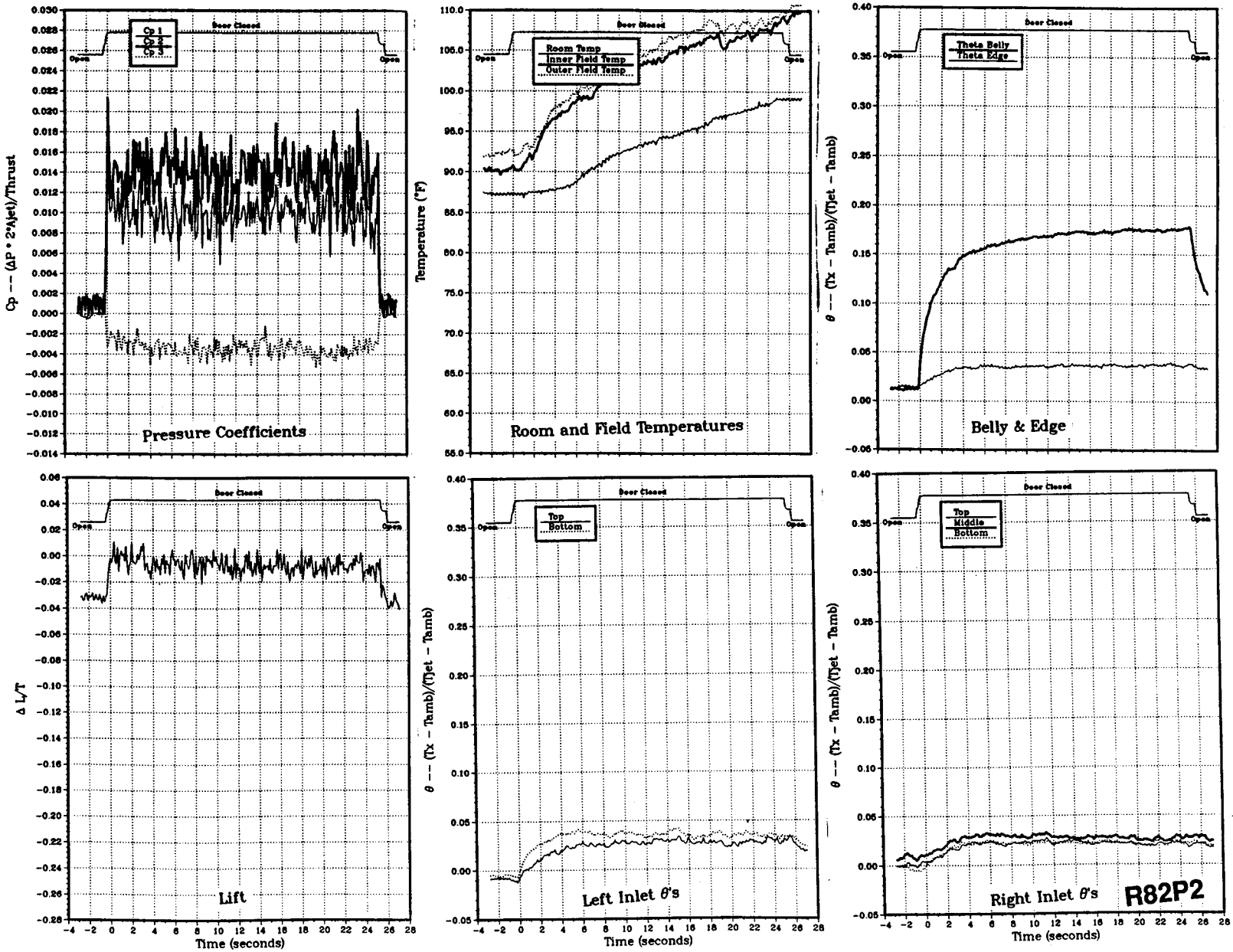

Figure 44(b). Body alone, no LIDs, NPR = 2.0, thrust = 50 lb, height = 6 in., Tjet = 500 °F, inlet position = 13 in.

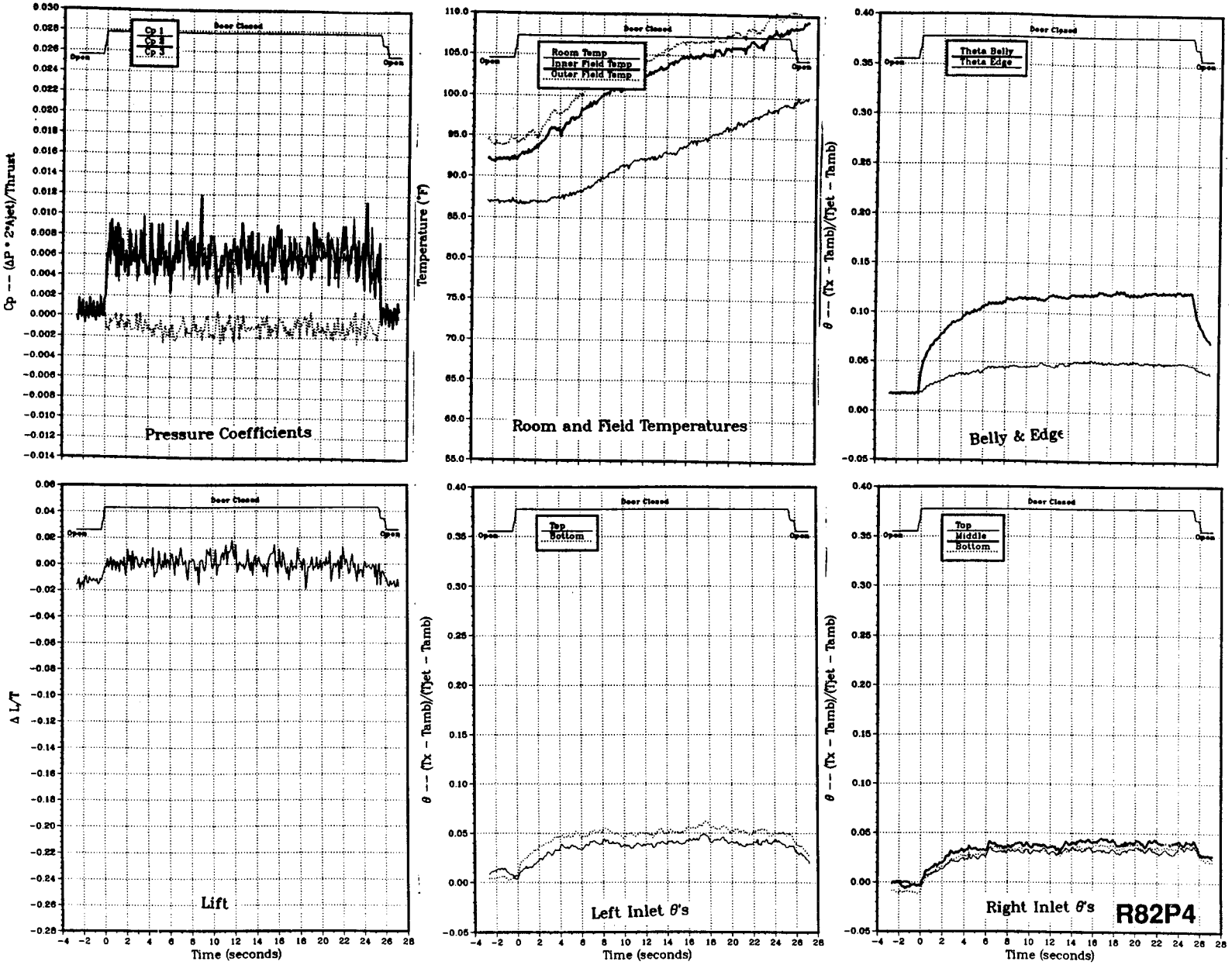

Figure 44(d). Body alone, no LIDs, NPR = 2.0, thrust = 50 lb, height = 10 in., Tjet = 506 °F, inlet position = 13 in.

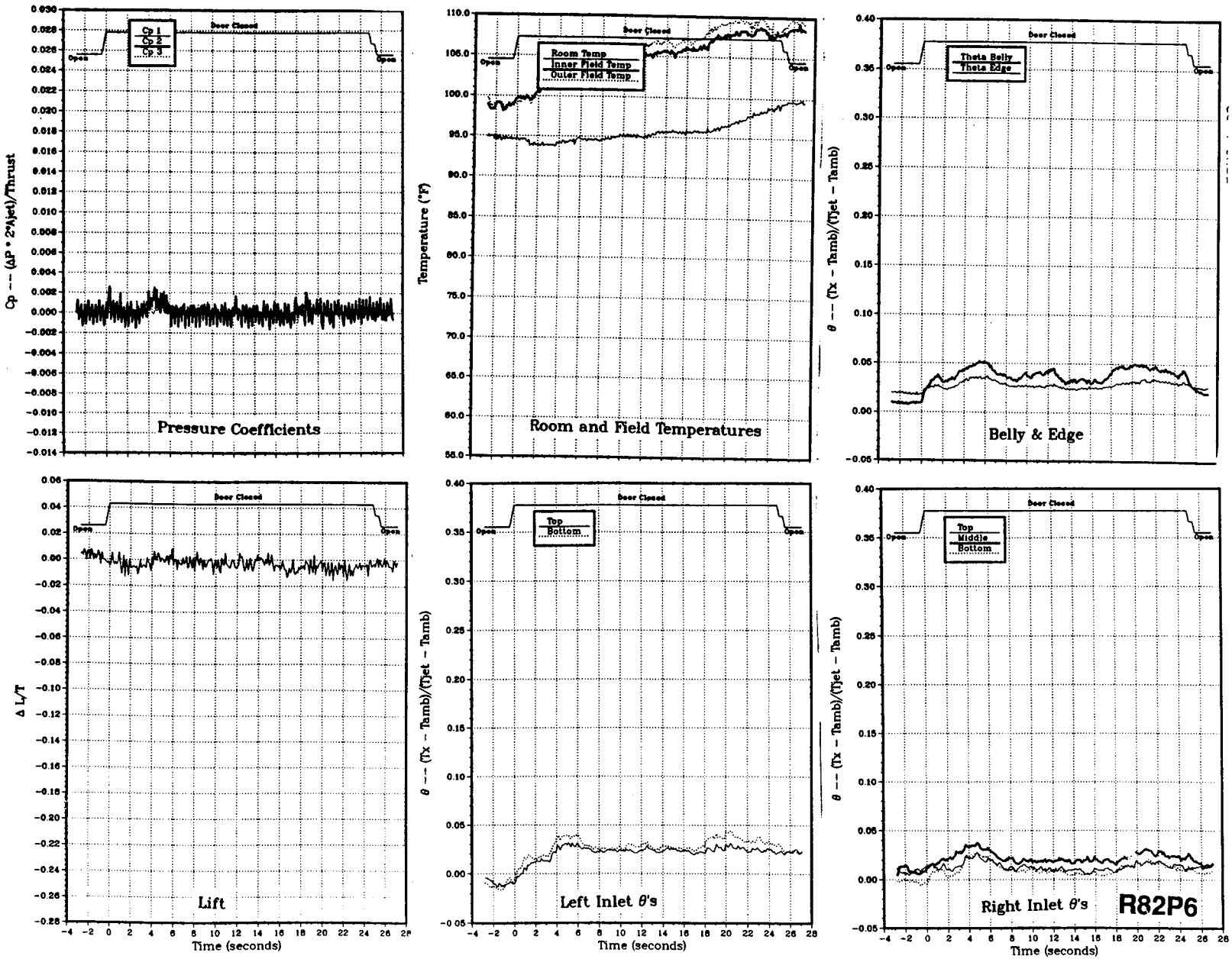

Figure 44(e). Body alone, no LIDs, NPR = 2.0, thrust = 50 lb, height = 20 in., Tjet = 511 °F, inlet position = 13 in.

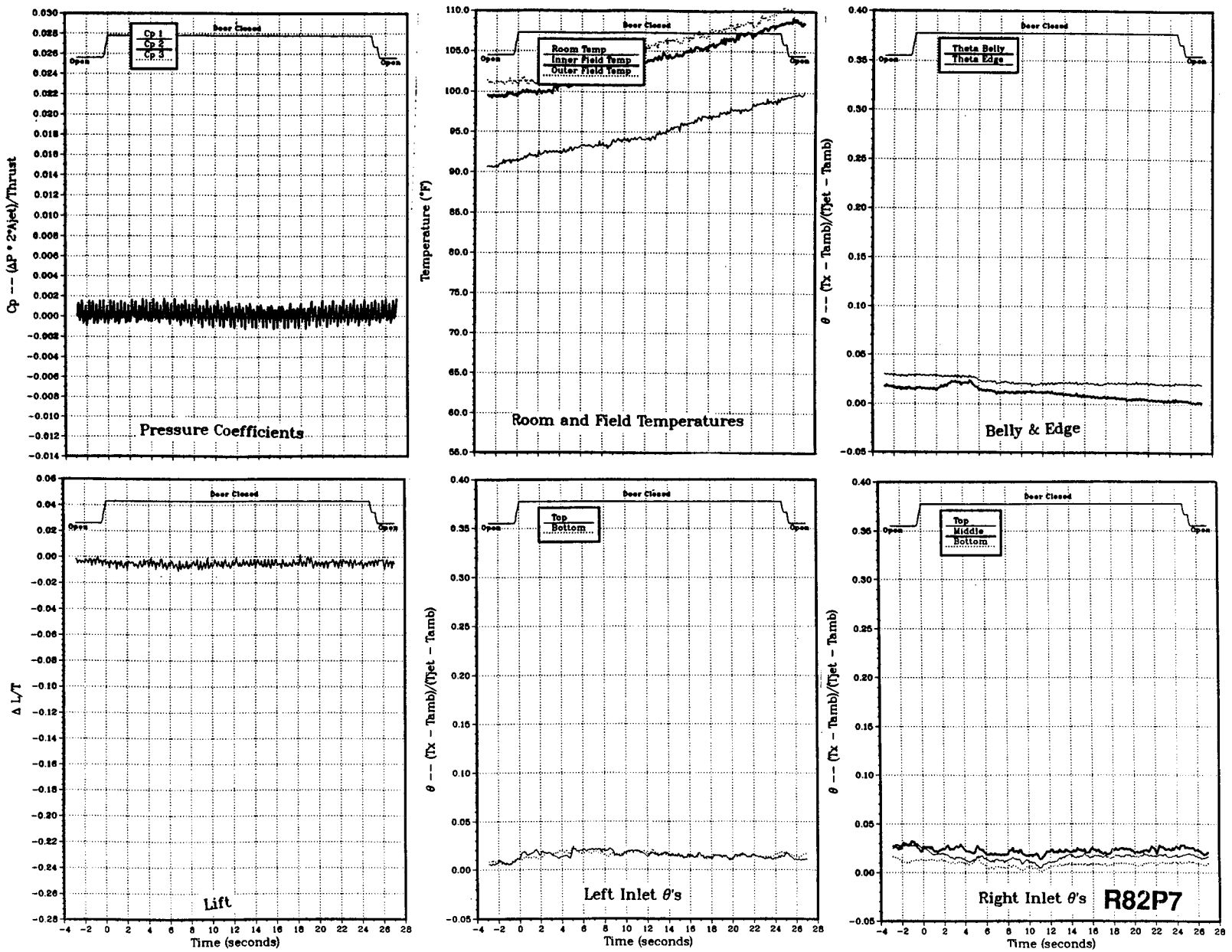

Figure 44(f). Body alone, no LIDs, NPR = 2.0, thrust = 50 lb, height = 30 in., Tjet = 514 °F, inlet position = 13 in.

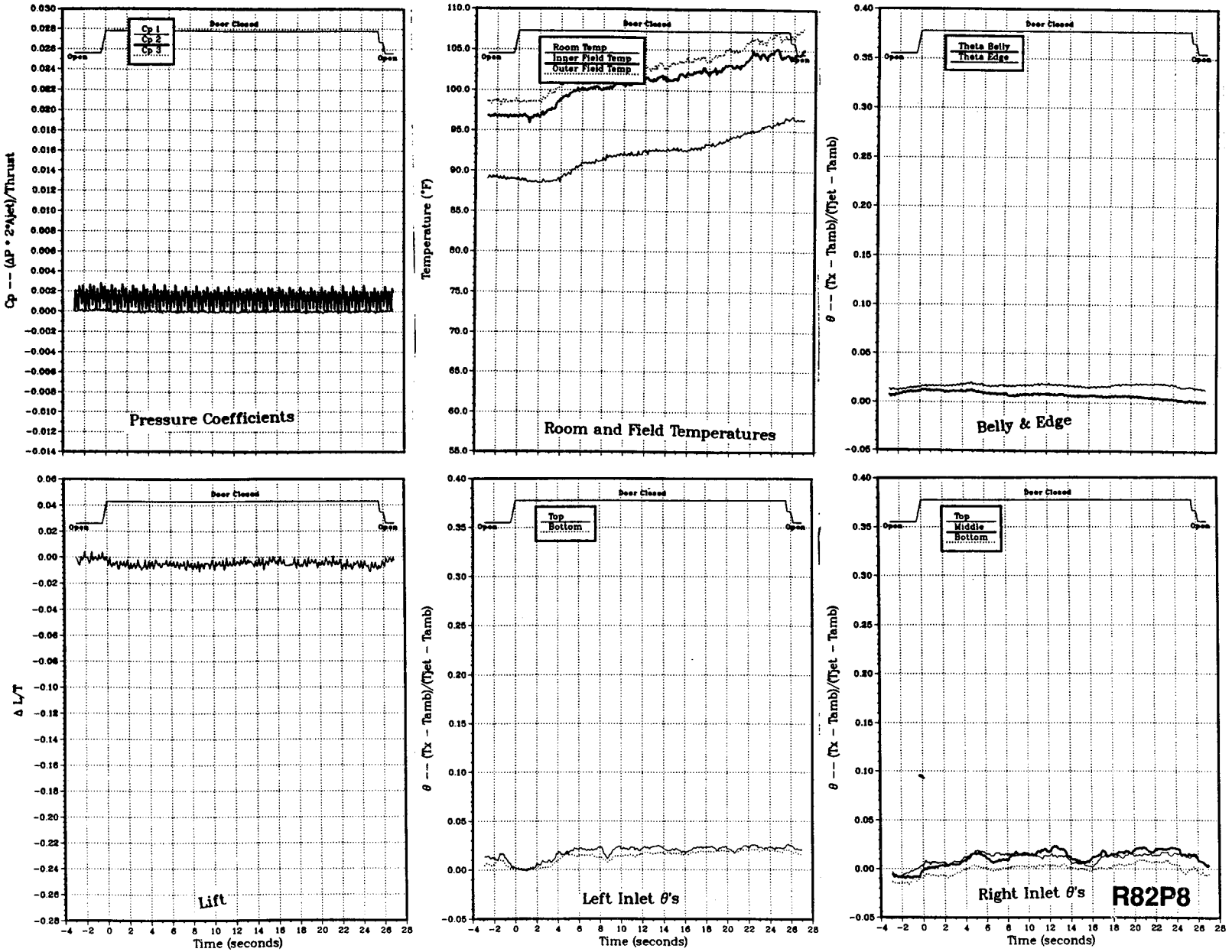

Figure 44(g). Body alone, no LIDs, NPR = 2.0, thrust = 50 lb, height = 40 in., Tjet = 515 °F, inlet position = 13 in.

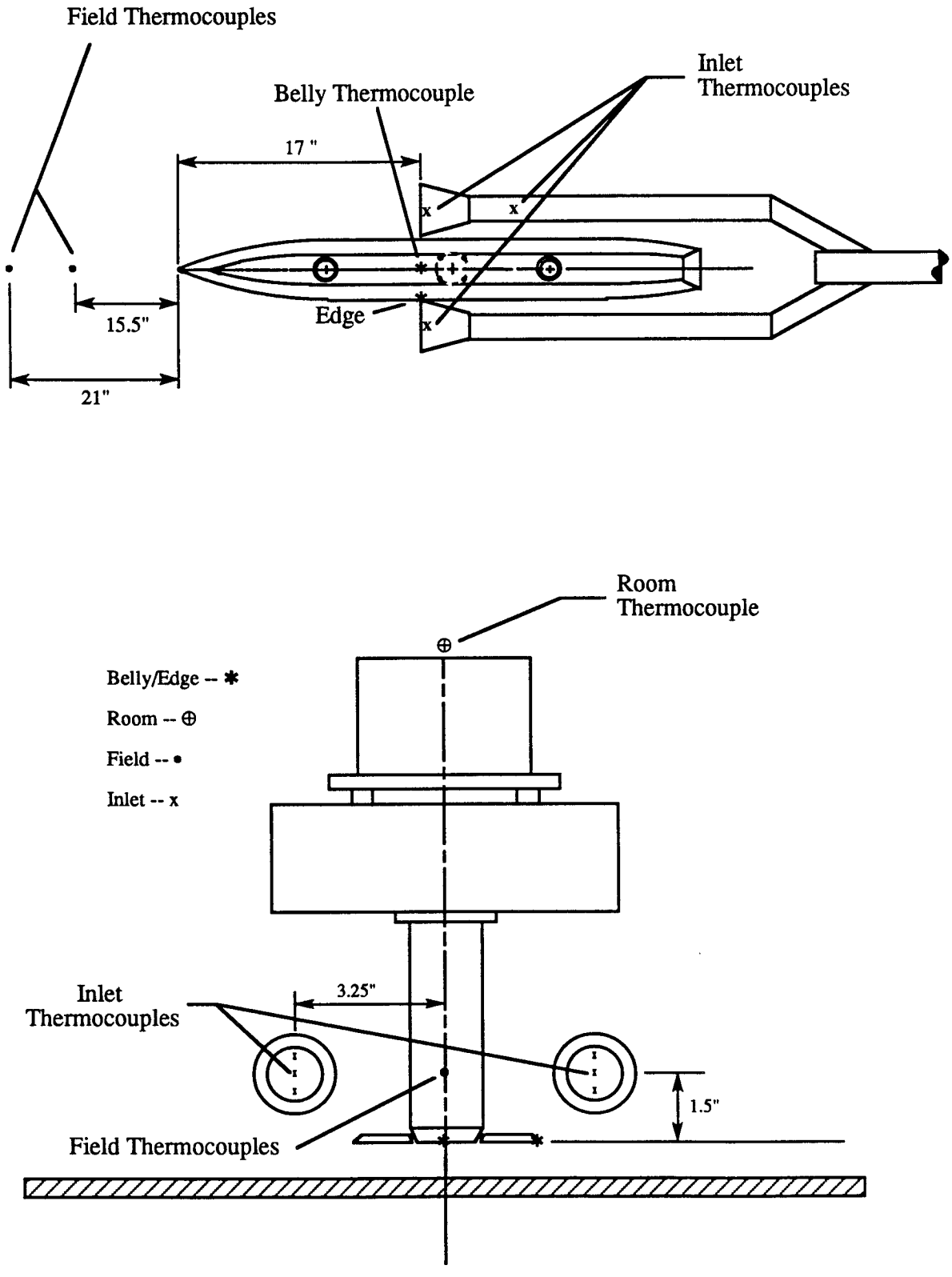

Figure 45. Locations of model and field thermocouples for data set 10.

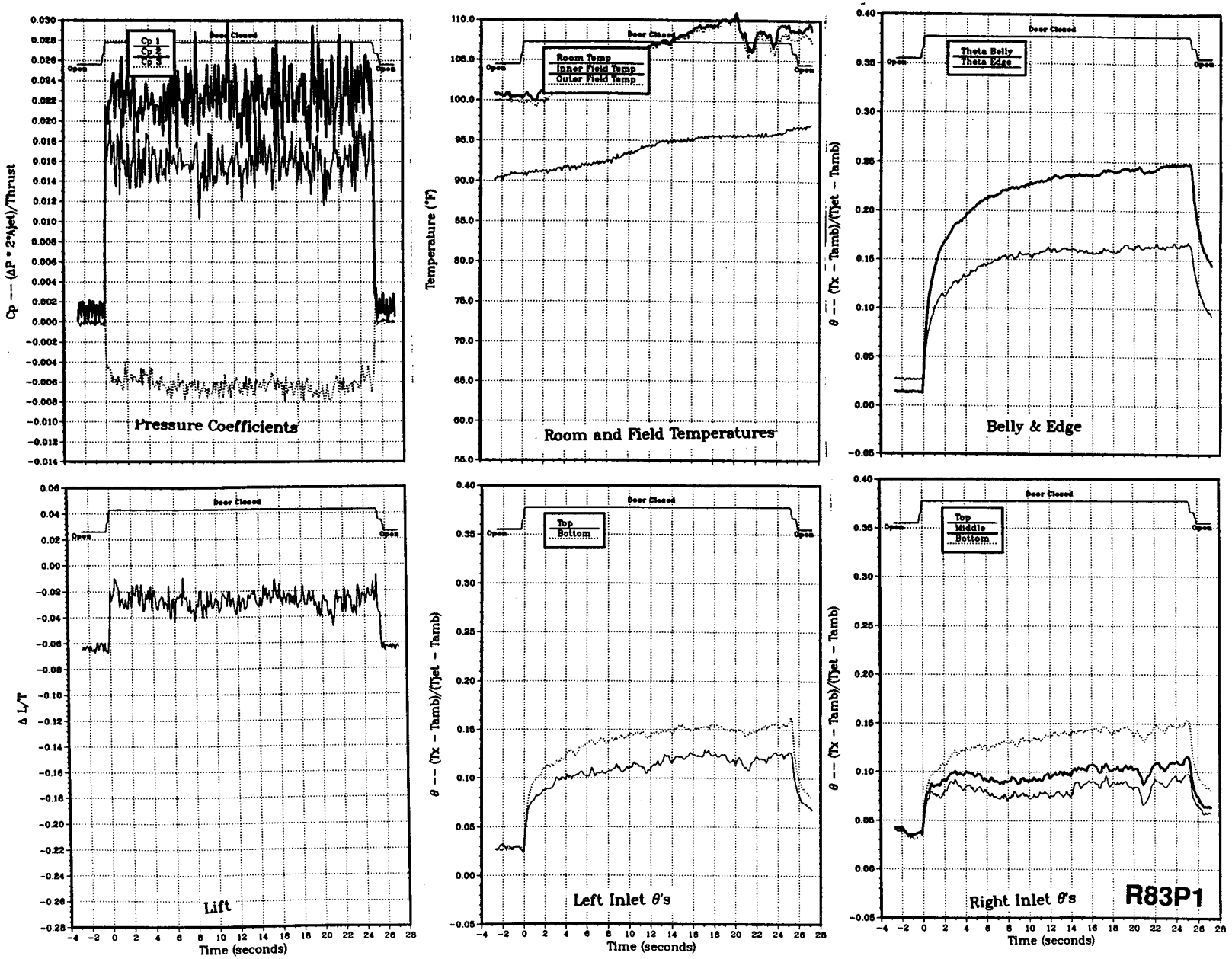

Figure 46(a). Body alone, no LIDs, NPR = 2.0, thrust = 50 lb, height = 4 in., Tjet = 506 °F, inlet position = 17 in.

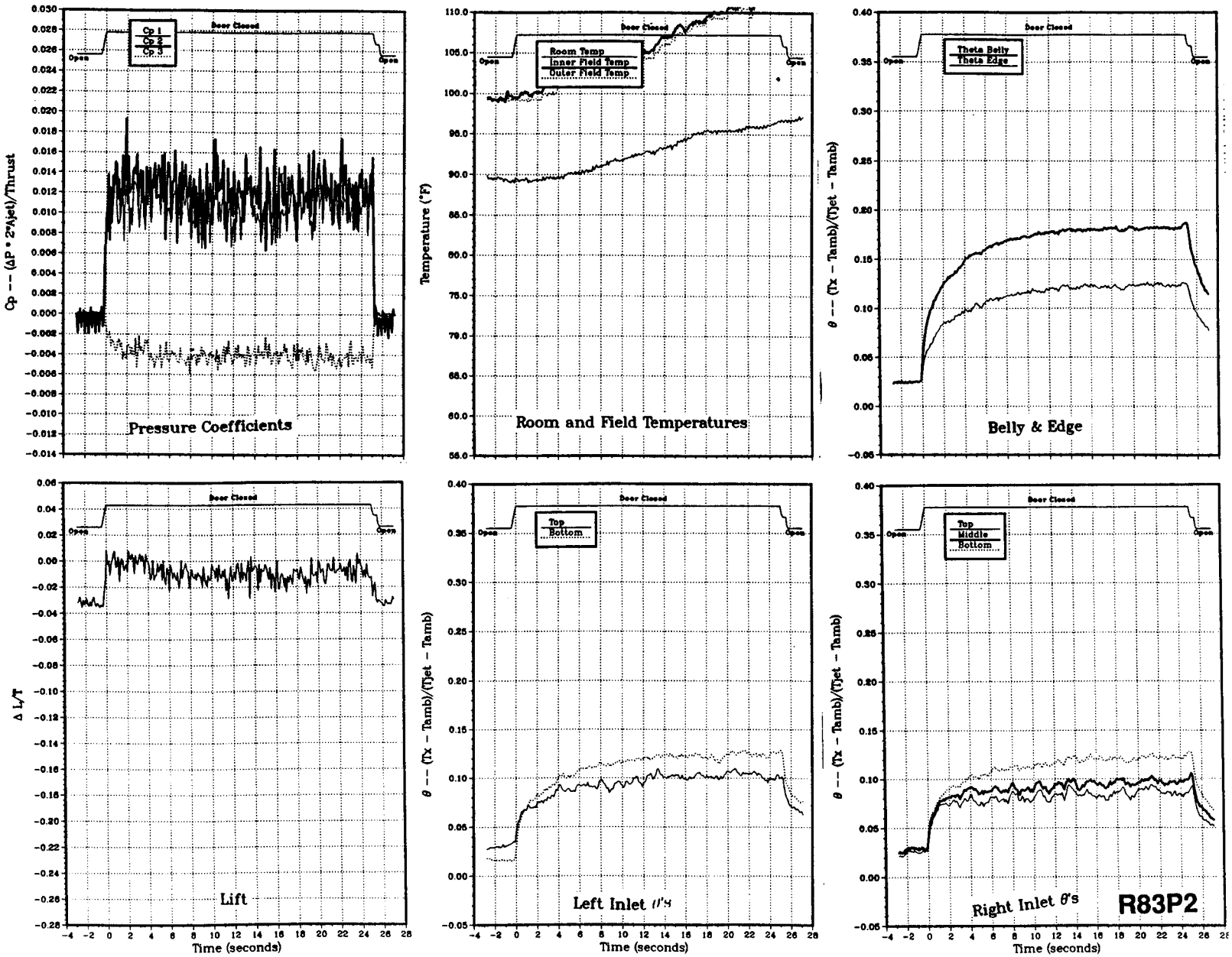

Figure 46(b). Body alone, no LIDs, NPR = 2.0, thrust = 50 lb, height = 6 in., Tjet = 508 °F, inlet position = 17 in.

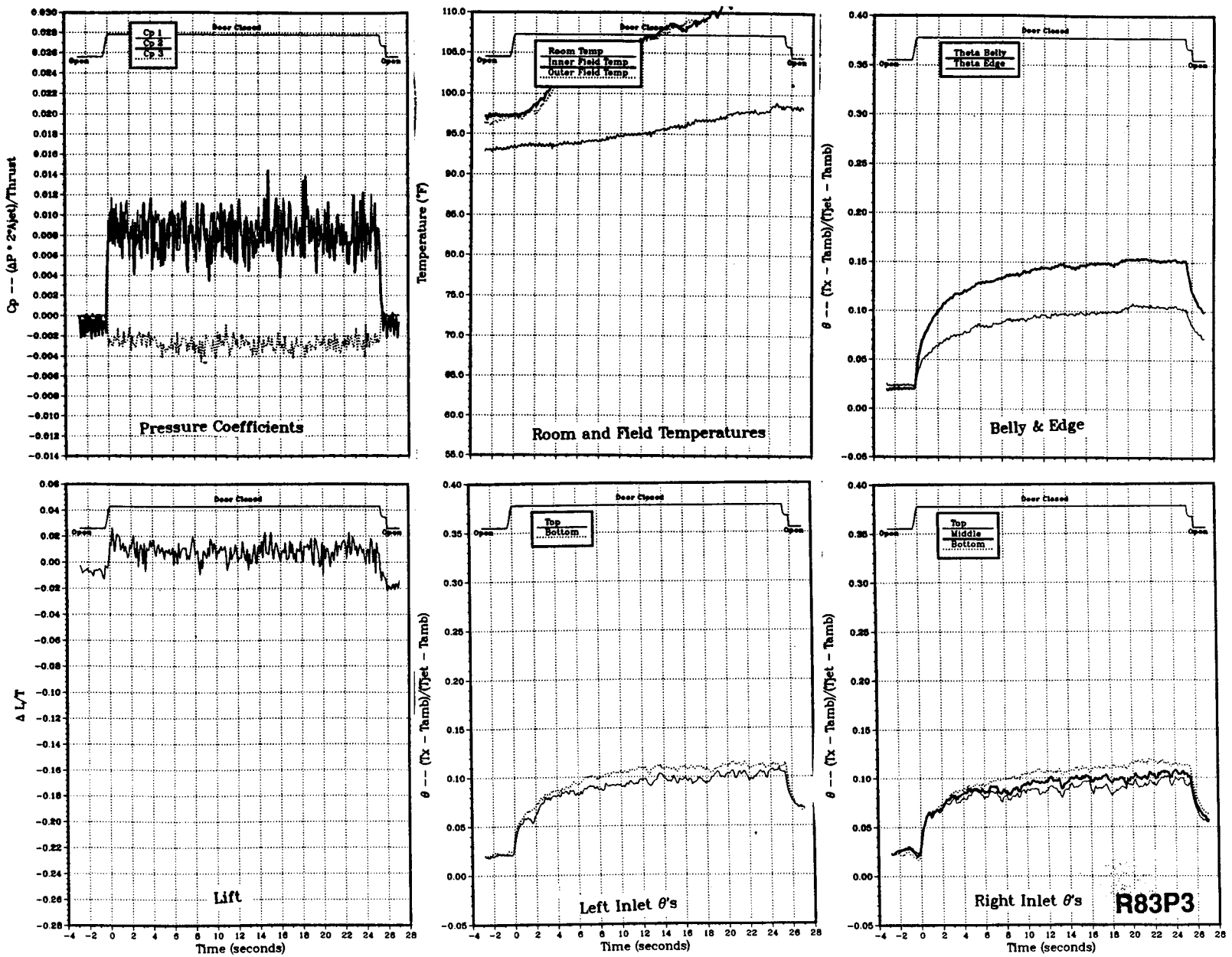

Figure 46(c). Body alone, no LIDs, NPR = 2.0, thrust = 50 lb, height = 8 in., Tjet = 511 °F, inlet position = 17 in.

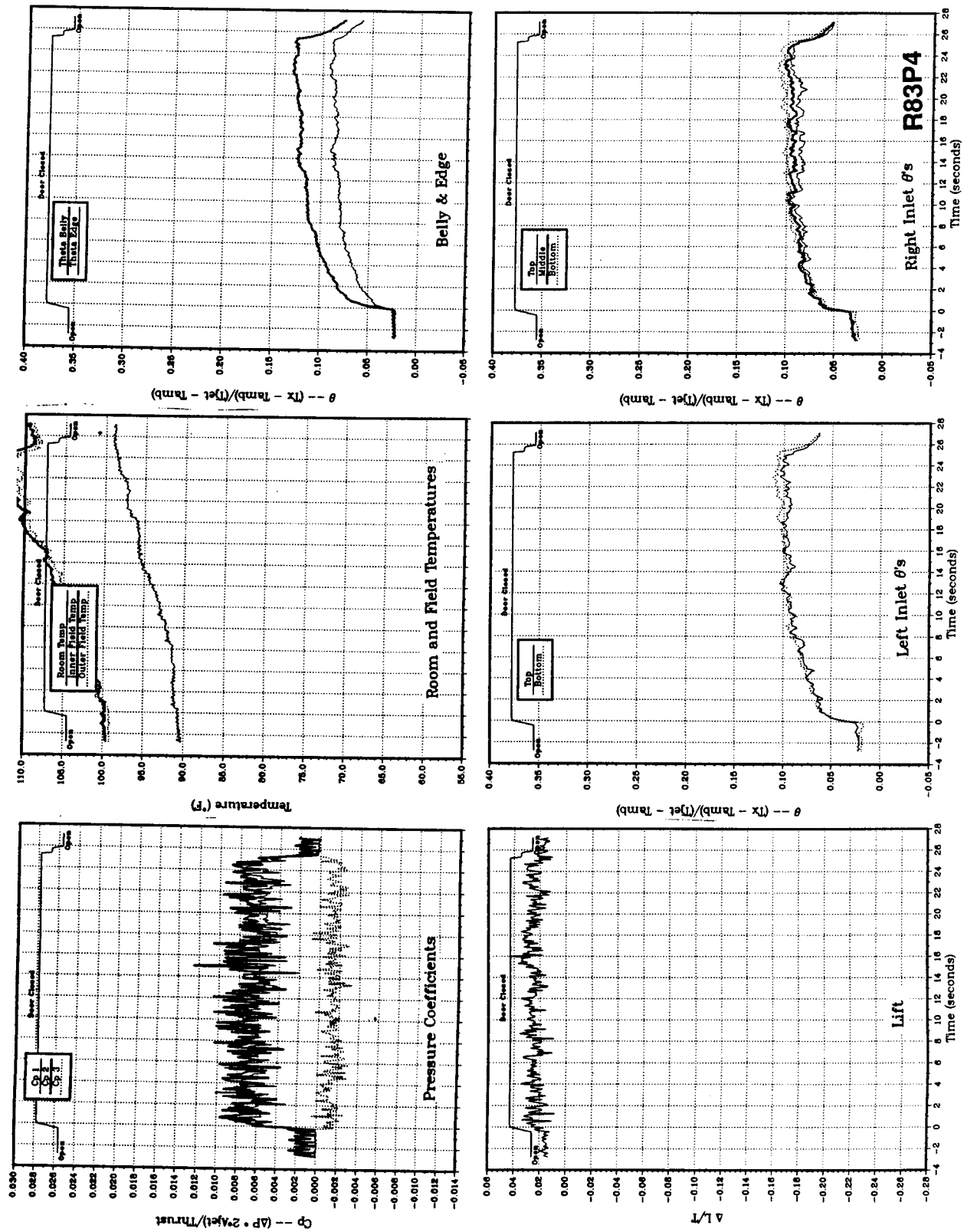

Figure 46(d). Body alone, no LIDs, NPR = 2.0, thrust = 50 lb, height = 10 in., Tjet = 513 °F, inlet position = 17 in.

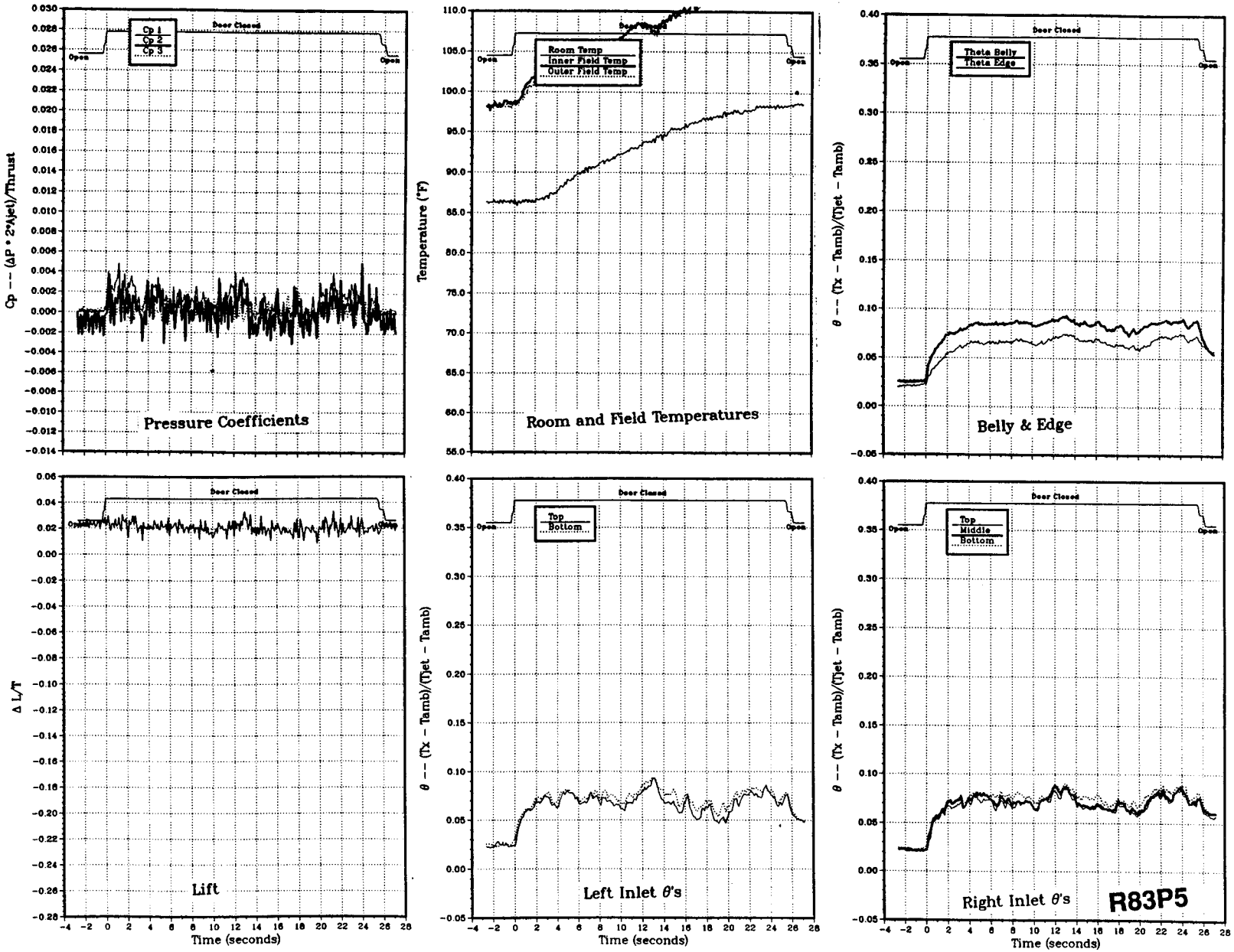

Figure 46(e). Body alone, no LIDs, NPR = 2.0, thrust = 50 lb, height = 15 in., Tjet = 514 °F, inlet position = 17 in.

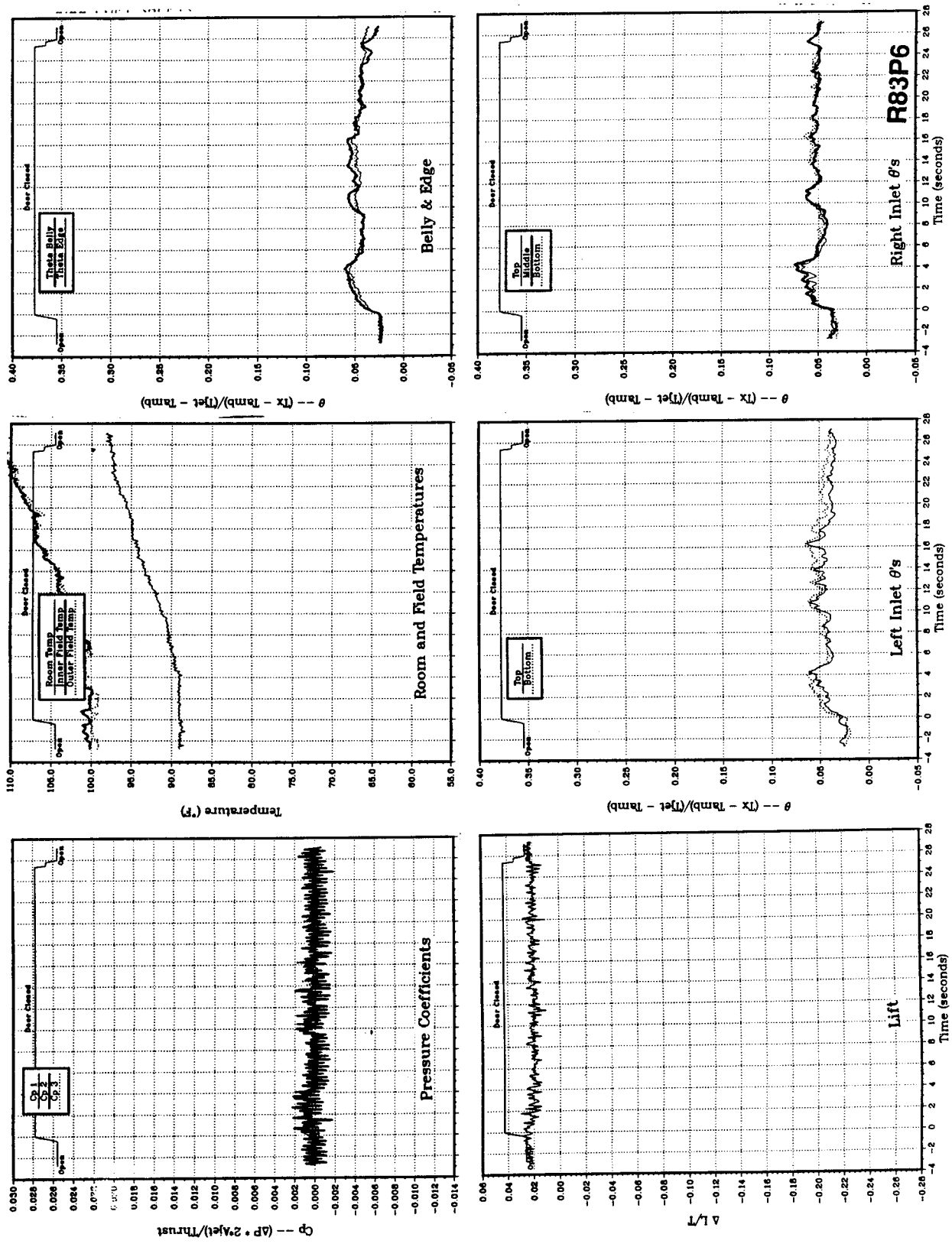

Figure 46(f). Body alone, no LIDs, NPR = 2.0, thrust = 50 lb, height = 20 in., Tjet = 516 °F, inlet position = 17 in.

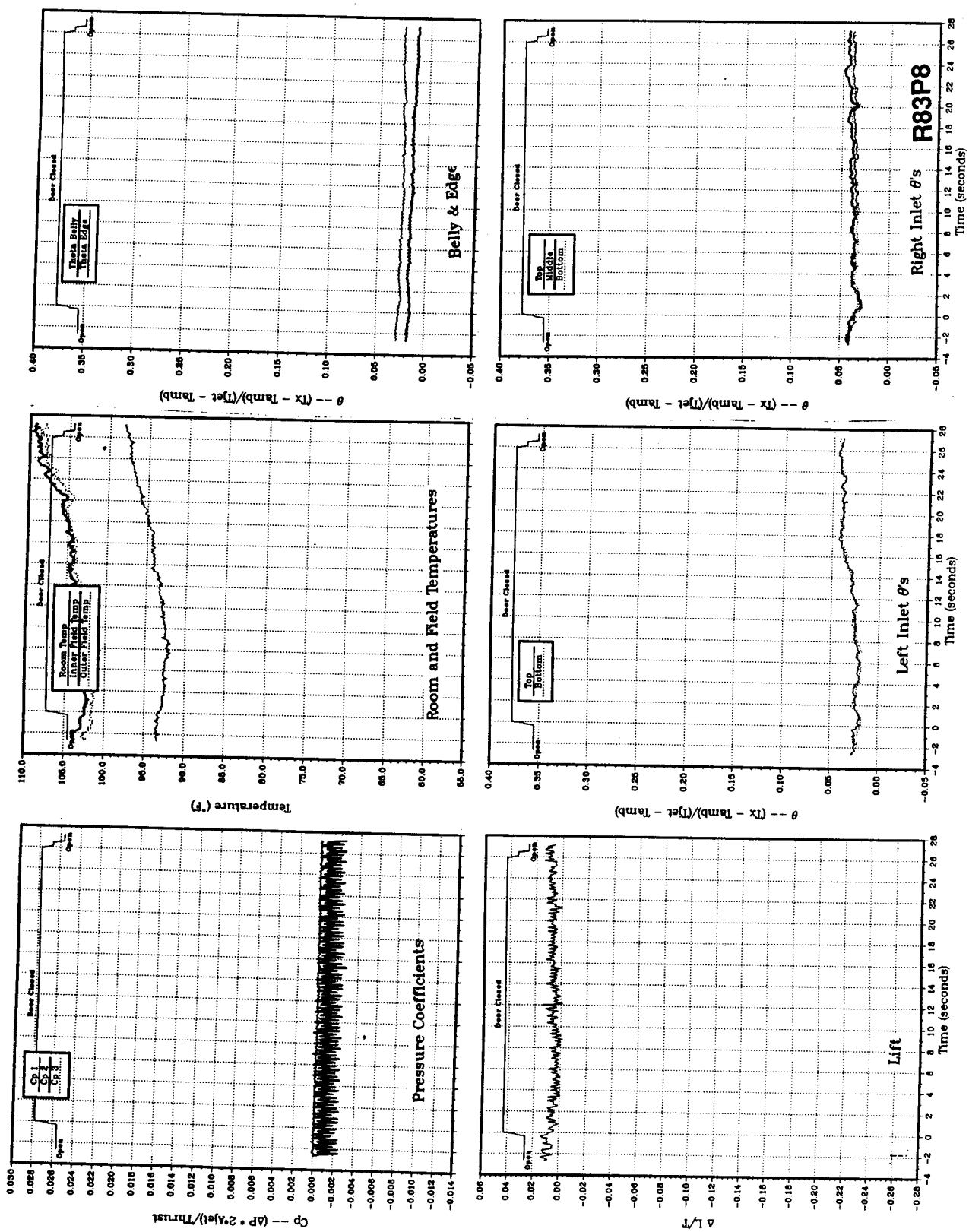

Figure 46(g). Body alone, no LIDs, NPR = 2.0, thrust = 50 lb, height = 40 in., Tjet = 518 °F, inlet position = 17 in.

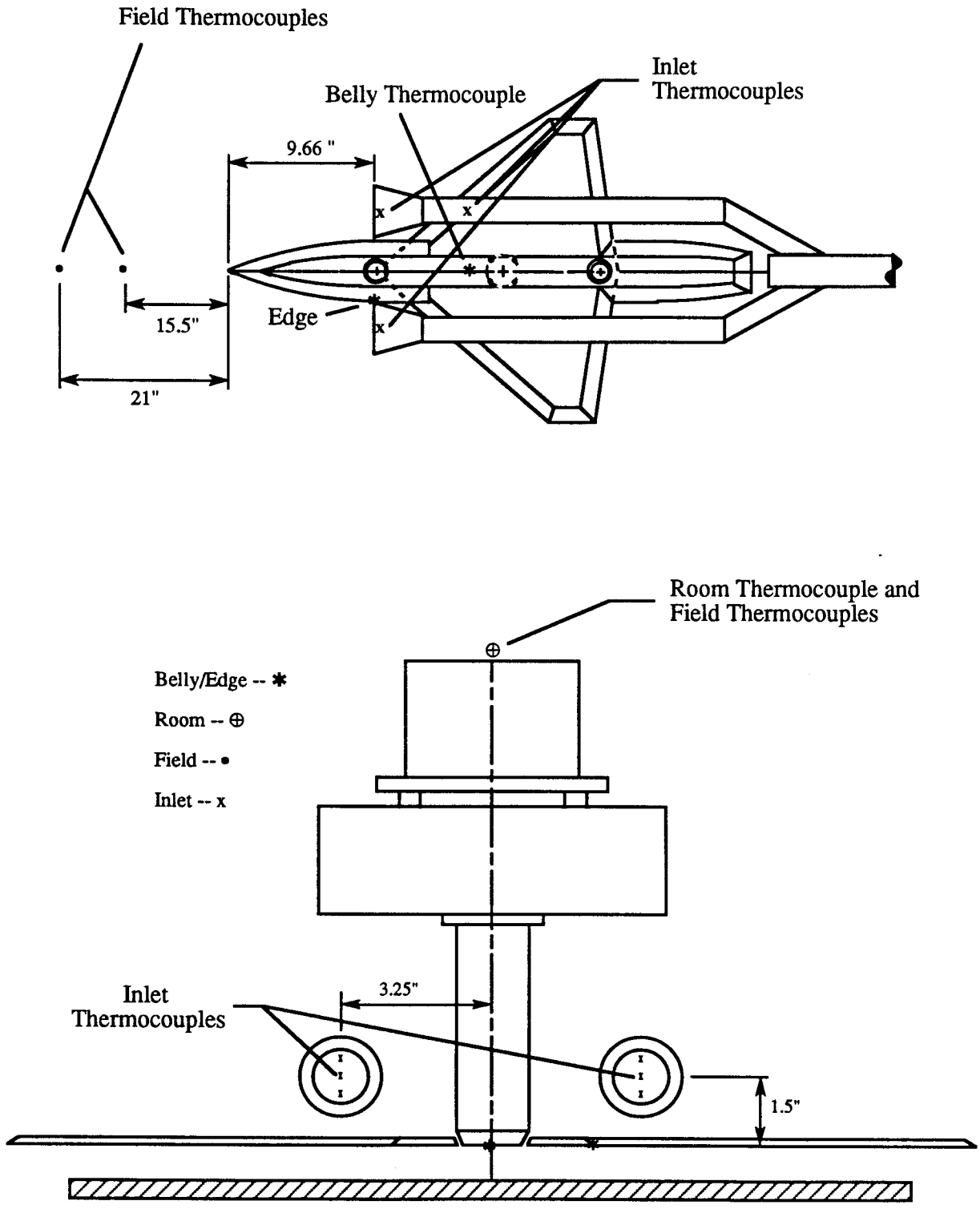

Figure 47. Locations of model and field thermocouples for data set 11.

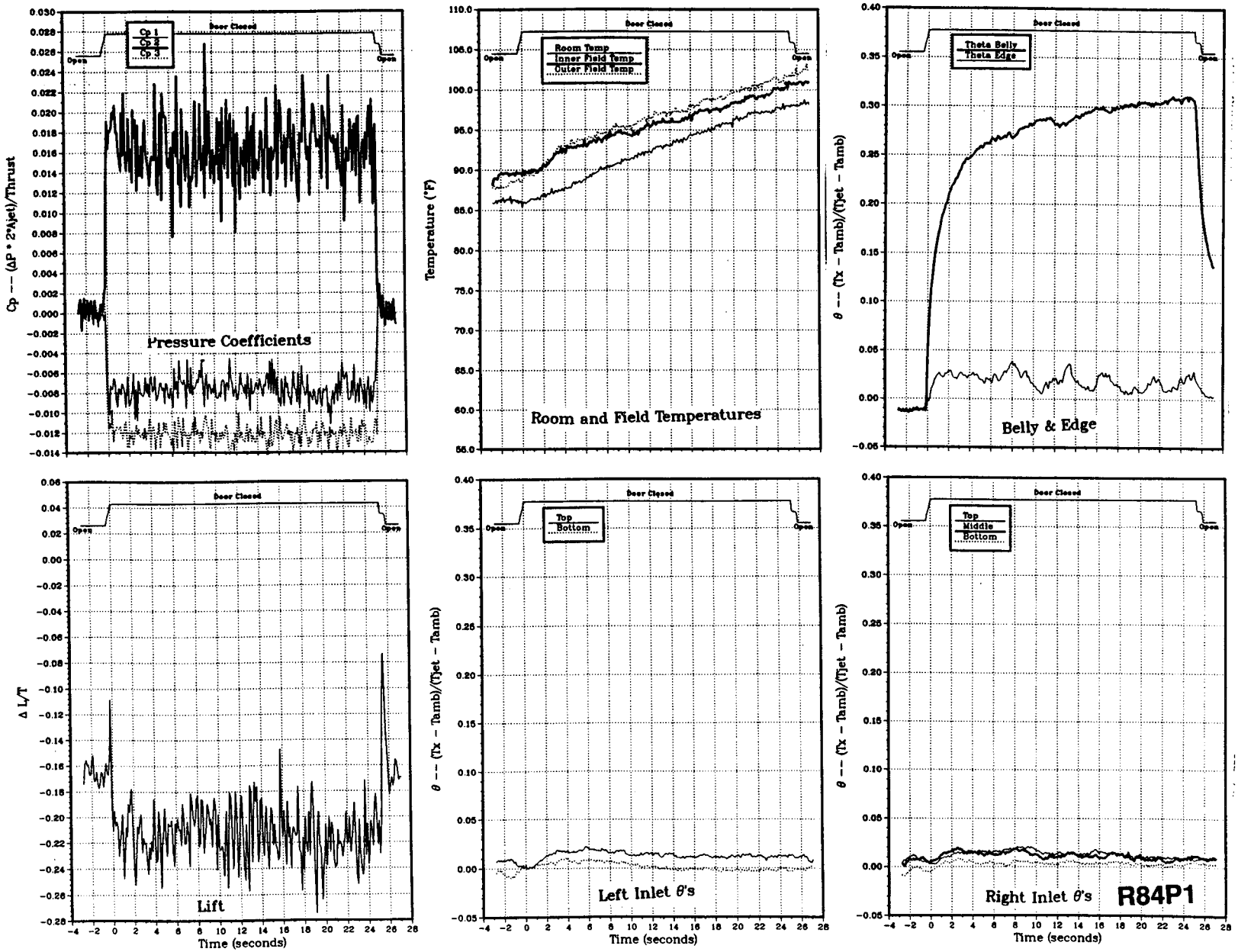

Figure 48(a). Wing/body, no LIDs, NPR = 2.0, thrust = 50 lb, height = 4 in., Tjet = 488 °F, inlet position = 9.66 in.

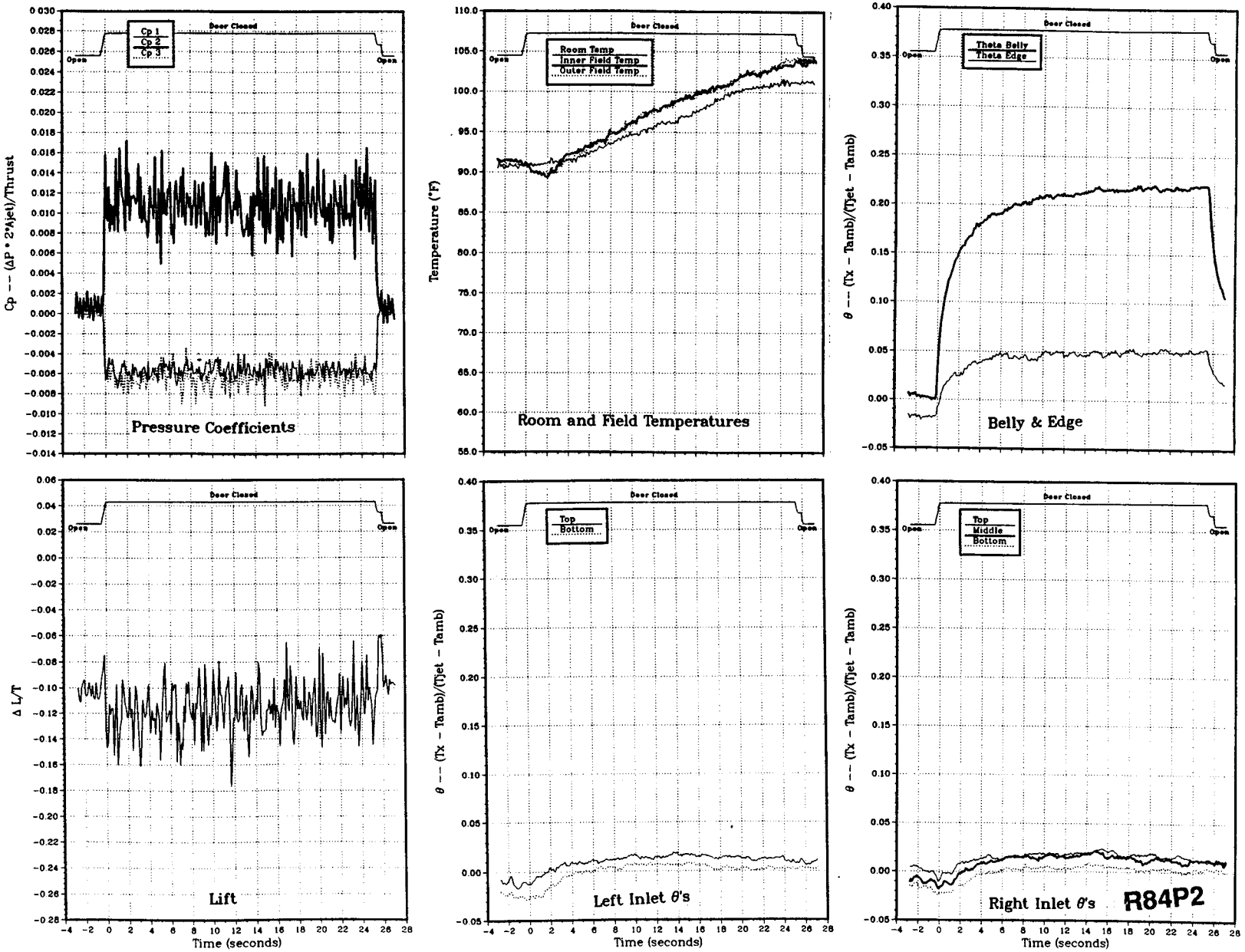

Figure 48(b). Wing/body, no LIDs, NPR = 2.0, thrust = 50 lb, height = 6 in., Tjet = 495 °F, inlet position = 9.66 in.

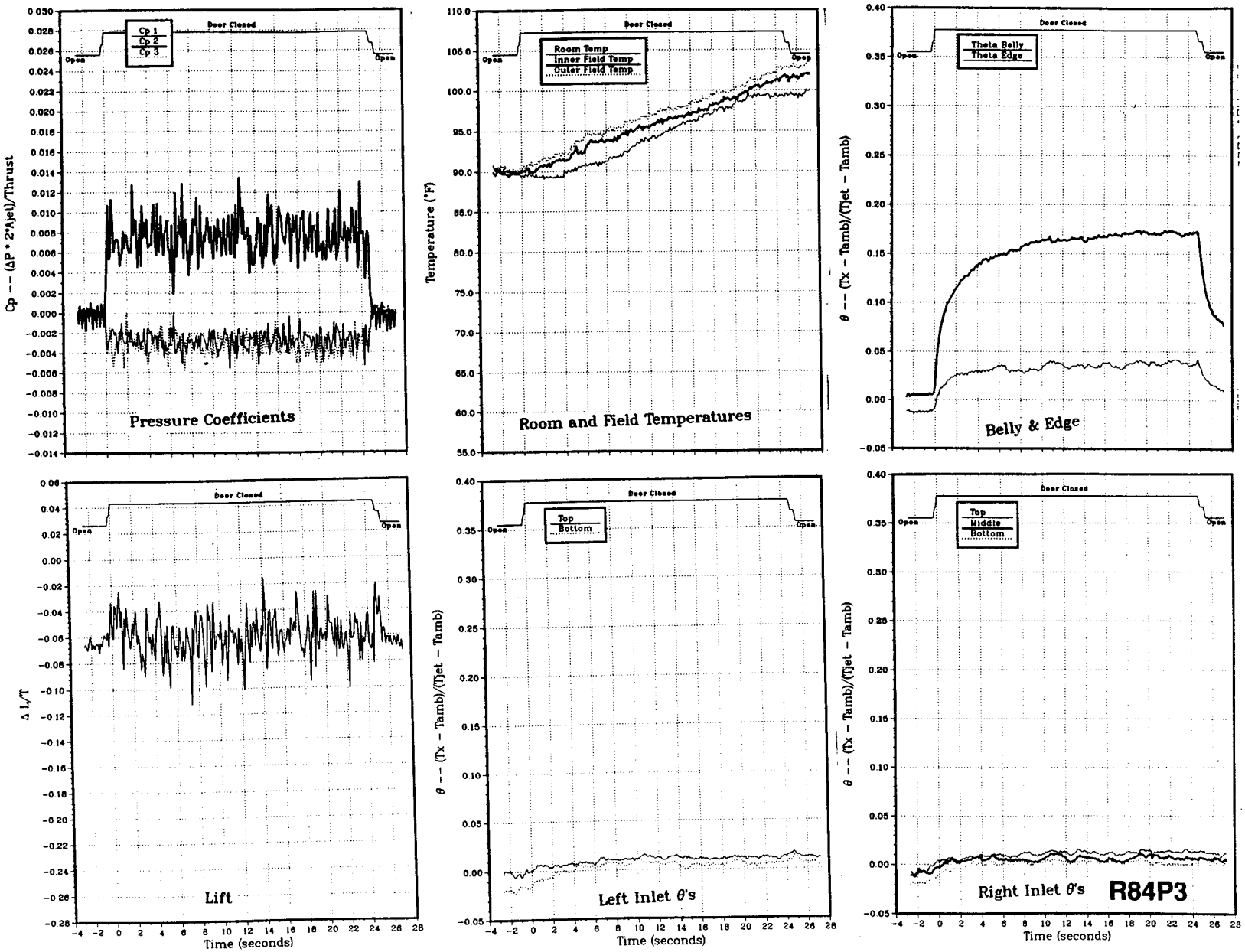

Figure 48(c). Wing/body, no LIDs, NPR = 2.0, thrust = 50 lb, height = 8 in., Tjet = 498 °F, inlet position = 9.66 in.

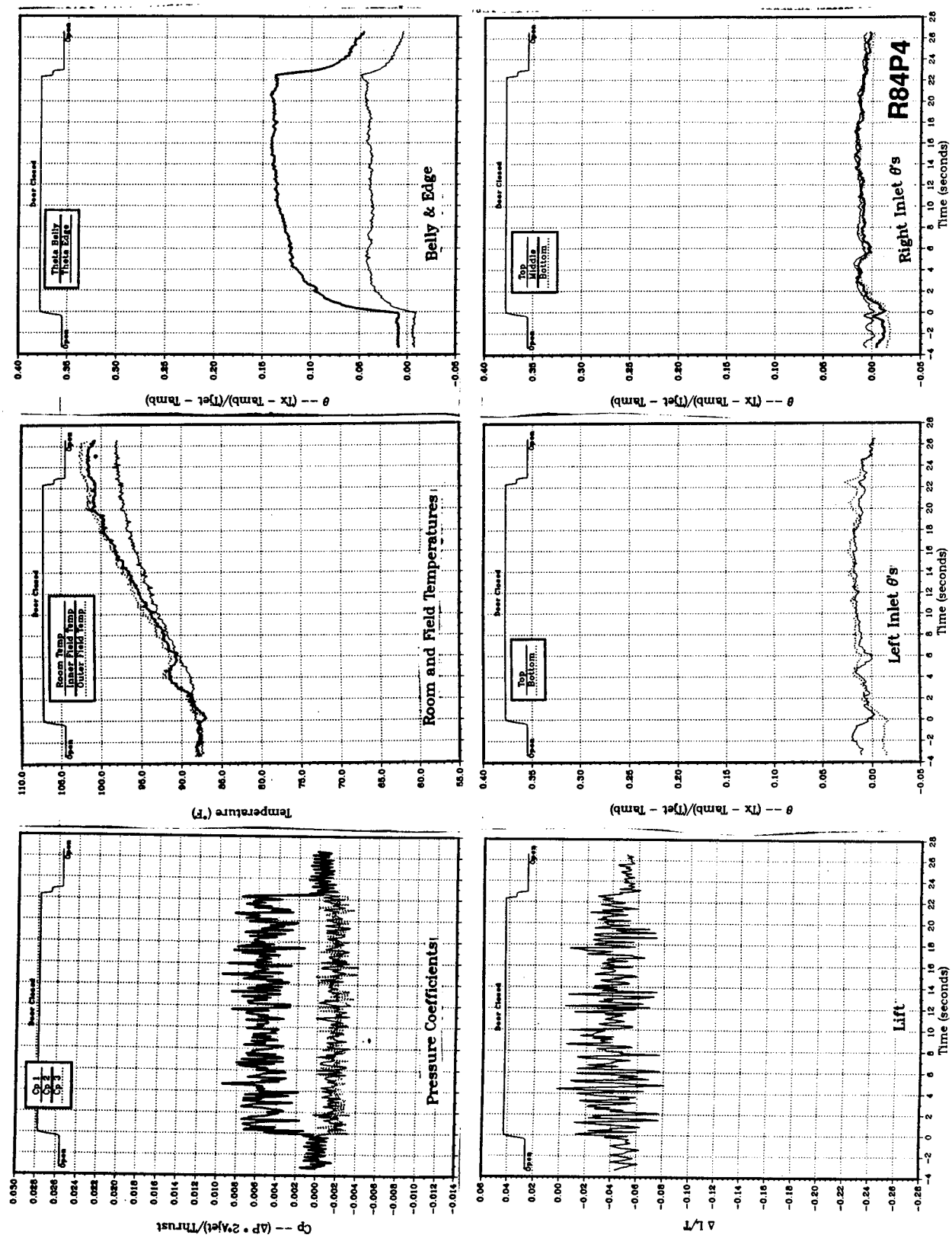

Figure 48(d). Wing/body, no LIDs, NPR = 2.0, thrust = 50 lb, height = 10 in., Tjet = 502 °F, inlet position = 9.66 in.

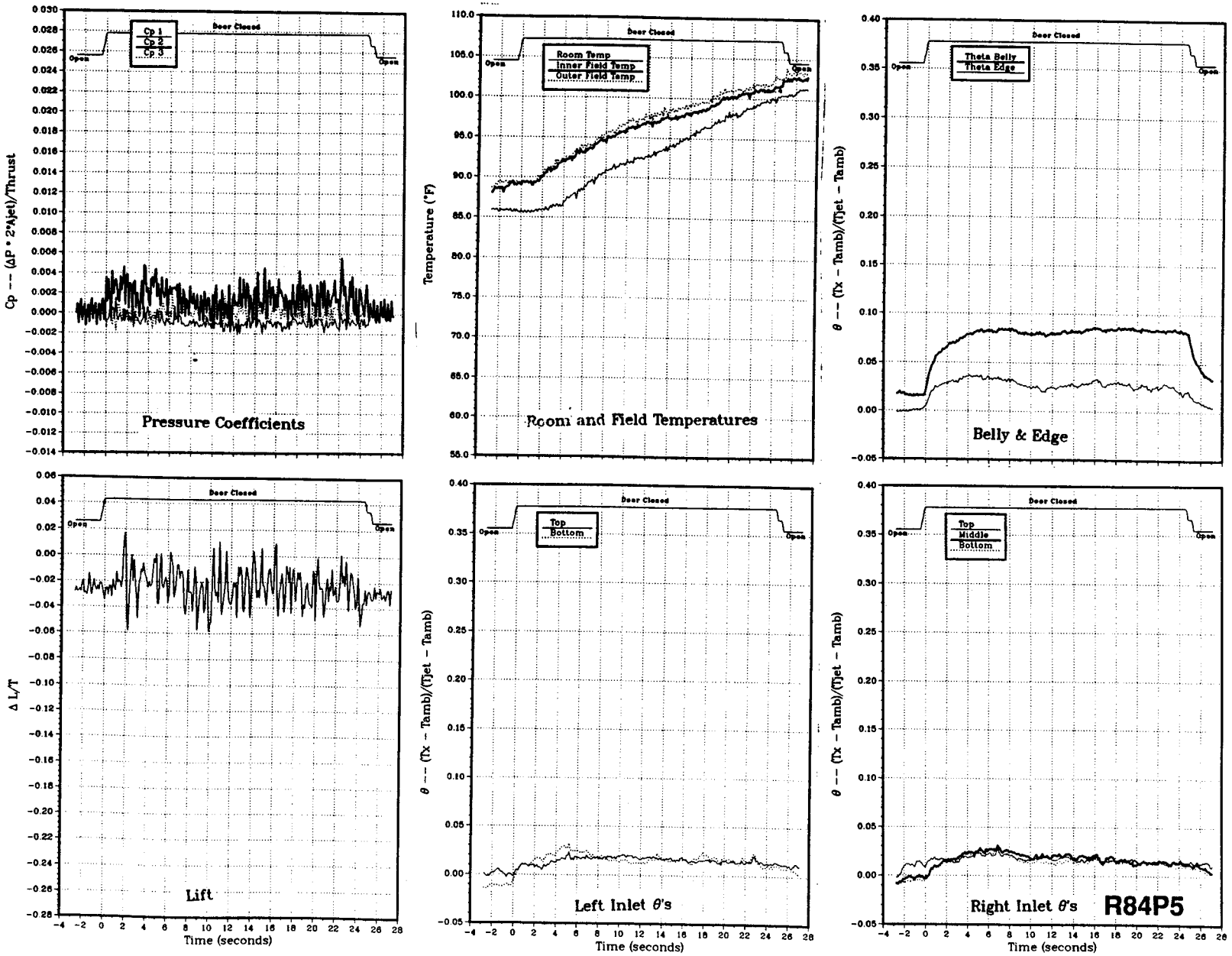

Figure 48(e). Wing/body, no LIDs, NPR = 2.0, thrust = 50 lb, height = 15 in., Tjet = 506 °F, inlet position = 9.66 in.

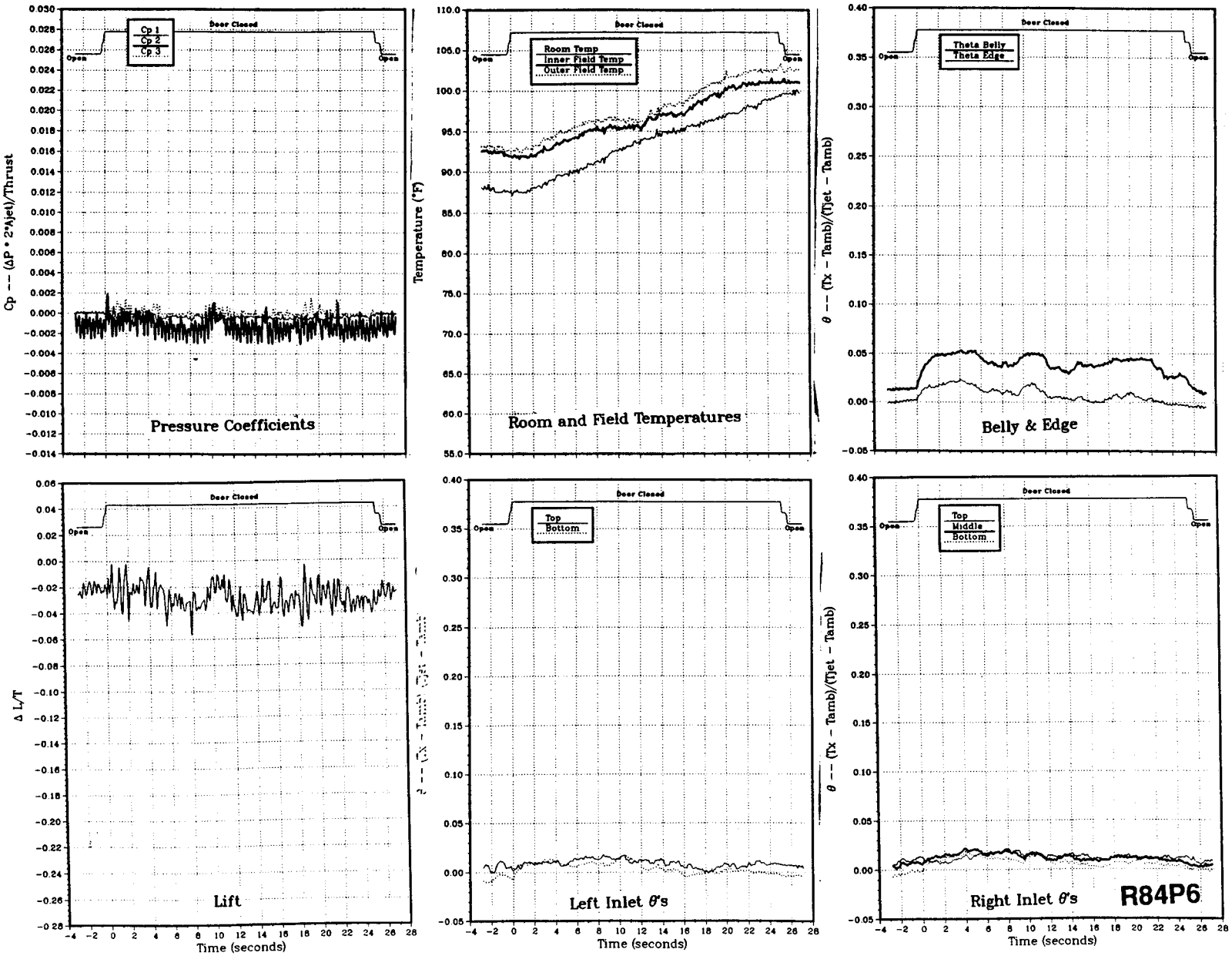

Figure 48(f). Wing/body, no LIDs, NPR = 2.0, thrust = 50 lb, height = 20 in., Tjet = 509 °F, inlet position = 9.66 in.

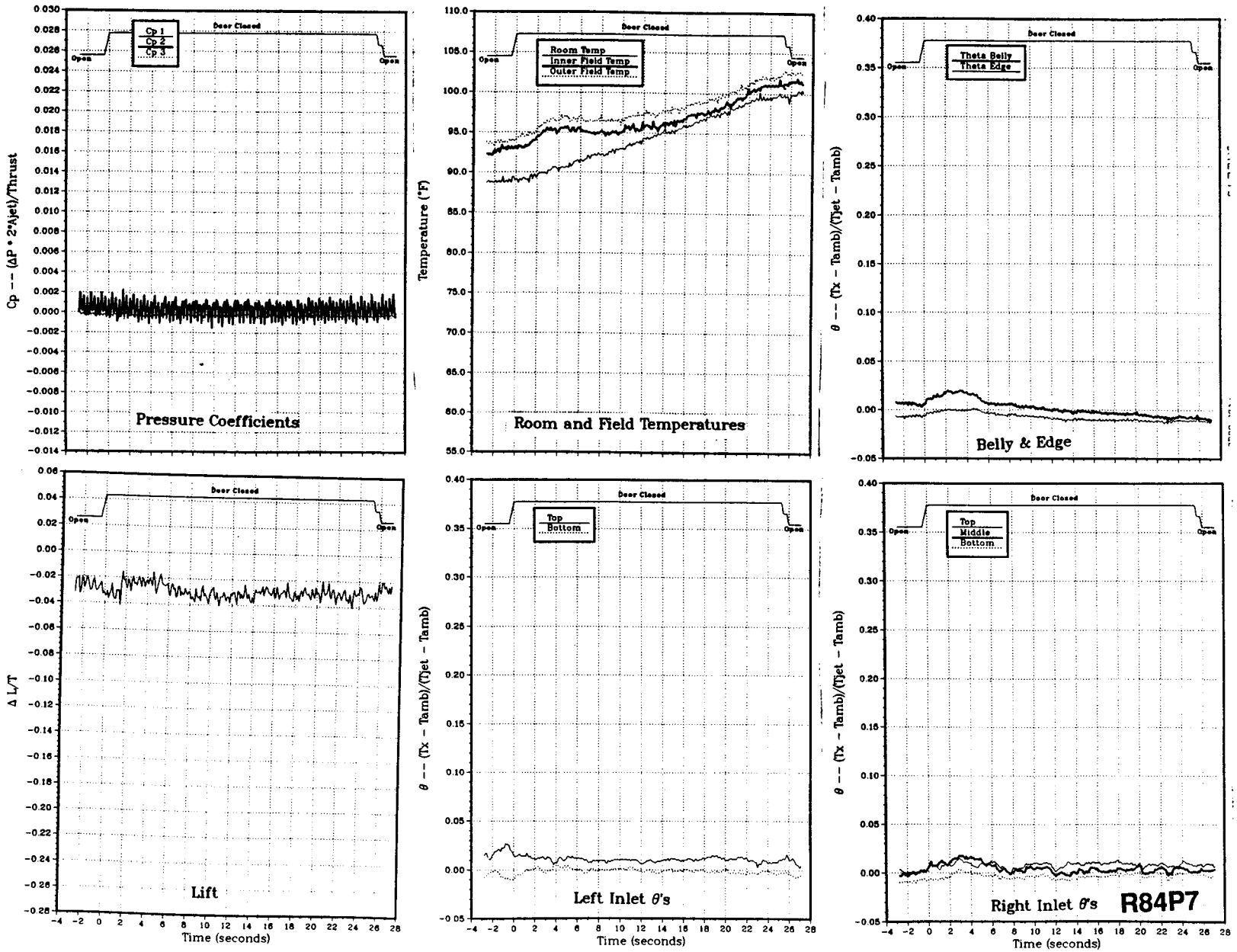

Figure 48(g). Wing/body, no LIDs, NPR = 2.0, thrust = 50 lb, height = 30 in., Tjet = 511 °F, inlet position = 9.66 in.

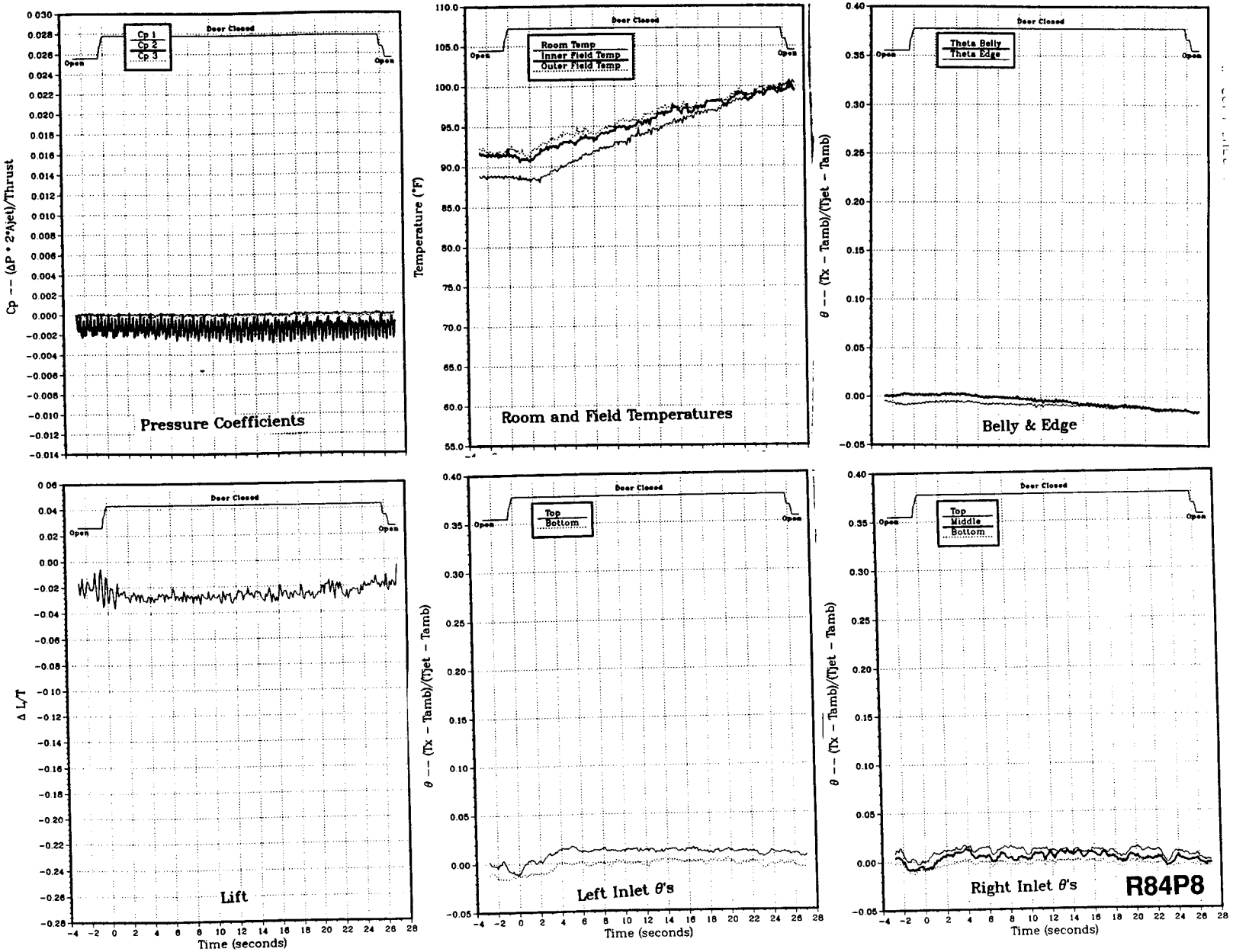

Figure 48(h). Wing/body, no LIDs, NPR = 2.0, thrust = 50 lb, height = 40 in., Tjet = 514 °F, inlet position = 9.66 in.

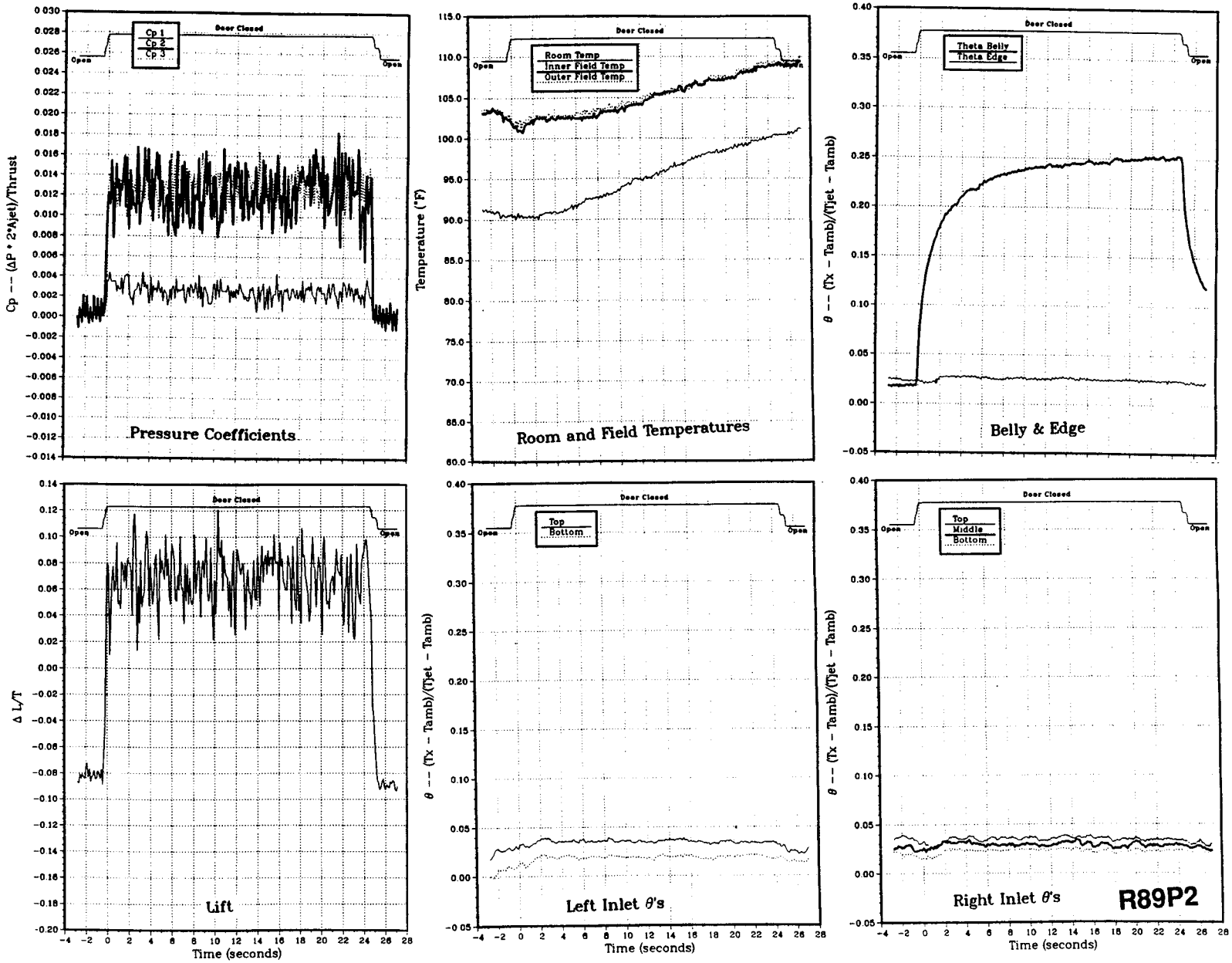

Figure 49(a). Wing/body, Box LIDs (12/21), NPR = 2.0, thrust = 50 lb, height = 6 in., Tjet = 512 °F, inlet position = 9.66 in.

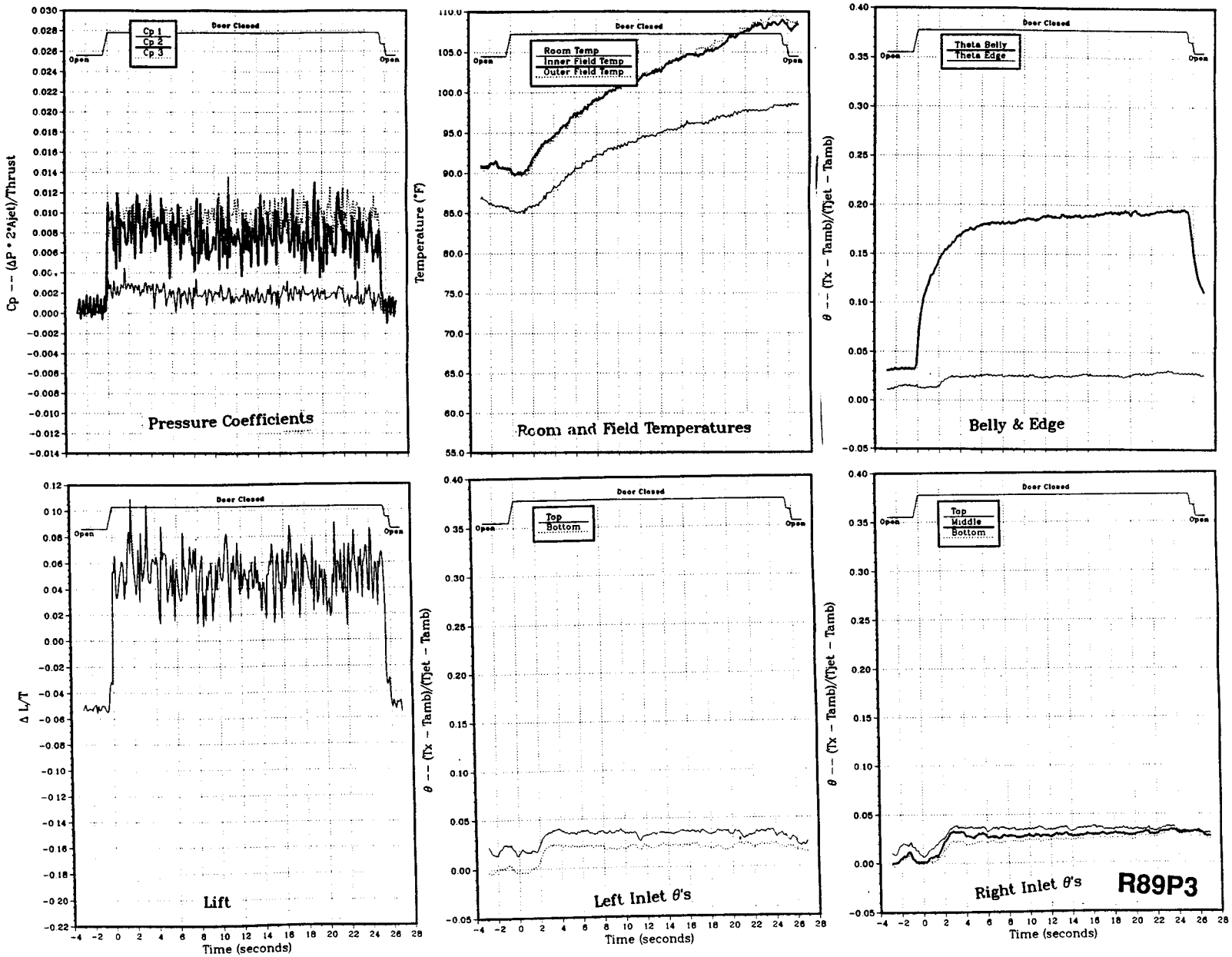

Figure 49(b). Wing/body, Box LIDs (12/21), NPR = 2.0, thrust = 50 lb, height = 8 in., Tjet = 514 °F, inlet position = 9.66 in.

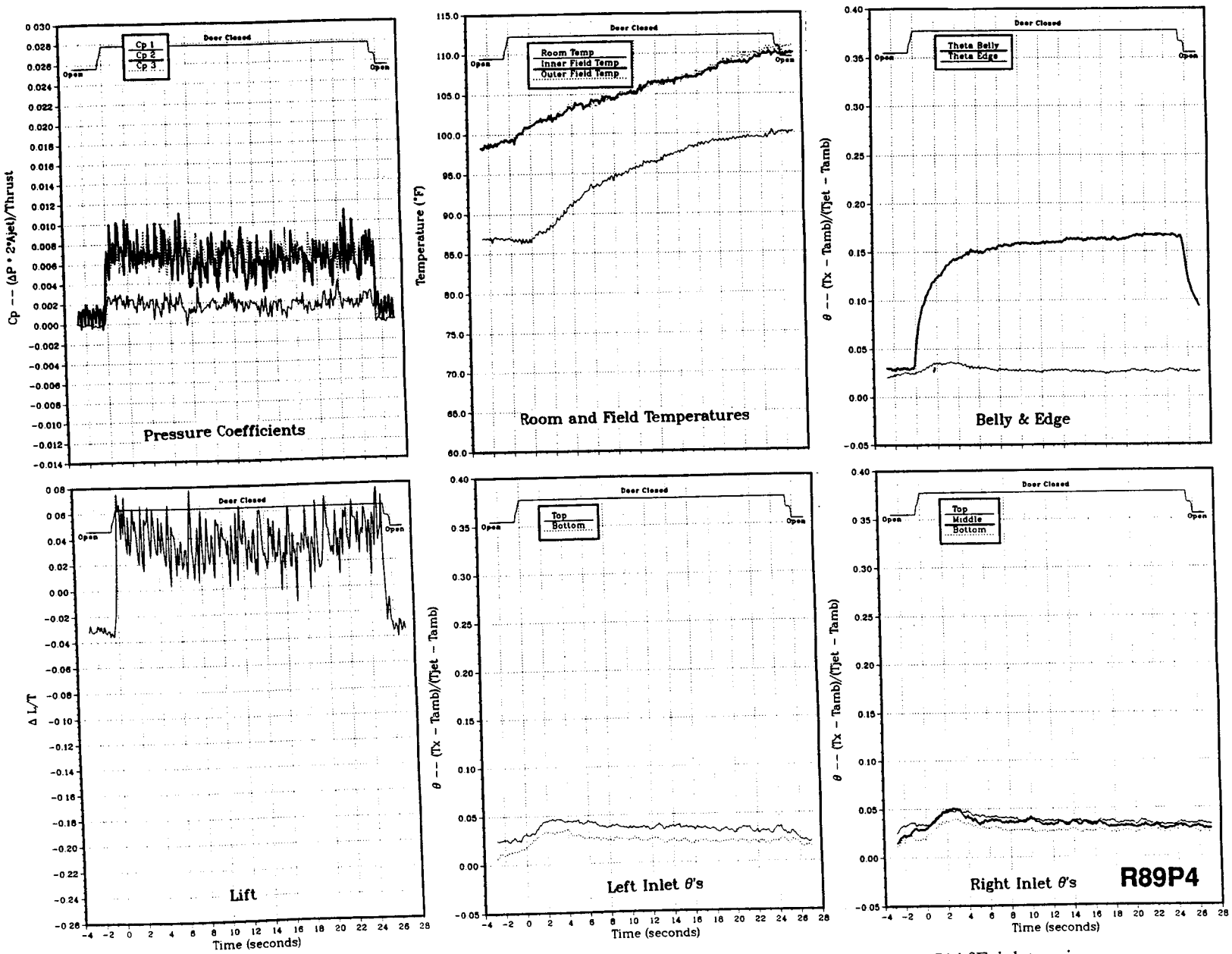

Figure 49(c). Wing/body, Box LIDs (12/21), NPR = 2.0, thrust = 50 lb, height = 10 in., Tjet = 514 °F, inlet position = 9.66 in.

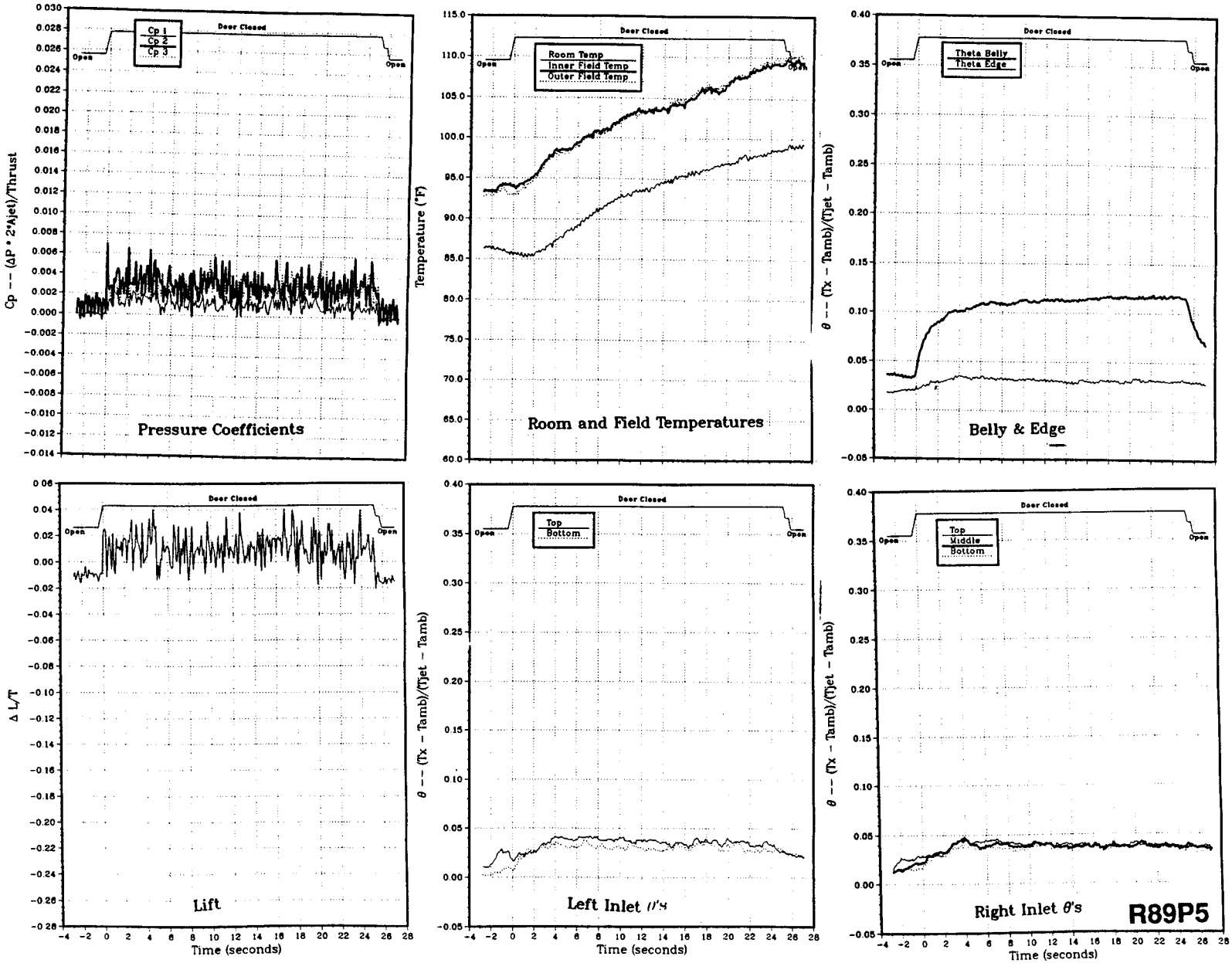

Figure 49(d). Wing/body, Box LIDs (12/21), NPR = 2.0, thrust = 50 lb, height = 15 in., Tjet = 515 °F, inlet position = 9.66 in.

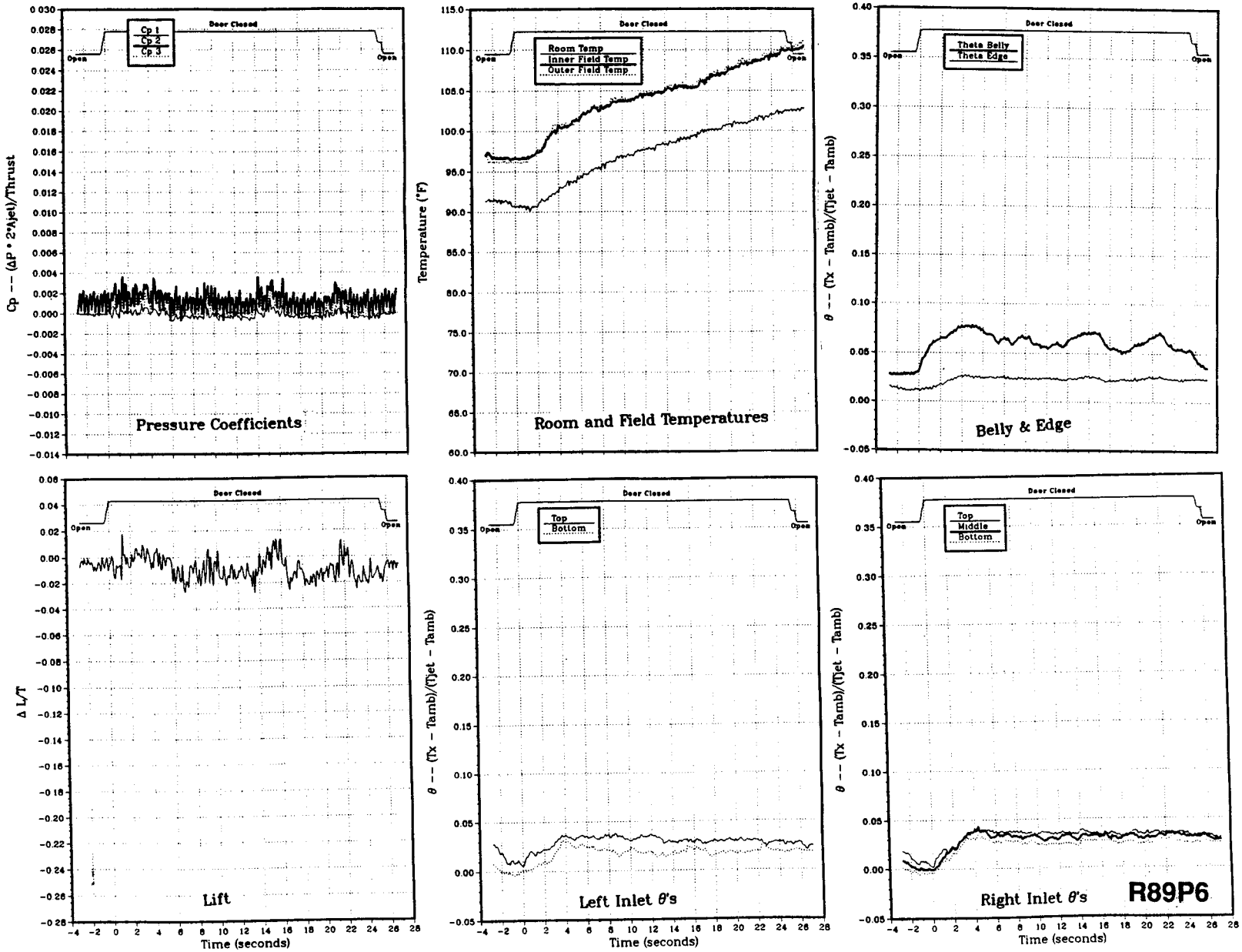

Figure 49(e). Wing/body, Box LIDs (12/21), NPR = 2.0, thrust = 50 lb, height = 20 in., Tjet = 515 °F, inlet position = 9.66 in.

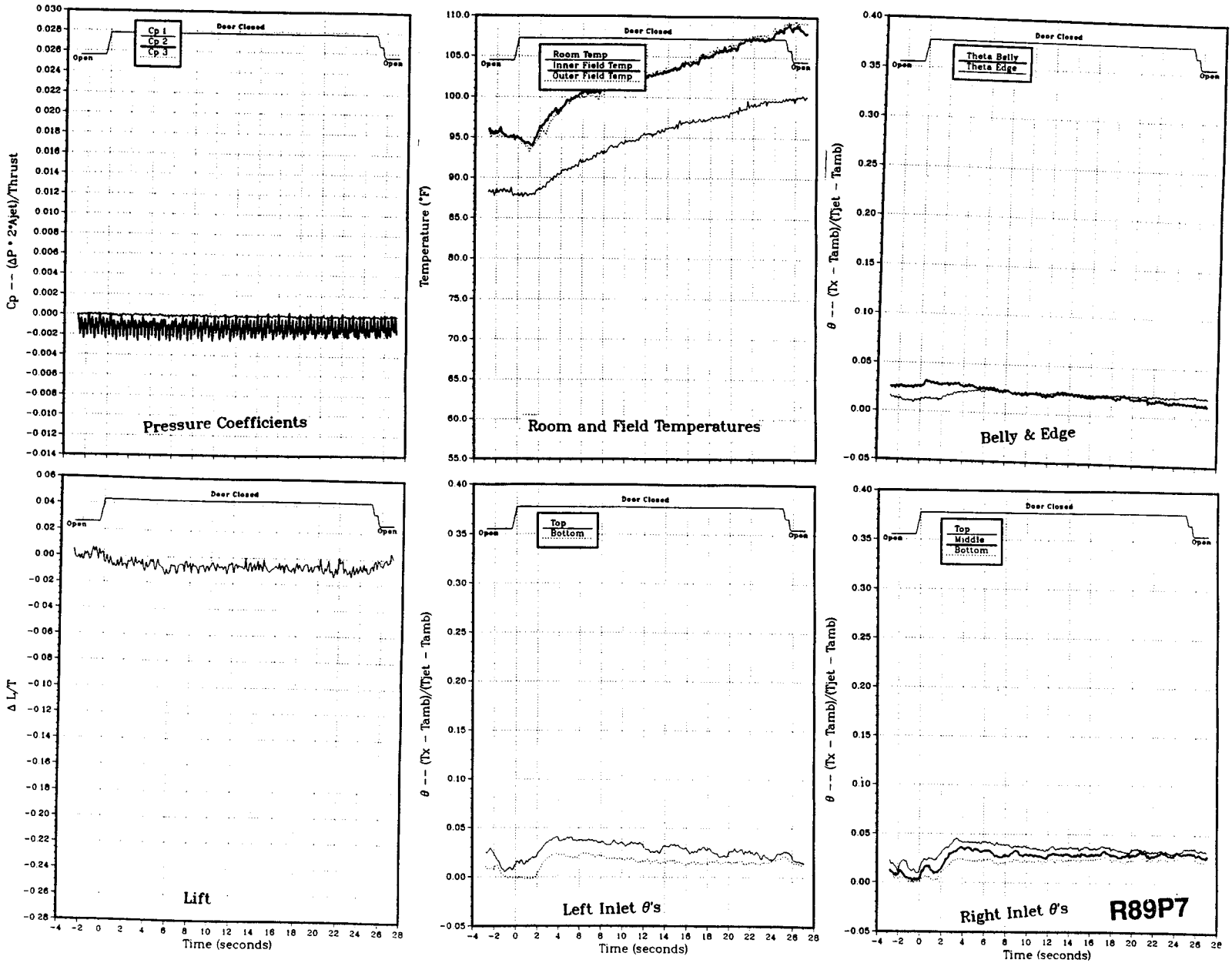

Figure 49(f). Wing/body, Box LIDs (12/21), NPR = 2.0, thrust = 50 lb, height = 30 in., Tjet = 517 °F, inlet position = 9.66 in.

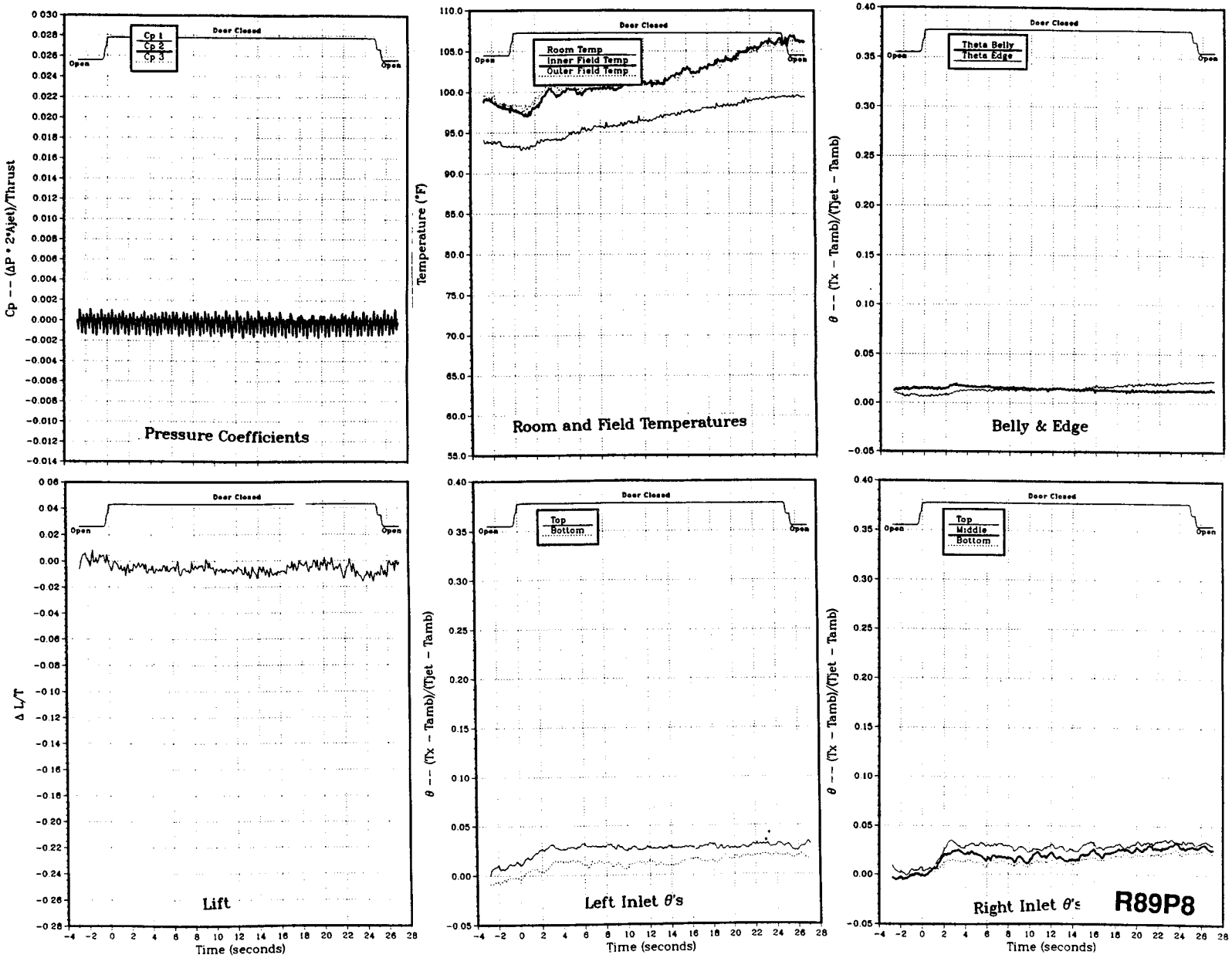

Figure 49(g). Wing/body, Box LIDs (12/21), NPR = 2.0, thrust = 50 lb, height = 40 in., Tjet = 517 °F, inlet position = 9.66 in.

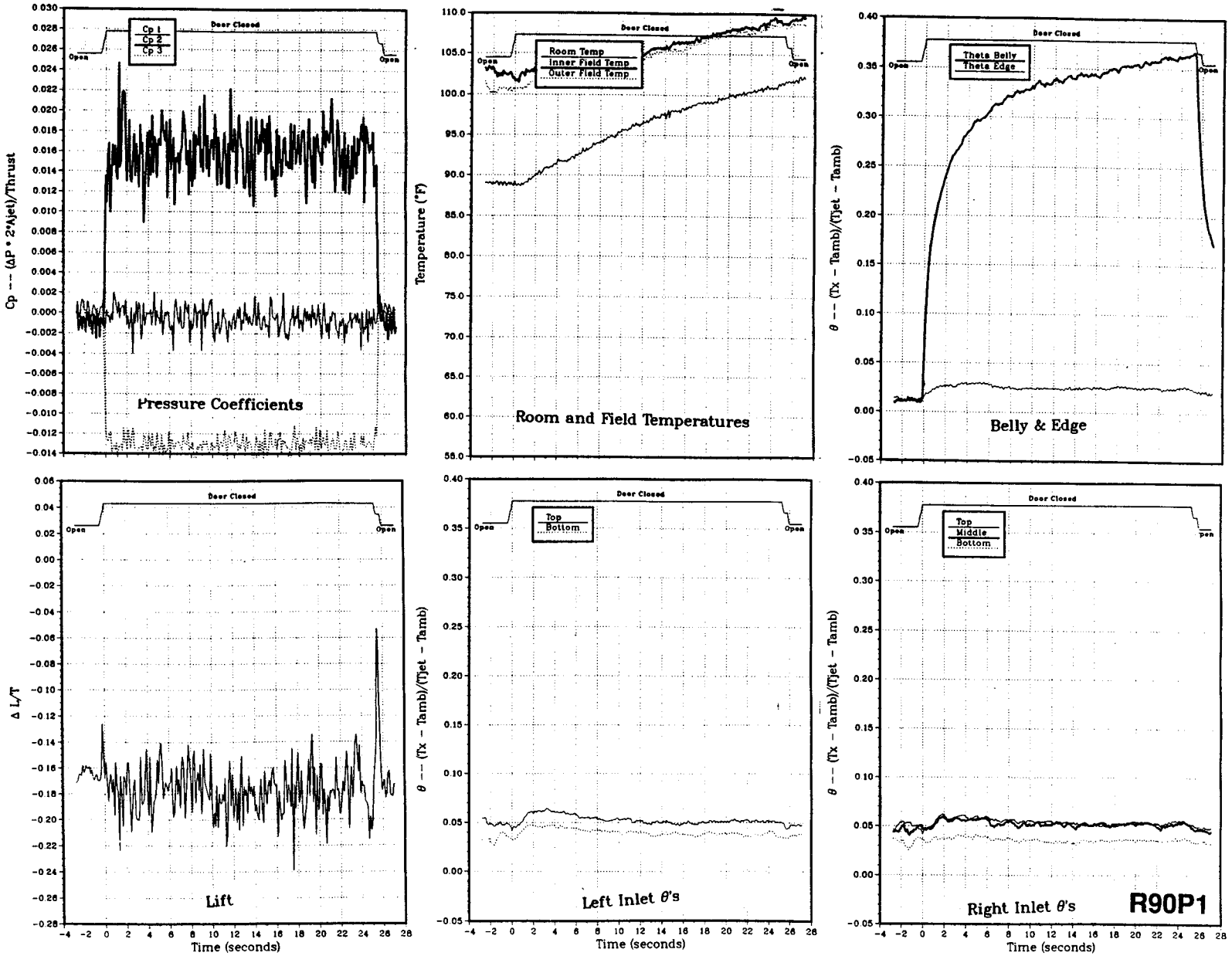

Figure 50(a). Wing/body, Box LIDs (12/no rear), NPR = 2.0, thrust = 50 lb, height = 4 in., Tjet = 507 °F, inlet position = 9.66 in.

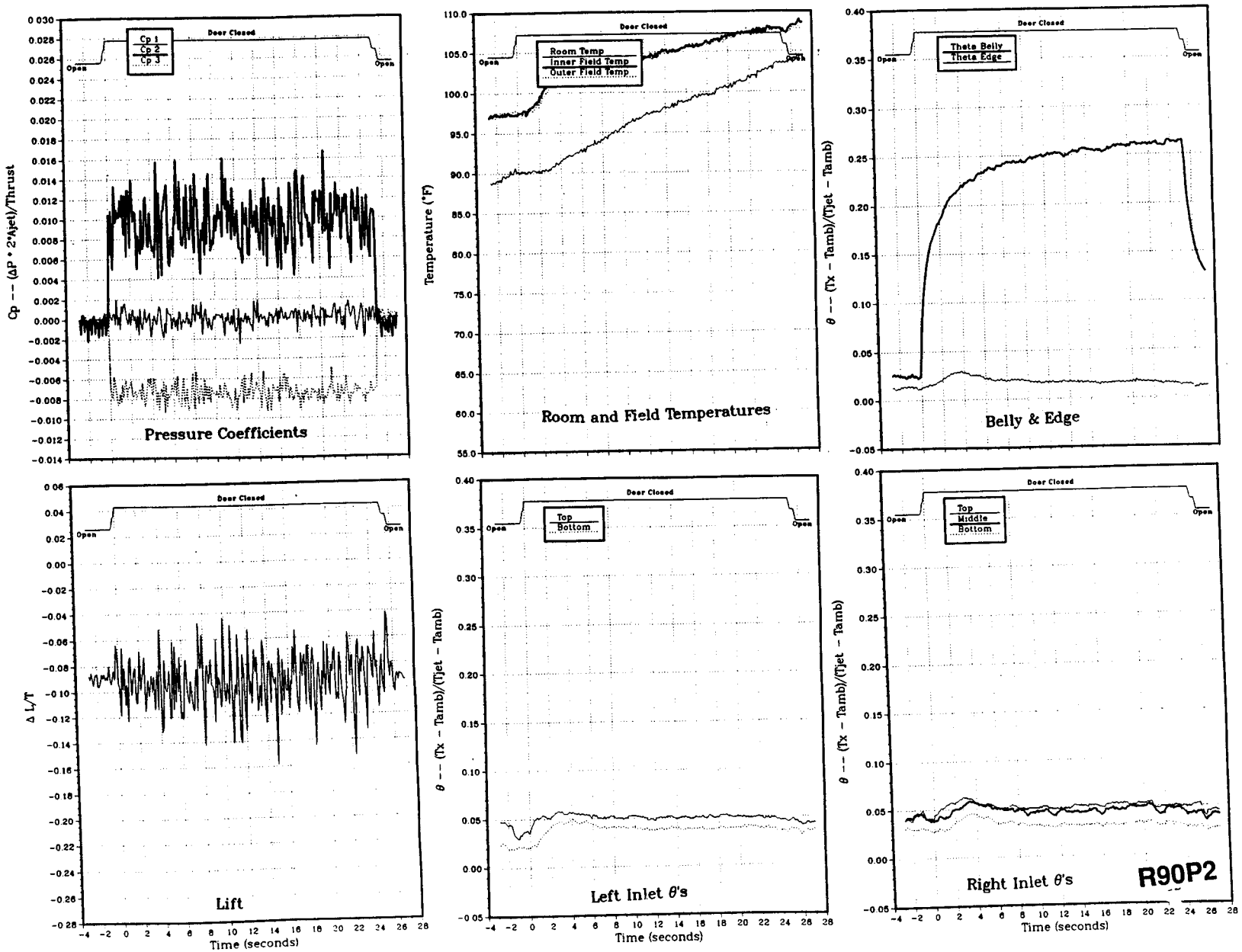

Figure 50(b). Wing/body, Box LIDs (12/no rear), NPR = 2.0, thrust = 50 lb, height = 6 in., Tjet = 509 °F, inlet position = 9.66 in.

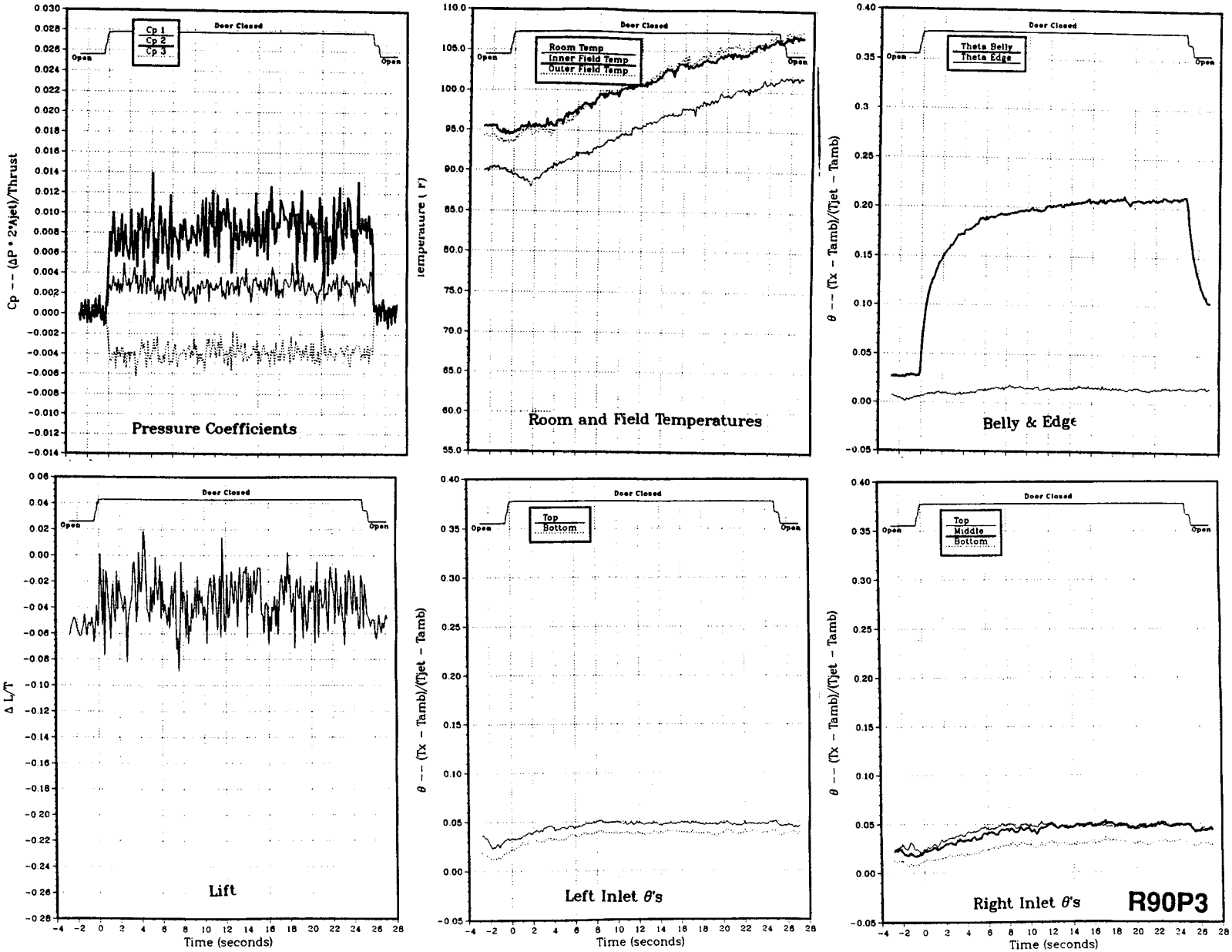

Figure 50(c). Wing/body, Box LIDs (12/no rear), NPR = 2.0, thrust = 50 lb, height = 8 in., Tjet = 510 °F, inlet position = 9.66 in.

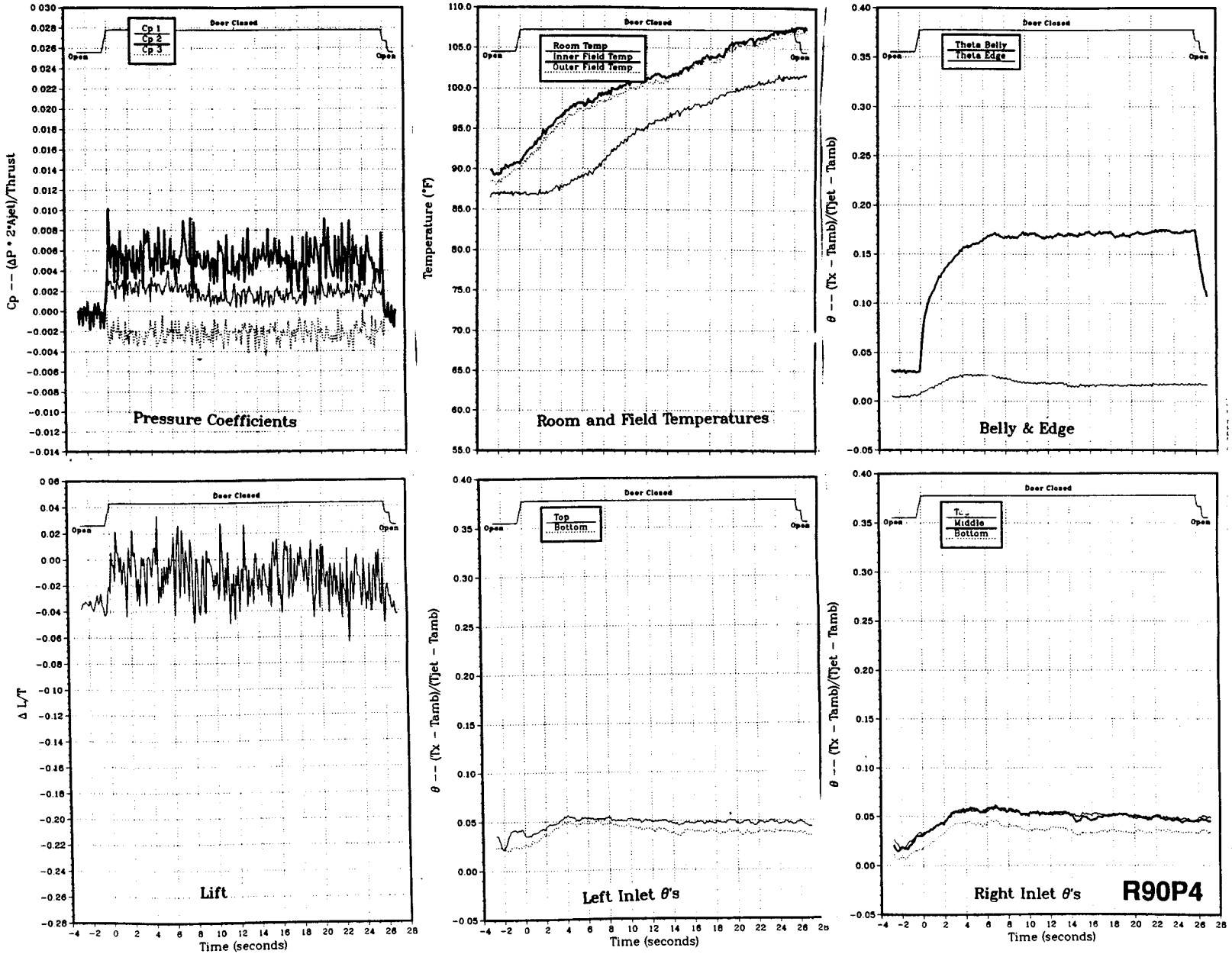

Figure 50(d). Wing/body, Box LIDs (12/no rear), NPR = 2.0, thrust = 50 lb, height = 10 in., Tjet = 510 °F, inlet position = 9.66 in.

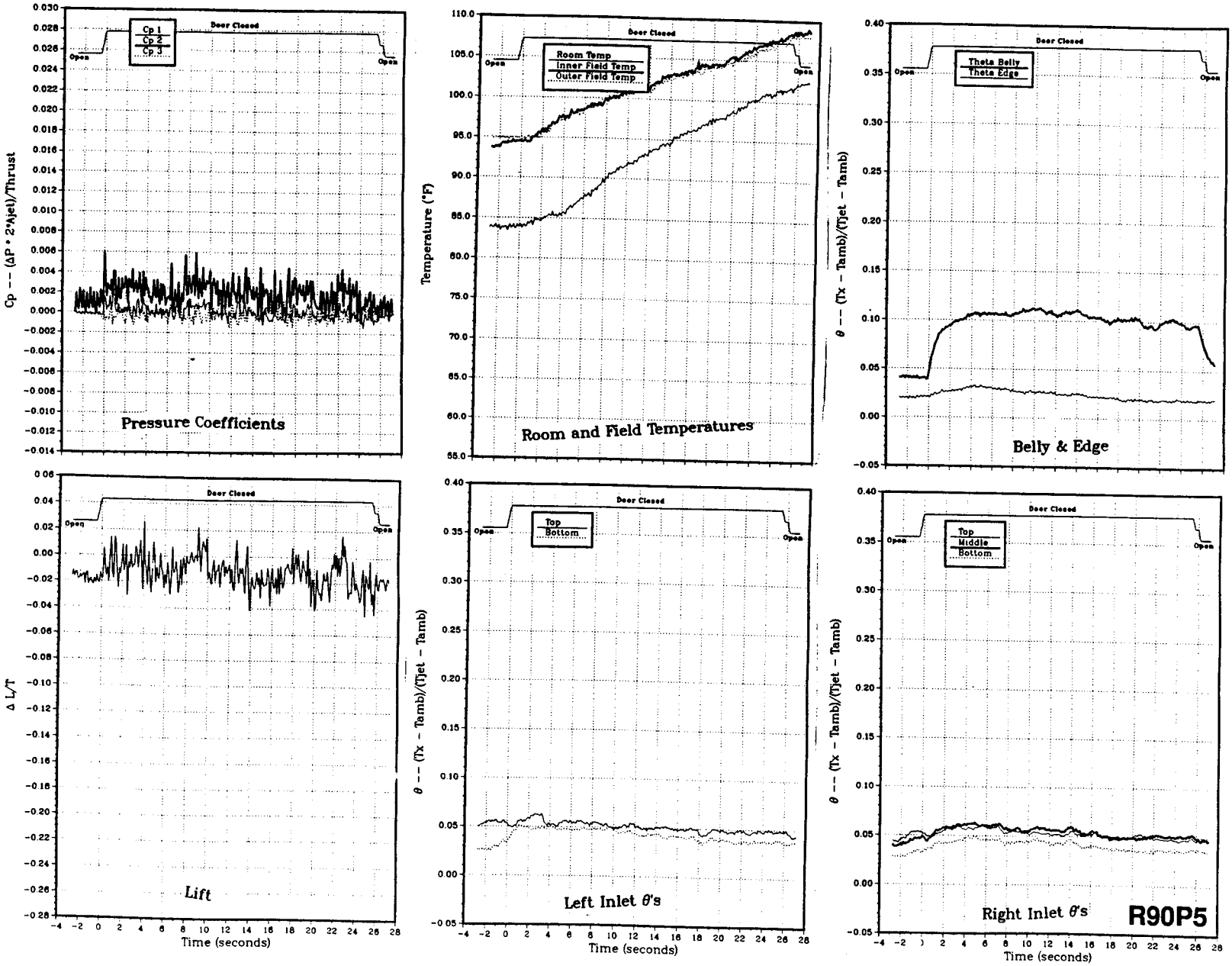

Figure 50(e). Wing/body, Box LIDs (12/no rear), NPR = 2.0, thrust = 50 lb, height = 15 in., Tjet = 512 °F, inlet position = 9.66 in.

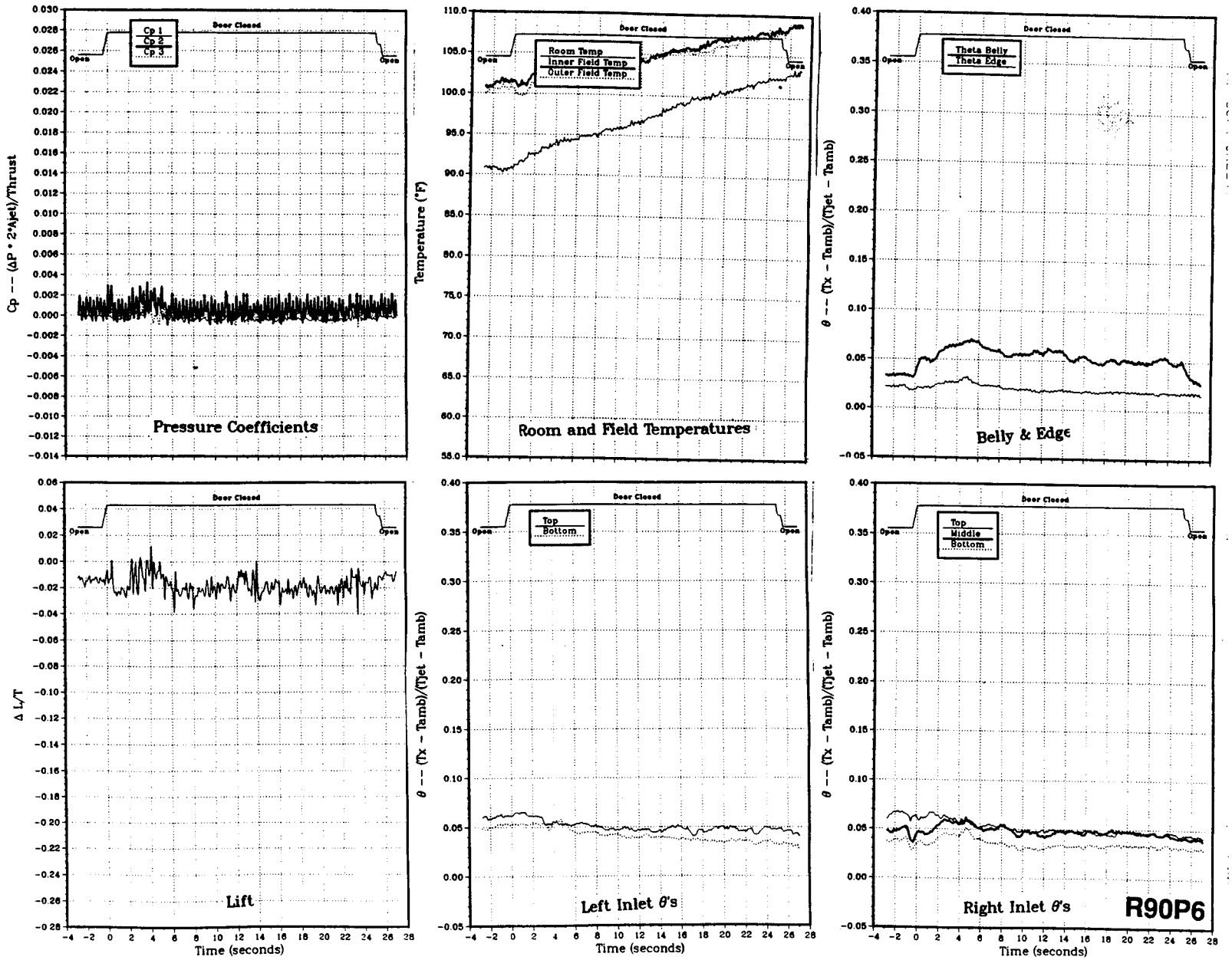

Figure 50(f). Wing/body, Box LIDs (12/no rear), NPR = 2.0, thrust = 50 lb, height = 20 in., Tjet = 514 °F, inlet position = 9.66 in.

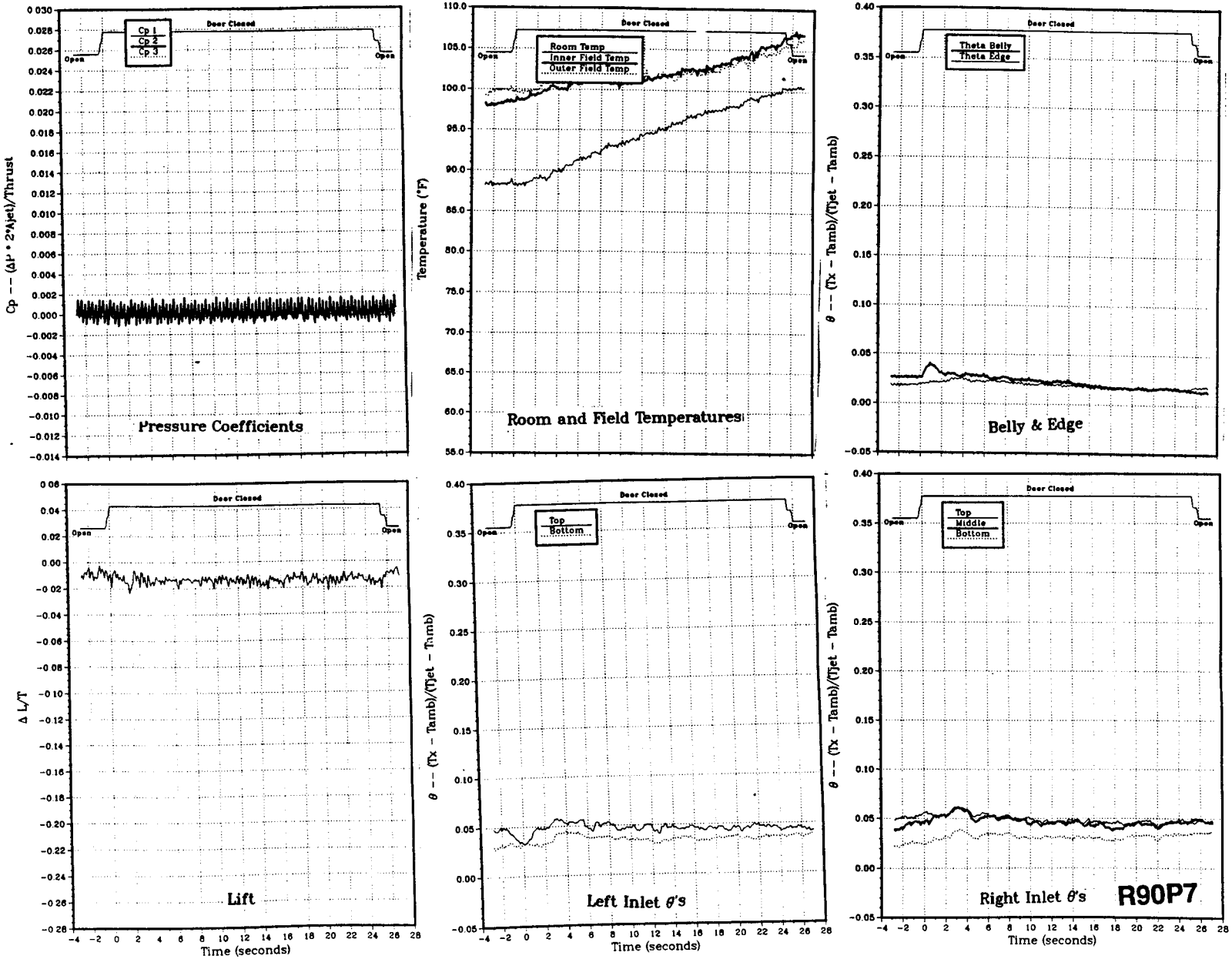

Figure 50(g). Wing/body, Box LIDs (12/no rear), NPR = 2.0, thrust = 50 lb, height = 30 in., Tjet = 515 °F, inlet posi-

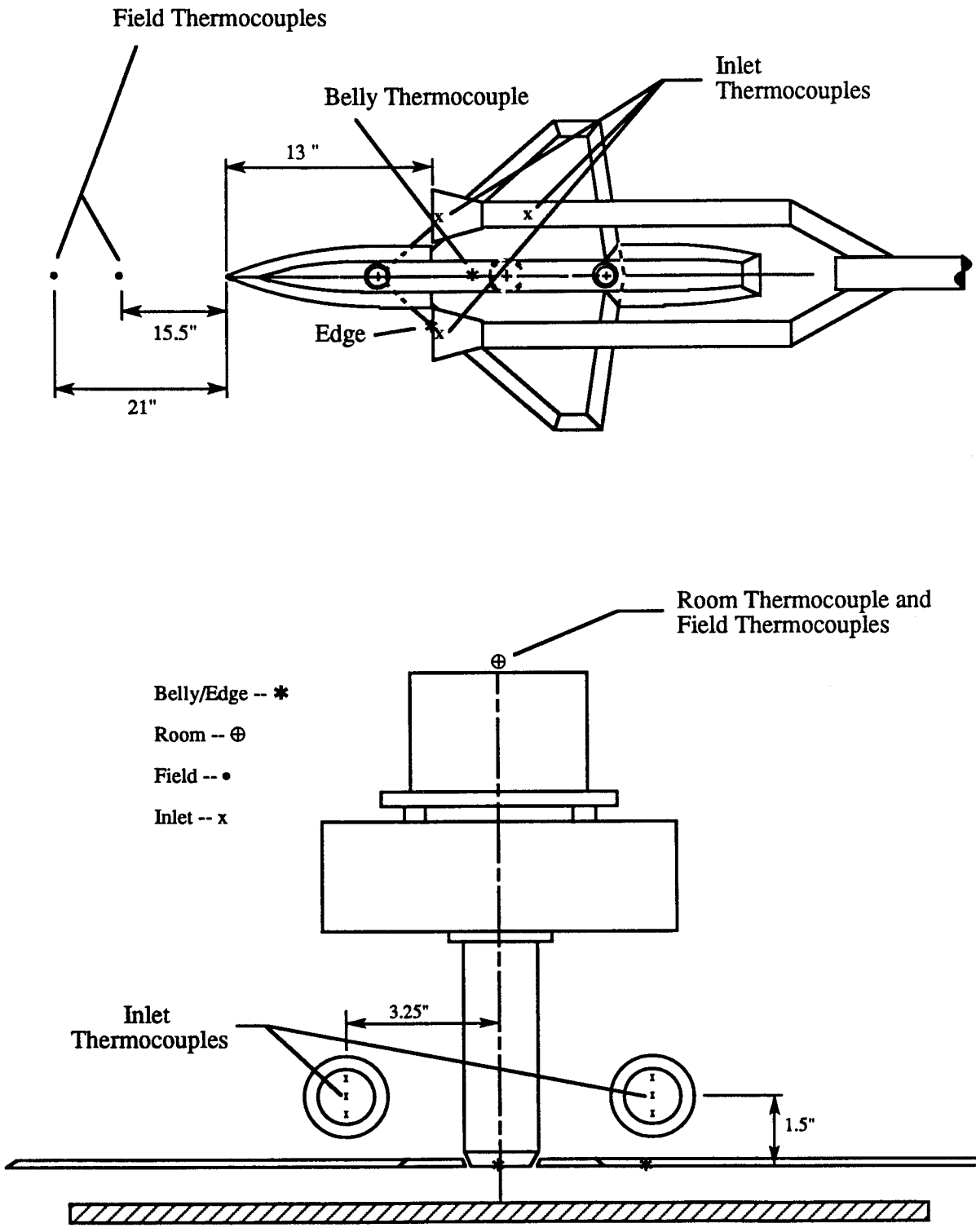

Figure 51. Locations of model and field thermocouples for data set 12.

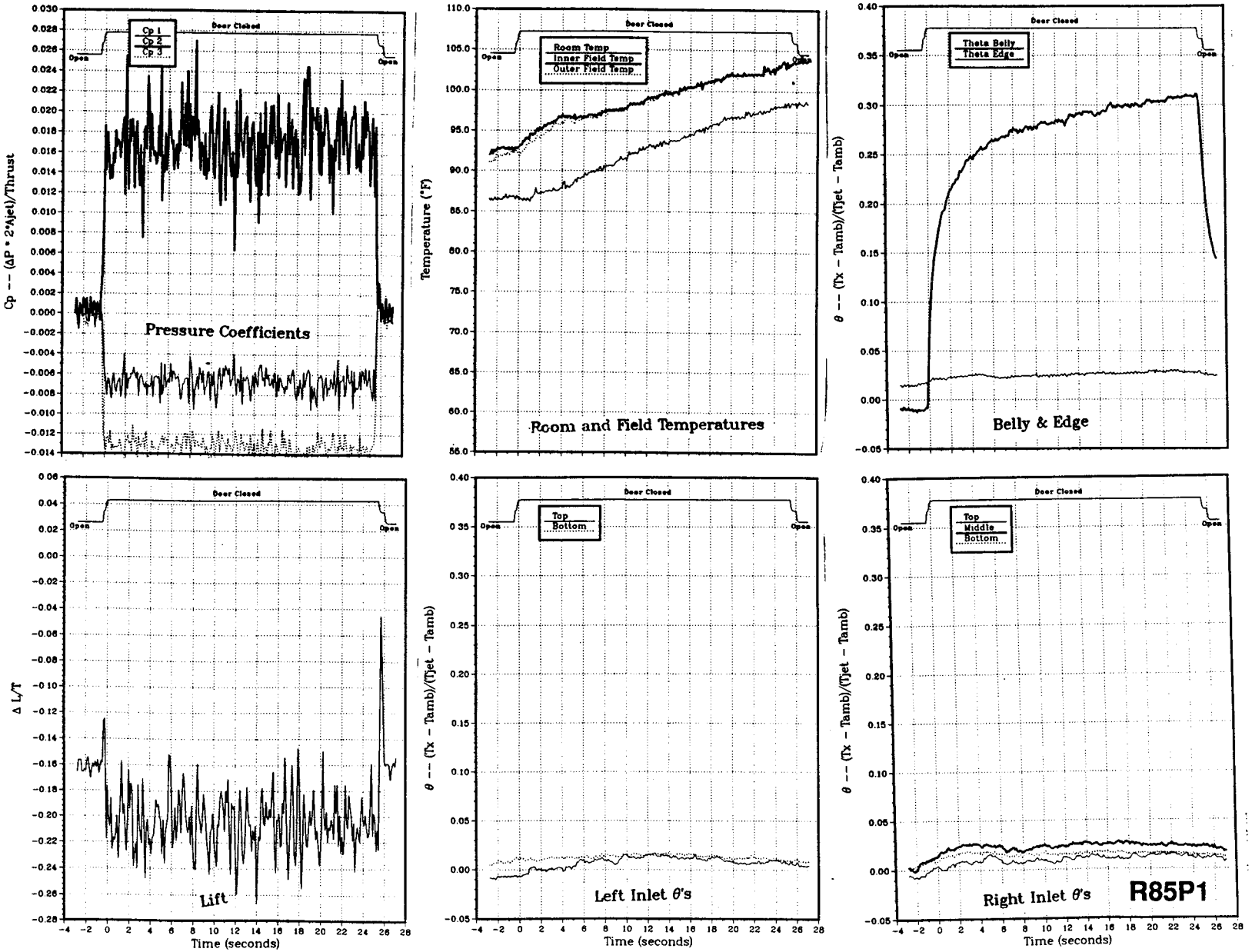

Figure 52(a). Wing/body, no LIDs, NPR = 2.0, thrust = 50 lb, height = 4 in., Tjet = 493 °F, inlet position = 13 in.

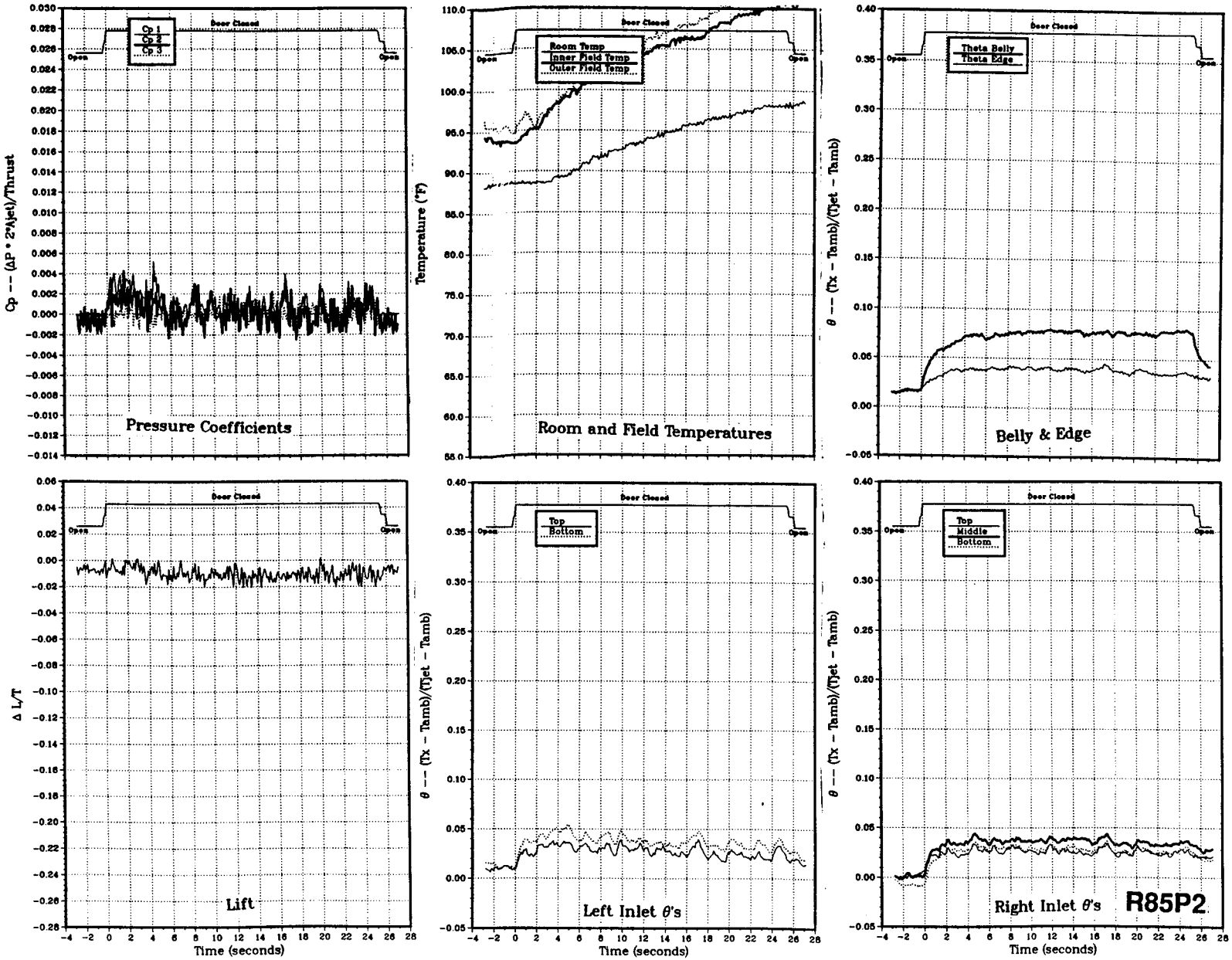

Figure 52(b). Wing/body, no LIDs, NPR = 2.0, thrust = 50 lb, height = 6 in., Tjet = 498 °F, inlet position = 13 in.

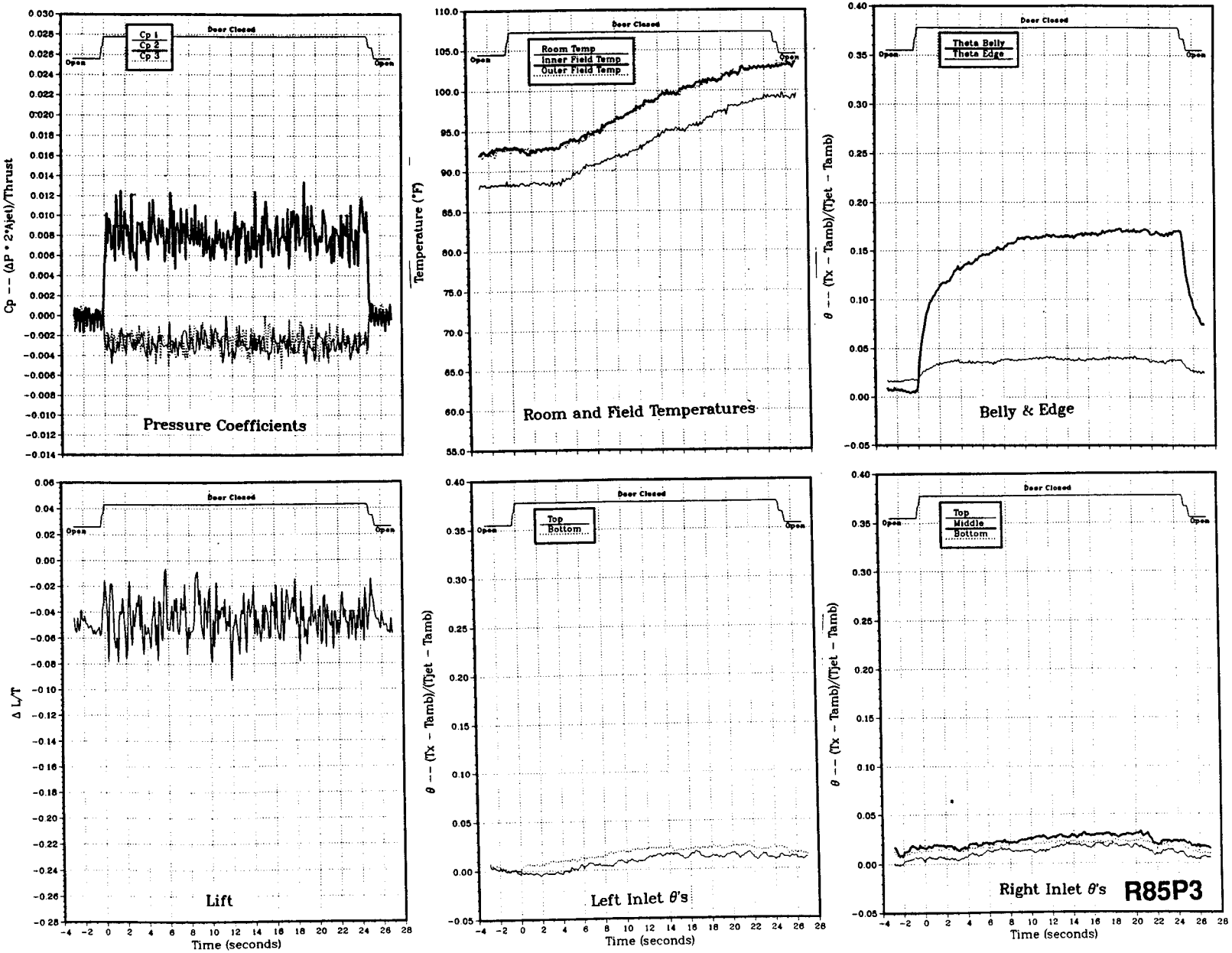

Figure 52(c). Wing/body, no LIDs, NPR = 2.0, thrust = 50 lb, height = 8 in., Tjet = 503 °F, inlet position = 13 in.

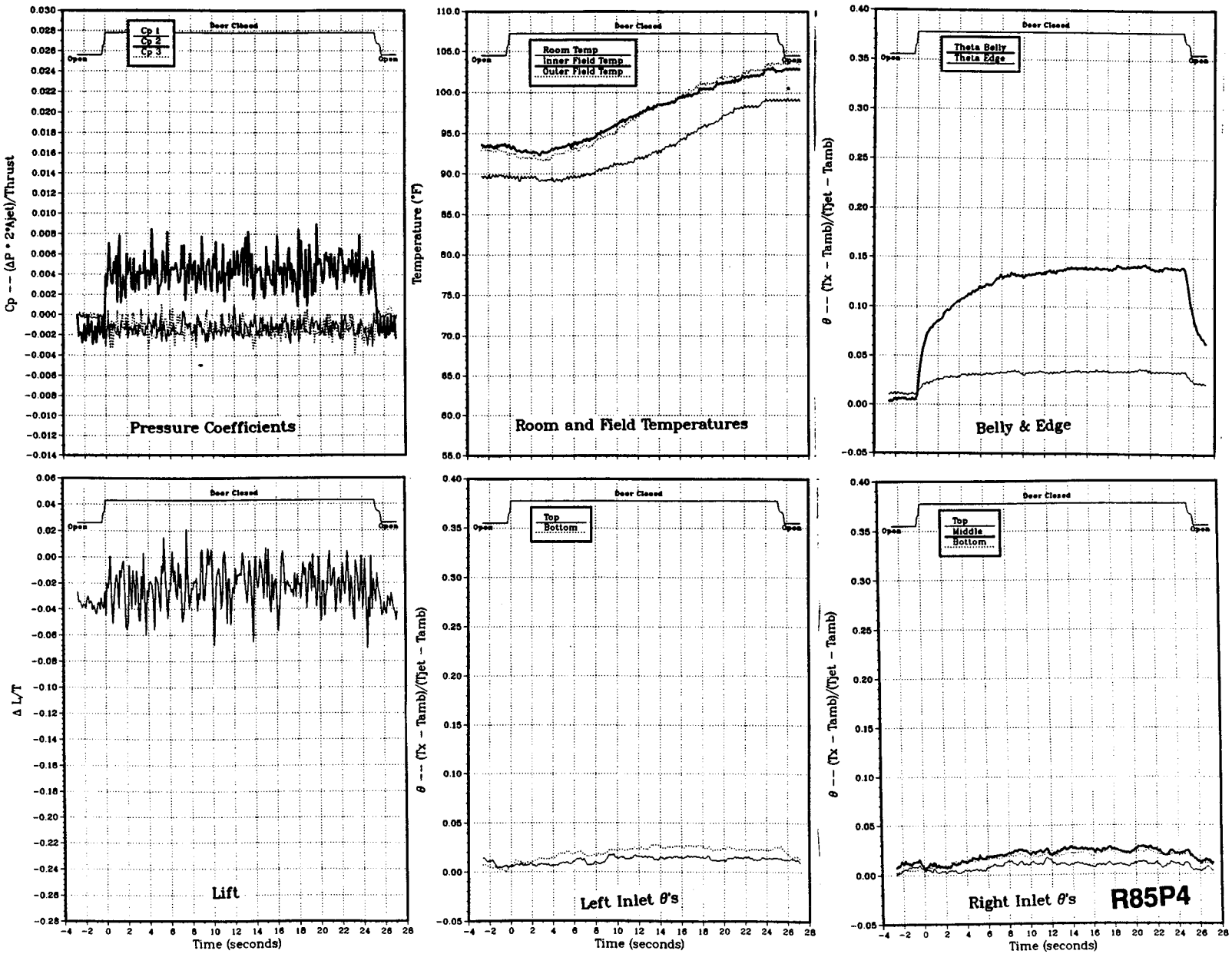

Figure 52(d). Wing/body, no LIDs, NPR = 2.0, thrust = 50 lb, height = 10 in., Tjet = 506 °F, inlet position = 13 in.

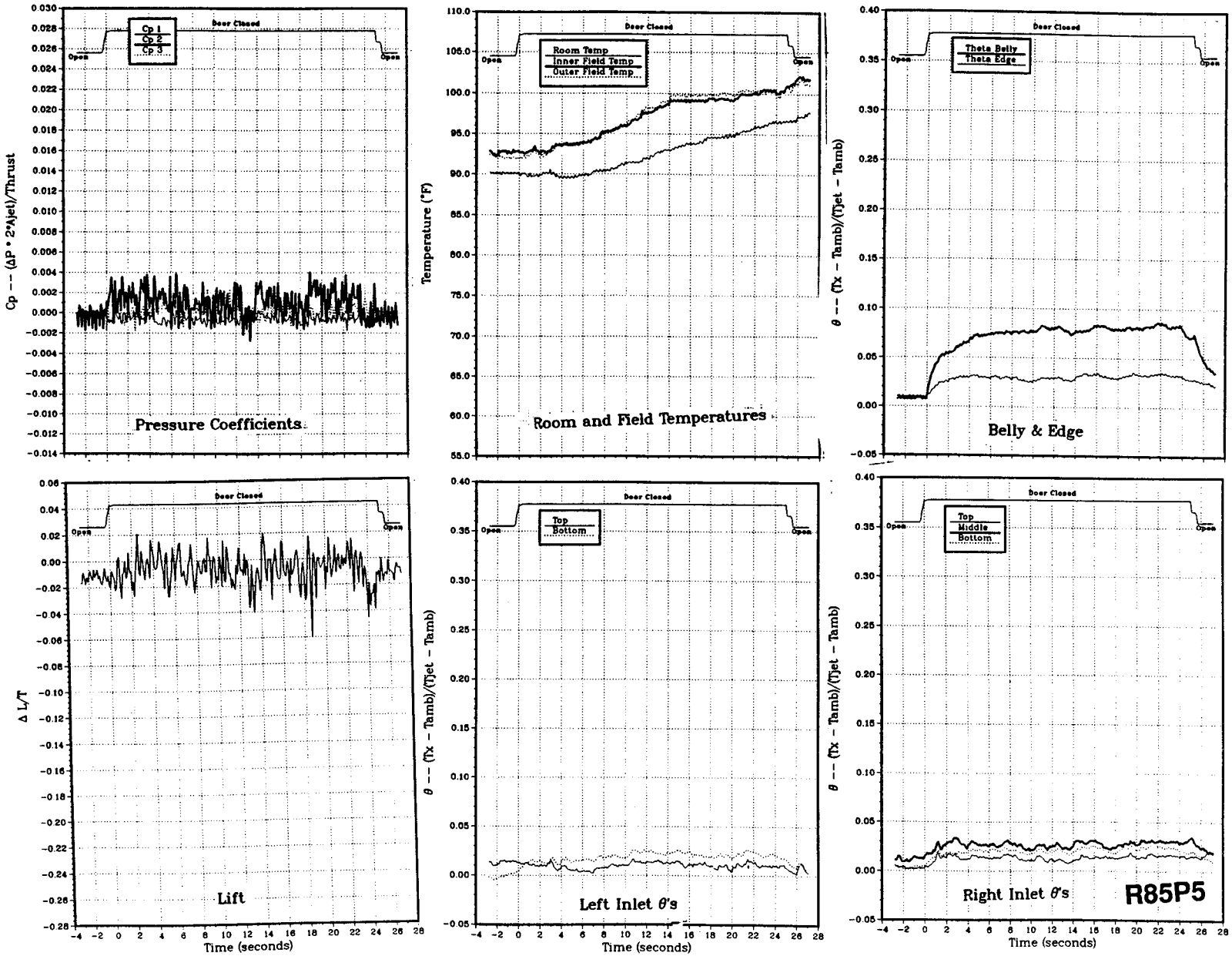

Figure 52(e). Wing/body, no LIDs, NPR = 2.0, thrust = 50 lb, height = 15 in., Tjet = 510 °F, inlet position = 13 in.

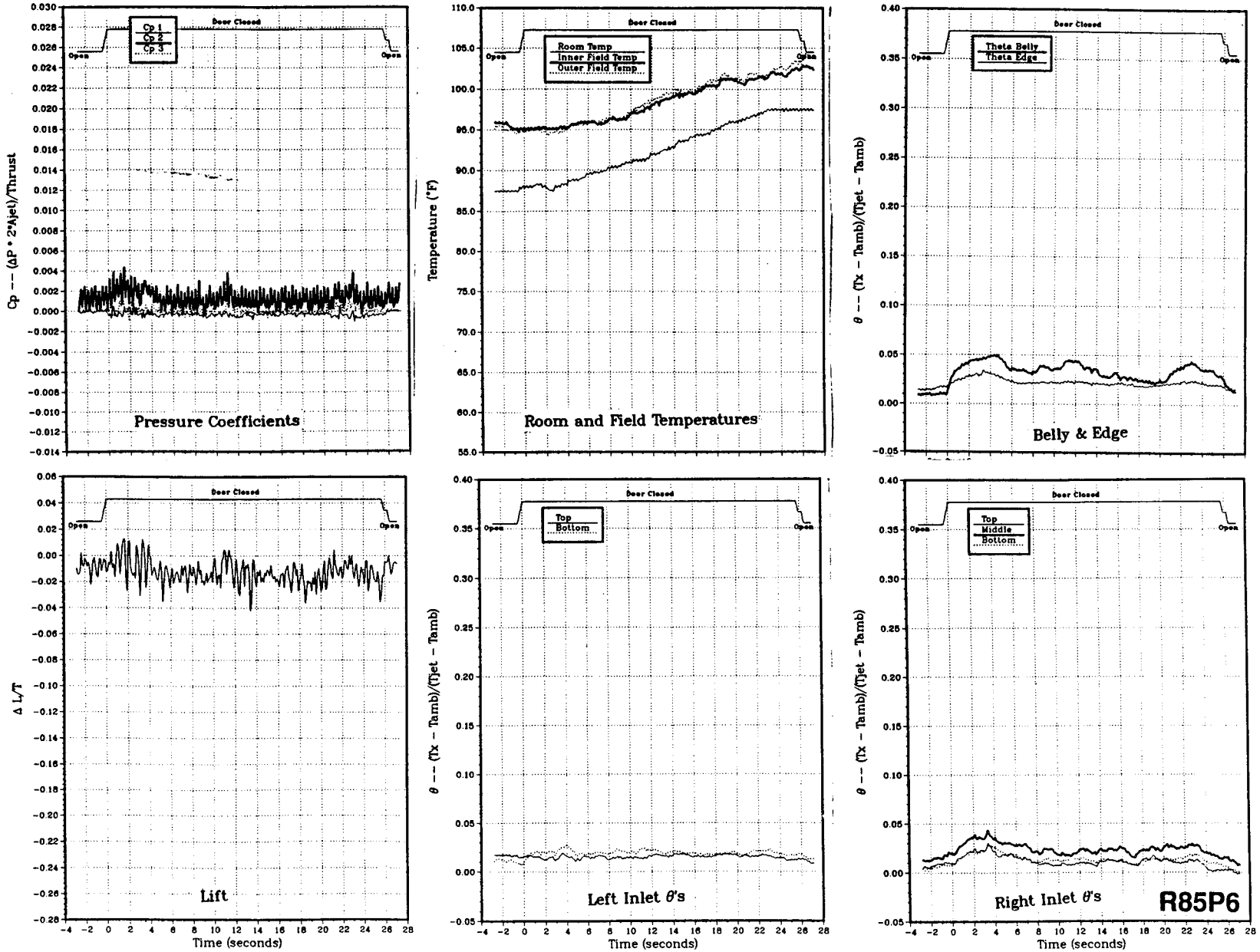

Figure 52(f). Wing/body, no LIDs, NPR = 2.0, thrust = 50 lb, height = 20 in., Tjet = 513 °F, inlet position = 13 in.

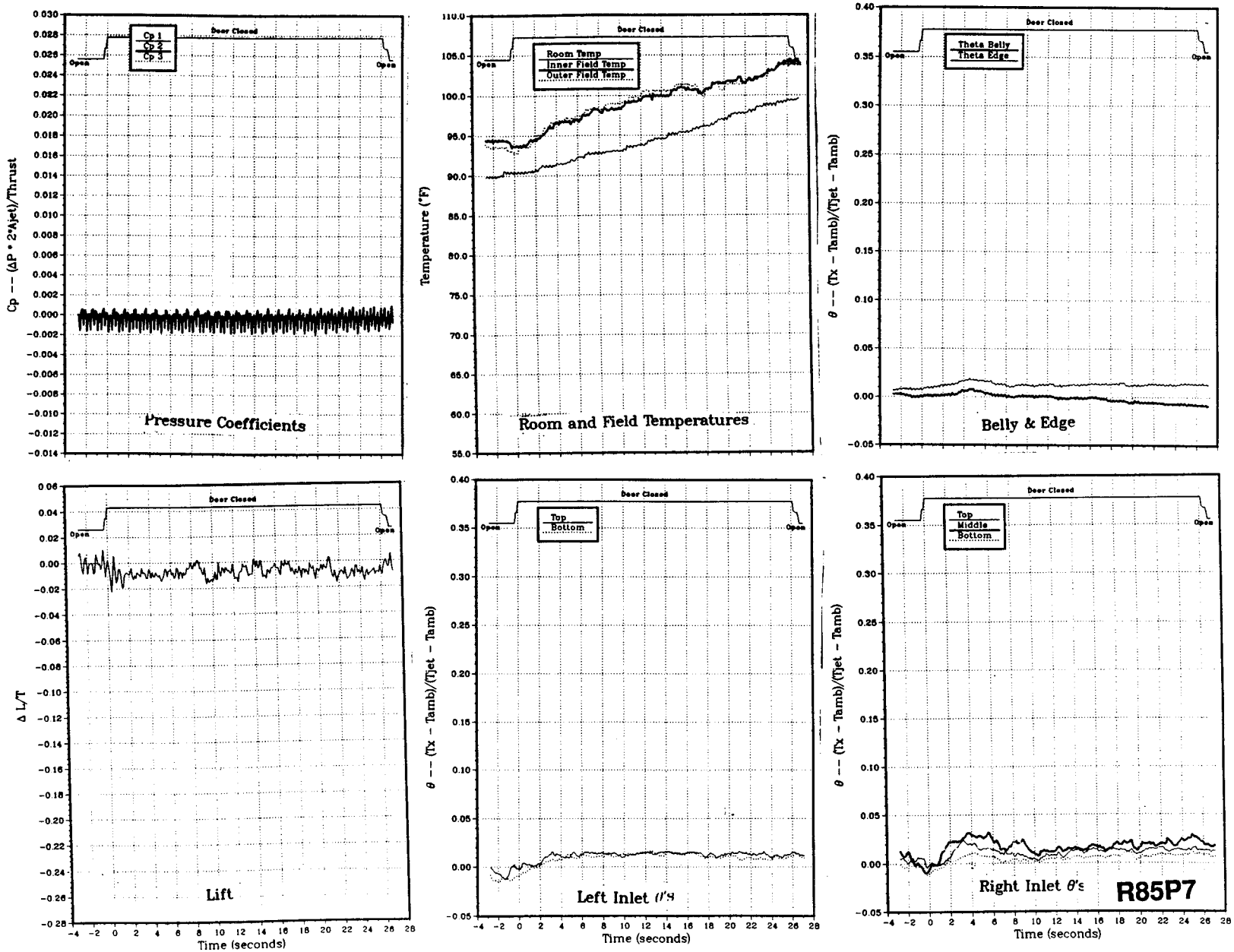

Figure 52(g). Wing/body, no LIDs, NPR = 2.0, thrust = 50 lb, height = 30 in., Tjet = 515 °F, inlet position = 13 in.

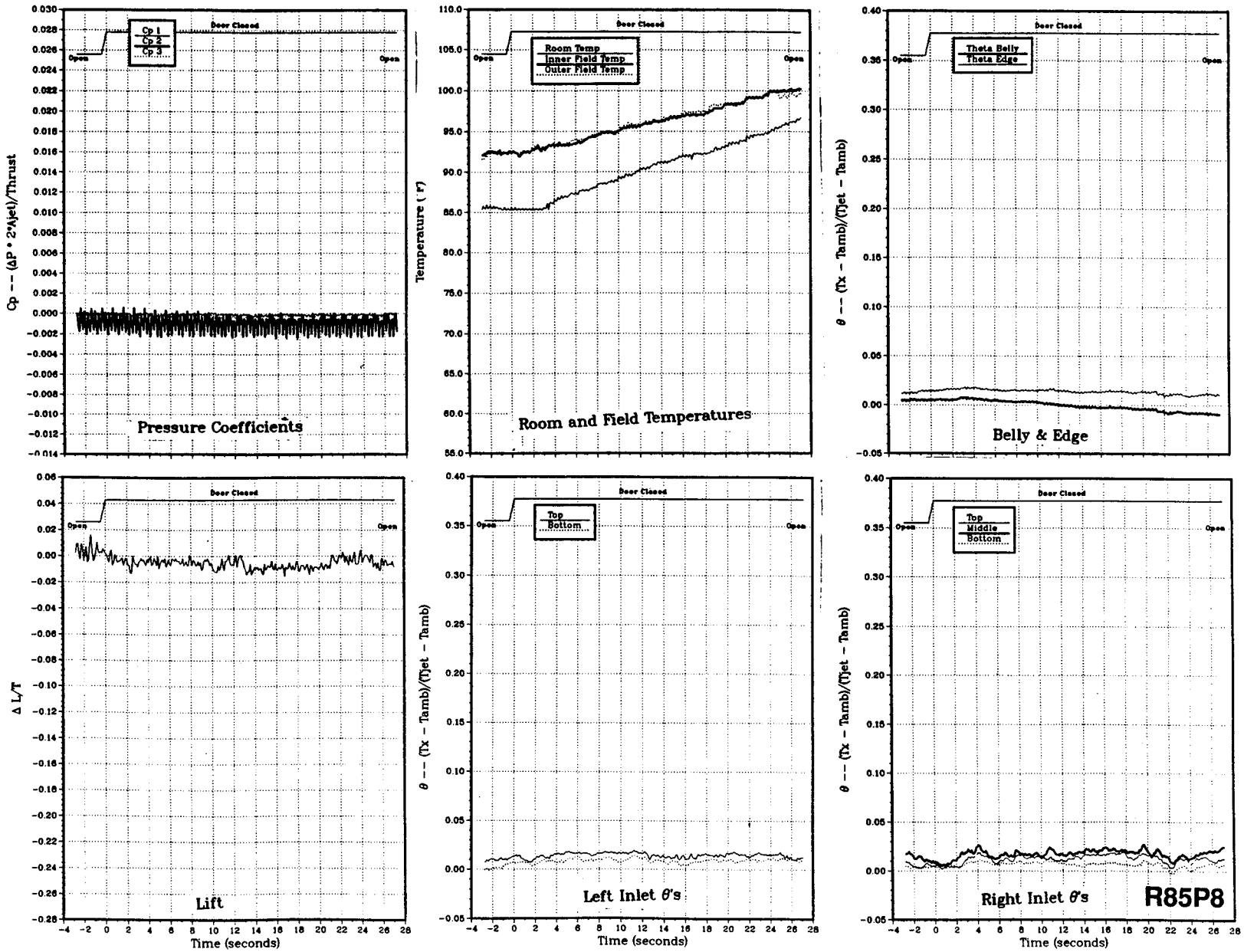

Figure 52(h). Wing/body, no LIDs, NPR = 2.0, thrust = 50 lb, height = 40 in., Tjet = 517 °F, inlet position = 13 in.

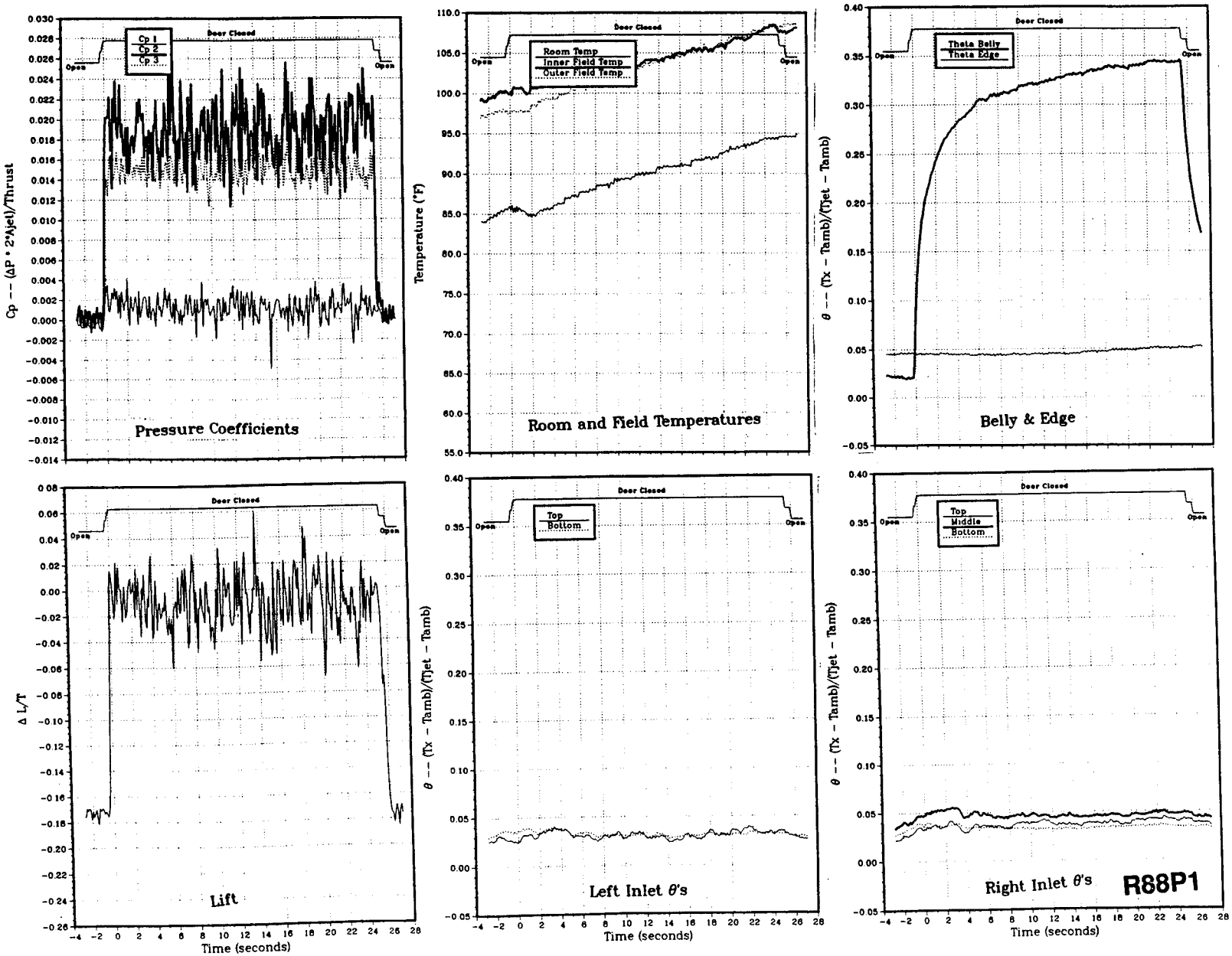

Figure 53(a). Wing/body, Box LIDs (12/21), NPR = 2.0, thrust = 50 lb, height = 4 in., Tjet = 495 °F, inlet position = 13 in.

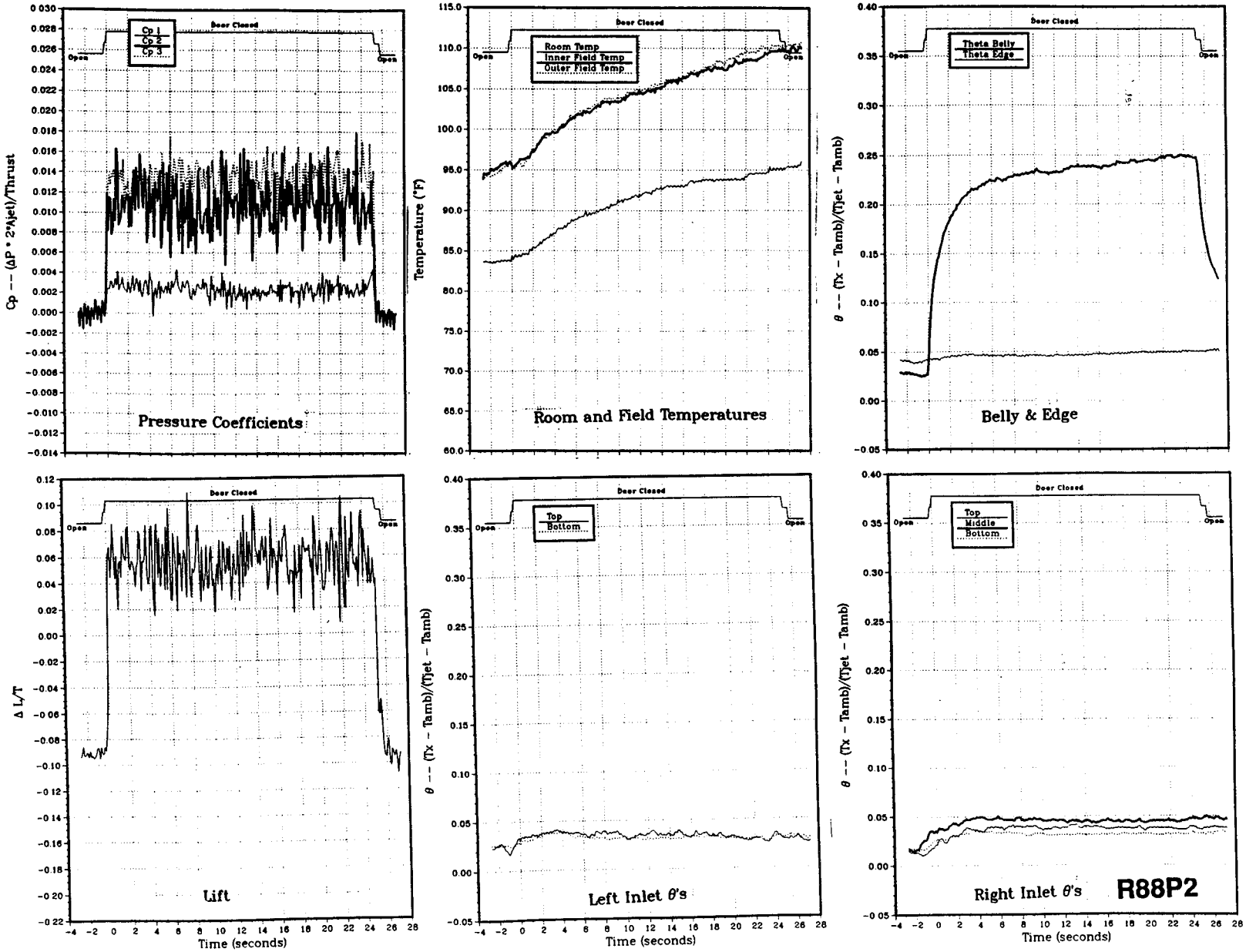

Figure 53(b). Wing/body, Box LIDs (12/21), NPR = 2.0, thrust = 50 lb, height = 6 in., Tjet = 499 °F, inlet position = 13 in.

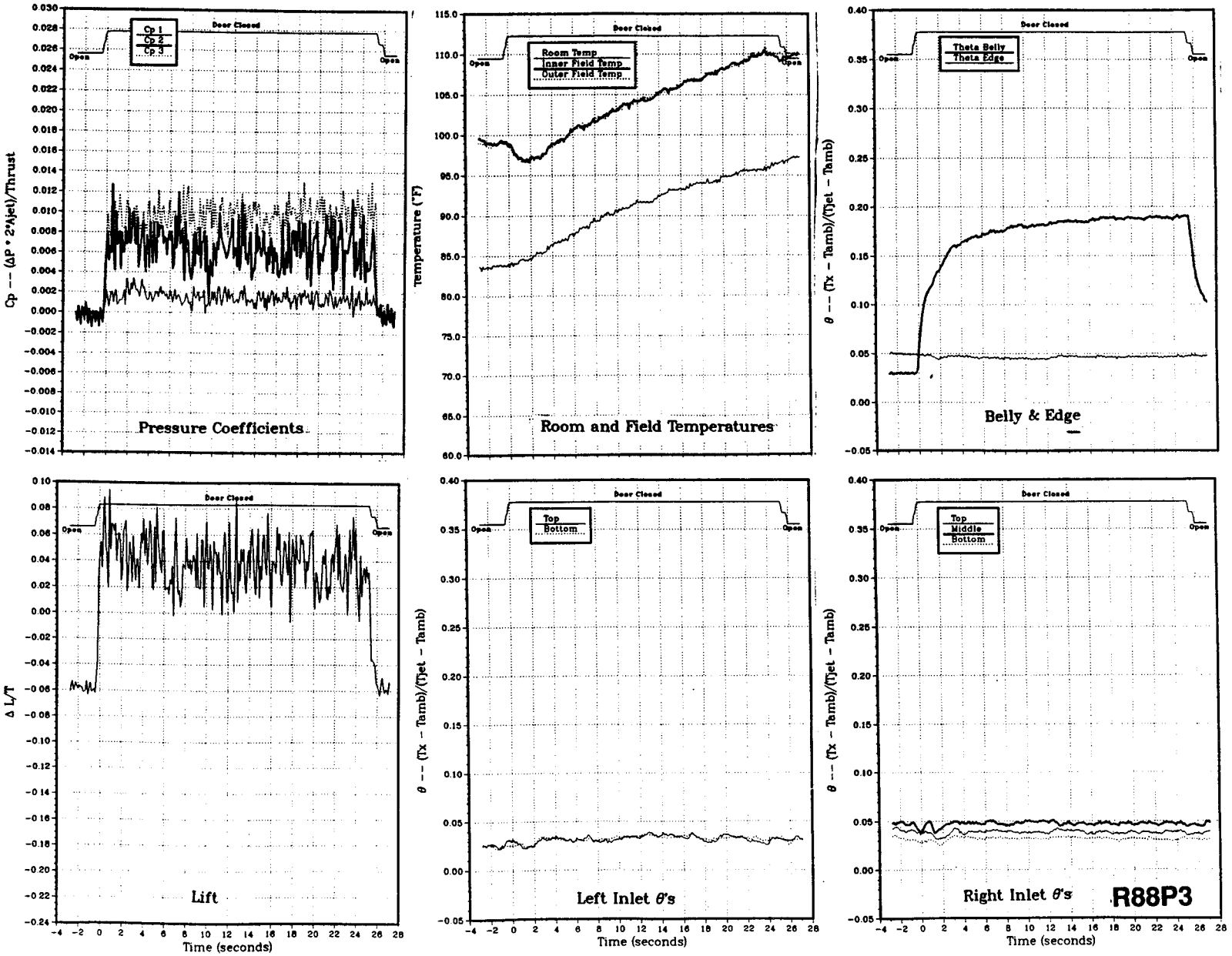

Figure 53(c). Wing/body, Box LIDs (12/21), NPR = 2.0, thrust = 50 lb, height = 8 in., Tjet = 502 °F, inlet position = 13 in.

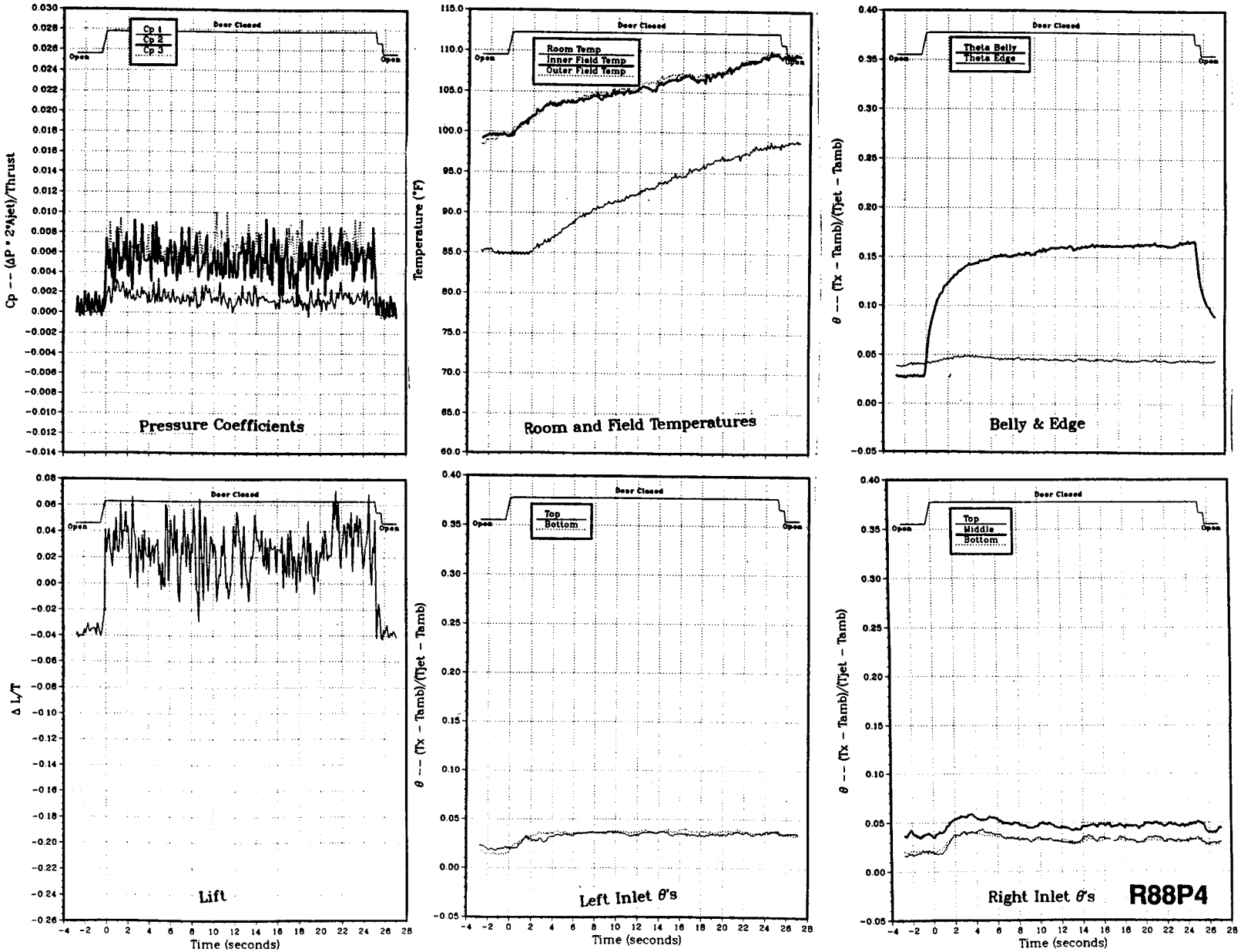

Figure 53(d). Wing/body, Box LIDs (12/21), NPR = 2.0, thrust = 50 lb, height = 10 in., Tjet = 504 °F, inlet position = 13 in.

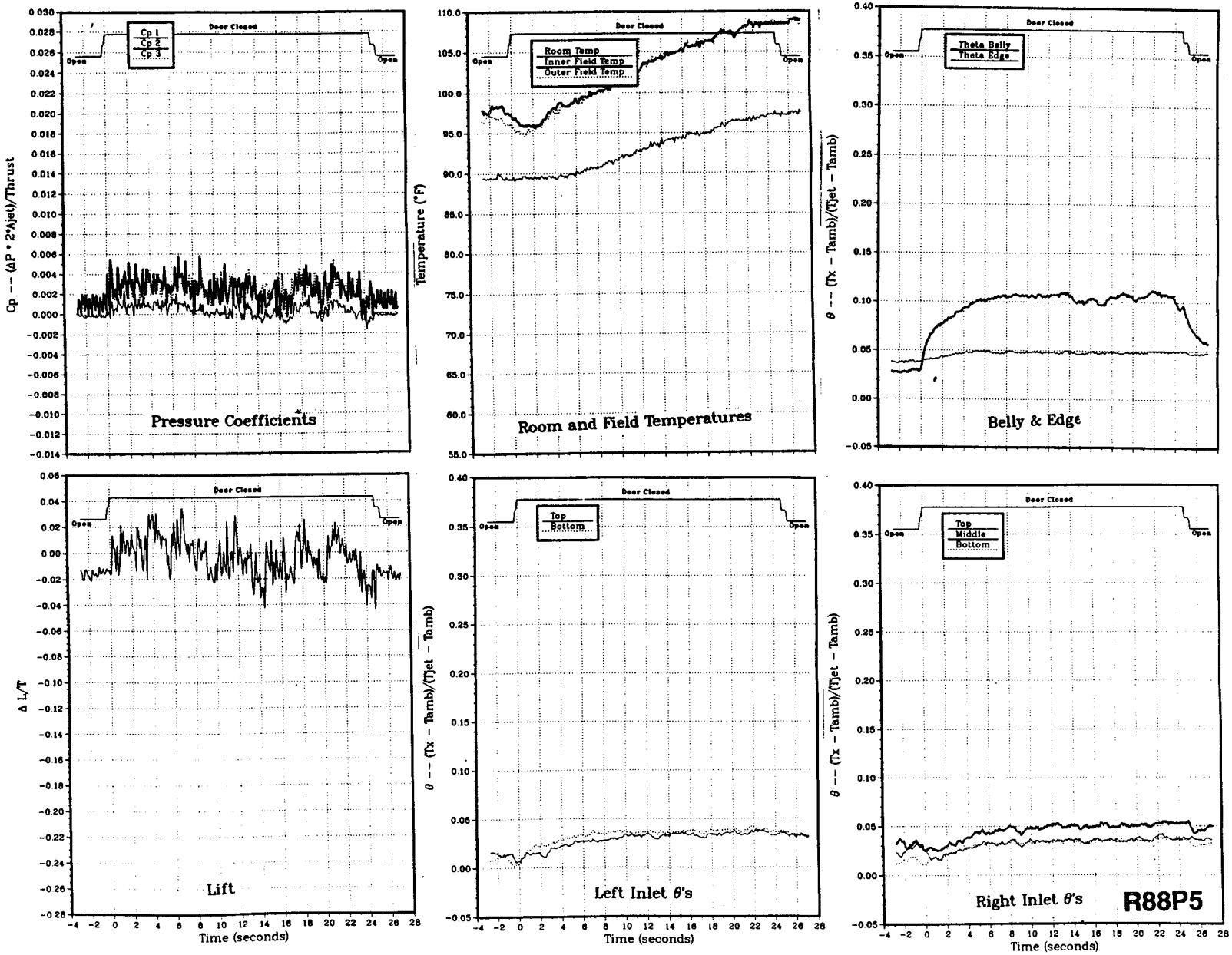

Figure 53(e). Wing/body, Box LIDs (12/21), NPR = 2.0, thrust = 50 lb, height = 15 in., Tjet = 507 °F, inlet position = 13 in.

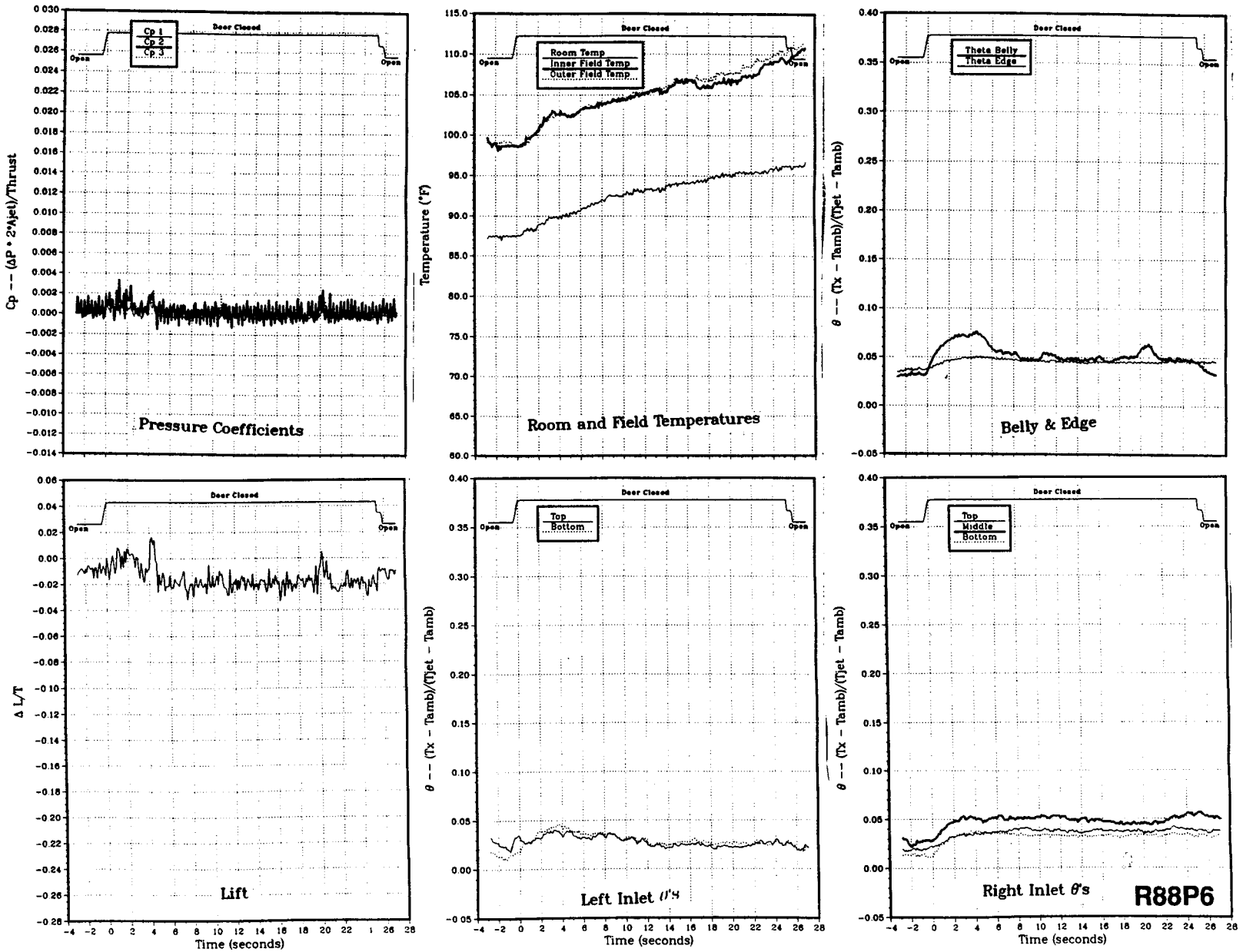

Figure 53(f). Wing/body, Box LIDs (12/21), NPR = 2.0, thrust = 50 lb, height = 20 in., Tjet = 508 °F, inlet position = 13 in.

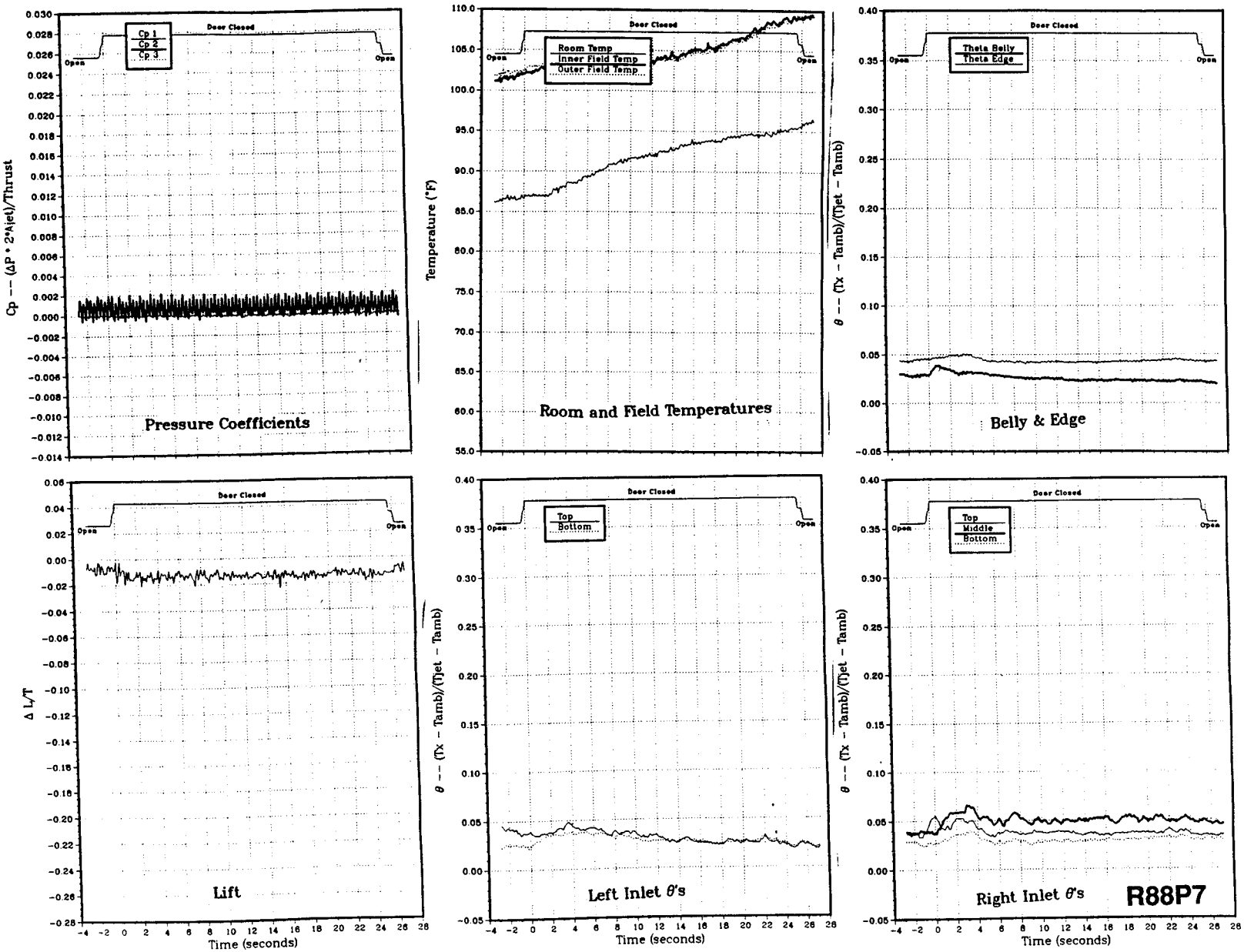

Figure 53(g). Wing/body, Box LIDs (12/21), NPR = 2.0, thrust = 50 lb, height = 30 in., Tjet = 511 °F, inlet position = 13 in.

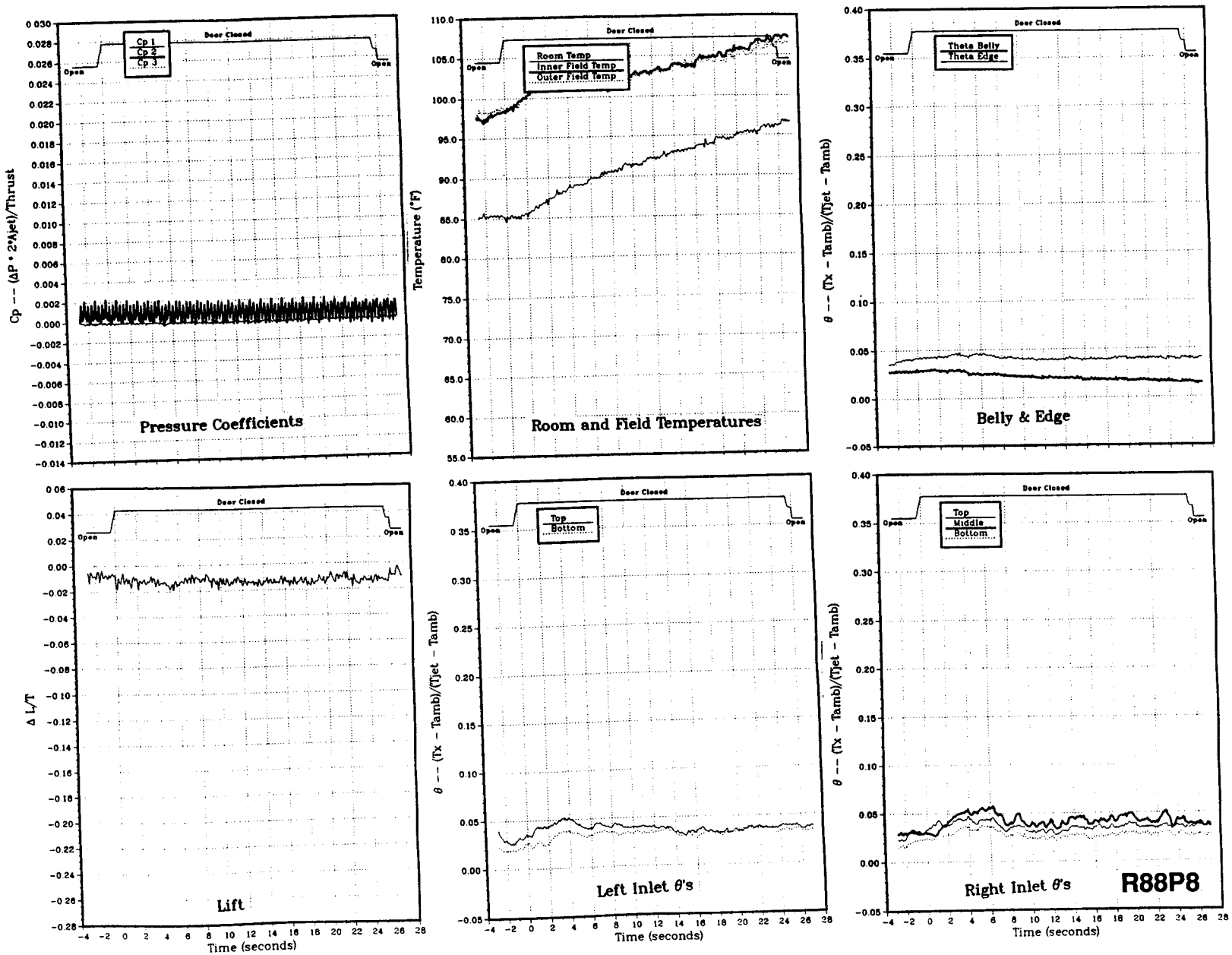

Figure 53(h). Wing/body, Box LIDs (12/21), NPR = 2.0, thrust = 50 lb, height = 40 in., Tjet = 512 °F, inlet position = 13 in.

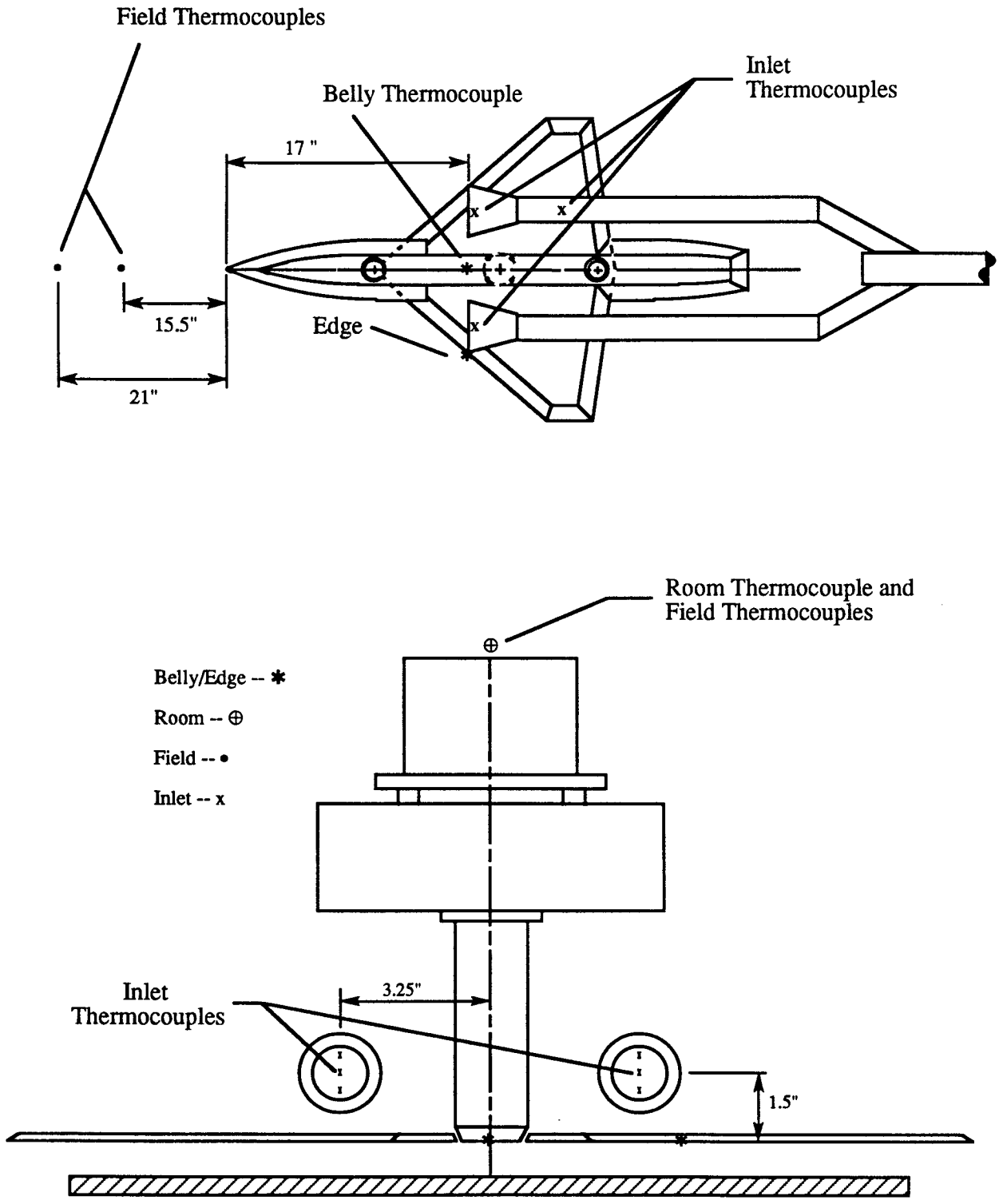

Figure 54. Locations of model and field thermocouples for data set 13.

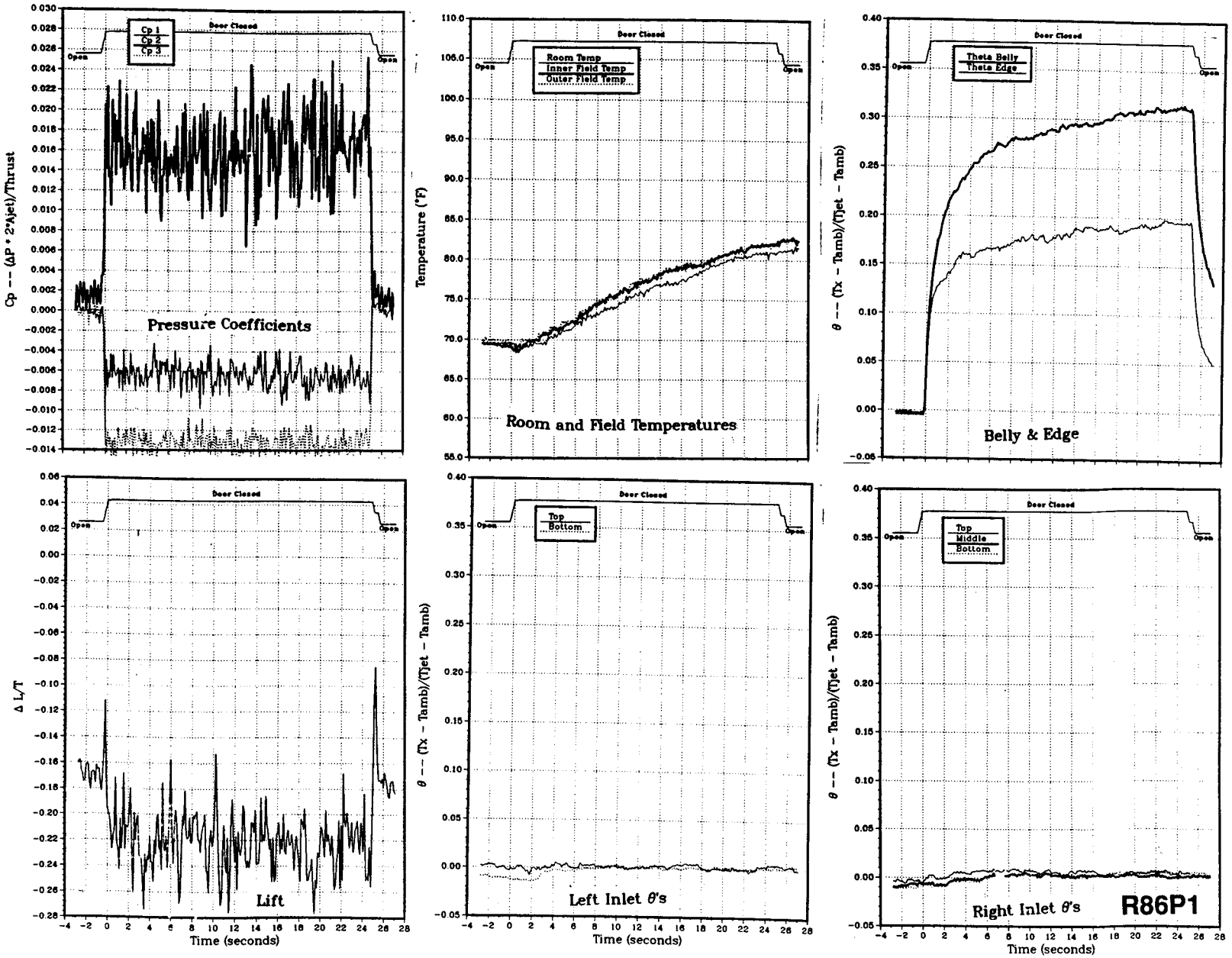

Figure 55(a). Wing/body, no LIDs, NPR = 2.0, thrust = 50 lb, height = 4 in., Tjet = 476 °F, inlet position = 17 in.

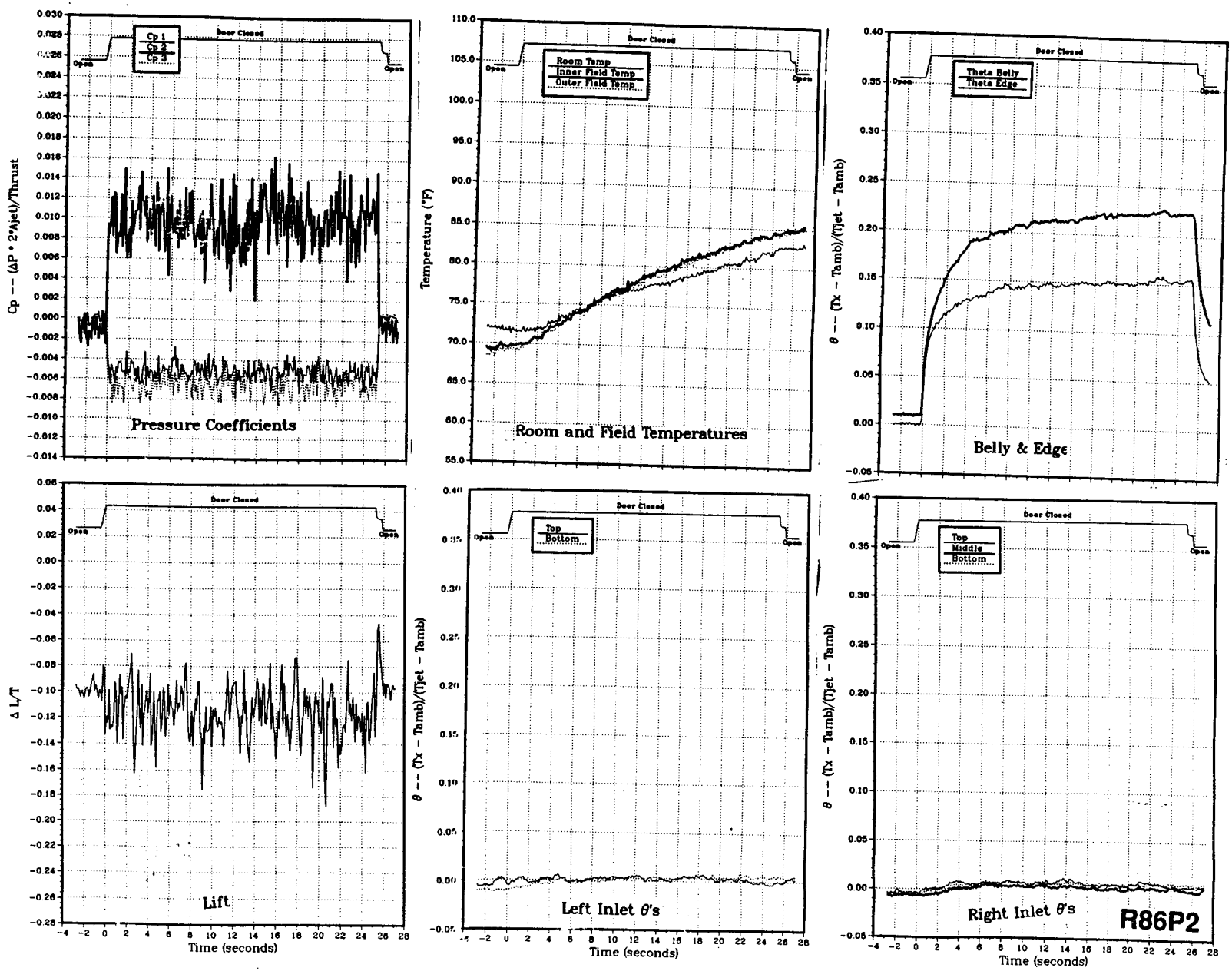

Figure 55(b). Wing/body, no LIDs, NPR = 2.0, thrust = 50 lb, height = 6 in., Tjet = 478 °F, inlet position = 17 in.

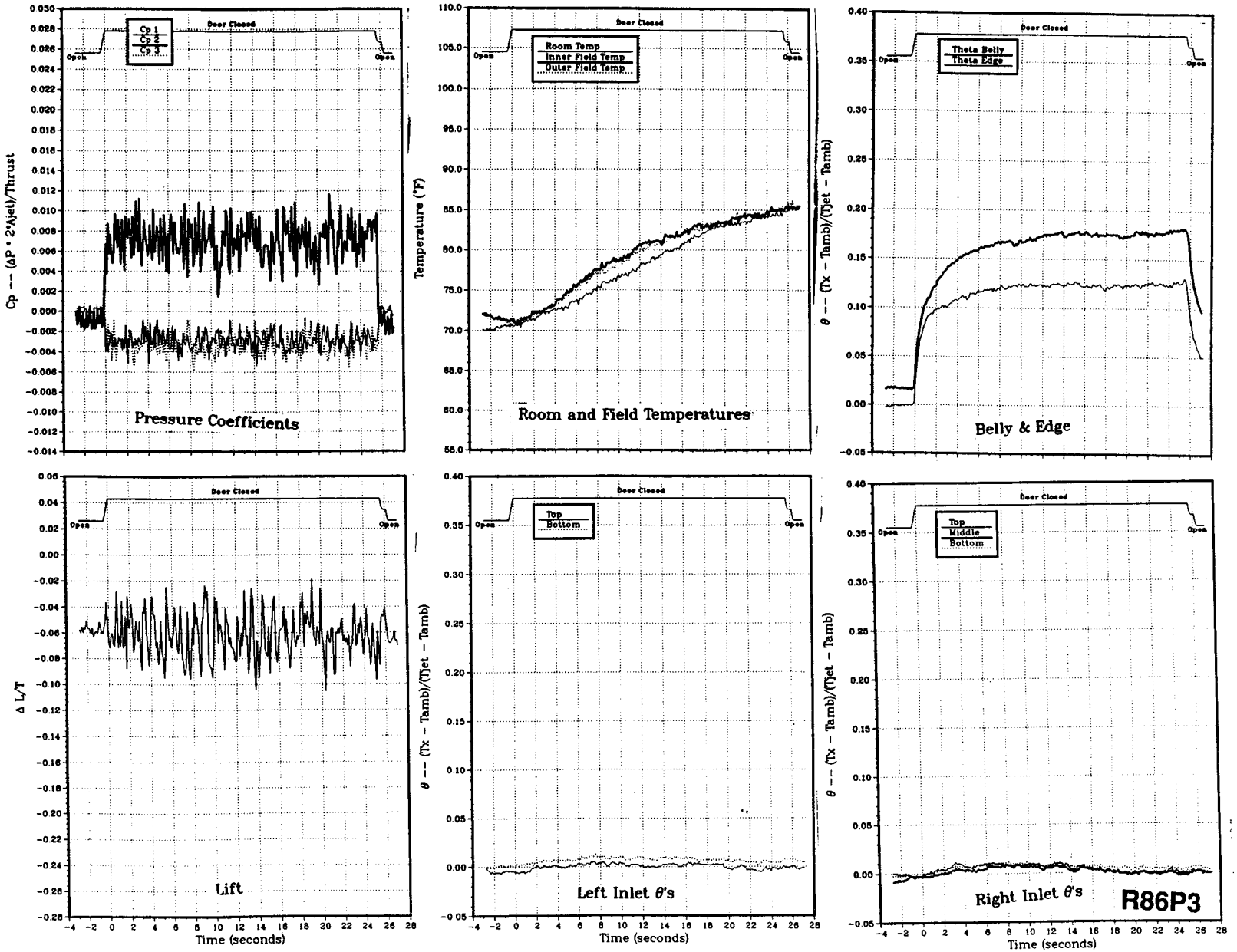

Figure 55(c). Wing/body, no LIDs, NPR = 2.0, thrust = 50 lb, height = 8 in., Tjet = 479 °F, inlet position = 17 in.

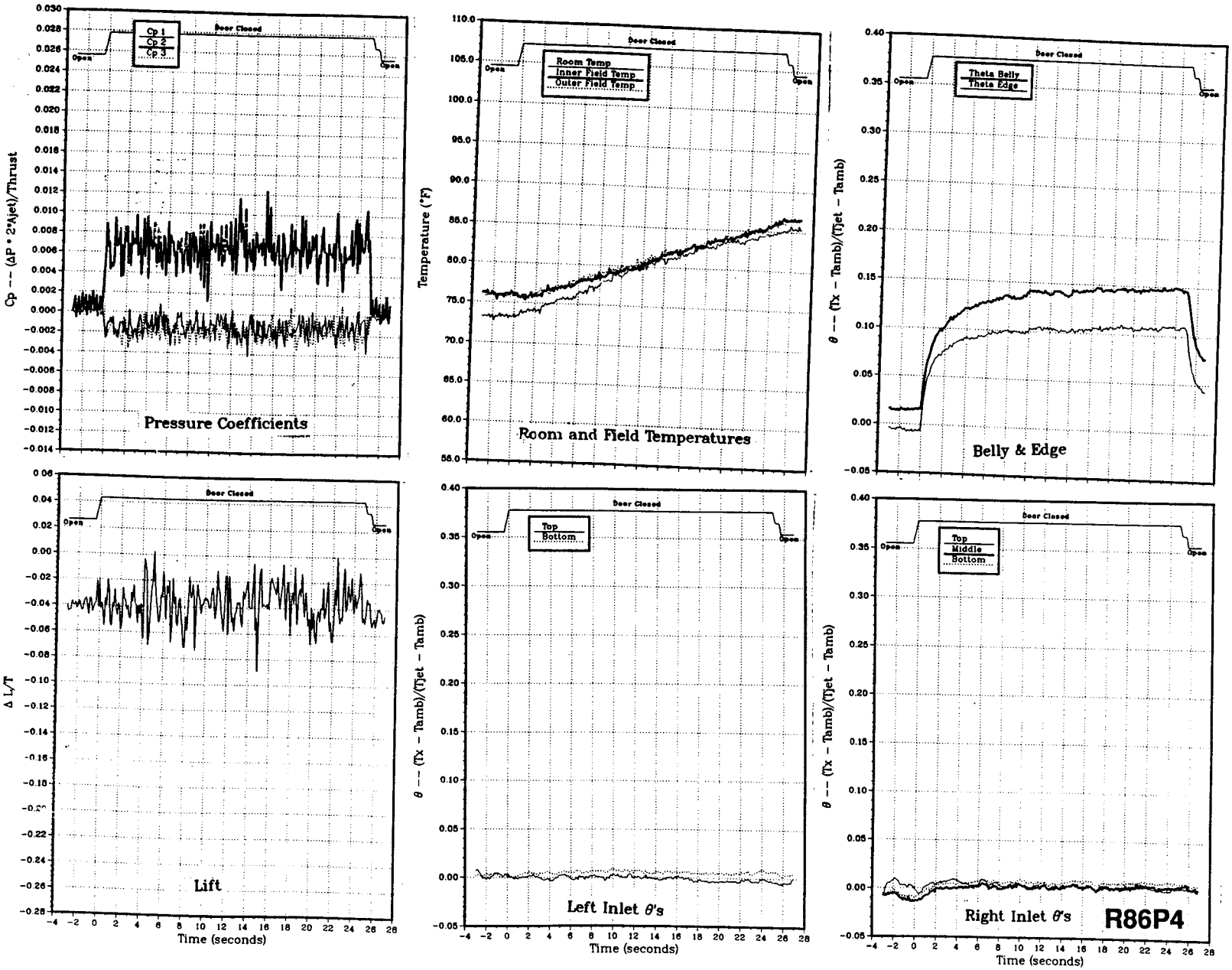

Figure 55(d). Wing/body, no LIDs, NPR = 2.0, thrust = 50 lb, height = 10 in., Tjet = 481 °F, inlet position = 17 in.

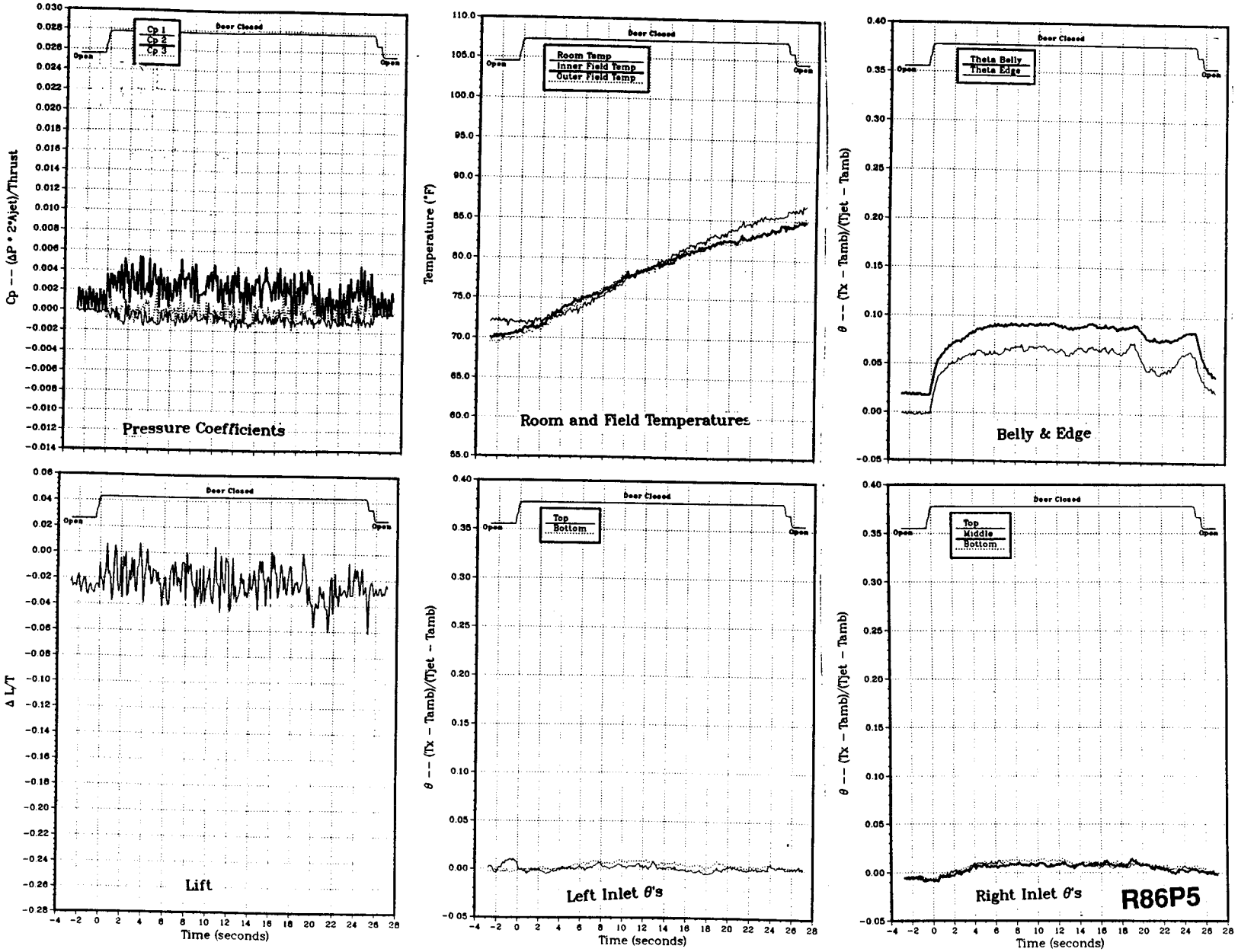

Figure 55(e). Wing/body, no LIDs, NPR = 2.0, thrust = 50 lb, height = 15 in., Tjet = 483 °F, inlet position = 17 in.

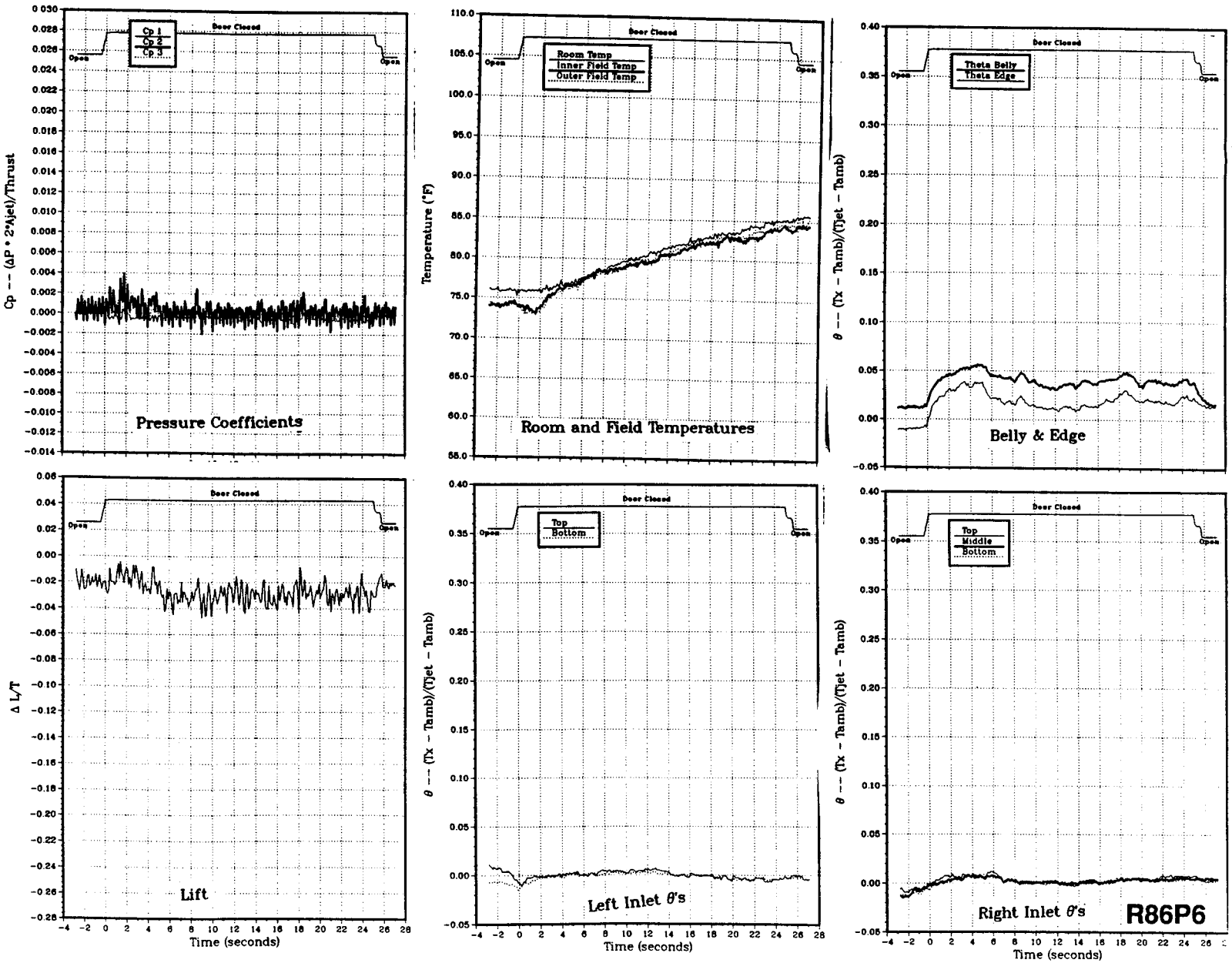

Figure 55(f). Wing/body, no LIDs, NPR = 2.0, thrust = 50 lb, height = 20 in., Tjet = 485 °F, inlet position = 17 in.

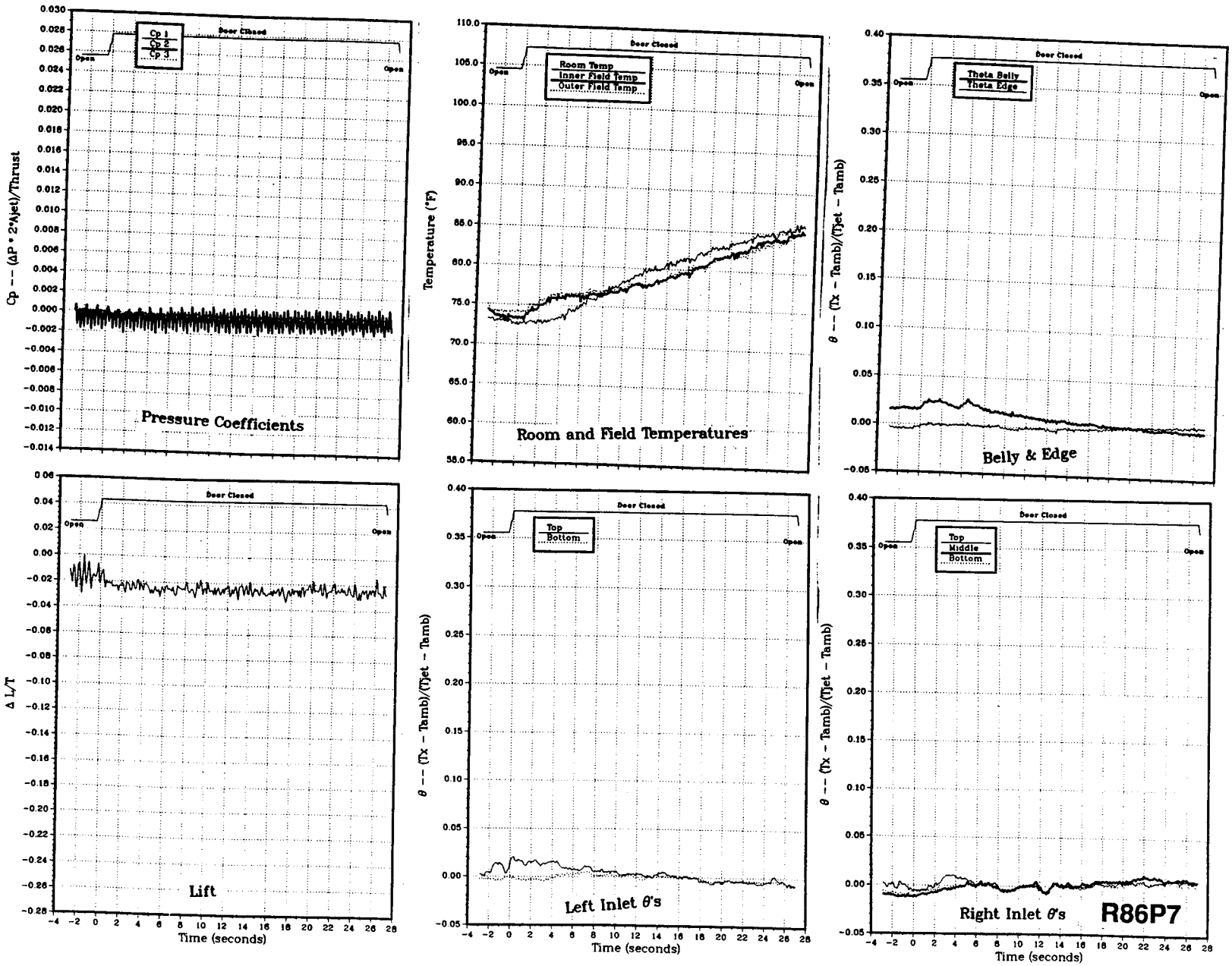

Figure 55(g). Wing/body, no LIDs, NPR = 2.0, thrust = 50 lb, height = 30 in., Tjet = 487 °F, inlet position = 17 in.

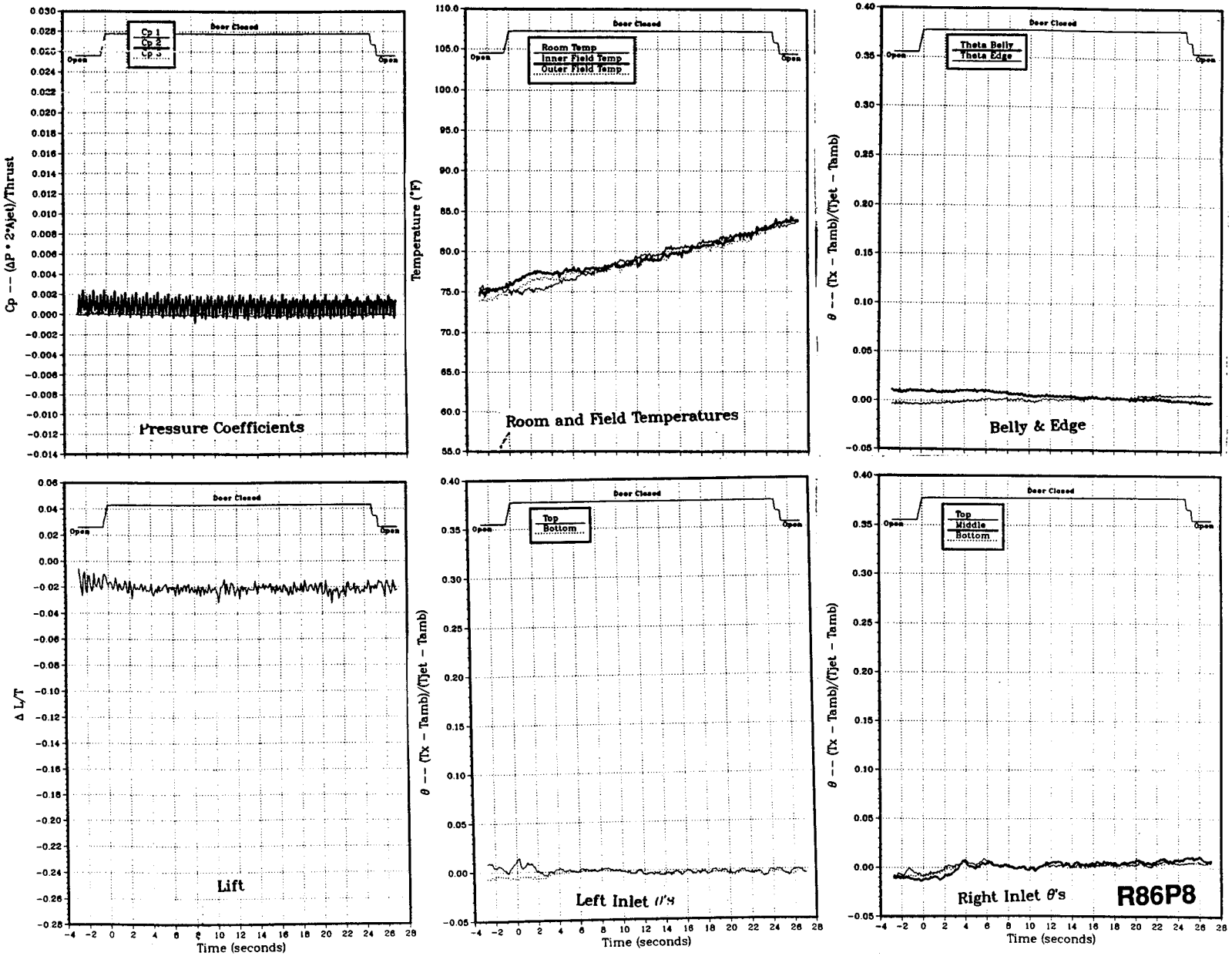

Figure 55(h). Wing/body, no LIDs, NPR = 2.0, thrust = 50 lb, height = 40 in., Tjet = 489 °F, inlet position = 17 in.

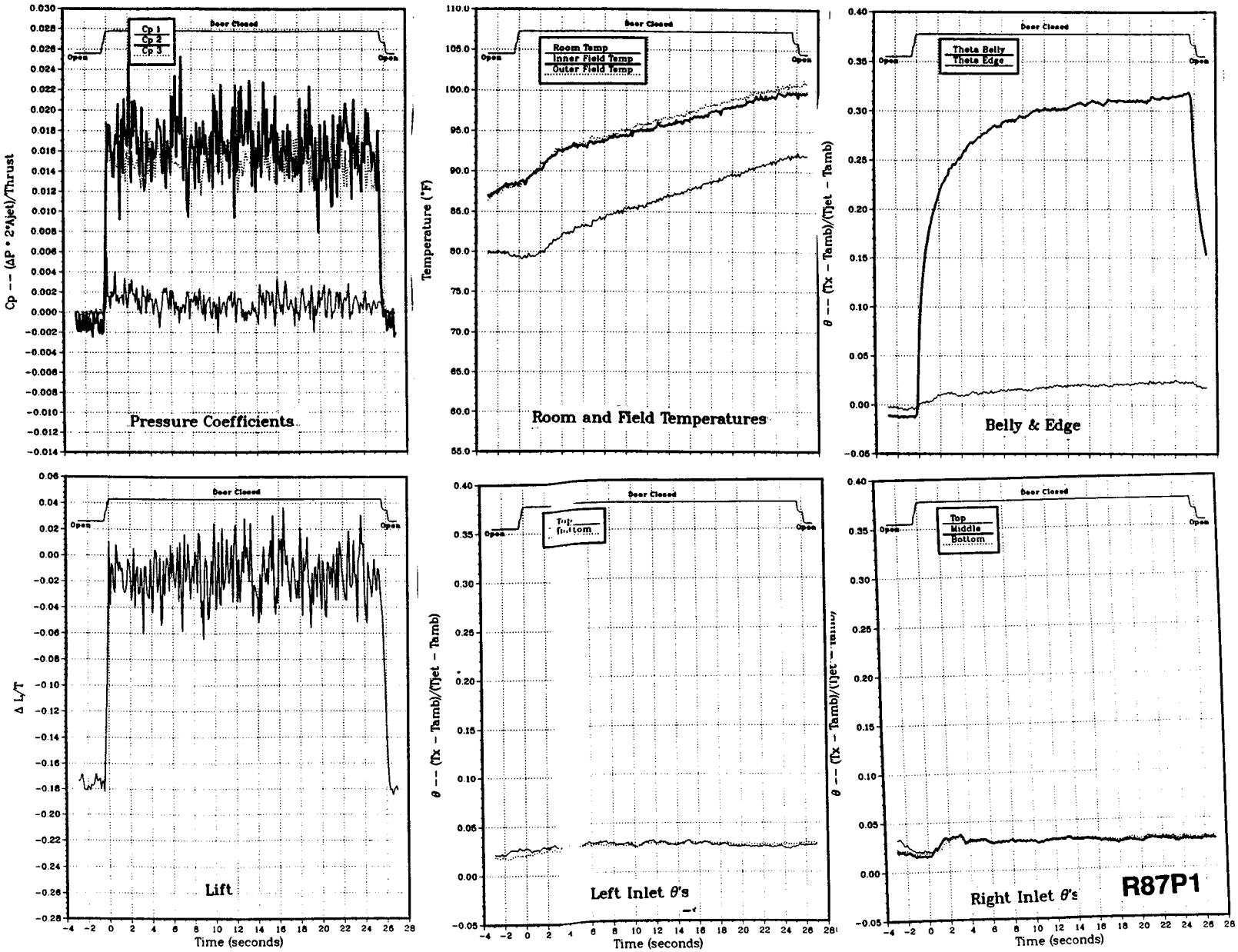

Figure 56(a). Wing/body, Box LIDs (12/21), NPR = 2.0, thrust = 50 lb, height = 4 in., Tjet = 509 °F, inlet position = 17 in.

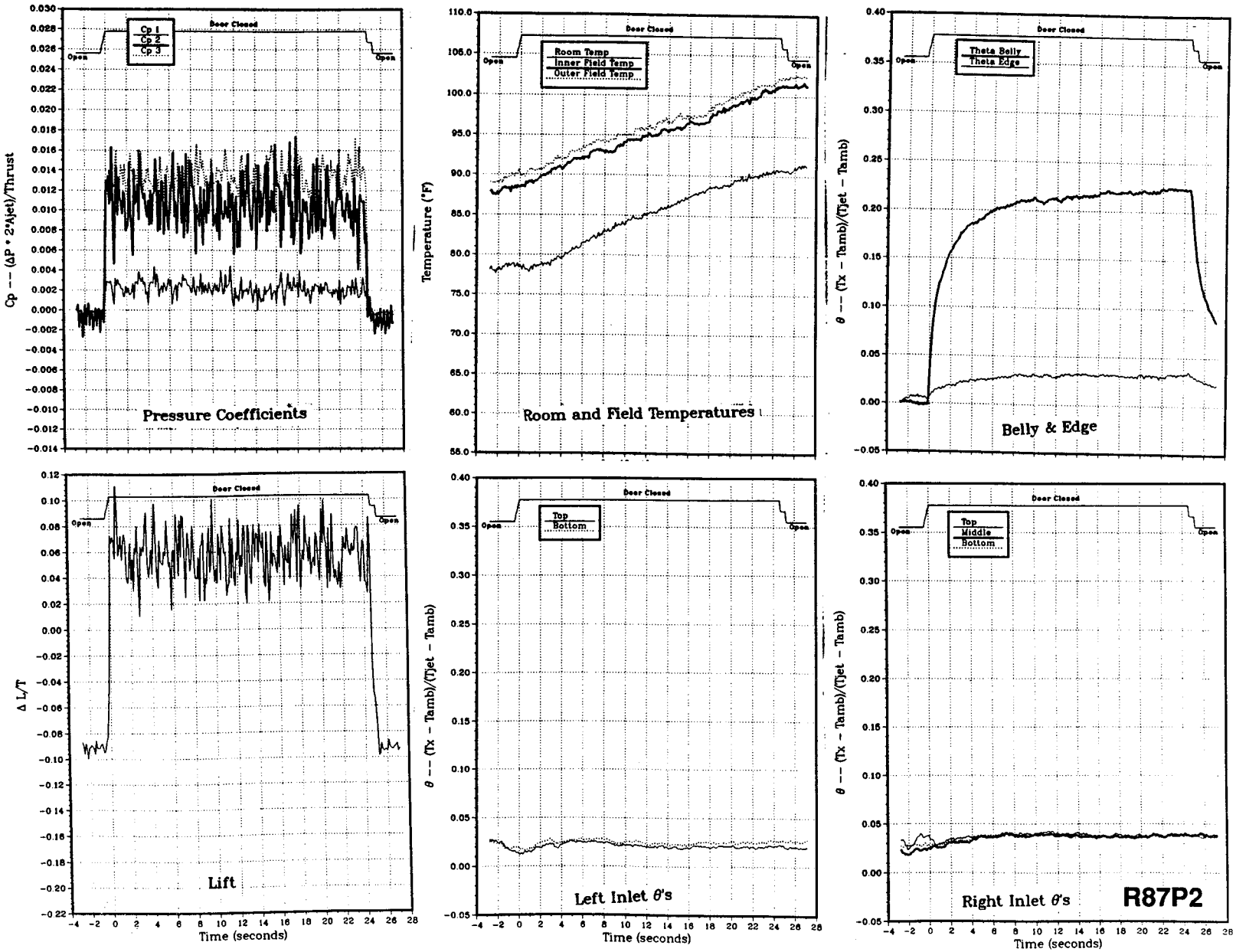

Figure 56(b). Wing/body, Box LIDs (12/21), NPR = 2.0, thrust = 50 lb, height = 6 in., Tjet = 510 °F, inlet position = 17 in.

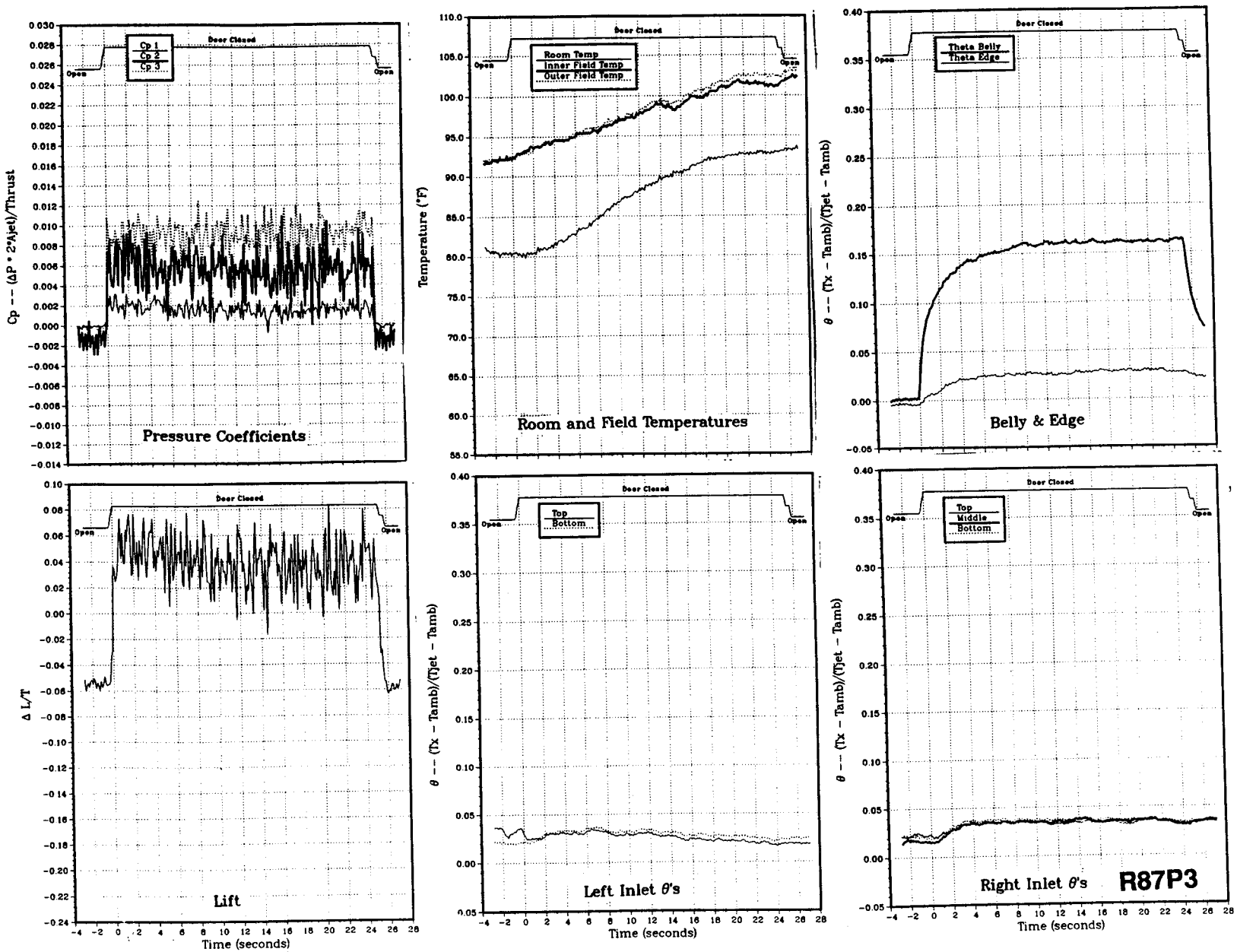

Figure 56(c). Wing/body, Box LIDs (12/21), NPR = 2.0, thrust = 50 lb, height = 8 in., Tjet = 510 °F, inlet position = 17 in.

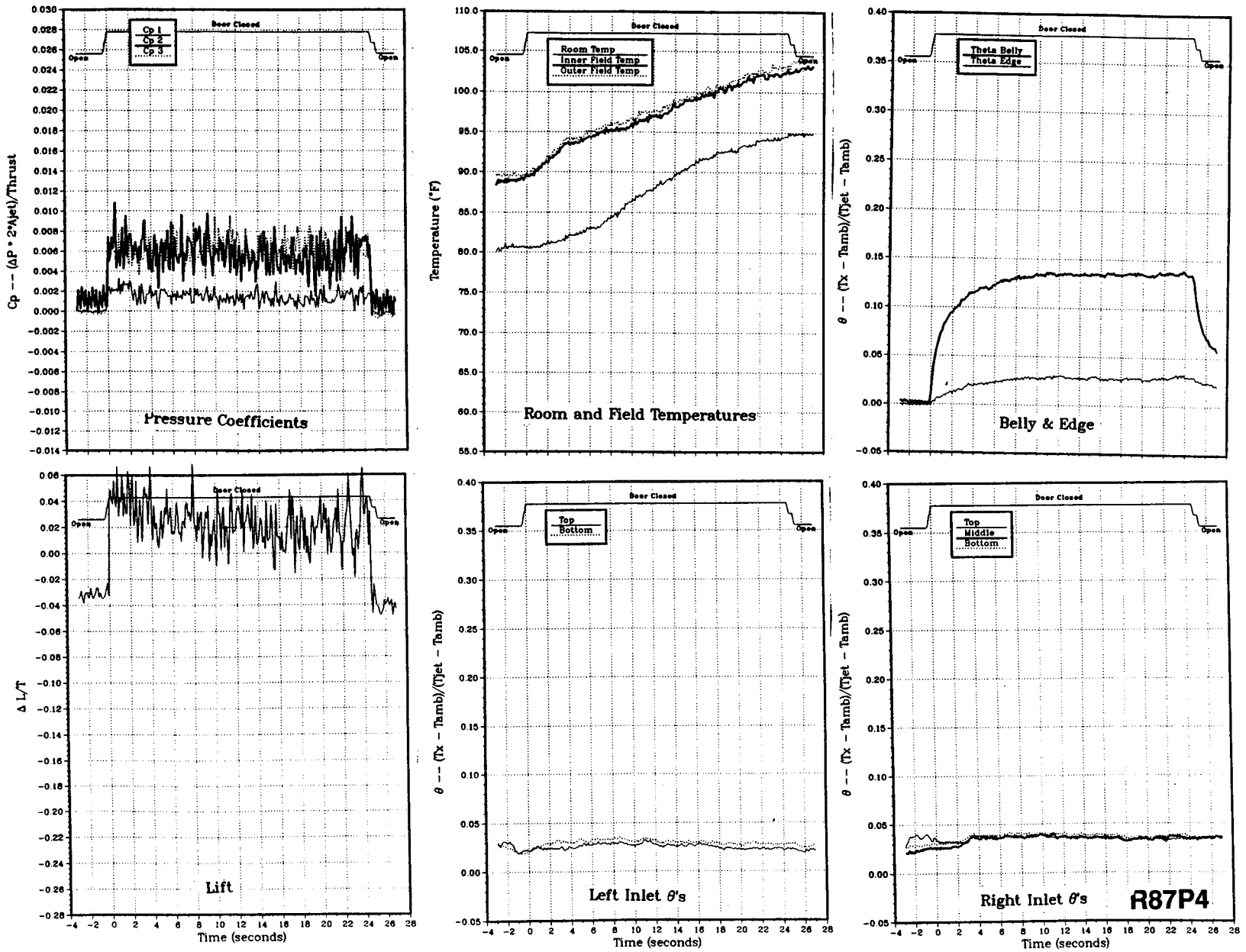

Figure 56(d). Wing/body, Box LIDs (12/21), NPR = 2.0, thrust = 50 lb, height = 10 in., Tjet = 511 °F, inlet position = 17 in.

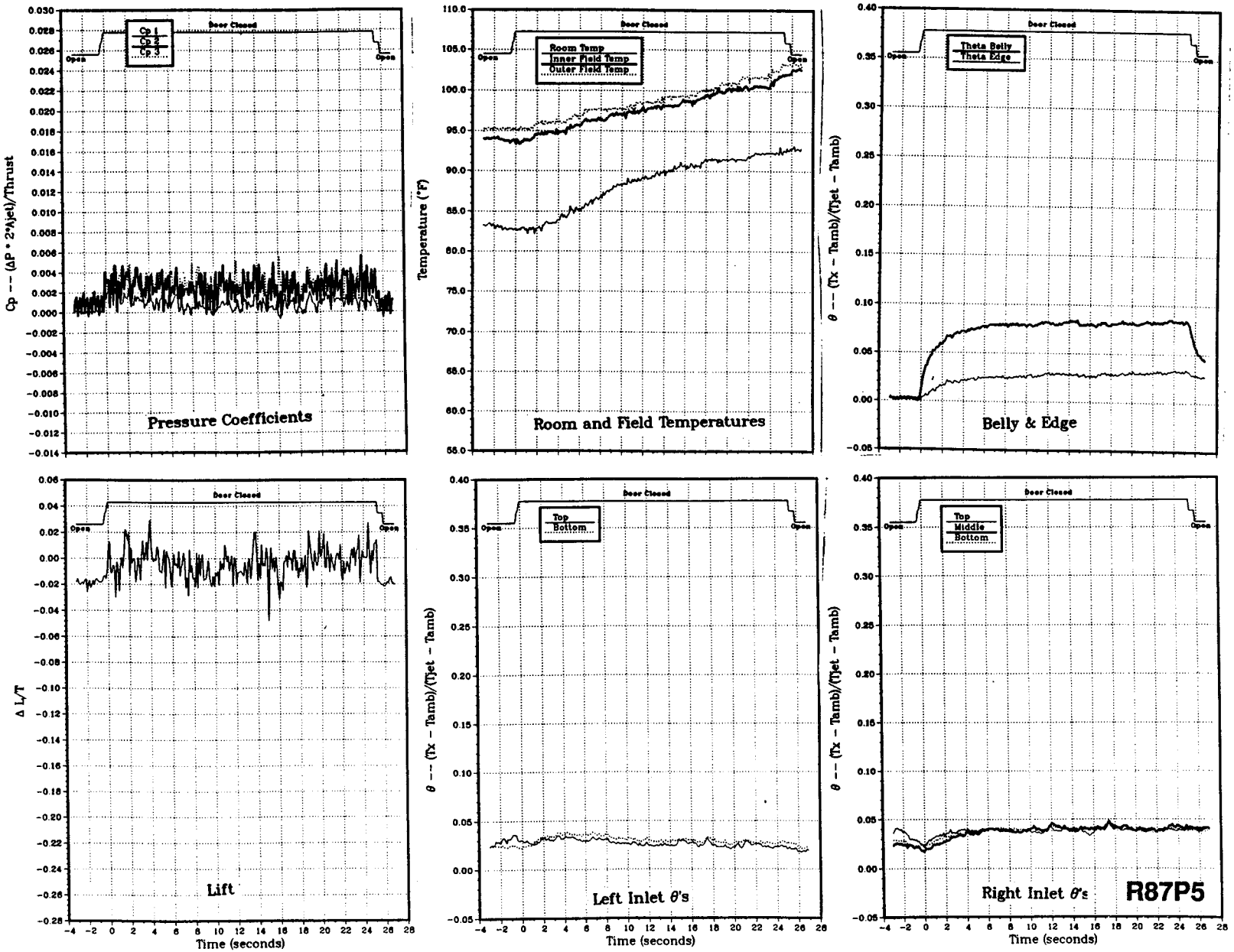

Figure 56(e). Wing/body, Box LIDs (12/21), NPR = 2.0, thrust = 50 lb, height = 15 in., Tjet = 511 °F, inlet position = 17 in.

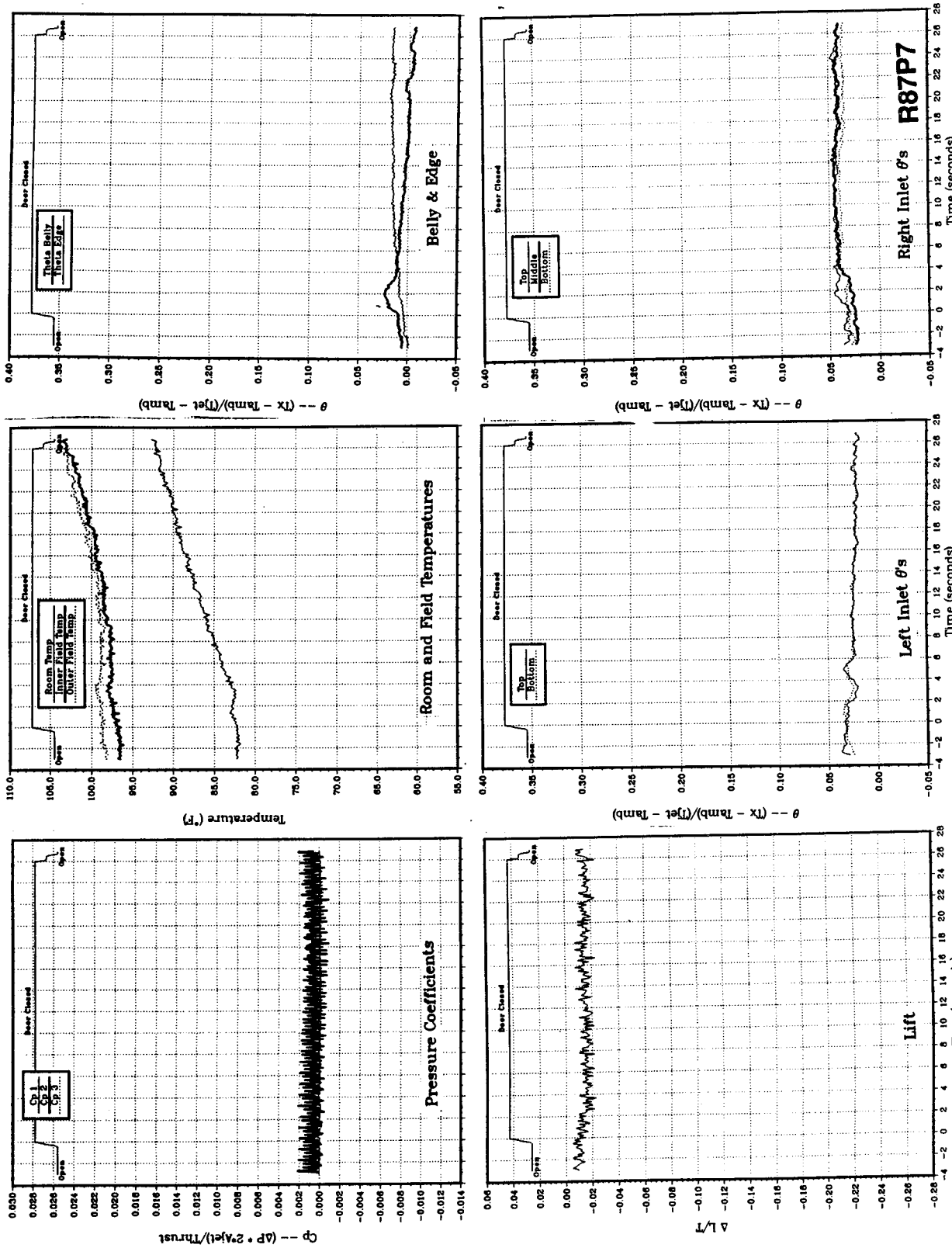

Figure 56(f). Wing/body, Box LIDs (12/21), NPR = 2.0, thrust = 50 lb, height = 30 in., Tjet = 511 °F, inlet position = 17 in.

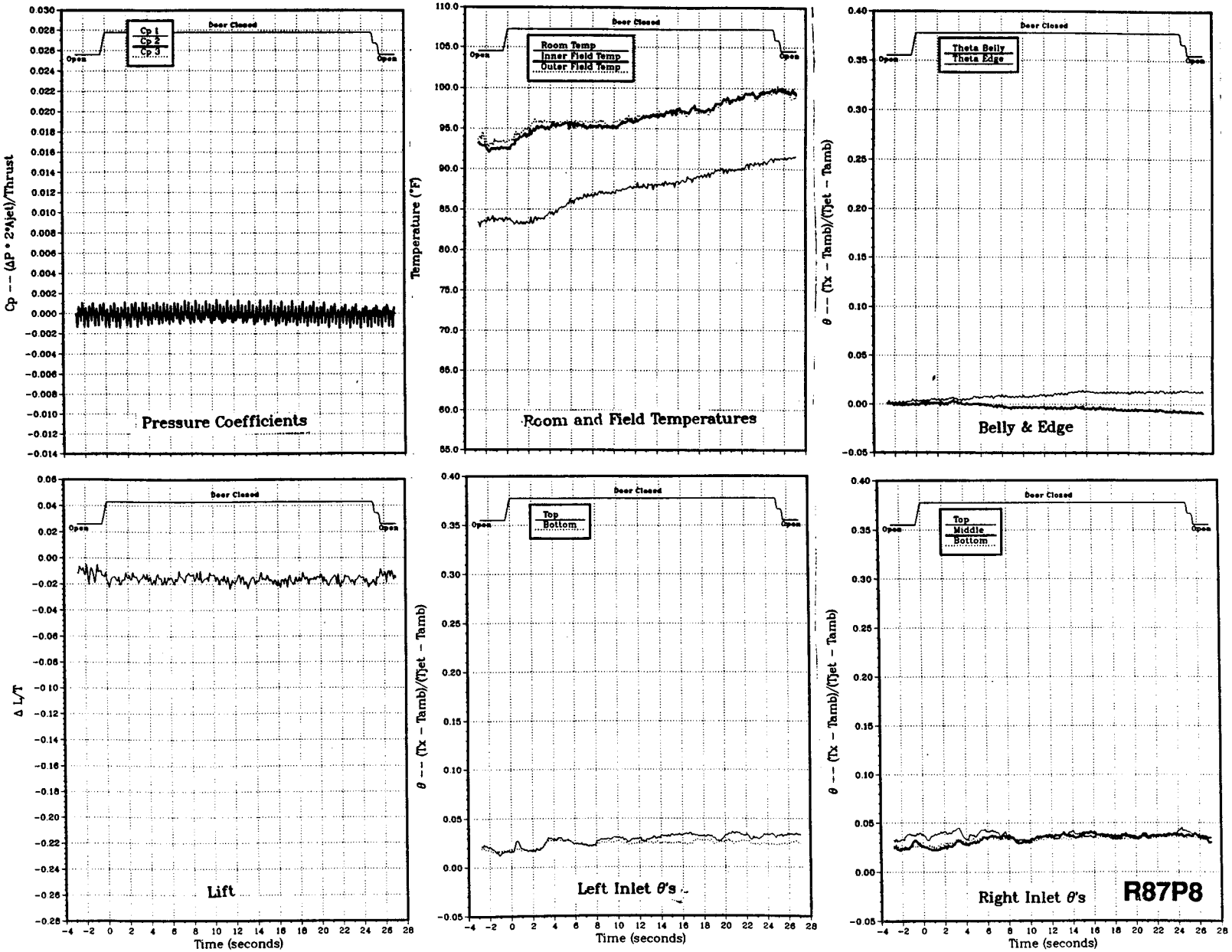

Figure 56(g). Wing/body, Box LIDs (12/21), NPR = 2.0, thrust = 50 lb, height = 40 in., Tjet = 511 °F, inlet position = 17 in.

REPORT DOCUMENTATION PAGE

Form Approved
OMB No. 0704-0188

1. AGENCY USE ONLY *(Leave blank)*	2. REPORT DATE	3. REPORT TYPE AND DATES COVERED
	July 1992	Technical Memorandum

4. TITLE AND SUBTITLE

Dynamic Response of Induced Pressures, Suckdown, and Temperatures for Two Tandem Jet STOVL Configurations

5. FUNDING NUMBERS

505-68-32

6. AUTHOR(S)

Douglas A. Wardwell, Victor R. Corsiglia, and Richard E. Kuhn

7. PERFORMING ORGANIZATION NAME(S) AND ADDRESS(ES)

Ames Research Center
Moffett Field, CA 94035-1000

8. PERFORMING ORGANIZATION REPORT NUMBER

A-90290

9. SPONSORING/MONITORING AGENCY NAME(S) AND ADDRESS(ES)

National Aeronautics and Space Administration
Washington, DC 20546-0001

10. SPONSORING/MONITORING AGENCY REPORT NUMBER

NASA TM-103934

11. SUPPLEMENTARY NOTES

Point of Contact: Douglas A. Wardwell, Ames Research Center, MS 237-3, Moffett Field, CA 94035-1000
(415) 604-6566 or FTS 464-6566

12a. DISTRIBUTION/AVAILABILITY STATEMENT

Unclassified-Unlimited
Subject Category – 02

12b. DISTRIBUTION CODE

13. ABSTRACT ***(Maximum 200 words)***

NASA Ames Research Center has been conducting a program to improve the methods for predicting the jet-induced lift loss (suckdown) and hot gas ingestion on jet Short Takeoff and Vertical Landing (STOVL) aircraft during hover near the ground. As part of that program, small-scale hover tests were conducted to expand the current data base and to improve upon the current empirical methods for predicting jet-induced lift loss and hot gas ingestion (HGI) effects.

This report is one of three data reports covering data obtained from hover tests conducted at Lockheed Aeronautical Systems, Rye Canyon Facility. It will include dynamic (time dependent) test data for both lift loss and HGI parameters (height, nozzle temperature, nozzle pressure ratio, and inlet location). The flat plate models tested were tandem jet configurations with three planform variations and variable position side-by-side sucking inlets mounted above the planform.

Temperature time lags from 8–15 seconds were observed before the model temperatures stabilized. This was larger than the expected 1.5-second lag calculated from literature. Several possible explanations for the flow temperatures to stabilize may include some, or all, of the following: thermocouple lag, radiation to the model surface, and heat loss to the ground board. Further investigations will be required to understand the reasons for this temperature lag.

14. SUBJECT TERMS

STOVL, V/STOL, Dynamic response, Induced pressures, Suckdown, Temperature, Hot gas ingestion, HGI

15. NUMBER OF PAGES

201

16. PRICE CODE

A10

17. SECURITY CLASSIFICATION OF REPORT	18. SECURITY CLASSIFICATION OF THIS PAGE	19. SECURITY CLASSIFICATION OF ABSTRACT	20. LIMITATION OF ABSTRACT
Unclassified	Unclassified		